The Dissertation Committee for Suk Ho Eun Certifies that this is the approved version of the following dissertation:

The role of *Drosophila auxilin* in Notch signaling

Committee:

Janice Ann Fischer, Supervisor

Paul Macdonald

Theresa O'Halloran

John Sisson

Wesley Thompson

The role of *Drosophila auxilin* in Notch signaling

by

Suk Ho Eun, B.S.; M.S.

Dissertation

Presented to the Faculty of the Graduate School of

The University of Texas at Austin

in Partial Fulfillment

of the Requirements

for the Degree of

Doctor of Philosophy

The University of Texas at Austin

December 2007

Dedication

To myself and family, especially Su Jung Kang

Acknowledgements

I would like to thank Janice for her time, guidance, generosity, encouragement and patience. I especially appreciate her comments to improve my writing, presentation skills and scientific understanding. Also, I would like to thank to all my committee members for constructive criticism, invaluable discussion, and recommendations. I am grateful to all the Fischer lab members previously and present. They helped me both scientifically and personally. I especially want to thank my wife, Su Jung, who has been very supportive in my graduate school. Her love always cheers me up during all of the difficult times. Finally, I would like to thank to my entire family in Korea.

The role of *Drosophila auxilin* in Notch signaling

Publication No._____

Suk Ho Eun, Ph.D.

The University of Texas at Austin, 2007

Supervisor: Janice Ann Fischer

The goal of my graduate study is to understand the role of endocytosis for signaling receptor activation during development, especially ligand endocytosis for Notch activation. Notch is a transmembrane receptor which is conserved in metazoans. I am using the *Drosophila* model system. Notch is required in almost every developmental context and abnormality in Notch signaling components is related to many human diseases. Delta, one of the Notch ligands, is also a transmembrane protein. To activate Notch, endocytosis of Delta in the signaling cells is essential. However, the exact mechanism of how Delta endocytosis regulates Notch activation is not known. Liquid facets (Lqf) is an endocytic protein, called epsin in vertebrates, which is required only in the signaling cells for Delta endocytosis and Notch activation. Overexpression of Lqf in the eyes results in malformed eyes. Using this phenotype as a background, an EMS-mutagenesis screen was performed and *auxilin* mutants were isolated as enhancers of the eye phenotype. Auxilin is a J-domain protein involved in fission and uncoating of clathrin-coated vesicles. Mosaic clonal analysis showed that auxilin functions in Notch

activation and that auxilin is required only in the signaling cells. The *auxilin* mutant phenotype was suppressed by addition of a clathrin heavy chain transgene. This result suggests that the *auxilin* phenotype is at least partly caused by clathrin depletion and that auxilin generates a pool of free clathrin which is required for Delta endocytosis. Auxilin is a multi-domain protein. Two C-terminal domains, the clathrin-binding and the J domains, are sufficient to function as auxilin in *Drosophila*.

One of the popular models to explain why Delta endocytosis is required in the signaling cells is the 'recycling model' in which inactive Delta is endocytosed and recycled to the plasma membrane in active form. Rab11 is a small GTPase that regulates recycling. If the recycling model is correct, *rab11* mutants may show a phenotype similar to *auxilin*, *lqf* and *Delta* mutants. The *rab11* hypomorphs or expression of *rab11* dominant negative result in fewer photoreceptor cells and less Delta protein in the eye. These phenotypes are the opposite of typical mutant phenotypes of Notch components. The *rab11* mutant phenotype argues against the recycling model.

Table of Contents

List of Figures

Chapter 1. Introduction

1.1. Notch signaling

Cell to cell communication plays an important role in controlling cell fate decisions and patterning in virtually every developmental context. Notch signaling is one of the most commonly used pathways regulating formation and maintenance of various organs. Notch is a transmembrane receptor conserved in all metazoans. Notch is activated upon binding of transmembrane ligands of the DSL family, Delta and Serrate from *Drosophila* and Lag-2 from *C. elegans*. Notch activation requires a series of proteolytic cleavages of the receptor, resulting in release of the Notch Intra-Cellular Domain (NICD) and its translocation into the nucleus, where it activates Notch target genes. The requirement for proteolysis distinguishes Notch signaling from other pathways. First, the proteolytic process is irreversible, and therefore, the intensity and duration of signaling cannot be regulated by removing the activated receptor from the plasma membrane. Second, the signaling is direct and does not use a secondary messenger so that signal amplification is limited (Schweisguth, 2004). Because of these features, Notch signaling may require tight regulation by the signaling cells.

1.1.1. Roles of Notch in intercellular communication

One of the important roles of Notch signaling is to restrict the number of neural cells by lateral inhibition (Fig.1.1.A). During lateral inhibition, equivalent cells possessing neural potential compete with each other to become neural cells. Through a

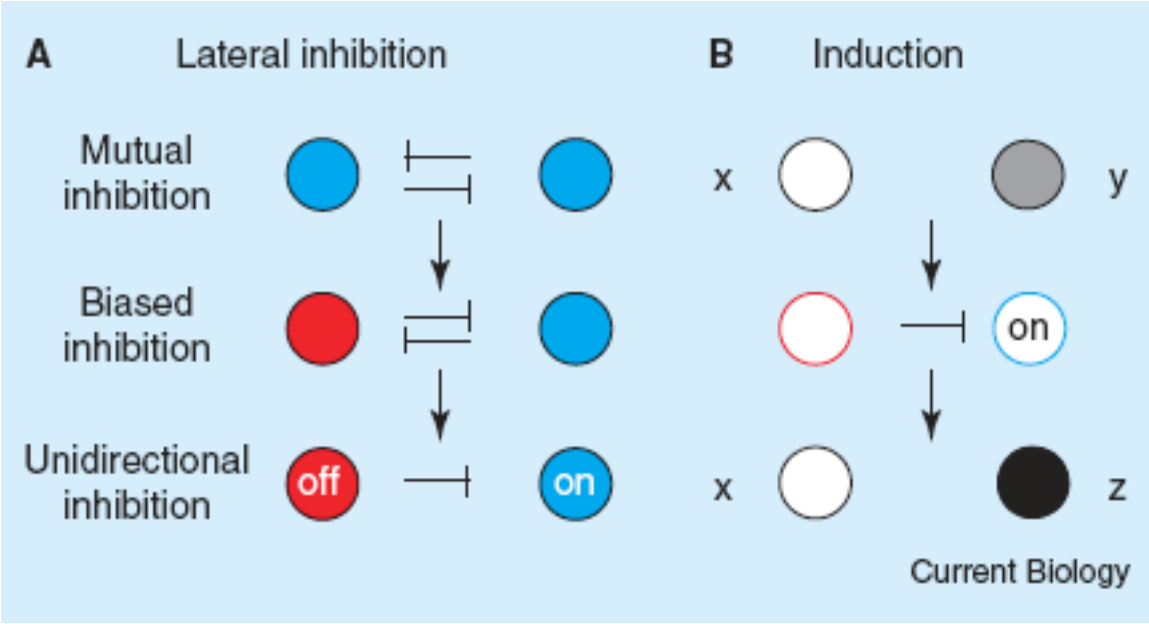

Figure 1.1. Notch signaling mediates both lateral inhibition and induction. (A) Lateral inhibition: Notch mediates reciprocal inhibitory signaling between cells that have similar developmental potential. Two cells are shown here for simplicity. Reciprocal signaling (top: mutual inhibition) is resolved over time into unidirectional signaling (bottom: unidirectional inhibition). The singling out of the signaling cell (red) results from a self-amplifying feed-back loop in which Notch inhibits the ability of the signal-receiving cell (blue) to produce inhibitory signaling. (B) Induction: Notch mediates unidirectional signaling between two cells, x and y, with distinct developmental potentials. The signal-sending cell (x, in red) activates Notch in the signal-receiving cell (y, in blue). In response to Notch activation, y becomes z. Figure and legend adapted form Schweisguth (2004).

variety of complex feedback mechanisms, one cell within a group becomes the signaler and thus the neural cell. Proneural clusters, special groups of cells containing neural

potential, are distinguished by expression of basic helix-loop-helix (bHLH) transcriptional activators known as proneural proteins. Notch signaling restricts the differentiation into neural cells by repression of the proneural genes (Parks et al., 1997). Therefore, many cases of Notch signaling failure result in neurogenic phenotypes. In *Drosophila*, repression of proneural genes is achieved by expression of *Enhancer of split* (*E(spl)*) complex genes. Activated Notch binds with CSL proteins (human CBF1, *Drosophila* Suppressor of Hairless (Su(H)), and *C. elegans* Lag-1) and activates transcription of *E(spl)* complex genes. Several repressor bHLH proteins in the E(spl) complex are expressed and these repressors probably bind directly to the regulatory region of proneural genes to block expression (Heizler et al., 1996).

There is also inductive Notch signaling between cells that are not equivalent (Fig. 1.1.B), for example at the *Drosophila* wing margin. Loss of Notch signaling at the wing margin (the dorsal/ventral boundary) results in elimination of the wing margin and a notched wing phenotype. Conversely, increased activation of Notch induces extra wing tissue (Lai, 2004). Notch signaling at the wing margin is mediated by *vestigial* expression. Vestigial is a co-activator of Notch target gene transcription that is important for wing development. In the wings, Notch is expressed in both dorsal and ventral sides. However, Notch in the dorsal side is modified by Fringe so that it is more sensitive to activation by Delta than by Serrate. Delta is expressed predominantly on the ventral side and signals to the dorsal side cells containing Fringe-modified Notch. Serrate is expressed predominantly in the dorsal side and signals to the ventral side cells containing unmodified Notch. Thus, Notch is activated in a narrow stripe of cells at the

dorsal/ventral midline and the result is that *vestigial* is expressed only there (de Celis and Bray, 1997; Fleming et al., 1997; Panin et al., 1997; Brukner et al., 2000).

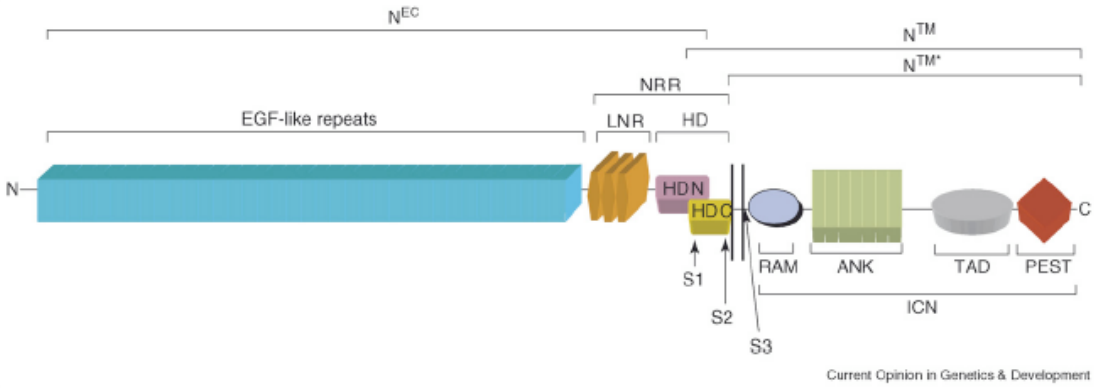

Figure 1.2. Notch receptor structure. A prototypic Notch receptor is shown. Cleavage at site S1 during receptor maturation generates two non-covalently associated subunits, NECD and NTM which are normally protected from premature activation by a negative regulatory region (NRR) composed of three LIN12–NOTCH repeats (LNRs), and the heterodimerization (HD) domain. Activation of Notch normally proceeds through ligand binding to the EGF-like repeats, which induces a cleavage at site S2 by ADAM-type metalloproteases. This is followed by an additional cleavage at site S3 by γ-secretase, which releases NICD. Abbreviations: ANK, seven iterated ankyrin-like repeats; PEST, degron sequence rich in the amino acids proline, glutamate, serine and threonine; RAM, RAM domain; TAD, transcriptional activation domain. Figure and legend adapted form Roy et al (2007).

1.1.2. Structure and modification of Notch

Notch is a single-pass transmembrane protein containing many functional domains (Fig. 1.2.). The extracellular domain of Notch homologs contains 10 to 36

epidermal growth factor-like repeats (ELRs) which bind to ELRs of its ligands (Fleming, 1998). ELRs are targets of glycosylation. Fucose is added to specific serine and threonine residues of ELRs by *O*-fucosyltransferase 1 (Meleony et al.,2000; Wang et al., 2001). This glycosylation of ELRs regulates interaction between Notch and its ligands. Down-regulation of fucosylation interferes with Notch-ligand interaction and an increase in fucosylation enhances the affinity of Notch for its ligands (Okajima et al., 2003). Fucose is further modified in the Golgi by the addition of *N*-acetylglucosamine. This process is catalyzed by Fringe, which binds to cysteine-containing repeats located in the Notch extracellular domain C-terminal to the ELRs (Bruckner et al., 2000; Ju at al., 2000). As mentioned above, Fringe modulates the specificity of Notch ligands. Fringe-modified Notch has higher affinity for Delta and unmodified Notch has higher affinity for Serrate (Panin et al., 1997; Bruckner et al., 2000). The ELRs are followed by three Lin12-Notch repeats (LNRs) which are found only in Notch homologs. LNRs are important for maintaining calcium-dependent association of Notch heterodimers before ligand binding (Rand et al., 2000). Also, two proteolytic cleavage sites (S1 and S2) are located on the extracellular domain. The intracellular domain also has a proteolytic cleavage site (S3) (see 1.1.3. below). After S3 cleavage, the NICD is released and translocated into the nucleus by two nuclear localization signals (Stifani et al., 1992). This NICD contains three important domains; the RBPjκ-associated molecule (RAM) domain, the six ankyrin repeats (ANKR) domain and the C-terminal PEST domain. Both the RAM and ANKR domains are important for the NICD to bind CSL for Notch target gene activation (Roehl et al., 1996). The RAM domain also binds specifically to Numb, a protein that antagonizes Notch function (Guo et al., 1996; Frise et al 1996). The ANKR domain is

important to bind to a positive regulator, Deltex (Diederich et al., 1994; Matsuno et al., 1995). The C-terminal PEST domain, which is enriched with proline, glutamate, serine and threonine, is involved in the negative regulation of Notch signaling. Phosphorylation of the PEST domain enhances degradation of the NICD through Sel-10 ubiquitin ligase in mammals and *C. elegans* (Hubbard et al., 1997; Oberg et al., 2001).

1.1.3. The proteolytic process for Notch activation

Notch (NICD) functions in the nucleus as a transcriptional factor. Release of the NICD is essential for it to move to the nucleus from the plasma membrane (Fig.1.3.). When the NICD is expressed in *Drosophila* and *C. elegans*, constitutive gain-of-function phenotypes are observed (Lieber et al., 1993: Roehl and Kimble, 1993, Struhl et al., 1993). Release of the NICD requires a series of proteolytic cleavages. The first cleavage (S1) occurs in the trans-Golgi network by a furin family protease before Notch reaches the plasma membrane (Logeat et al., 1998). This process is required for Notch activation in mammals (Logeat et al., 1998) but is not essential in *Drosophila* (Kidd and Lieber, 2002). These two cleaved Notch domains, Notch extracellular domain (NECD) and membrane-tethered domain (NTM), interact non-covalently in a calcium dependent manner (Rand et al 2000). The physical interaction between ELRs within the Notch extracellular domain and its ligand triggers extracellular cleavage (S2). A truncated Notch protein which does not contain the NECD has constitutive activity, like the NICD. This result suggests that S2 cleavage is the determining step and the following proteolytic cleavage is spontaneous (Fortini et al., 1993). S2 cleavage removes the ectodomain of Notch and generates Notch extracellular truncation (NEXT) fragment. The S2 cleavage is

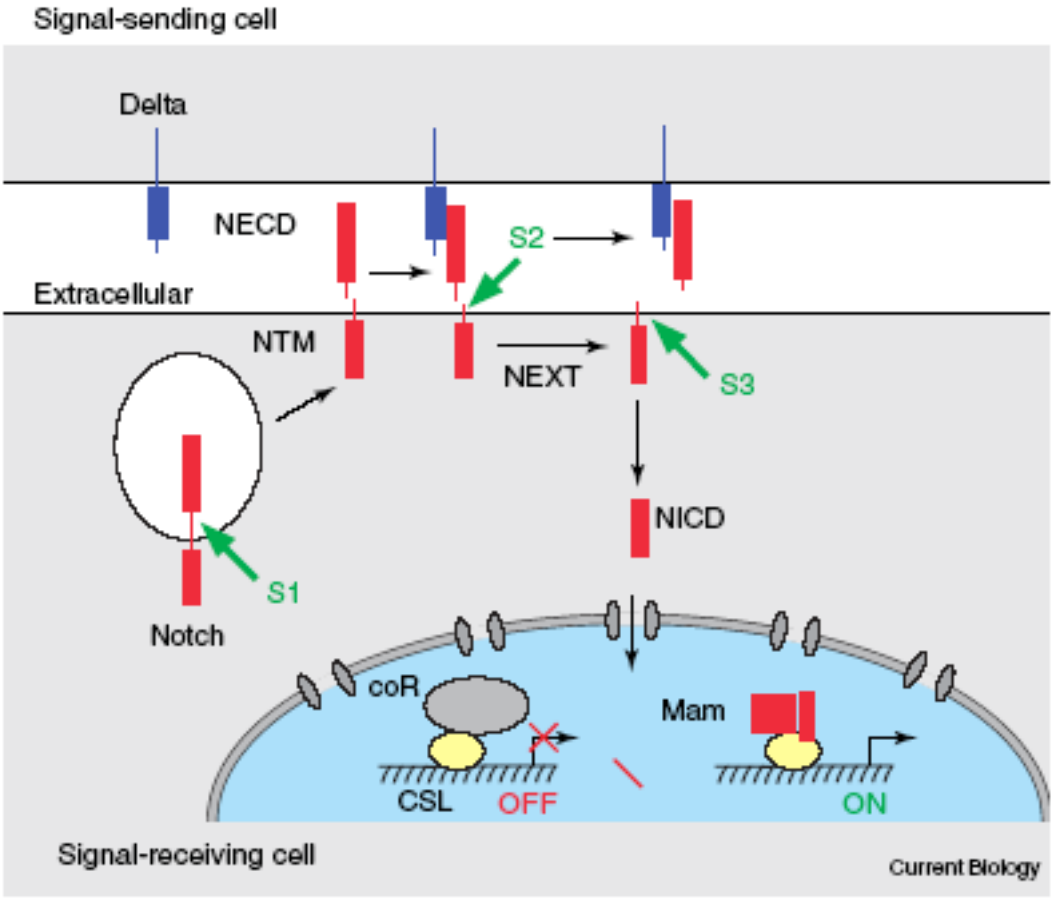

Figure 1.3. A model of CSL-dependent signaling. Delta at the surface of signaling cell (top) binds S1 processed Notch at the surface of the responding cell (bottom). Ligand dependent S2 cleavage of Notch generates NEXT, which is further processed at the S3 site. This releases NICD (which translocates into the nucleus) and NECD. NICD associates with CSL and Mam, thereby triggering a switch from repression, mediated by CSL-corepressor (coR) complexes, to activation. Figure and legend adapted form Schweisguth (2004).

performed by Kuzbanian, an ADAM family metalloprotease (Mumm et al., 2000; Lieber et al., 2002). Finally, NEXT is cleaved (S3) intracellularly by γ-secretase and generates

the active form of Notch, NICD (Scroeter et al., 1998). The NICD translocates into the nucleus and binds to the CSL complex already in the nucleus. The affected complex activates Notch target genes such as *Drosophila* (*E(spl)*). The CSL complex has dual function. Without the NICD, CSL functions as a repressor and after binding of the NICD functions as an activator of Notch target genes (Bray and Furriols, 2001). So far, the fate and function of the transmembrane remains of NEXT after S3 cleavage is not known.

1.1.4. The role of Notch signaling in *Drosophila* eye development

The *Drosophila* eye is composed of approximately 800 facets (ommatidia) and each facet contains 19 cells; 8 photoreceptor cells (R-cells), three classes of pigment cells and a bristle complex. The R-cells are divided by two classes; R1 through R6 are outer R-cells and R7 and R8 are inner R-cells. The rhabdomere size of outer R-cells is bigger than that of inner R-cells. R7 is positioned on top of R8. While outer R-cells express broad spectrum rhodopsin1, inner R-cells express other rhodopsins, for example rhodopsin3, 4, 5, or 6 which are involves in color vision and UV-detection. The adult eye develops from a monolayer of epithelial cells called the eye imaginal disc. The eye disc is formed from about 20 cells set aside during embryonic development. Until the 2nd larval instar, cells in the eye disc undergo mitosis without differentiation until there are 1300-1600 cells. During the 3rd larval instar, a wave of morphogenesis known as the morphogenetic furrow moves from the posterior to the anterior. Every two hours, a row of assembling evenly spaced ommatidia emerges posterior to the furrow and continues to mature as the furrow moves forward. About five rows posterior to the furrow, the undifferentiated cells

between developing ommatidia undergo a final round of mitosis. During pupation, the eye disc everts to expose the retinal epithelium (Wolff and Ready, 1993).

Notch signaling is required at nearly every stage of *Drosophila* eye development. When a temperature-sensitive allele of *Notch* is shifted to the restrictive temperature, in different rows of ommatidia (different stages of maturation), at successive time intervals, various phenotypes are produced from no eyes to overneuralization (Cagan and Ready, 1989). Notch signaling and EGF signaling function upstream of eye specific genes and antagonize each other in eye tissue development. Loss of Notch function in this very early stage transforms the eye to an antenna (Kumar and Moses, 2001a). R-cell differentiation initiates from the intersection of the dorsal/ventral midline and the posterior edge. In the 2nd larval instar, Fringe is expressed only on the ventral side of eye disc (Cho and Choi, 1998; Dominguez and de Celis, 1998). As discussed above (see 1.1.2.), Fringe is a glycosyltransferase that modifies Notch to increase the affinity between Notch and Delta by adding *N*-acetylglucosamine (Brukner et al., 2000). Determination of the dorsal/ventral boundary in the eye requires Notch inductive signaling similar to the wing (see 1.1.1.) In early eye discs, Delta is expressed only dorsally and Serrate is expressed only ventrally. The ventral expression of Fringe restricts Notch activation to the dorsal/ventral midline where Fringe-modified Notch meets dorsal Delta. The boundary of Fringe expression is essential for Notch activation and defines the dorsal/ventral midline. The absence of Fringe or its ubiquitous expression causes the loss of the eyes (Cho and Choi, 1998; Dominguez and de Celis, 1998). Cell specification starts with the initiation of the morphogenetic furrow and Notch is also required for the furrow initiation (Kumar and Moses, 2001b). At the furrow, R8 is the founder cell that

differentiates first in each ommatidium. R8 specification depends on expression of the proneural gene, *atonal*. Atonal is expressed uniformly ahead of the morphogenetic furrow and becomes restricted only to R8 in the furrow. During this transition, Atonal expression is retained in groups of about 12 cells called neural clusters. Notch activation is required to maintain Atonal expression at a high level, a phenotype called proneural enhancement (Baker et al., 1996; Baker, 2002 book). The absence of Notch or Delta function during proneural enhancement results in the absence of neural determination and thus no R-cells (Baker and Yu, 1997). Next, Notch is needed for lateral inhibition that restricts Atonal to R8. When Notch function is reduced at this stage, up to ten R8 cells appear in each proneural cluster (Baker and Zitron, 1995). After R8 cell specification within the furrow, R2 and R5 cells are specified followed by R3 and R4. R3 and R4 cells appear equivalent at first and later adopt asymmetric positions. Notch activation in R4 distinguishes it from R3. Loss of Notch in R3 and R4 results in two R3s and Notch activation in both cells results in two R4s (Fanto and Mlodzik, 1999; Cooper and Bray, 1999). R3 and R4 specification is followed by R1 and R6 specification. R7 is the last R-cell to be specified. In addition to activation of Sevenless by Boss on R8 and EGFR activation in R7, Notch signaling from R1 and R6 cells is required for R7 cell specification. The reduction of Notch activity in R7 precursors transforms them into R1 or R6, and activation of Notch in R1 and R6 transforms them into R7 or cone cells (Cooper and Bray, 2000). The four cone cells are recruited after all R-cells are specified. Notch and EGFR are activated in cone cells by signaling from R-cells. This signaling is essential for their cell fate (Flores et al., 2000). After their fate is determined, the cone cells also express Delta to specify primary

pigment cells. If cone cells are not specified, the primary pigment cells do not form (Cagan and Ready, 1989; Parks et al., 2000).

1.1.5. Notch in human development and disease

In the human genome, four Notch receptors (Notch 1-4) are identified with five ligands including Delta-like ligands (Dll-1, -3, and -4) and Serrate-like ligands (Jagged-1, and -2). Because Notch performs essential roles throughout human development for the formation and maintenance of tissues and organs, it is not surprising that deregulation of the Notch pathway is associated with many human diseases.

One well-known example of the relationship between aberrant activity of Notch and human disease is T-cell acute lymphoblastic leukaemia, a malignancy of thymocytes that preferentially affects children and adolescents. A chromosomal translocation [t(7;9)] causes deletion of most of the Notch extracellular domain, resulting in constitutive and ligand-independent Notch activity. Also, the translocation results in expression of truncated Notch under the control of the T-cell receptor-β locus. Although fewer than 1% of patients with this disease have the chromosomal translocation [t(7;9)] (Grabher et al., 2006), more than 50% of T-cell acute lymphoblastic leukaemia cell lines possess mutations in the *Notch 1* gene. These include missense mutations in the heterodimerization domain and short insertions or deletions in the C-terminal PEST domain (Weng et al., 2004).

In some instances, the Notch activation pathway shares common components with disease pathways. One example is Alzheimer's, a common neurodegenerative disease (AD). In AD, neurotoxic peptides, so-called amyloid-β (Aβ), accumulate as plaques.

Amyloid-β precursor protein is cleaved into Aβ by the membrane-bound proteases, β-secretase and γ-secretase (Iwatsubo, 2004). Presenilin is the catalytic component of the γ-secretase complex. In humans, mutations of two *Presenilin* genes, *PS1* and *PS2*, are often detected in early-onset familial Alzheimer's disease (Tanzi and Bertram, 2001). Presenilin mutations alter the cleavage pattern of Aβ and change it to a prolonged and more cytotoxic form (Wolfe and Haass, 2001; Selkoe, 2004). As mentioned above, the γ-secretase/Presenilin complex also functions in Notch activation. The NICD is released by the proteolytic activity of γ-secretase, and Presenilin is essential for Notch pathway signaling (Wolfe and Kopan, 2004).

Schizophrenia may also be related to Notch signaling in some cases. Schizophrenia is a a mental illness characterized by impairments in the perception of reality. Linkage disequilibrium mapping in 80 British parent-offspring trios showed that *Notch4* is a candidate site for Schizophrenia susceptibly (Wei and Hemmings, 2000).

In addition to the previous examples, defects in Notch signaling have been linked to a number of human diseases including Alagille syndrome, associated with mutation in *Jagged 1*, cerebral autosomal dominant arteriopathy with subcortical infarcts and leukoencephalopathy (CADASIL), associated with mutations in the ELRs of *Notch3*, and spondylocostal dysostosis, associated with mutations in *Dll-3* (Gridley, 2003; Harper et al., 2003; Lasky and Wu, 2005).

1.2. Endocytosis is required for Notch signaling

Endocytosis plays diverse roles in eukaryotes. By internalizing vesicles at the plasma membrane, endocytosis limits the levels of proteins and lipids on the plasma membrane accumulated from the secretory process. Also, uptake of essential nutrients and many extracellular signals such as neurotransmitters, growth factors and metabolic signals are controlled by endocytosis. Moreover, cell-to-cell signaling often depends on endocytosis. The most well-known example is attenuation of EGFR signaling by transferring EGFR to the lysosome for degradation following endocytosis. Endocytosis can be clathrin-dependent or clathrin-independent.

1.2.1. Clathrin-dependent endocytosis

Clathrin-dependent endocytosis (Fig. 1.4.) takes places continuously in eukaryotic cells to internalize essential nutrients for example, low-density lipoprotein (LDL) that binds to the LDL receptor and iron-loaded transferrin that binds to the transferrin receptor (Schmid, 1997; Brodsky et al., 2001; Conner and Schmid, 2003). Clathrin-dependent endocytosis starts at a clathrin-coated pit (CCP), an assembly of clathrin and a multisubunit adapter protein complex called AP2. CCPs assemble on a defined membrane area which is constrained by the actin cytoskeleton (Gaidarov et al., 1999). After invagination, CCPs are pinched-off and become clathin-coated vesicles (CCVs). The large GTPase, dynamin, plays an important role in the fission (pinching off) of CCVs. However, dynamin is not specific for clathrin-dependent endocytosis. Dynamin also functions in phagocytosis and clathrin-independent endocytosis (Hinshaw, 2000). The basic assembly unit of clathrin is the clathrin triskelion which is composed of three molecules of Clathrin heavy chain (Chc) and three molecules of Clathrin light chain

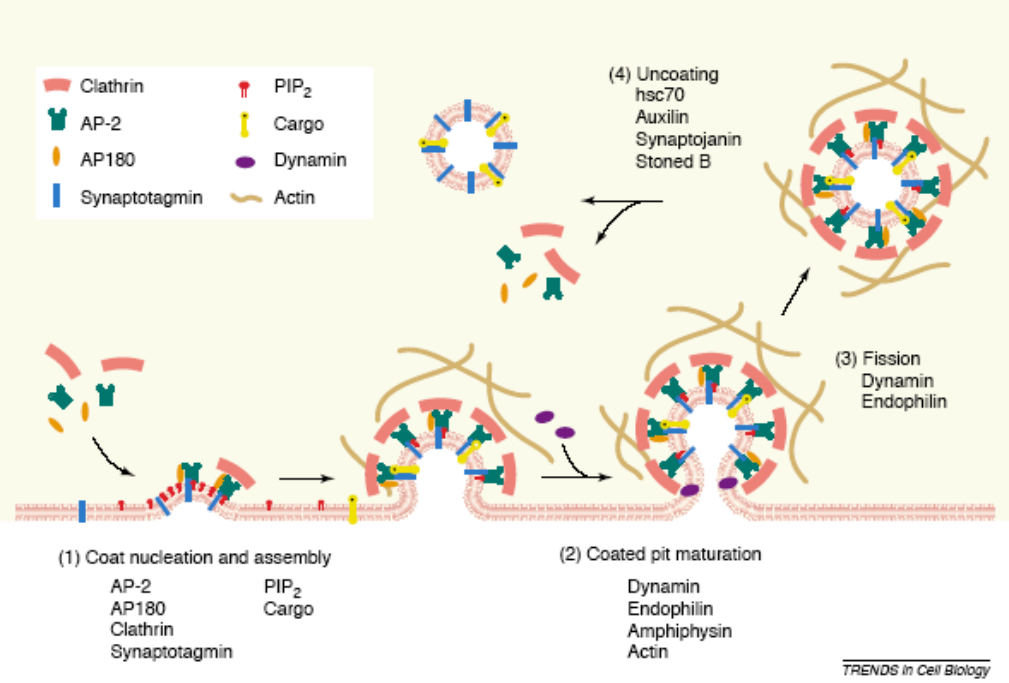

Figure 1.4. Overview of the steps involved in clathrin-mediated endocytosis. Shown are the sequential steps involved in clathrin-mediated endocytosis and several key components that function in each step. Figure and legend adapted form Takei and Haucke (2001).

(Clc). The hub region of the clathrin triskelion is composed of the C-termini of three molecules of Chc (Brodsky et al., 2001). In vitro, clathrin triskelions self-assemble spontaneously to form polygonal cages. However, in physiological conditions, cage formation requires adapter proteins such as AP2 (Conner and Schmid, 2003). AP2 is a protein complex composed of two large subunits, α-adaptin, and β2-adaptin, a medium subunit, μ2, and a small subunit σ2. The α-adaptin subunit is involved in targeting AP2

to the plasma membrane. The β2-adaptin subunit is important for the interaction with clathrin and is capable of inducing clathrin assembly. The μ2 subunit binds to internalization motifs of the cytoplasmic domain of cargo proteins and functions in cargo recognition. Phosphorylation of the μ2 subunit increases the affinity of AP2 for the internalization motifs. The σ2 subunit binds to α-adaptin probably to play a structural role (Conner and Schmid, 2003; Mousavi et al., 2004). AP180, a monomeric assembly protein, is expressed in neurons and functions in clathrin assembly and recycling of synaptic vesicles. AP180 cannot recognize cargo proteins but it has greater clathrin assembly activity than AP2 (McMahon, 1999). AP180 can interact with AP2. Probably, AP2 and AP180 have a synergistic effect on clathrin assembly (Hao et al., 1999). There are other accessory proteins, such as Eps15, epsin, endophilin and amphiphysin that interact with AP2 and clathrin, and function during clathrin-dependent endocytosis (Brodsky et al., 2001; Mousavi et al., 2004).

After CCVs bud off from the plasma membrane, vesicles must release clathrin coats prior to fusion with the proper endosomal structures. So far, four proteins (Hsc70, auxilin, synaptojanin and endophilin) have been found that function during uncoating. Auxilin binds to CCVs and recruits Hsc70, an ATPase that releases clathrin (Ungewickell et al., 1995). Synaptojanin is a polyphosphoinositide phosphatase that dephosphorylates at the 3, 4, and 5 positions of the inositol ring to decrease affinity of coat proteins assembled on CCVs (Cremona, et al., 1999). Endophilin has many functions in endocytosis. For the uncoating process, endophilin recruits synaptojanin to the CCVs (Gad et al., 2000; Verstreken et al., 2003).

1.2.2. Clathrin-independent endocytosis

Endocytosis also takes place in a clathrin-independent manner at lipid rafts where cholesterol, glycosphingolipids, sphingomyelin, phospholipids with long, unsaturated acyl chains, glycosylphosphatidylinositol (GPI)-linked proteins and some membrane-spanning proteins are enriched (Simons and Ikonen, 1997; Simons and Toomre, 2000; Nichols, 2003). The lipid rafts are membrane microdomains resistant to extraction of non-ionic detergents such as Triton X-100 because of a different lipid composition to surrounding area (Heerklotz, 2002; Edidin, 2003; Schuck et al., 2003). Cholesterol is thought to play an important role during lipid-raft endocytosis. The depletion of cholesterol blocks accumulation of proteins and lipids in lipid rafts (Simons and Ikonen, 1997) and blocks internalization of molecules that are known to be endocytosed in a clathrin-independent way (Nichols and Lippincott-Schwartz, 2001).

Caveolae are non-coated spherical invaginations of the plasma membrane (Stan, 2002), formed from lipid rafts by self-assembling of hairpin-like integral membrane proteins, caveolins (Parton, 1996). Expression of caveolins is sufficient to promote formation of caveolae in cells lacking such structures (Fra et al., 1995). Although caveolins are the major components in caveolae, the mechanism by which caveolins regulate clathrin-independent endocytosis is not understood. Surprisingly, mice that have null mutations in *caveolin 1*, are viable, although their cells lack obvious caveolae (Drab et al., 2001; Razani et al., 2001). Several experiments suggest that caveolin 1 negatively regulates caveolar budding. Overexpression of caveolin 1 inhibits clathrin-independent endocytosis (Minshall et al., 2000; Le and Nabi, 2003) while decreased expression of caveolin 1 increases clathrin-independent endocytosis (Le et al., 2002). Also, the

majority of caveolin 1 is immobile on the plasma membrane and only a minority of caveolin 1-positive vesicles are internalized (Pelkmans et al., 2001; Thomsen et al., 2002). Clathrin-independent endocytosis of cholera toxin and interleukin-2 receptors is not defective in cells naturally lacking caveolin1 and caveolar structures (Orlandi and Fishman, 1998; Lamaze et al., 2001). In *Drosophila*, there are no caveolin homologs (Razzaq et al., 2001) so clathrin-independent endocytosis must work without caveolin if there is clathrin-independent endocytosis in flies.

Some proteins internalized by a clathrin-independent pathway are delivered to caveosomes, endosome structures containing caveolin-1 (Pelkmans et al., 2001). Caveosomes are assumed to be distinct from other endosomes because endosomes containing caveolin 1 do not colocalize with typical early and recycling endosomal markers (Nichols, 2002). Trafficking of SV40 form the plasma membrane to the ER and trafficking of GPI-anchored protein undergo through caveosomes (Pelkmans et al., 2001, Nichols, 2002).

1.2.3. Ubiquitin in endocytosis

Ubiquitin is a 76 amino acid peptide which can become attached covalently to internal lysine residues of target proteins via an isopeptide bond. Ubiquitin conjugation occurs through three enzyme activities; a ubiquitin-activating enzyme (E1), a ubiquitin-conjugating enzyme (E2), and a ubiquitin ligase (E3). The E1 activates ubiquitin and forms a thiolester linkage between E1 and ubiquitin. The activated ubiquitin is transferred to the E2 by transthioesterification. The E3 recognizes substrates and transfers ubiquitin from the E2 to substrates. There are two types of E3 ligases. RING domain E3s can

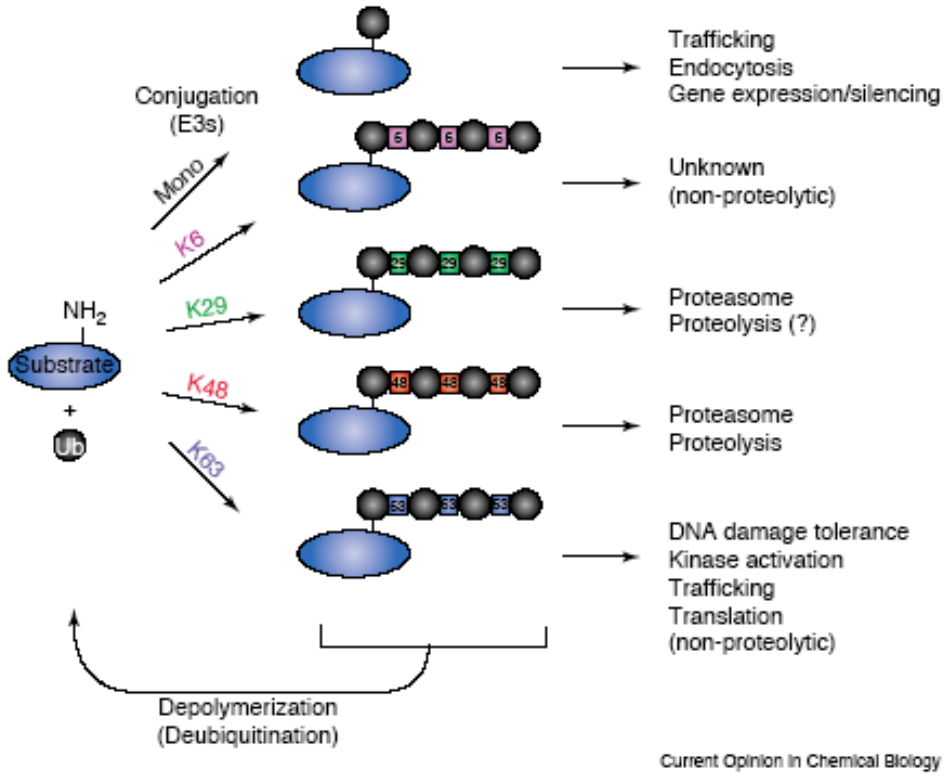

Figure 1.5. Influence of signal structure on the consequences of ubiquitination. The differently colored squares denote linkage of the corresponding ubiquitin chains through different ubiquitin lysine residues, as defined in the left-hand set of arrows. Figure and legend adapted form Pickart and Fushman (2004).

transfer ubiquitin directly from the E2 and HECT domain E3s use a covalent E3-ubiquitin intermediate. There are different types of ubiquitination. Monoubiquitination is attachment of a single ubiquitin. Polyubiquitination is attachment of a ubiquitin chain which can be through linkages that use K48, K63, K6 and K29 of ubiquitin, or possibly other linkages as well (Fig. 1.5.). Usually, K48-linked ubiquitin chains target proteins for degradation by the 26S proteasome (Aguilar and Wendland, 2003; Pickart and Fushman,

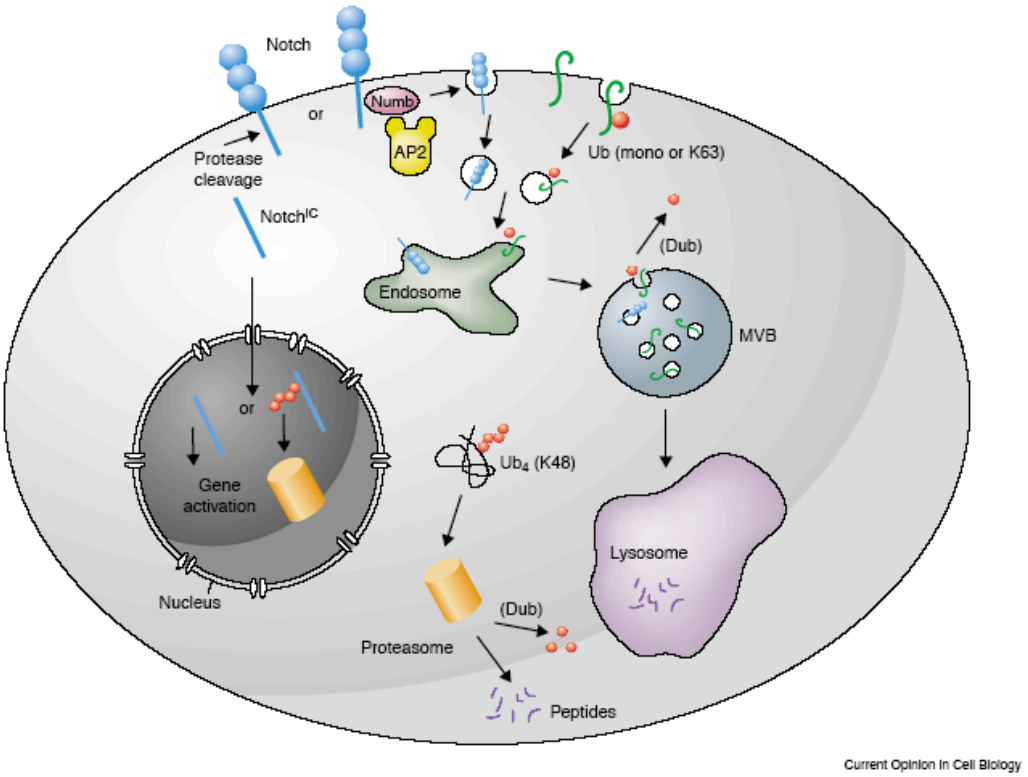

Figure 1.6. overview of some of the cellular compartments where ubiquitin functions. The proteasome (orange barrel) degrades cytosolic or nuclear proteins containing a chain of four ubiquitin molecules joined by K48 linkages. The transmembrane receptor Notch has several modes of regulation: one in which Notch internalization is promoted by association with Numb and AP2, and another involving proteolytic cleavage of NICD, followed by transport of NICD to the nucleus, where it either activates transcription or is degraded. Finally, transmembrane proteins at the plasma membrane (green) can use ubiquitin (red) as a signal for inclusion in endocytic vesicles. Moreover, a ubiquitin signal can direct sorting of transmembrane proteins into the lumenal vesicles of the MVB. Deubiquitination enzymes (Dubs) remove covalently attached ubiquitin to allow its reuse. Figure and legend adapted form Aguilar and Wendland (2003).

2004), whereas monoubiquitination serves as an internalization signal or controls protein

activity (Fig. 1.6.) (Hicke, 2001; Hicke and Dunn, 2003). Other polyubiquitin chains are poorly understood. Ubiquitin can regulate internalization in two ways. First, ubiquitination of a transmembrane protein can be an internalization signal. Second ubiquitination of endocytic proteins can control their activity (Aguilar and Wendland, 2003; Hicke and Dunn, 2003). The early evidence of ubiquitination as an internalization signal came from yeast. Ligand binding to a G protein-coupled plasma membrane receptor induces ubiquitination and endocytosis. Finally, endocytosed protein is transferred to the lysosome for degradation (Hicke and Riezman, 1996). For this endocytosis event, monoubiquitination is sufficient to function as an internalization signal (Terrell et al., 1998). Also, in mammalian cells, monoubiquitination at multiple sites is sufficient for the endocytosis and degradation of receptor tyrosine kinases (Haglund et al., 2003). However, recent papers suggest that polyubiquitin is perfered to monoubiquitin as an internalization signal in mammalian cultured cells (Barriere st al., 2006; Hawryluk et al., 2006). Particular E3 ubiquitin ligases, such as the Nedd4 and Cbl families, ubiquitinate transmembrane proteins (Dupre et al., 2004).

The internalization of ubiquitinated cargo proteins may be mediated by endocytic proteins containing ubiquitin-interacting motifs (UIMs) such as eps15 and epsin (Dupre et al., 2004). Eps15 is also monoubiquitinated. UIMs may play dual roles in recognizing transmembrane proteins and also in regulation of the endocytic protein itself. UIMs are essential for Eps15 ubiquitination but they are not the sites for the ubiquitination (Polo et al., 2002; Klapisz et al., 2002). One interpretation is that UIMs mediate interaction between an E3 ligase and eps15. Blocking eps15 ubiquitination does not affect the targeting or internalization of cargo proteins (Klapisz et al., 2002). Ubiquitination of

eps15 may regulate its function, possibly in a process other than endocytosis. After internalization, ubiquitinated cargo proteins are also transported by UIM-containing proteins such as Hrs (Bilodeau et al., 2002; Raiborg et al., 2002) which is also ubiquitinated (Polo et al., 2002; Katz et al., 22002; Urbe et al., 2003)). The role of Hrs ubiquitination is not known, either. Epsin is also a target of ubiquitination. Details about ubiquitination of epsin will be discussed later (see 1.3.2.).

1.2.4. Notch signaling and endocytosis

A requirement for endocytosis during Notch signaling was first shown with *shibire* temperature-sensitive mutants. Shibire is the *Drosophila* homolog of mammalian dynamin (Poodry, 1990). Analysis of *shibire* mutant clones suggestes that endocytosis is required both in the signaling cells and in the receiving cells (Seugnet et al., 1997).

1.2.4.1. Endocytosis in the signaling cells

A decade ago, it was shown that dynamin in the signaling cells is essential for Notch activation in the receiving cells (Seugnet et al., 1997). It has been shown that internalization of Notch ligands by the signaling cells is necessary (Parks et al., 2000; Pavlopoulos et al., 2001; Le Borgne and Schweisguth, 2003; Overstreet et al., 2004; Wang and Struhl, 2004). We still do not understand how Delta endocytosis regulates Notch activation (Fig. 1.7.). The Notch S2 cleavage depends on binding of its ligands. Parks et al (2000) showed that NECD is trans-endocytosed into the Delta expressing cells. They suggested that trans-endocytosis of Notch is important to expose the S2 cleavage site, and thus for Notch activation. Recently, it has been shown that release and

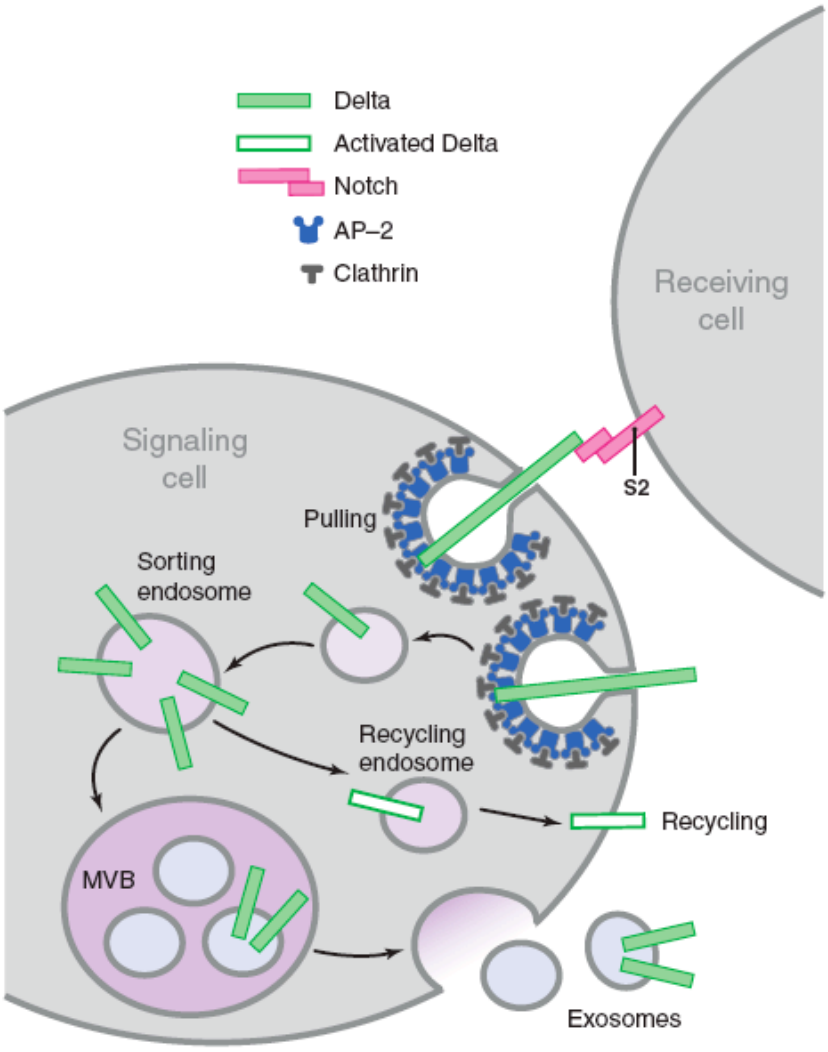

Figure 1.7. Models for why Delta endocytosis by the signaling cells is required for signaling. Delta internalization by the signaling cell may facilitate S2 cleavage (pulling). Alternatively, Delta endocytosis may enable the activation of Delta in an endosome as well as its return to the plasma membrane in active form (recycling). In a similar model, Delta internalization allows formation of Delta-containing exosomes. Figure and legend adapted from Fischer et al (2006). Reprinted, with permission, from the Annual Review of Cell and Development Biology, Volume 22 (c)2006 by Annual Reviews www.annualreviews.org

trans-endocytosis of NECD does not require S2 cleavage. In addition, endocytosis of

ligands may physically dissociate Notch heterodimers before S2 cleavage. Defects in ligand endocytosis reduce both trans-endocytosis of NECD and Notch activation in the receiving cells, probably by reducing Notch heterodimer dissociation (Nichols et al., 2007). These data suggest a model where endocytosis provides a mechanical force to physically dissociate the Notch heterodimer, which is essential for Notch activation. However, this model is at odds with the observation that S1 cleavage is not required for Notch activation in *Drosophila* (Kidd and Lieber, 2002) even though S1 cleavage takes place in *Drosophila*.

Another popular model is that ligand endocytosis is required to generate active ligands. There are several endocytic proteins that function in the signaling cells. Two E3 ubiquitin ligases, Neuralized (Neur) and Mind bomb (Mib), are key regulators of ligand endocytosis that function complementarily in different developmental contexts. Monoubiquitination of DSL ligands by Neur or Mib is thought to serve as an internalization signal by allowing binding to adapter proteins that contains UIMs (Wang and Struhl, 2005; Lai et al., 2005; Le Borgne et al., 2005; Itoh et al., 2003; Pitsouli and Delidakis, 2005). Liquid facets (Lqf), the *Drosophila* homolog of mammalian endocytic epsin, functions only in the signaling cells and controls endocytosis of DSL ligands (Overstreet et al., 2004; Wang and Struhl, 2004). Neur, Mib and Lqf are essential only in a small subset of ligand endocytosis events that are required for Notch activation. A large amount of Delta endocytosis occurs in the mutants of *neur*, *mib* and *lqf*. As these mutant cells do not signal, Delta endocytosis in these mutants, referred to as 'bulk endocytosis,' is not related to Notch activation (Wang and Struhl, 2004; Wang and Struhl, 2005). When the intracellular domain of Delta is replaced by the intracellular domain of the LDL

receptor, this chimeric protein overcomes the requirement for Lqf. Upon binding of LDL, internalized LDL receptor is brought back to the plasma membrane after dissociation of its ligand. This result leads to a model where Lqf-dependent ligand endocytosis routes ligand to special endosomes where ligand is processed into active form and recycled back to the plasma membrane (Le Borgne and Schweisguth, 2003; Wang and Struhl, 2004). Several subsequent experiments support the recycling model (Emery et al., 2005; Jafar-Nejad et al., 2005). Still, it is not clear how Delta endocytosis regulates Notch activation and several issues need to be resolved: Is there an active processed form of Delta? What is its structure? Is ubiquitination of Delta by Neur and Mib mono- or poly-ubiquitination? Does Lqf bind Delta? Is ubiquitination prerequisite for Lqf binding to Delta? Is recycling of Delta Rab11-dependent?

Lipid rafts may be functional during DSL endocytosis. In *C. elegans*, *bre-3*, *bre-4* and *bre-5* were isolated from a suppressor screen using an egg-laying defect phenotype associated with elevated Notch activity. These genes are involved in the synthesis of glycosphingolipids, components of lipid rafts. Genetic analysis showed that Bre-5 is required for Notch activation in a non-cell-autonomous manner and is functions prior to the S2 cleavage (Katic et al., 2005).

1.2.4.2. Endocytosis in the receiving cells

When there is no dynamin in the receiving cells, Notch activation fails. At the border of mosaic clones where mutant cells containing a hypermorphic, ligand-dependent *Notch* allele are adjacent to wild-type cells, signaling is always from wild-type cells to mutant cells. In other words, Notch is always activated in the mutant cells. However,

when the hypermorpic *Notch* cells are also *dynamin* mutants, Notch is not activated in the mutant cells. Expression of various constitutively active forms of Notch including membrane-bound constitutively active Notch overcomes the requirement for dynamin. These results suggest that Notch endocytosis is required for Notch downstream gene activation (Seugnet et al., 1997). However, it is not known exactly why Notch endocytosis is required for Notch activation. Several endocytic proteins control Notch activation in the receiving cells. Numb is a membrane-associated protein that negatively regulates Notch (Frise et al., 1996; Guo et al., 1996). Numb interacts with Itch, an E3 ligase, to promote ubiquitination and proteasome-dependent degradation of Notch before Notch activation (McGill and McGlade, 2003). Numb also functions as an endocytic protein. Numb interacts with α-adaptin, a subunit of AP2, and eps15 (Santolini et al., 2000; Berdnik et al., 2002). Additionally, Numb binds to Sanpodo, a four-pass membrane protein localized on the plasma membrane. Membrane-localized Sanpodo interacts with Notch for activation. Numb inhibits membrane localization of Sanpodo by inducing endocytosis of Sanpodo to prevent interaction between Sanpodo and Notch (O'Connor-Gilesa and Skeath, 2003; Skeath and Doe, 1998; Hutterer and Knoblich, 2005). In summary, Numb negatively regulates Notch by removing it from the plasma membrane where it is activated and by blocking interaction with a positive regulator, Sanpodo.

Two other E3 ubiquitin ligases, Suppressor of deltex (Su(dx)) and Nedd4, down-regulate Notch. Nedd4 ubiquitinates Notch and is involved in constitutive Notch endocytosis which targets Notch for lysosomal degradation (Sakata et al., 2004). Blocking of Nedd4 function activates Notch target genes in a ligand-independent manner and this effect is enhanced by expression of Deltex (see below). Therefore, Nedd4

antagonizes Deltex function for ligand-independent Notch activation (Sakata et al., 2004). Su(dx) regulates Notch endosomal sorting from early endosomes to late endosomes to block recycling to the plasma membrane. However, it is not clear whether Su(dx) ubiquitinates Notch (Wilkin et al., 2004).

Ubiquitination of Notch does not always result in down-regulation of Notch signaling. Deltex, another E3 ligase, functions as a downstream positive regulator. Deltex is required in canonical Su(H)-dependent Notch signaling. Also, Deltex can activate Notch in a ligand- and Su(H)-independent manner (Hori et al., 2004). Deltex lacking its RING-finger domain, which is essential for ubiquitination, acts as a dominant negative to inhibit Notch signaling (Matsuno et al., 2002). Deltex induces accumulation of Notch in the late endosomes, which is not transferred to lysosomes. Thus, it is suggested that Deltex protects Notch from lysosomal degradation. Overexpression of a dominant negative form of Rab5 blocks Notch delivery to the late endosomes and inhibits Deltex-mediated Notch activation. This result suggests that Notch accumulation in late endosomes is important for ligand- and Su(H)-independent Notch activation. However, the mechanism by which endosomal Notch functions is not understood (Hori et al., 2004). Deltex activity is also regulated by ubiquitination. Itch polyubiquitinates Deltex for degradation (Chastagner et al, 2006).

1.3. Fat facets and Liquid facets

1.3.1. Fat facets

Fat facets (Faf) is important to restrict the number of outer R-cells in ommatidia during *Drosophila* eye development (Fischer-Vize et al., 1992). Eyes of *faf* null mutants have extra R-cells. *faf* encodes a deubiquitination enzyme, which removes ubiquitin from particular ubiquitinated substrates (Huang et al., 1995). Lqf is the critical substrate of Faf in the eye. In the eye, the overneuralized phenotype of *faf* is suppressed by Lqf overexpression. Probably, Faf regulates the level of Lqf by removing a polyubiquitin chain that targets Lqf for proteosomal degradation (Cadavid et al., 2000; Chen et al., 2002). As evidence of this idea, the level of Lqf in *faf* null flies is less than half of that in wild-type flies. Also, a ladder of higher molecular weight forms of Lqf is detected in *faf* mutant protein extracts in a Western blot experiments using α-Lqf antibody. This ladder pattern of bands is typically observed from polyubiquitinated proteins (Chen et al., 2002). Extra R-cells are the only phenotype detected in the eyes. This phenotype is generally caused by failure of Notch signaling during R-cell restriction in R2/5 and R3/4 cells. Expression of Lqf in these cells is sufficient to complement the *faf* null phenotype. This result indicates that Faf function is essential only for R-cell restriction. Why is Faf required only during R-cell restriction? A *faf-lacZ* translational fusion experiment showed that Faf is expressed ubiquitously in eye discs except in the morphogenetic furrow (Fischer-Vize et al., 1992). One plausible explanation is that R-cell restriction is the most sensitive among Notch signaling events in the eye. This idea is consistent with the observation that weak mutant alleles of Notch signaling components show a similar extra R-cell phenotype.

1.3.2. The structure of Liquid facets and endocytosis

Lqf is the *Drosophila* homolog of mammalian epsin, a multi-modular protein (Fig. 1.8.). The epsin N-terminal homology (ENTH) domain is the most highly conserved region among epsin homologs. The ENTH domain is targeted to the plasma membrane by binding membrane lipid phosphatidylinositol-4,5-bisphosphate (PI-(4,5)P_2) (Itoh et al., 2001). ENTH domain binding to PI-(4,5)P_2 induces the formation of an amphipathic α-helix at the N-terminus of Lqf. This α-helix induces membrane curvature (Ford et al., 2002). In yeast, there are two *epsin* homologous genes, *ent1* and *ent2*. Yeast with a deletion of either one of these genes is viable and grows normally but deletion of both genes is lethal. Expression of at least one intact ENTH domain of either gene is sufficient for viability whereas the C-terminal regions are dispensable. Therefore, in yeast, the

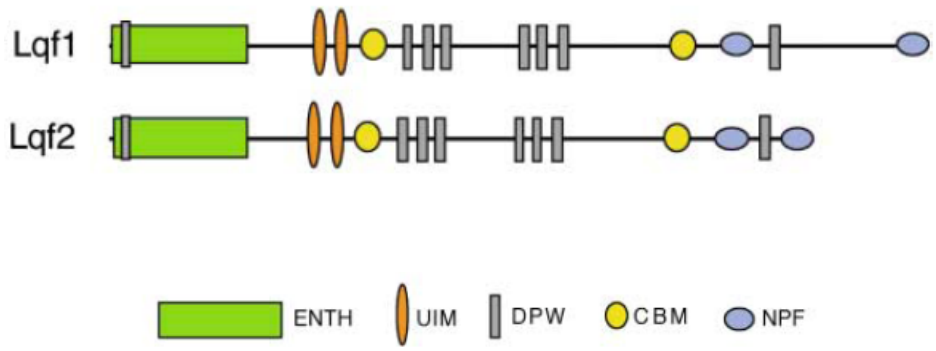

Figure 1.8. Modular Structure of Lqf. The *lqf* gene encodes two different proteins by alternate mRNA splicing. Figure and legend adapted from Overstreet et al (2004).

ENTH domain is sufficient for the essential function of epsin (Wendland et al., 1999). Interestingly, in *Drosophila*, both the ENTH domain alone and ENTHless Lqf retain a significant amount of activity. Probably, the ENTH domain and the remains of Lqf are redundant with other proteins (Overstreet et al., 2003). After the ENTH domain, two UIMs, which provide sites for ubiquitin binding, are present. As mentioned above (1.2.3.) UIM-containing proteins are often themselves ubiquitinated in a UIM-dependent manner (Klapisz et al., 2002). Oldham et al (2002) showed that epsin is monoubiquitinated and that the monoubiquitination is not related to protein degradation. Also, the UIMs are essential for ubiquitination but are not the target sites for ubiquitination. These data are in conflict with the ladder of ubiquitinated Lqf bands observed in *faf* mutants and the idea that Faf regulates the level of Lqf to prevent its degradation (Chen et al., 2002). It is possible that epsin is regulated differently in flies and vertebrates. Further experiments in both systems are needed to resolve this issue. It is also possible that epsin is recruited to the monoubiquitinated cargo via UIMs. The C-terminal part of Lqf contains several other conserved motifs that bind other endocytic proteins such as clathrin-binding motifs (CBMs), DPW motifs which bind to AP2, and NPF motifs which may bind eps15 or other EH-domain proteins. In mammalian cells, epsin binds to the α-adaptin subunit of AP2 (Chen et al., 1998). However, the *lqf* loss-of-function phenotype caused by defects in Delta endocytosis is not enhanced significantly by *α-Adaptin* mutations (Cadavid et al., 2000). Whether interaction between Lqf and AP2 is necessary for Delta internalization is not clear.

1.3.3. Liquid facets and Notch signaling

Lqf was identified as the substrate of Faf in the eye (Fischer et al. 1997; Cadavid et al., 2000). Lqf is required for viability, in all three Notch signaling events near the morphogenetic furrow (proneural enhancement, lateral inhibition and R-cell restriction) (Fig. 1.9.), and also for wing and leg development (Cadavid et al., 2000; Overstreet et al., 2004; Wang and Struhl, 2004). The null alleles of *lqf* are homozygous lethal and

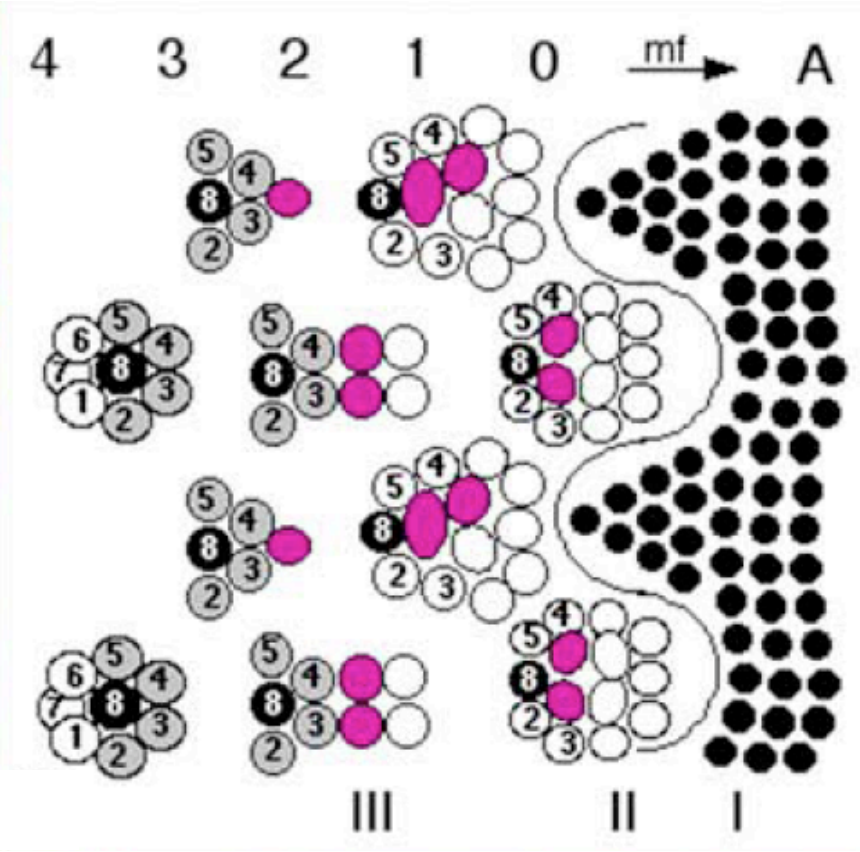

Figure 1.9. Diagram of the three defined Notch/Delta signaling events near the morphogenetic furrow. I is proneural enhancement, II is lateral inhibition, and III is R-cell restriction. The numbers at top indicate rows of developing ommatidia. The pink cells become ectopic R-cells when R-cell restriction fails in *aux* hypomorphs. mf=morphogenetic furrow, moving in the direction of the arrow; A=anterior; P=posterior.

homozygous flies of a weak allele of *lqf* have a very similar eye phenotype to *faf* null mutants. Hypomorphic mutants of *lqf* have wing and leg defects as well as eye defects (Cadavid et al., 2000). These observations suggest that Lqf is required in general for Notch signaling. Lqf is essential for Delta internalization that is associated with signaling (Overstreet et al., 2003; Overstreet et al., 2004; Wang and Struhl, 2004). Consistent with the requirement for Delta endocytosis, Lqf functions only in the signaling cells but not in the receiving cells (Overstreet et al., 2004; Wang and Struhl, 2004). However, only a small subset of Delta endocytosis is Lqf-dependent. In *lqf* null wing clones, the number of vesicles containing Delta is not different from that in the wild-type side. Therefore, Lqf is required only for Delta endocytosis for Notch activation and most endocytosed Delta (at least the Delta positive vesicles that are not sent to the lysosome right away) is not related to Notch activation (Wang and Struhl, 2004). Replacements of the Delta cytosolic domain with random 50 amino acids containing two lysine residues, possible targets for ubiquitination, or with a single ubiquitin, allow these chimeric proteins to be internalized in a Lqf-dependent manner. Further mutation of the two Lysine residues of the 50 amino acids to block ubiquitination withdraws the ability for internalization. These results suggest that mono-ubiquitination is sufficient to serve as a signal for Delta internalization by Lqf (Wang and Struhl, 2004).

1.3.4. Function of Liquid facets in endocytosis

Epsin contains CBMs and has been suggested to function during clathrin-dependent endocytosis (Chen et al., 1998; Morinaka et al., 1999). In HeLa cells, with a low dose of EGF, EGFR is internalized in a clathrin-dependent way without

ubiquitination of EGFR. However, with a high dose of EGF, EGFR is ubiquitinated and internalized in a clathrin-independent way. Epsin is required for EGFR endocytosis only when EGFR is ubiquitinated and endocytosed in clathrin-independent way (Sigismund et al., 2005). To investigate the interactions among ubiquitin, clathrin and epsin during endocytosis, Chen and Di Camilli (2005) analyzed the location of monoubiquitinated GFP targeted to the membrane protein in HeLa cells. Endocytosis of this chimeric protein is not defective when clathrin is depleted and only a small amount of wild-type epsin colocalizes with the chimeric protein. However, epsin lacking clathrin-binding and AP2 binding motifs colocalizes more intensively with the ubiquitin chimera. These results suggest that epsin recognizes ubiquitinated plasma membrane proteins to regulate clathrin-independent endocytosis and that clathrin antagonizes epsin function. The fact that the E3 ligases, Neur and Mib, are essential for Delta endocytosis suggests that ubiquitination is the normal signal for Delta endocytosis. Lqf is essential for Delta endocytosis. These observations lead to a model where Lqf binds to ubiquitinated Delta and induces clathrin independent endocytosis. However, this model conflicts with the genetic interaction between *lqf* and *chc*. A null mutant of *chc* dominantly enhances the *lqf* (and *faf*) phenotypes (Cadavid et al., 2000). Recently, it has been shown that in cultured mammalian cells, polyubiquitin serves as an interanlization signal and that epsin binds to the polyubiquitinated membrane proteins and associates with AP-2 and clathrin, components of clathrin-dependent endocytosis. Also, colocalization between epsin and AP-2 and clathrin is not alterend by the different concentration of EGF. Thses results suggest that epsin functions in clathrin-dependent endocytosis of ubiquitinatied cargo proteins (Barriere st al., 2006; Hawryluk et al., 2006). In this thesis, analysis of *auxilin*

mutants strongly supports the idea that in Notch signaling, epsin function depends on clathrin although not necessarily for CCV formation. Delta endocytosis may depend on clathrin directly or indirectly. For example, clathrin may regulate epsin, which mediates vesicle formation without clathrin.

1.4. Auxilin

1.4.1. Auxilin functions during clathrin-dependent endocytosis

Clathrin is used to transfer selected proteins from the cell surface or Golgi to endosomes. After clathrin-coated vesicles (CCVs) are pinched off from the membrane, they must be uncoated to allow fusion to the proper endosomal compartments. Also, for the subsequent round of clathrin-dependent endocytosis, a pool of free clathrin should be regenerated by uncoating of CCVs. Uncoating requires ATPase activity and the 'uncoating ATPase' was identified as Hsc70 (Heat shock cognate 70) (Chappell at al., 1986). Hsc70 is a constitutively expressed member of the heat shock protein family. Hsc70 has functions in many processes including folding of newly synthesized proteins, translocation of proteins, assembly of multi-subunit protein complex, stabilization of proteins under stress, and antigen presentation (Bukau and Horwich, 1998; Mayer and Bukau, 1998). Hsc70 requires J domain proteins as adapters to bind specific proteins. For CCV uncoating, Hsc70 binds the J domain protein, auxilin. Auxilin functions catalytically: it binds clathrin cages, and then transfers the clathrin to Hsc70, and

stimulates Hsc70 ATPase activity (Ungewickell et al., 1995). Auxilin, Hsc70 and ATP are sufficient for uncoating in vitro. Clc is not a target of uncoating (Ungewickell et al., 1995). The structure of the auxilin binding location on CCVs was determined to 12 Å resolution. Three auxilin molecules bind each clathrin triskelion. Auxilin binds the clathrin lattice where N-terminal ankle segments are crossed (Fig. 1.10.). Binding of

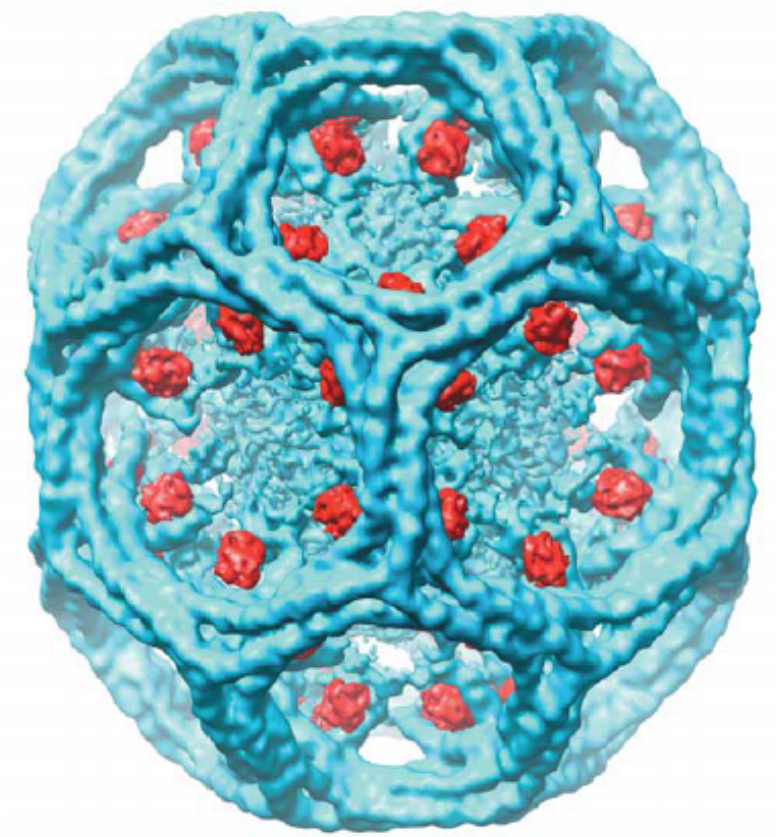

Figure 1.10. Three-dimensional image reconstruction of a clathrin D6 barrel (the hub assembly) with bound auxilin at 12 Å resolution. The auxilin fragment is rendered in red, whereas the rest of the structure is blue. Figure and legend adapted from Fotin et al (2004).

auxilin changes Chc contacts to generate a global distortion (FIG. 1.11.) (Fotin et al., 2004). Hsc70 binds two sites on clathrin-coated vesicles. The major interaction site is the sides of spurs near the hub regions and another interaction site is the N-terminal ankle region probably via auxilin (Heymann et al., 2004). Mammalian auxilin is brain-specific and there is another auxilin variant, cyclin-G associated kinase (GAK), also known as auxilin 2, which is expressed ubiquitously. Although GAK associates directly with cyclin-G, the significance of this interaction is not understood (Kanaoka et al., 1997). GAK also functions in uncoating in non-neural cells (Umeda et al., 2000; Greener et al., 2000; Zhang et al., 2005).

Auxilin functions also with dynamin. GTP-bound dynamin binds to both Hsc70 and auxilin directly and independently. The interaction between auxilin and dynamin is not dependent on the J domain of auxilin. Auxilin has two dynamin binding sites. When these sites are overexpressed, endocytosis is inhibited neither due to failure of uncoating nor due to altered clathrin distribution. From the interaction between auxilin and dynamin, a role for auxilin at the fission step has been suggested (Newmyer et al., 2003). However, auxilin may not be directly required at the fission itself. When auxilin is depleted in cultured cells, vesicle constriction is decreased but fission itself is not affected (Sever et al., 2005). Auxilin inhibits the GTPase activity of dynamin. Dynamin forms dimers in its basal state and assembly of dynamin tetramers induces cooperative GTP binding. This GTP-bound tetramer conformation is the active state and depends on interaction with auxilin and Hsc70. Therefore, auxilin may function as an effector of dynamin (Sever et al., 2005). Auxilin is recruited transiently to the plasma membrane just before and right after clathrin-coat assembly completion. One or both of these

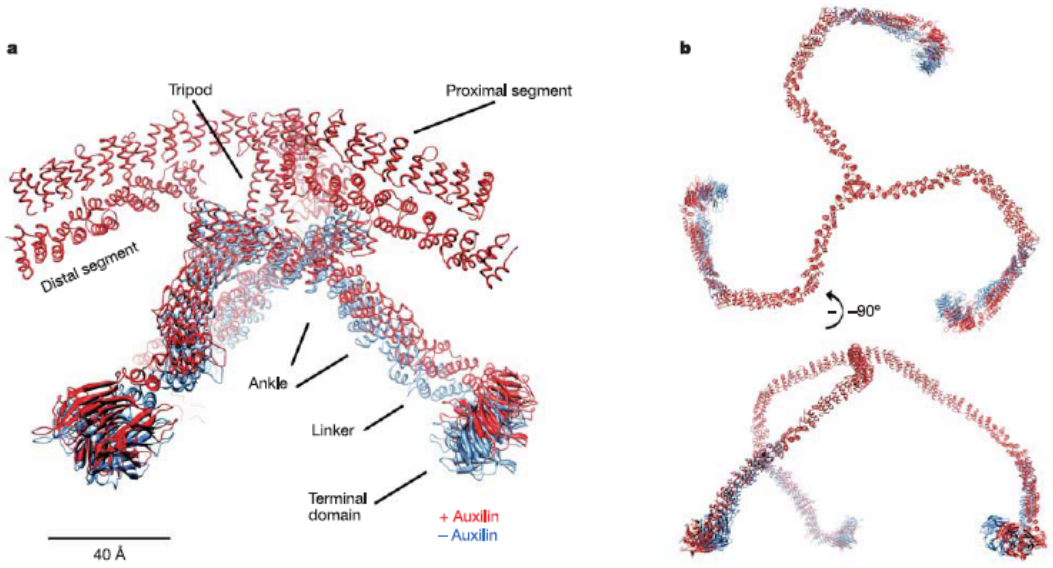

Figure 1.11. Changes in clathrin heavy-chain contacts produced by auxilin binding. (A) Comparison of the arrangement of clathrin legs in the region around a vertex of the D6 barrel (the hub assembly). The model from the 7.9 Å resolution analysis of a D6 barrel is in blue; the one obtained by adjusting that model to fit the 12 Å auxilin-bound D6 barrel is in red. The ankle-crossing angles change in such a way that the terminal domains move radially outwards with respect to the outer shell. (B) Superposition of clathrin triskelions from corresponding locations in the auxilin-bound D6 barrel (red) and the auxilin-free D6 barrel (blue). Figure and legend adapted from Fotin et al (2004).

recruitments may require the PTEN domain of auxilin (Lee et al., 2006; Massol et al., 2006). However, the expression of the PTEN domain only did not affect the fission of vesicles (Newmyer et al., 2003). While maturation of CCPs, clathrin rearrangement must occur to form spherical structure from planar membrane. During CCP invagination,

exchange between membrane-bound clathrin and cytosolic free clathrin occurs instead of adding a small amount of clathrin triskelions to the edges of growing clathrin-coated pits. Probably, clathrin exchange is required to ensure the arrangement of clathrin on the curved lattice of the invaginating CCPs. (Wu et al., 2001). The suggested mechanism for how auxilin functions in the fission of CCVs is that auxilin and Hsc70 exchange clathrin bound to clathrin-coated pits with free clathrin in the cytosol to constrict clathrin-coated pits. In addition, they stabilize dynamin in its active state.

1.4.2. In vivo studies of auxilin in *C. elegans* and yeast

C. elegans contains only one auxilin homolog. When its expression is knock-downed by RNAi, endocytosis is reduced and development is arrested. Also, failure of clathrin exchange was detected by fluorescence recovery after photobleaching. Interestingly, expression of Chc suppresses the arrest of development, probably by overcoming the defect in endocytosis due to failure of clathrin recycling (Greener et al., 2001). Yeast auxilin is encoded by the *swa2* gene. Distinct form other auxilin homologs, only Swa2 contains three tetratricopeptide repeat (TPR) motifs located between the clathrin-binding domain and the J domain (Fig 1.12.). The TPR motif is a protein-protein interaction module with which Hsp70 and Hsp90 proteins mediate interactions (Blatch and Lassle, 1999). The strains with *swa2* deletions are viable but grow very slowly. Protein sorting from the trans-Golgi network to the endosomal system also utilizes CCVs. Deletion of *swa2* also causes mislocalization of a late Golgi protein and accumulation of assembled clathrin (Gall et al., 2000). A different group studied yeast Swa2 and showed that depletion of Swa2 impairs transport of a Golgi protein to the vacuole and that the

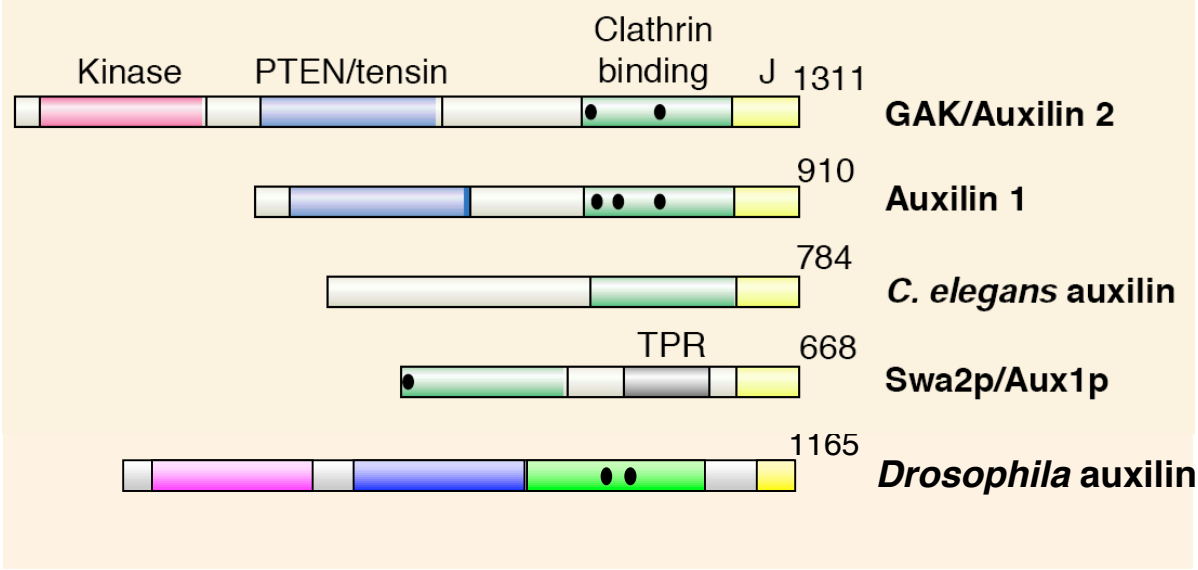

Figure 1.12. Domain structures of auxilins. The domain arrangement of human GAK/Auxilin 2, bovine auxilin 1, *C. elegans* auxilin, yeast Swa2p/Aux1p and *Drosophila* auxilin are shown with the kinase, PTEN, clathrin-binding and J domains indicated. The TPR domain is only found in yeast auxilin, and all but the worm auxilin contain 'DPF' AP-2-binding motifs (black dots). Figure and legend adapted from Lemmon (2001).

number of clathrin-coated vesicles are increased (Pishvaee et al., 2000). These results indicate that clathrin-dependent membrane trafficking is affected by failure of clathrin uncoating in *auxilin* mutants.

1.4.3. The domains of auxilin

Drosophila auxilin is 40% identical to GAK. Only *Drosophila* auxilin and GAK contain the kinase domain and both also contain DPF motifs that can bind AP2 (Fig. 1.12.) (Lemmon, 2001; Scheele et al., 2003). Phosphorylation and dephosphorylation of AP2 regulates clathrin-dependent endocytosis. In vitro, GAK can phosphorylate the μ1

subunit of AP1 and the μ2 subunit of AP2 (Umeda et al., 2000; Korolchuk and Banting, 2002). AP1 and AP2 are adapter proteins required respectively in the Golgi and at the plasma membrane during clathrin-dependent membrane trafficking. Phosphorylation of the μ2 subunit of AP2 is required for endocytosis (Olusanya et al., 2001). Adapter-associated kinase 1 (AAK 1) can also phosphorylate the μ1 subunit of AP1 and the μ2 subunit of AP2 (Conner and Schmid, 2002). Probably, AAK 1 must have a redundant role with GAK. Because mammalian auxilin as well as *C. elegans* and yeast auxilin homologs do not contain the kinase domain, probably the kinase domain of GAK is not essential for the uncoating function. The PTEN domain is common among mammalian auxilin, GAK and *Drosophila* auxilin but is not found in *C. elegans* and yeast auxilin homologs. The tumor suppressor, PTEN, can dephosphorylate PI-(3,4,5)-P_3 which is a lipid second messenger involved in cell growth signaling (Maehama and Dixon, 1999). However, the auxilin PTEN domain does not have the essential cysteine residue for the phosphatase activity. Although the exact function of the PTEN domain is not understood, it is thought that the PTEN domain recruits auxilin to the membrane containing phosphatidylinositide. As mentioned before, the PTEN domain may be required for transient recruitment of auxilin to the plasma membrane before and/or after CCV budding (Lee et al., 2006; Massol et al., 2006). Two C-terminal domains, the clathrin-binding domain and the J domain, are well-conserved among auxilin homologs. A truncated form of auxilin containing only the clathrin-binding domain and the J domain is sufficient to uncoat CCVs just like intact auxilin, in vitro (Holstein et al., 1996; Greener et al, 2000). The clathrin-binding domains of auxilin in different organisms (except *C. elegans*) contain a variable number of DPF motifs which is known to bind AP2 (Lemmon, 2001).

Mammalian auxilin has three DPF motifs, which bind cooperatively to the α-ear domain of AP-2 and are involved in the interactions with clathrin (Scheele et al., 2003). The J domain is composed of about 70 amino acids and is highly conserved even in prokaryotes. The J domain contains the invariant HPD motif that binds specifically to Hsc70 and stimulates its ATPase activity (Holstein et al., 1996; Jiang et al., 2000). Two dynamin binding sites are identified in mammalian auxilin. One is located between the PTEN domain and the clathrin-binding domain. The other is located in the clathrin-binding domain (Newmyer et al., 2003).

1.5. Rab proteins

Rab proteins are small GTPases in the Ras-super family that control vesicle trafficking such as membrane tethering, vesicle budding, and vesicle mobility. Each Rab protein is localized to a distinct membrane structure. For example, Rab5 is on the early endosomes, Rab7 is on the late endosomes, and Rab11 is on the recycling endosomes (Zerial and McBride, 2001). In vertebrates, more than 75 *rab* genes have been identified and in *Drosophila* there are 33 *rab* genes (Zhang et al., 2007).

1.5.1. Controlling of Rab activity

Rab proteins cycle between a GTP-bound active form and a GDP-bound inactive form. The active GTP-bound form is proposed to regulate membrane docking with the target membrane structures. In the cytosol, a Rab protein is in the GDP-bound inactive

form by binding of GDP dissociation inhibitor (GDI). After the Rab protein is delivered by GDI to the target membrane compartment, GDI is released by a GDI displacement factor (GDF). Then, the Rab protein is converted to the GTP-bound active form by guanine nucleotide exchange protein (GEP). The GTP-bound Rab protein interacts with downstream effectors for the specific functions of Rabs. After the Rab protein functions on the membrane, the GTP-bound form is converted to the GDP-bound form by GTPase-activating protein (GAP). The GDP-bound form of the Rab protein is released from the downstream effectors and binds to GDI to be relocalized to the cytosol. This cycle event controls temporal and spatial Rab activity (Fig. 1.13.) (Takai et al., 2001; Seabra and Wasmeier, 2004; DerMardirossian and Bokoch, 2005). Prenylation is the addition of either a farnesyl or a geranyl-geranyl moiety, which are hydrophobic molcules, to the C-terminal cysteine of the target protein to facilitate attachment to cell membranes. One or two geranylgeranyl groups are added to the C-termini of Rabs to associate with membranes by Rab geranylgeranyl transferase (RGGT) (Seabra, 1998). Rab escort proteins (REPs) are required for newly synthesized Rabs to be recognized by RGGT (Andres et al., 1993). REPs also deliver newly prenylated Rabs to the target membrane structures (Alexandrov et al., 1994). When Rabs are recycled, GDI delivers Rabs to the target membrane (Wilson et al., 1996)

1.5.2. Structure of Rabs

The structure of Rab proteins is similar to other Ras-related GTPases in their overall folding. Rab proteins are defined structurally by unique switch domains (Fig. 1.14.). Similar to other Ras analogs, Rabs contain two switch domains, Switch I and

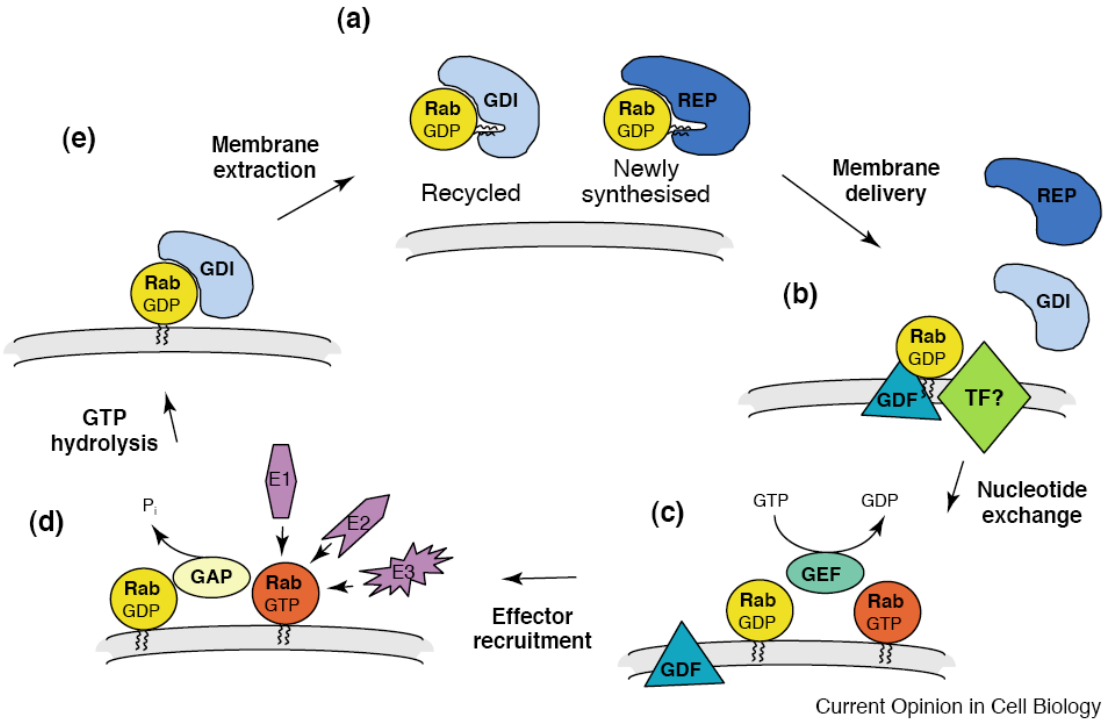

Figure 1.13. Schematic representation of the Rab cycle showing membrane recruitment and activation. (a) GDP-bound Rab proteins form a cytosolic complex with RabGDI. (b) Membrane delivery and Rab-GDI displacement are mediated by a GDF, probably aided by unidentified targeting factors, followed by (c) Rab activation through GEF-catalysed nucleotide exchange. (d) GTP-bound Rab recruits effector molecules to the membrane. (e) GAP-mediated GTP hydrolysis returns the Rab to its inactive state, resulting in re-extraction from the membrane by GDI. Figure and legend adapted from Seabra and Wasmeier (2004).

Switch II. These domains are regions which change conformation by exchange of nucleotides (Pereira-Leal and Seabra, 2000; Pfeffer, 2005). A specific interaction between each Rab protein and its effectors takes place on the complementarity-determining domains which form a deep pocket (Ostermeier and Brunger, 1999).

Conserved hydrophobic residues within the switch domains also contribute to interaction with effectors (Pfeffer, 2005). The C-terminus of Rab proteins is the hypervariable domain which is most distinct element of different Rabs. The length of the hypervariable domains vary form 23 to 42 amino acids and usually two cysteine residues are located at the termini for geranylgeranylation. Probably, the importance of the hypervariable domain is to provide flexibility between the geranylgeranylation site and GTPase site (Chavrier et al., 1991).

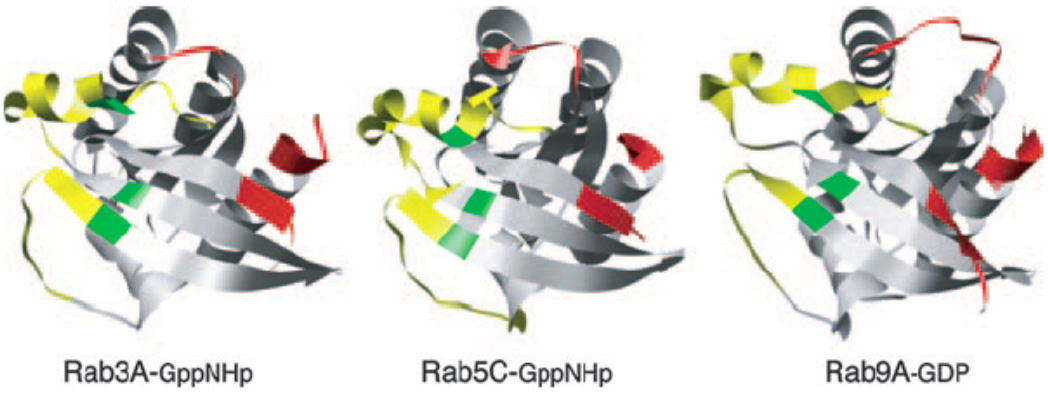

Figure 1.14. Comparison of the structures of three Rab proteins. Shown in yellow are Switch regions and in red are domains that correspond to the complementarity-determining regions. Green positions represent the hydrophobic triad residues in which side chains have different orientation in Rab structures despite their identical sequences. Figure and legend adapted from Pfeffer (2005).

1.5.3. Rab11

Rab11 is present in Golgi and recycling endosomes. When a mutant form of Rab11 that binds GDP predominantly is overexpressed in cultured cells, the morphology of recycling endosomes is altered and recycling of the transferrin receptor, which follows recycling pathway, fails (Ullrich et al., 1996). Rab11 also functions in trans-Golgi network to plasma membrane transport (Chen et al, 1998).

1.5.3.1. Effectors of Rab11

Several effectors of Rab11 have been identified. Rab11BP, also known as Rabphilin-11, functions during recycling. In HeLa cells, Rab11BP colocalizes with Rab11 along microtubules (Zeng et al., 1999; Mammoto et al, 1999). Another rab11 effector, Rip11 is important for protein trafficking from recycling endosomes to the plasma membrane. Rip11 is recruited to the endosomal membrane by binding to Rab11 as well as by interaction of the C2 domain, which targets proteins to the membrane, with neutral phospholipids (Prekeris et al, 2000). Rab11-FIP2 functions in recycling and it can associate with a motor protein, myosin-Vb. Probably, Rab11-FIP2 is involved in actin-dependent recycling vesicle transport (Hales et al., 2001). Rab11-FIP2 also functions in receptor-mediated endocytosis. Thus, it is possible that Rab11-FIP2 connects endocytosis and the subsequent endosomal sorting (Cullis et al., 2002). Rab coupling protein (RCP) binds Rab4 as well as Rab11 (Lindsay et al, 2002). Rab4 is another Rab protein involved in recycling. It has been suggested that Rab4 is involved in fast recycling. (Sonnichsen et al., 2000). RCP may act as an intermediate that connects the two Rab proteins. An exocyst is a protein complex that functions in the secretory pathway. An exocyst

component, Sec15, colocalizes with Rab11 and interacts with Rab11 in a GTP-dependent way. Probably, Sec15 is an effector of Rab11 during protein transport from Golgi to the plasma membrane (Zhang et al 2004). Rab11-FIP3/Arfophilin-1 and Rab11-FIP4/Arfophilin-2 deliver Rab11 to the cleavage furrow by interaction with ADP ribosylation factor 6 (Arf 6), a monomeric GTPase regulating actin dynamics, and the exocyst (Fielding et al., 2005; Shiba et al., 2006).

1.5.3.2. *Drosophila* Rab11

Drosophila Rab11 has been studied in a few developmental contexts. Mutant alleles of *rab11* were isolated from a screen that detected alteration of the localization of *oskar* mRNA at the posterior pole of oocyte (Jankovics et al, 2001). Localization of *oskar* mRNA and other mRNAs depends on polarization of the microtubule cytoskeleton. Rab11 localizes to distinct compartments at the posterior end of the oocyte and is required to establish and maintain the microtubule plus ends at the posterior pole (Dollar et al 2002). Rab11 is also required for cellularization during embryogenesis. Vesicle trafficking through Rab11 endosomes is important for lateral membrane growth. During this process, Rab11 functions with its effector Nuclear-fallout (Nuf) a *Drosophila* homolog of Rab11-FIP4/Arfophilin-2 (Pelissier et al., 2003; Riggs et al., 2003).

Drosophila Rab11 functions both in recycling and exocytic membrane trafficking. *Rab11* mutant germ line clonal analysis showed that transferrin receptor internalization takes place, but the recycling of transferrin receptor fails in *rab11* mutants (Dollar et al., 2002). The exocytic function of Rab11 has been studied in eye development. Rab11 is localized to the trans-Golgi network in R-cells. Expression of a

dominant negative form of Rab11 blocked the transport of rhodopsin, a rhabdomere-residing protein, from Golgi to the rhabdomere which is an apically located membrane compartment (Satoh et al. 2005).

Rab11 function during Notch signaling has been suggested. During asymmetrical division of sensory organ precursor (SOP) cells, Rab11 asymmetry is established. In pIIb cells where Delta signaling occurs, Rab11 accumulates around the centrosome. A significant number of Delta-positive vesicles are often Rab11-positive. However, in pIIa cells where Notch is activated, Rab11 accumulation is inhibited (Emery et al., 2005). Jafar-Nejad et al (2005) showed that *sec15* mutants cause transformation of pIIa to pIIb, probably due to failure of Notch activation during SOP development. Sec15, a Rab11 effector protein, colocalizes with Rab11 in wild-type cells and Rab11 accumulates aberrantly in *sec15* mutant cells. From these observations, the authors suggested that *sec15* mutants result in a Delta recycling defect that blocks the Notch activation. However, a functional study of Rab11 during Notch activation using *rab11* mutants has not been published.

Chapter 2. Identification of auxilin mutants as enhancers of the *liquid facets* gain-of-function eye phenotype

2.1. Introduction

The data described in this chapter have been published in *Genetics* (see Eun et al., 2007)

Lqf is the *Drosophila* homolog of mammalian endocytoic epsin. Lqf is a multi-modular protein containing an N-terminal ENTH domain and several protein-protein interacting motifs such as ubiquitin-interacting motifs, clathrin-binding motifs, DPW motifs which bind AP2, and NPF motifs which bind other accessory proteins. The ENTH domain, which binds PI-(4,5)P_2 at the plasma membrane, is thought to recruit epsin to the plasma membrane and it also inserts into the membrane and induces curvature (Ford et al., 2002). However, in *Drosophila*, either the ENTH domain alone or an ENTH-less Lqf rescues the *lqf* mutant eye phenotype. Thus, Lqf probably has two distinct functions, each of which is partially redundant with another protein or pathway or with each other (Overstreet et al., 2003).

Drosophila Lqf was identified as a substrate of Fat facets (Faf), a deubiquitinating enzyme that prevents overneuralizaton in the eye (Fischer et al., 1997; Cadavid et al., 2000). In the eye, ubiquitination of Lqf is thought to target the protein for proteasomal degradation. By preventing degradation, Faf helps to sustain Lqf at the proper level of

activity (Chen et al., 2002). Consistent with this idea, weak mutant alleles of *lqf* have a similar phenotype to *faf* mutants. *lqf* null mutant eyes have a much more complex mutant phenotype that resembles *Delta* loss-of-function (Cadavid et al., 2000).

In *lqf* mutant cells, Delta accumulates at the apical surface of eye discs and Notch activation fails in neighboring cells. This indicates that Lqf is essential for Delta endocytosis and it is required specifically in the Delta-expressing signaling cells. In *faf* mutants, the amount of Lqf is decreased and Delta endocytosis also fails (Chen et al., 2002; Overstreet et al., 2004). Faf is required only for neural inhibition by R-cells. In contrast, Lqf is required for all Notch function near the furrow. Lqf function appears to be specific for Delta endocytosis. Lqf probably functions in all Delta signaling events (Overstreet et al., 2004; Wang and Struhl, 2004).

When Lqf is overexpressed by the eye-specific *glrs* promoter, it results in a rough eye phenotype (Fig. 2.1.). Adult eye sections show extra R-cells and missing R7 cells (Fig. 2.1.E,F,G). The *glrs-lqf* transgene cannot rescue the *lqf* loss-of-function eye phenotype of the weak viable allele, lqf^{FDD9}. The *glrs* promoter expresses genes starting at 3-4 rows posterior to the morphogenetic furrow. This is too late for rescuing neural inhibition by R-cells, a known part of the lqf^{FDD9} phenotype. The mutant phenotype of overexpression of a wild-type *lqf* gene likely results from titration of the proteins that bind Lqf and function synergistically with it. The idea behind the modifier screen is that the rough eye phenotype will be modified by lowering the amount of the proteins that Lqf requires to function or that Lqf binds. Consistent with the idea, c*lathrin heavy chain* (*chc*) mutants are dominant enhancers of the rough eye phenotype of *glrs-lqf*. *chc* mutations are also enhancers of *lqf* hypomorphs indicating that lqf^{+} requires chc^{+} to function (Cadavid

et al., 2000). The *glrs-lqf* mutant phenotype is dose-dependent; flies with two copies of the transgene have much rougher eyes than flies with one copy (Fig. 2.1.H,I,J). These

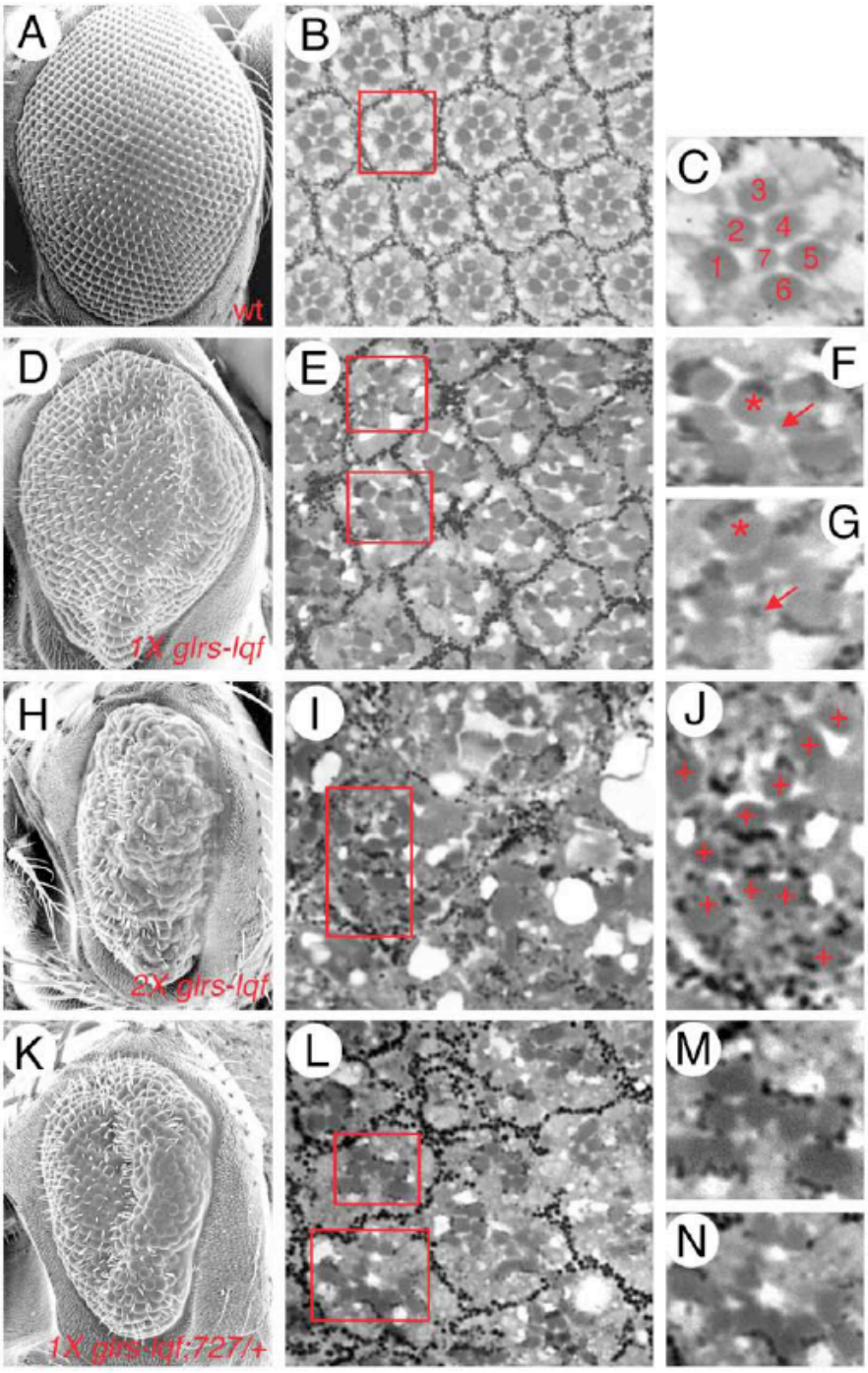

Figure 2.1 The *glrs-lqf* eye phenotype. Scanning electon micrographs (A, D, H, K) and tangential sections (B, C, E-G, I, J, L-N) of adult eyes are shown. The genotypes are: (A-C) wild-type (wt); (D-G) *1Xglrs-lqf*; (H-J) *2Xglrs-lqf*; (K-N) *2Xglrs-lqf*; *727*/+. The boxes in B, E, I, and L correspond to the enlargements in C, F-G, J, and M-N, respectively. The numbers in C refer to R-cells. In F and G, asterisks indicate ectopic R-cells and arrows indicate degenerated R7s. The plus signs in J indicate R-cells. The *2Xglrs-lqf* eyes are homozygous for the *1Xglrs-lqf* P element. The rough eye phenotype of *2Xglrs-lqf* is unlikely to be affected by a mutation caused by the P element insertion because flies with one copy of this P element and an additional copy at a different location show similarly rough eyes. In eyes with *1Xglrs-lqf*, some facets have more than the normal number of 6 outer R-cells (Figure 1, B, C and E – G). Adult eyes with *2Xglrs-lqf* have more severely disrupted eye morphology; organized facets are absent, although some R-cells do form (Figure 1I, J). Also, degeneration of R7 is observed in *glrs-lqf* transformants (Figure 1B, C, and E-G).

characteristics suggest that flies with one copy of *glrs-lqf* are a good background to screen for *lqf*-related genes.

To screen for autosomal enhancers of the eye phenotype caused by overexpression of Lqf, male flies were mutated using ethylmethylsulfonate (EMS) and then crossed with females bearing one copy of *glrs-lqf* (Fig. 2.2). About 30,000 F1 males (~24 mutagenized genomes) were screened. This screen was performed by Janice Fischer and Kristi Lea. F1 males with enhanced eye roughness were backcrossed and those that bred were mapped to chromosome 2 or 3 and balanced (Fig. 2.2.). From the screen, 16 enhancers on chromosome 2 and 74 enhancers on chromosome 3 were isolated. Only enhancers on homozygous lethal chromosomes were used subsequently in complementation tests. There was one second chromosome complementation group. The

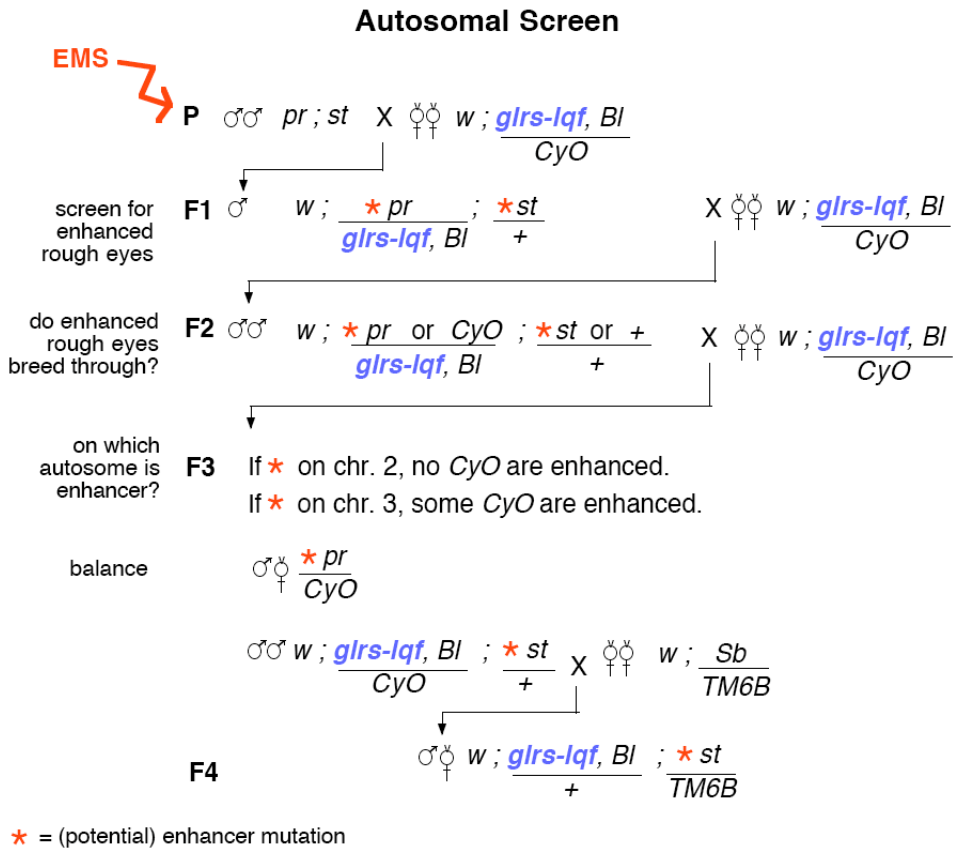

Figure 2.2. Mutagenesis screen for autosomal enhancers of the *glrs-lqf* eye phenotype. A cross scheme is shown for the screen of the autosomes for dominant enhancers of the *glrs-lqf* rough eye.

mapping results indicate that these are *spen* alleles. Spen is a RNA binding protein containing three RNA recognition motifs. In the absence of Spen, Notch expression is normal but the expression of Su(H), a major component of Notch signaling, is reduced dramatically. Spen functions downstream of the Notch receptor as a transcriptional regulator (Kuang et al., 2000). Many other laboratories work on the function of Spen and so I decided not to work on it. However, as epsin may have a function in the nucleus

(Hyman et al., 2000; Spradling et al., 2001), it remains an intriguing possibility that epsin might bind Spen directly. The third chromosome enhancers represent several different lethal complementation groups. Meiotic and deficiency mapping were performed to locate each of them on the third chromosome. One large complementation group whose representative allele is *727* was being mapped when I joined this project. Meiotic recombination had located *727* between two recessive mutant markers, *th* and *cu*. Flies containing chromosome 3 deletions between *th* and *cu* had been crossed with *727* flies to narrow down the mutation location. No available deficiency within this region uncovered *727*. Several P elements in this region had been used for male recombination mapping. I continued to map this complementation group using male recombination.

To identify X chromosome enhancers of *glrs-lqf*, a separate EMS screen was performed by Janice Fischer and Samuel Stevens and approximately 15,000 F1 females were screened. Flies which still showed an enhanced eye phenotype after mutated chromosome 2 and 3 are removed were collected and eight enhancer chromosomes were isolated. Of these eight mutant chromosomes, two were homozygous lethal (*AA1* and *BB2*), and one was hemizygous viable with morphological phenotypes and male sterility (*EE1*). *AA1* and *BB2* were identified as mutant alleles of *chc* by complementation tests with a rescue transgene and a duplication. Using deletion and duplication chromosomes, *EE1* was mapped physically to a small gene region including *Rala,* a Ras-like small GTPase that functions in many different pathways including regulation of vesicle trafficking (Feig, 2003). *EE1* is homozygous viable with morphological phenotypes and male sterility. The *EE1* homozygous phenotype is similar to the phenotype reported previously for a *Rala* dominant negative transgene. Expression of a wild-type *Rala*

cDNA (*Act5C-gal4>UAS-Rala*) complements the morphological phenotypes of *EE1*. These experiments were performed by Janice Fischer and Samuel Stevens and I determined the DNA lesion in the *Rala* coding region on the *EE1* chromosome.

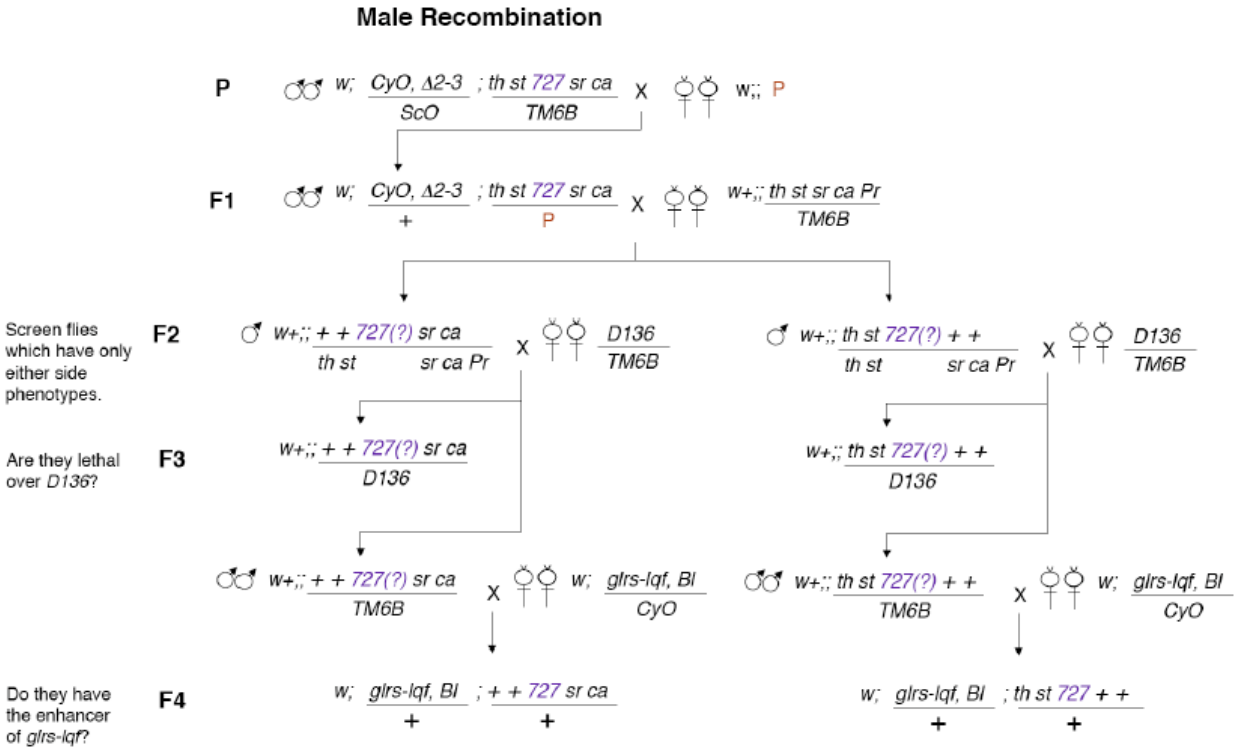

Figure 2.3. Male recombination mapping of *727*. A cross scheme is shown for the male recombination mapping for the lethality over *D136* and dominant enhancerment of the *glrs-lqf* rough eye. The table shows the number of flies in which recombination occurs and the corresponding location of the P elements.

P elements (location)	phenotype	Number of flies	Enhancement/ lethality	Location from P
KG03229 (80A1)	*th- sr+*	2	No	**Right**
	th+ sr-	2	Yes	
KG00844 (80A2)	*th- sr+*	1	No	**Right**
	th+ sr-	0		
KG06133a (80B3)	*th- sr+*	1	No	**Right**
	th+ sr-	2	Yes	
KG08740 (82A1)	*th- sr+*	4	No	**Right**
	th+ sr-	1	Yes	
CG14641 (82A1)	*th- sr+*	2	No	**Right**
	th+ sr-	0		
KG03023 (82A4)	*th- sr+*	2	Yes	**Left**
	th+ sr-	0		
CG1103 (82A5)	*th- sr+*	5	Yes	**Left**
	th+ sr-	2	No	
j1E6 (82A3/5)	*th- sr+*	0		**Left**
	th+ sr-	1	No	
EY01545 (82B1)	*th- sr+*	4	Yes	**Left**
	th+ sr-	0		

Figure 2.3. Continued

2.2. Results

2.2.1. Identification of the *727* complementation group

The *727* complementation group is the largest enhancer complementation group on the third chromosome. Originally, The complementation group consists of 9 alleles: *727, C2, D136, D128, J26, K5, N7, L7* and *F37*. *L7* was isolated as a homozygous lethal chromosome and could not complement the lethality of the other complementation group members initially. However, the chromosome is homozygous viable without any obvious phenotypes and *in trans* to the other *727* complementation group members, there are escapers with eye and wing phenotypes. Using meiotic recombination and male recombination using several P elements (Fig. 2.3.), the cytogenetic location of the *727* complementation group determined to be between 80C1 and 82A6. With the help of Kristi Lea, I performed the 2nd round male recombination using nine P elements and narrowed down the gene region to one that includes six genes (Fig. 2.4.). Because the *727* complementation group has many alleles, I expected the gene to be large. *auxilin* is the largest gene in this region, and *auxilin* was known to function in clathrin-mediated endocytosis.

There were no existing *auxilin* mutant alleles to use for complementation tests. I checked complementation with expression of an *auxilin* cDNA using *Actin5c* promoter. The expression of the cDNA complements completely *727/D136* heterozygotes (strong alleles-see below). Therefore, I concluded that the gene corresponding to the *727*

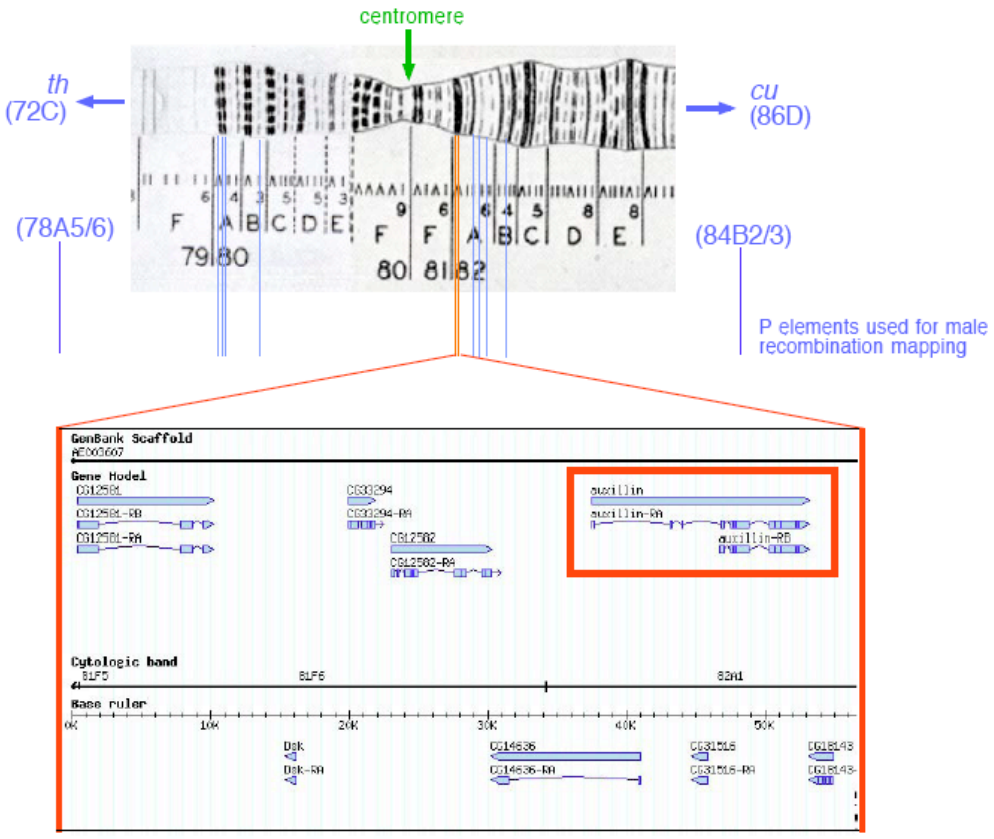

Figure 2.4. Localization of *727* to the *auxilin* region. A diagram summarizing how *727* was localized to the *auxilin* region using male recombination is shown. The blue lines indicate the polytene positions (between 78A5/6 and 84B2/3) of the different P elements used for male recombination mapping. The red lines indicate the two P elements found to flank *727* most closely. See Materials and Methods and text for details. The polytene chromosome drawing is from Sorsa, 1988. The gene region map is from FLYBASE (Grumbling et al., 2006).

complementation group is *auxilin*. Using sequencing analysis, I confirmed that the members of the *727* complementation group are alleles of *auxilin* (Fig. 2.5.).

Initially, *L24*, *K47*, and *K48* were thought to be a different complementation group. From meiotic mapping, the mutation was located between *th* and *cu*. The allelic

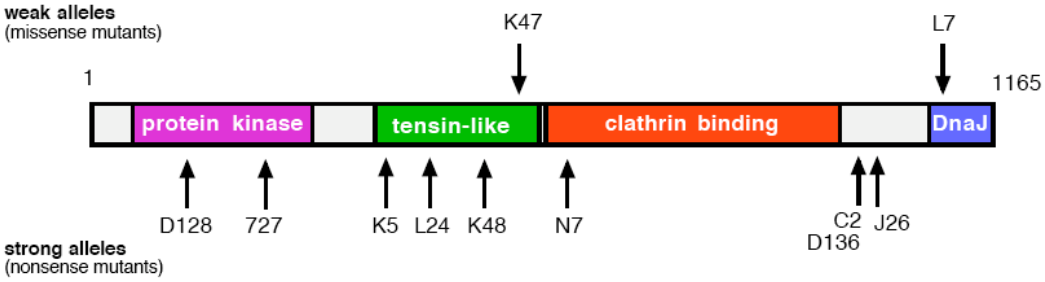

allele	aa change	codon change
D128	Q172 → stop	**C**AG → **T**AG
727	W254 → stop	T**G**G → T**A**G
K5	Q404 → stop	**C**AG → **T**AG
L24	Q486 → stop	**C**AG → **T**AG
K48	Q594 → stop	**C**AG → **T**AG
N7	K734 → stop	**A**AG → **T**AG
C2	Q1018 → stop	**C**AG → **T**AG
D136	Q1018 → stop	**C**AG → **T**AG
J26	Q1037 → stop	**C**AA → **T**AA
eF37	?	?
K47	C671Y	T**G**T → T**A**T
L7	P1111S	**C**CT → **T**CT

Figure 2.5. Molecular analysis of *auxilin* mutant alleles. The *Drosophila* auxilin protein is diagrammed, numbers are amino acids 1 – 1165. Arrows indicate approximate positions of the codon changes in each mutant allele. The table shows each nucleotide change and the corresponding codon changes. The functional domains of *Drosophila* auxilin were inferred by amino acid sequence similarity to GAK (cyclin G-associated kinase) also known as vertebrate auxilin 2.

combinations of *K47/K48* and *K47/L24* have lethal escapers with morphological phenotypes similar to the phenotypes of *L7 in trans* to the other *727*complementation group members. Complementation tests were performed between these three mutant chromosomes and *727* complementation group members and all failed to complement lethality. Therefore, I concluded that *L24*, *K47*, and *K48* are alleles of *auxilin* and I

confirmed this with the sequencing analysis (Fig 2.5.).

There were other 3rd chromosome lethal complementation groups: ① *A2* and *E184*, ② *C47*, and *I58* ③ *D13* and *L25*, ④ *G56* and *E142*. While Janice Fischer was mapping these complementation groups, lethal and enhancer function separated.

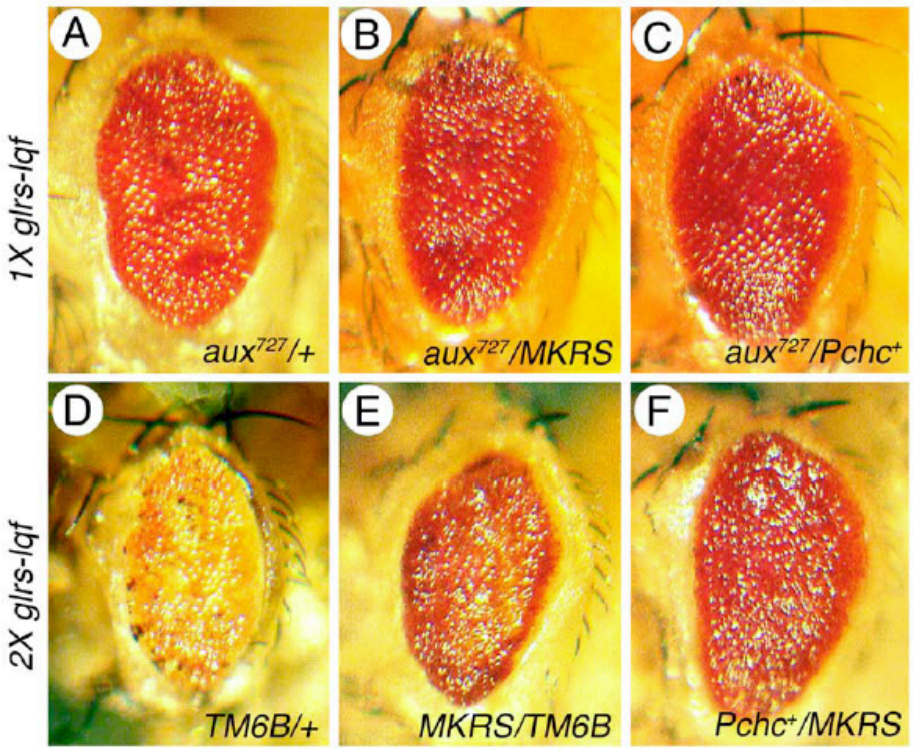

Figure 2.6. Suppression of the *glrs-lqf* phenotype by chc^{+} overexpression. Eyes of flies with the genotypes indicated and also with one copy (A-C) or two copies (D-F) of the *glrs-lqf* transgene are shown. (A-C) The enhancement of the *1Xglrs-lqf* rough eye by aux^{727} /+ is suppressed partially by an additional copy of chc^{+} genomic DNA. (The flies in B and C came from a single cross.) (D-F) The *2Xglrs-lqf* rough eye is suppressed partially by an additional copy of chc^{+}. (The flies in E and F came from a single cross.)

Therefore, lethality *in trans* is not caused by the mutations which enhance *glrs-lqf*. These complementation groups were not analyzed further.

2.2.2. A P element containing *chc*+ genomic DNA suppresses the *glrs-lqf* phenotype.

Lqf contains clathrin-binding motifs and the *chc* gene was isolated as an enhancer of *glrs-lqf*. Therefore, I wondered if the *glrs-lqf* rough eye phenotype might result at least partly from titration of clathrin from the cytoplasm. To address this question, I added one extra copy of a genomic chc^{+} gene to the *glrs-lqf* background. The enhanced phenotype of 1X *glrs-lqf* with aux^{727}/+ is suppressed by the addition of the chc^{+} transgene (Fig. 2.6.C). It is possible that the extra copy of the chc^{+} gene suppresses 1X *glrs-lqf* and/or the *auxilin* mutant. (Also, I found that an extra chc^{+} gene does suppress the *auxilin* phenotype (see chapter 4)). The addition of a wild-type chc^{+} gene suppresses partially the eye phenotype of 2X *glrs-lqf* (Fig. 2.6.F). These data suggest that the rough eye phenotype caused by overexpression of Lqf is also suppressed by the addition of clathrin and thus may result at least in part by clathrin depletion. Maybe, Lqf overexpression titrates clathrin.

2.2.3. DNA sequence determination of *auxilin* alleles and *EE1*

I wanted to confirm molecularly that the *727* complementation group alleles are *auxilin* mutants. In addition, I wanted to determine if the characteristics and severity of the phenotypes correlate in any way with the molecular lesions in the mutants. Most of the *auxilin* mutant alleles are homozygous lethal and the alleles die as small larvae. I balanced the mutant chromosomes with a *TM6B* balancer containing a GFP marker.

Homozygous larvae (not glowing) were gathered using the GFP microscope and genomic DNA was isolated. For the viable allele, *L7*, I used a single adult fly to prepare genomic DNA. From each allele, the *auxilin* gene region was amplified by PCR and exons and splice junctions of the *auxilin* coding region were sequenced.

Nine nonsense mutations (*D128, 727, K5, L24, K48, N7, D136, C2, J26*; the order corresponds to the location of the nonsense mutation along the ORF) and two missense mutations (*K47, L7*) were identified (Fig. 2.5.). Meiotic mapping and male recombination mapping had located *F37* in the same region of *auxilin* mutants. Also, *F37* failed to complement all *auxilin* alleles but I was not able to find any mutation in the coding region nor splicing donor and acceptor sites from sequence analysis. This suggests that *F37* might have a mutation in a regulatory region.

EE1 was isolated as an X-linked enhancer. A homozygous viable *EE1* was physically mapped into a small gene region containing *Rala*. To identify whether *EE1* is an allele of *Rala*, I isolated DNA from a single adult male and sequenced the *Rala* gene region of the *EE1* chromosome. I found a missense mutation: Ser154 (TCG) is mutated to Leu154 (TTG). Ser154 is conserved in human Ral proteins and also in human Kras, and amino acids 152 through 156 are required for nucleotide binding.

2.2.4. Genetic interactions between *auxilin* and *lqf*

The main purpose of the screen we performed was to identify more genes that function with lqf^{+} in Delta signaling. The background we used was overexpression of lqf^{+} in the eyes. Using loss-of-function alleles, I wanted to look for genetic interaction between *auxilin* and *lqf* in a more physiological context. If the two genes function in the

same direction in a pathway, the strong *auxilin* alleles may act as dominant enhancers of *lqf* hypomorphs and vice versa. First, I tested strong *auxilin* alleles (aux^{D128}, aux^{727}, aux^{N7}, aux^{C2}, aux^{D136}, and aux^{F37}) in a *lqf* hypomorphic background (lqf^{FDD9}/lqf^{FDD9}). I could not observe any enhancement of the eye or wing phenotypes. Second, I tested whether a *lqf* null mutation (lqf^{ARI}) acts as a dominant enhancer of homozygous viable *auxilin* allelic combinations between nonsense mutations (aux^{D128}, aux^{727}, aux^{K5}, aux^{L24}, aux^{K48}, aux^{N7}, aux^{J26}, aux^{D136}, and aux^{C2}) and missense mutations (aux^{K47} and aux^{L7}). At 25°C, these combinations are semi-lethal and I could detect escapers which show abnormal eye and wing phenotypes. When I introduced one copy of lqf^{ARI}, I could not detect any viable flies. This result suggests that the *lqf* mutation enhances *auxilin* mutant phenotypes.

2.2.5. Allelic series based on the severity of phenotype

I determined the strength of *auxilin* mutant alleles using the eye phenotype and numbers of escapers. The number of escapers and the severity of the eye phenotype correlate; allelic combinations that have fewer numbers of escapers show more severe eye phenotypes. I concluded that the two missense mutations (aux^{K47} and aux^{L7}) are weaker than any nonsense mutations. The eye phenotype of aux^{K47}/aux^{D128} is stronger than aux^{L7}/aux^{D128} (Fig. 2.7.B,C). Therefore, I concluded that among missense mutations, aux^{K47} is a stronger loss-of-function mutation than aux^{L7}. The earlier nonsense mutations seem to cause stronger phenotypes than the later nonsense mutations. The eye phenotype of aux^{K47}/aux^{D128} is more severe than that of aux^{K47}/aux^{D136} (Fig. 2.7.B,D). Also, there are fewer escapers from aux^{K47}/aux^{D128} and aux^{K47}/aux^{727} than any other allelic

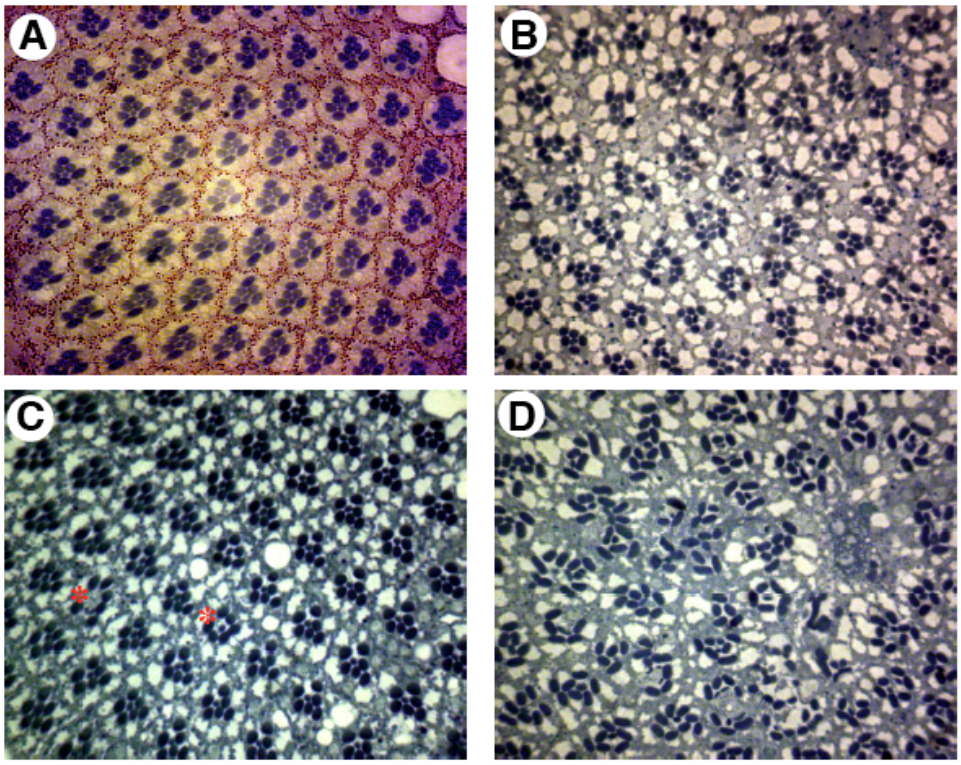

Figure 2.7. Tangential sections of adult eyes of *auxilin* mutants. The genotypes are: (A) wild-type; (B) aux^{K47}/aux^{D136}; (C) aux^{L7}/aux^{D136}; (D) aux^{K47}/aux^{D128}. In C. asterisks indicate mutant facets. *auxilin* mutant eye have various phenotype such as extra R-cells, missing R-cells, loss of chimetrics, misorganized facets, loss of facets, and fused facets. The order of phenotypic severity among the shown allelic combination is aux^{L7}/aux^{D136}, aux^{K47}/aux^{D136}, aux^{K47}/aux^{D128} form weakest to strongest.

combinations. However, this idea is not consistent with the result of rescue by a truncated protein containing only the clathrin-binding domain and the J domain, and the dominant negative characteristic of J-less protein (see chapter 4). Maybe the differences in

nonsense mutant phenotypes are due to other EMS-linked mutations on these chromosomes.

From the experiment to test the genetic interaction between *auxilin* and *lqf*, I was able to place aux^{N7} as the weakest nonsense mutation. I observed that aux^{N7}/aux^{K47} and aux^{N7}/aux^{L7} genotype flies were viable and I could not detect any obvious eye phenotype. Subsequently, I looked for a wing phenotype as well and found that aux^{N7}/aux^{L7} flies

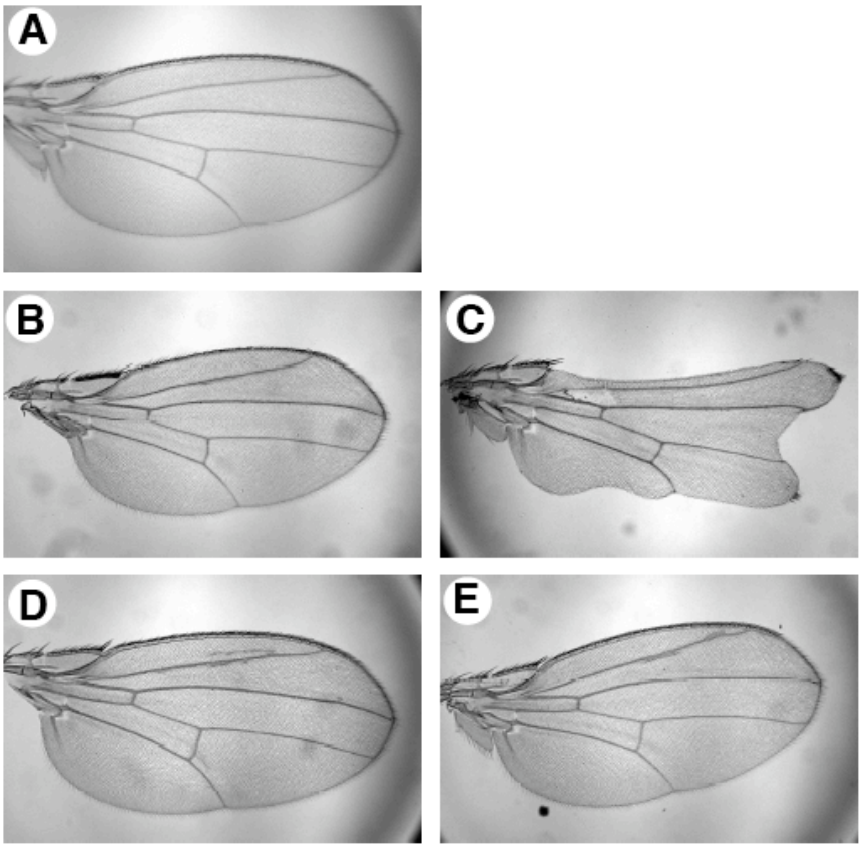

Figure 2.8. Wing phenotypes of allelic combinations with aux^{N7}. The genotypes are: (A) wild-type; (B) aux^{K47}/aux^{N7}; (C) aux^{K47}, lqf^{ARI}/aux^{N7}; (D) aux^{L7}/aux^{N7}; (E) aux^{L7}, lqf^{ARI}/aux^{N7}.

have abnormal wings. However, I could not observe any abnormality of aux^{N7}/aux^{K47} wings (Fig. 2.8.). Viable aux^{N7}/aux^{K47} and aux^{N7}/aux^{L7} flies that are also $lqf^{ARI}/+$ flies have abnormal eyes and wings while the other nonsense mutations over aux^{K47} or aux^{L7} with $lqf^{ARI}/+$ do not produce viable progeny (Fig. 2.8.). These results suggest that aux^{N7} is weaker than any other *auxilin* nonsense mutants I have, even though the stop codon in aux^{N7} is further upstream in the open reading frame. Maybe the characteristics of aux^{N7} are also because of other EMS-linked mutations on the chromosome.

I also examined wings of viable *auxilin* allelic combinations (Fig. 2.9.). The wing phenotype is highly variable, so it was difficult for me to determine the order of allelic strength. However, I conclude that the allelic hierarchy differs in the wing and eye. Sometimes, flies with the aux^{L7} allele have more severely mutant wings than flies with aux^{K47} (Fig. 2.9) though aux^{K47}, lqf^{ARI}/aux^{N7} flies have more severe wing phenotype than aux^{L7}, lqf^{ARI}/aux^{N7} flies (Fig. 2.8.). The expression of *auxilin* or the requirement for it might be different in the wings and eyes.

aux^{L7} is cold sensitive. At 25 °C, heterozygotes between aux^{L7} and any nonsense mutant are semi-viable and escapers have mutant eyes and wings. By contrast, at 18 °C these same heterozygous combinations are completely lethal.

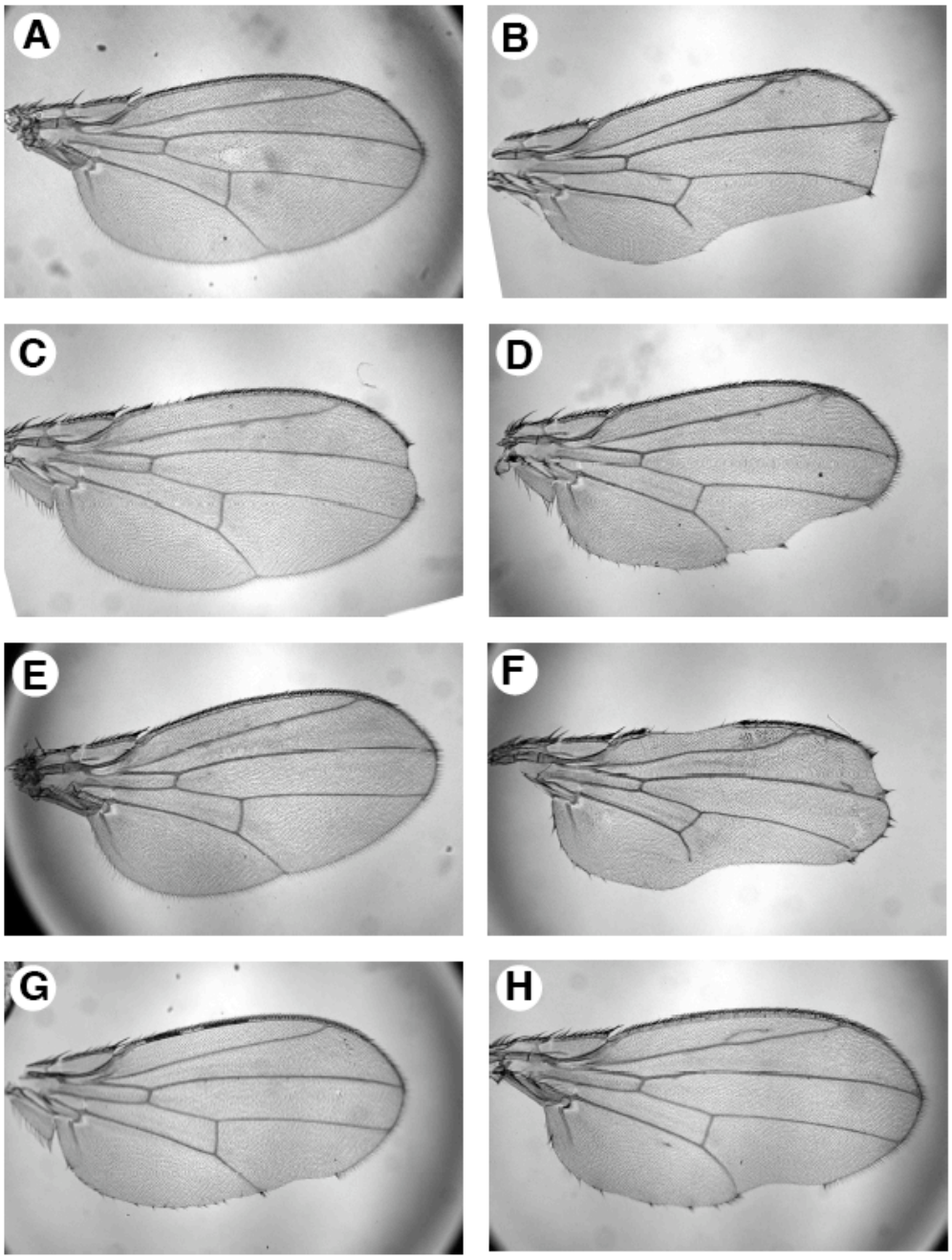
A
B
C
D
E
F
G
H

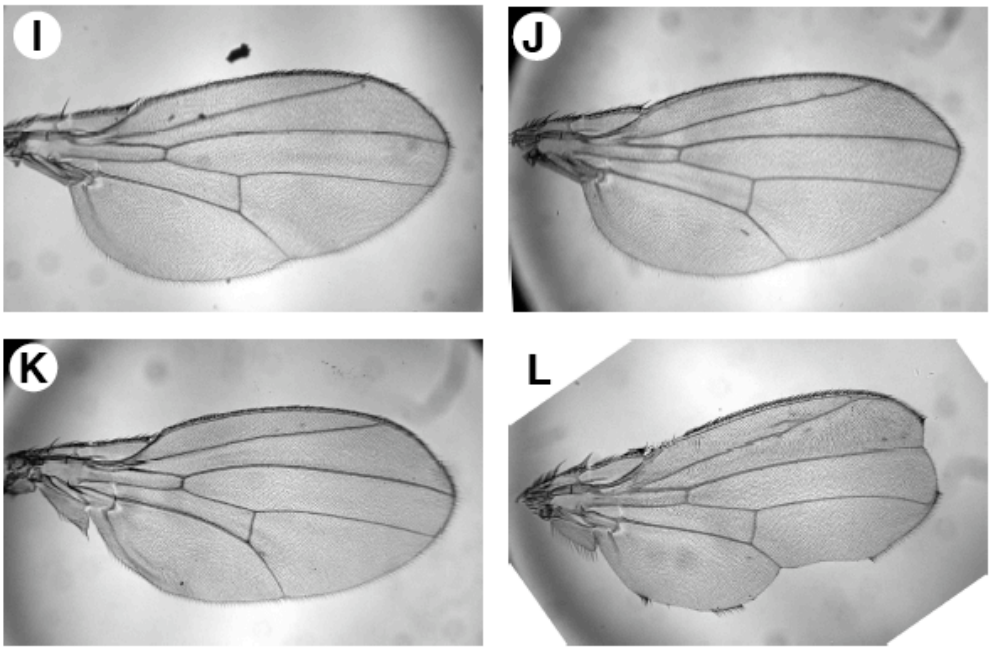

Figure 2.9. Wing phenotypes of *auxilin* hupomorphs. The genotypes are: (A) aux^{K47}/aux^{K5}; (B) aux^{L7}/aux^{K5}; (C) aux^{K47}/aux^{K48}; (D) aux^{L7}/aux^{K48}; (E) aux^{K47}/aux^{D136}; (F) aux^{L7}/aux^{D136};(G) aux^{K47}/aux^{C2}; (H) aux^{L7}/aux^{C2}; (I) aux^{K47}/aux^{J26}; (J); aux^{L7}/aux^{J26} (K) aux^{K47}/aux^{F37}; (L); aux^{L7}/aux^{F37}. For all escaper genotypes, the wing phenotypes show widely variable expressivity. The strongest pehnotypeof each genotype is shown.

2.3. Discussion

2.3.1. How *auxilin* was identified from the enhancer screen.

The *glrs-lqf* eye has extra outer R-cells and also no R7 cells. I did not determine exactly how this phenotype is caused by Lqf overexpression. However, I can think of two possible explanations for this phenotype. One is that overexpression of Lqf affects

directly the normal function of Lqf by titrating the components of Notch signaling. For R7 cell specification, Notch signaling is required. Therefore, it is possible that the phenotype was caused by the failure of Notch activation. The other idea is that the phenotype is caused by clathrin depletion. The addition of one copy of chc^{+} suppresses the *glrs-lqf* eye phenotype. This suggests that the eye phenotype is at least partly caused by clathrin depletion. It is also possible that the *glrs-lqf* phenotype is caused by both effects. Previously, our lab showed that *chc* dominantly enhances *lqf* hypomorphs (Cadavid et al., 2000) and my data support that Lqf-dependent Delta endocytosis is clathrin-dependent even if CCV formation is not required (see chapter 4). Therefore, clathrin depletion may cause Notch signaling defects. In chapter 4, I show that *auxilin* mutations also result in clathrin depletion. Thus, it seems possible that *auxilin* was recovered from this screen because both *auxilin* mutation and *glrs-lqf* deplete clathrin. Alternatively, *auxilin* mutants may have been isolated as enhancers of a Notch signaling failure due to *glrs-lqf*. However, *auxilin* mutants do not dominantly enhance the lqf^{FDD9} homozygous phenotype, so *auxilin* would not be recovered from a screen using *lqf* hypomorphs as the background.

2.3.2. Characteristics of *auxilin* alleles

From this screen, I isolated 12 mutant alleles of *auxilin* and I determined the molecular lesions of 11 alleles. Compared to the DNA sequence annotation in the FlyBase web site, all alleles contain the same DNA polymorphism: Glu28 (GAG) to Gly 28 (GGG). This polymorphism must be from the original isogenized parent generation.

There were no deficiency chromosomes that uncover the *auxilin* gene region, so I was not able to test if any of my alleles behave genetically like amorphs. (Now, there is one deficiency line, *Df(3R)ED5021*, which was added to FlyBase recently.) The clathrin-binding domain and the J domain of auxilin are necessary and sufficient for function in *Drosophila* (see chapter 4). Thus, one can expect that nonsense mutations that do not produce the clathrin-binding domain and the J domain would act as null mutants. Allelic combinations of nonsense and missense alleles show various degrees of severity. Even among nonsense mutations upstream of these domains, the degree of the phenotypes was different. Probably, each allele has different background effects on *auxilin* phenotypes. The two earliest nonsense alleles, aux^{D128} and aux^{727}, have stop codons in the kinase domain and their phenotypic severity is similar to each other. These two alleles may act like null mutations.

Among two missense alleles, aux^{K47} and aux^{L7}, I expected aux^{L7} to have a more severe phenotype because the aux^{K47} missense mutation is located in the PTEN domain which is unnecessary for auxilin function, while aux^{L7} has a mutation in the J domain which recruits Hsc70 and is necessary for function (see chapter 4). However, It is hard to compare these two missense alleles directly because aux^{L7} is cold-sensitive. At 25 °C, aux^{K47} has a more severe phenotype than aux^{L7} but at 18 °C, aux^{L7} has more severe phenotype. How can missense mutation in the unnecessary PTEN domain have a mutant phenotype? One possible explanation is that this specific mutation affects the overall conformation of auxilin.

Chapter 3. Role of auxilin in Notch signaling

3.1. Introduction

3.1.1 *Drosophila* auxilin

The uncoating role of auxilin has been studied in vitro (Ungewickell et al., 1995; Holstein et al., 1996; Jiang et al., 2000; Umeda et al, 2000; Scheele et al., 2003). Uncoating of CCVs is necessary for vesicle fusion with endosomes and maintenance of the free clathrin pool. Using the J domain, auxilin can bind and function with the Hsc70 ATPase that uncoats clathrin from CCVs (Ungewickell et al., 1995). In other organisms, it has been shown that auxilin always functions with Hsc70. However, the *hsc70* phenotype is more complicated than that of *auxilin* mutants. Hsc70 is more pleiotropic than auxilin and uncoating CCVs is only one of its functions. Null alleles of *hsc70* are cell lethal and weak alleles of *hsc70* show defects in endocytosis (Chang et al., 2002). Endocytic defects in *hsc70* mutants have not been studied in the context of Notch signaling. Recent publications show that auxilin also functions in fission of CCVs in cell culture. During this step, *auxilin* interacts with the GTP-bound form of dynamin as well as Hsc70 (Newmyer et al., 2003; Sever et al., 2005).

While my experiments were well in progress, Hagedorn et al (2006) published that auxilin functions in Notch activation. They found one missense allele and two nonsense alleles from a screen directed to find *auxilin* mutants using deficiencies. In *auxilin* mutants, they observed neurogenic phenotypes in the eye and the embryo. Also, they found that *auxilin* interacts genetically with *hsc70* and *Notch* in a manner that

implied that these genes work synergistically. Eye-specific expression of a dominant negative form of Hsc70 causes rough eyes and *auxilin* mutants enhance this phenotype. Also, *auxilin* mutants enhance the wing phenotypes of a haploinsufficient *Notch* mutant and the eye phenotype caused by eye-specific overexpression of full-length Notch that probably disrupts Notch-dependent processes. Using epistasis experiments, they concluded that auxilin functions upstream of the Notch receptor.

3.1.2 Endocytosis and Notch signaling

Endocytosis plays an important role in Notch signaling. Mosaic clonal analysis of *shibire* mutants (*shibire* encodes dynamin) during bristle formation showed that endocytosis is essential in the signaling cells as well as in the receiving cells (Seugnet et al., 1997). In *shibire* mutants, the signaling activity of ligand-independent membrane-bound Notch is unaffected. This result indicates that dynamin is not necessary for transferring signaling from Notch receptor to downstream components. Thus, dynamin function during endocytosis must be important for Notch activation (Seugnet et al., 1997). However, the reason why endocytosis is required in the receiving cells and in the signaling cells is not known. Lqf (epsin) is required in the signaling cells but not in the receiving cells (Overstreet et al., 2004; Wang and Struhl, 2004). The requirement for Lqf suggests that ligand endocytosis regulates Notch activation. Several models have been proposed to explain this. The first popular model is the 'pulling model.' In this model, endocytosis of Delta renders the mechanical force to expose the S2 cleavage site of Notch. A series of proteolytic cleavages of Notch is necessary for the downstream gene activation. Among those, S2 cleavage depends on endocytosis of Delta in the singling

cells. In the signaling cells, the extracellular domain of Notch is detected with Delta in the endosomal structure (Parks et al., 2000). A recent paper showed that Delta endocytosis is required for dissociation of the Notch heterodimer that is essential for Notch activation (Nichols et al., 2007). The second popular model is the 'recycling model.' When Delta inner membrane portion is replaced by LDL receptor inner membrane portion, it overcomes the failure of Delta endocytosis caused by *lqf* mutants. After internalization, LDL receptor is recycled to the plasma membrane. This result suggests that epsin-dependent Delta recycling is required for Notch activation. Wild-type cells contain a certain Delta cleavage form which is not detected in *lqf*$^{-}$ cells. Thus, Delta recycling might be required to convert Delta to an active form (Wang and Struhl, 2004). The requirement in the signaling cells for Sec15 and Nuf, which function with Rab11 to regulate recycling, supports the recycling model (Emery et al., 2005; Jafar-Nejad et al., 2005). However, a requirement for recycling in the signaling cells has not been shown directly. Also, it is not known whether or not there is a truncated or modified active form of Delta. The third popular model is the 'exosome model.' In this model, endocytosed Delta accumulates in vesicles within multi-vesicular bodies (MVB) and clustered Delta is released as exosomes (Le Borgne and Schweisguth, 2003). In *C. elegans* and mammalian cultured cells, soluble DSL ligands can activate Notch signaling (Fitzgerald and Greenwald, 1995; Li et al., 1998; Wang et al., 1998). This model may explain the long-range activity of Delta sometimes observed. However, in most cases, Notch activation requires cell-cell interaction and in flies, a secreted form of DSL ligand acts as a dominant negative (Hukriede and Fleming, 1997; Hukriede et al., 1997; Sun and Artavanis-Tsakonas, 1997). I think that these models are not mutually exclusive. A single

cell could require Delta endocytosis more than one thing or different cells during different developmental stages may require Delta endocytosis for the different regions.

3.1.3. Ubiquitin, clathrin, and Lqf in Delta internalization

Ubiquitination is used as an internalization signal for many signaling receptors. The E3 ubiquitin ligase genes, *neuralized* and *mind bomb*, are important for Delta and Serrate signaling and ubiquitination of Delta. These results suggest that ubiquitination is a signal for Delta internalization. Our lab showed previously that Delta endocytosis that can activate Notch in neighboring cells is Lqf-dependent (Overstreet et al., 2004). Lqf contains clathrin-binding motifs and ubiquitin binding motifs. In mammalian cells, EGFR is endocytosed either in a clathrin-independent pathway with ubiquitination or in a clathrin-dependent pathway without ubiquitination. It has been shown that for EGFR endocytosis, epsin functions only in the clathrin-independent pathway (Sigismund et al., 2005). Other cell culture data suggest that epsin can bind either clathrin or ubiquitin but not both at the same time. Delta uses ubiquitin as an internalization signal and Delta endocytosis is Lqf-dependent (Chen and De Camilli, 2005). Does this mean that Delta is endocytosed in a clathrin-independent way? Loss-of-function mutations in the *chc* gene are strong enhancers of *lqf* hypomorphs. This suggests that *chc* functions synergistically with *lqf*. The mammalian cell culture data seems to conflict with the genetic interaction between *chc* and *lqf*, unless we can come up with a model where *chc* positively regulates Notch ligand endocytosis without CCV formation (see below). Also, recent papers suggested that epsin binds ubiquitinated membrane proteins and functions in clathrin-dependent endocytosis (Barriere et al., 2006; Hawryluk et al., 2006).

Here I show that auxilin is required for Notch activation only in the signaling cells at least in part in order to maintain the free clathrin pool. My data suggests that Delta endocytosis for Notch activation is clathrin-dependent but not necessarily through CCV formation. I discuss the implications of auxilin function for the functions of clathrin and epsin in Notch signaling.

3.2 Results

3.2.1 The phenotypes of *auxilin* hypomorphs

auxilin mutants were identified as enhancers of the phenotype caused by lqf^{+} overexpression in the eye (see chapter 2). Certain allelic combinations of *auxilin* mutants produce lethal escapers with *Notch*-like morphological phenotypes. If auxilin functions in the same pathway with Lqf and Delta, *auxilin* mutants should show a similar phenotype to *lqf* and *Delta* mutants. There are noticeable eye and wing phenotypes in *auxilin* hypomorphs. I examined hypomorphic *auxilin* phenotypes in aux^{D128}/aux^{K47} flies, because they show the strongest phenotype among the viable *auxilin* allelic combinations. The exterior eyes of these flies show roughness. In adult eye sections, many facets have extra R-cells (Fig. 2.7.), a typical phenotype of weak Notch pathway mutants. Shortly after the morphogenetic furrow passes through, Notch signaling is important to restrict the outer R-cell number to six. Failure of Notch signaling at this point causes the extra R-cell phenotype. Hypomorphic mutants of *lqf* or *Delta* show the same phenotype

(Overstreet et al., 2004). This phenotype suggests that *auxilin* may function during Notch signaling. Also, most facets are disorganized and some facets have fewer photoreceptor cells. Notch signaling is required in many contexts during eye development. These latter phenotypes could be caused by failure of Notch signaling in different eye developmental contexts such as lateral inhibition.

Hypomorphic *auxilin* mutants have wing phenotypes such as notched wings, extra veins and missing veins (Fig. 2.9.). These phenotypes are also similar to the phenotypes of *lqf* and *Delta*. The *auxilin* mutant wing phenotypes also suggest that *auxilin* functions during Notch signaling.

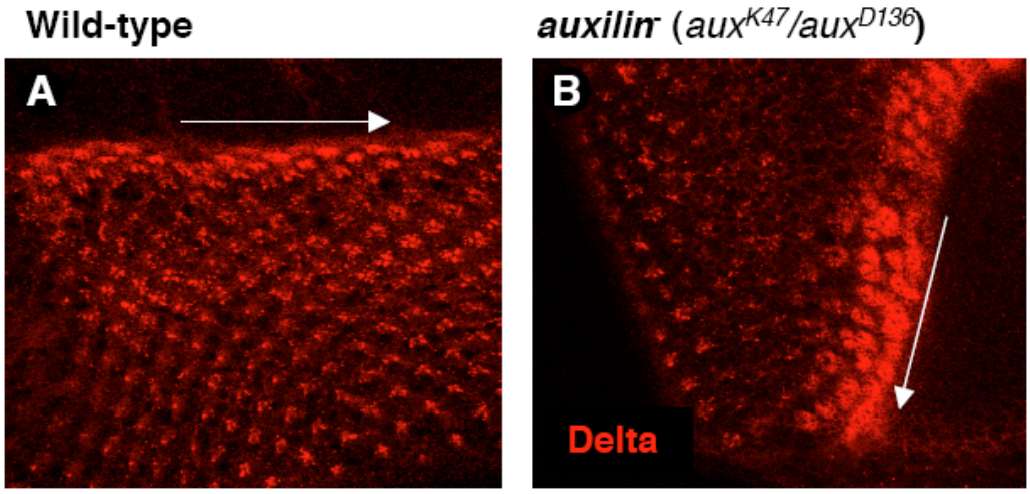

Figure 3.1. Delta accumulates at the morphogenetic furrow in *auxilin*⁻ eye discs. Wild-type (A) and *auxilin* hypomorph (aux^{K47}/aux^{D136}) (B) eye discs are labeled with Delta antibody. A disc hypomorphic for *auxilin* activity has excessive Delta on plasma membranes near the furrow (arrow) compared with wild-type cells.

Another *lqf* phenotype is accumulation of Delta at the morphogenetic furrow (Overstreet et al., 2004). This phenotype can be caused by a failure in Delta signaling during lateral inhibition. Failure of lateral inhibition results in transcriptional upregulation of Delta. The Delta accumulation may also be due to endocytosis failure of Delta (see 3.2.5 below). I stained *auxilin* hypomorphic eye discs with α-Delta antibody (Fig. 3.1.). The failure of Notch signaling at the morphogenetic furrow induces excess Delta transcription. Similar to *lqf*, Delta accumulates at the morphogenetic furrow in *auxilin* mutants.

Because in yeast, *auxilin* mutants result in an increase in membrane accumulated clathrin, for example, CCPs and CCVs, I expected more clathrin puncta in *auxilin* hypomorphs (Gall et al., 2000). In order to see the clathrin vesicle morphology in *auxilin* mutants, I compared the GFP-clc staining pattern between aux^{D128}/aux^{K47} and wild-type eye discs. I performed this experiment before I realized that GFP-Clc and Chc do not coincide. Because there is no *clc* mutant, I cannot determine whether *GFP-clc* is functional or not. I showed that *chc* mutants enhance *lqf* and *auxilin* phenotypes and that addition of chc^{+} suppresses *lqf* and *auxilin* phenotypes (see chapter 4). However, *GFP-clc* expression enhances *lqf* and *auxilin* phenotypes (Fig. 3.2). I think that the *GFP-clc* transgene has a dominant negative characteristic probably by quenching Chc or other proteins. In *auxilin* hypomorphs, I detect fewer and larger GFP-Clc positive puncta (Fig. 3.3.) though this result is not informative. A better way to perform this experiment is probably to use α-Chc antibody.

3.2.2 Generation of *auxilin* mosaic clones

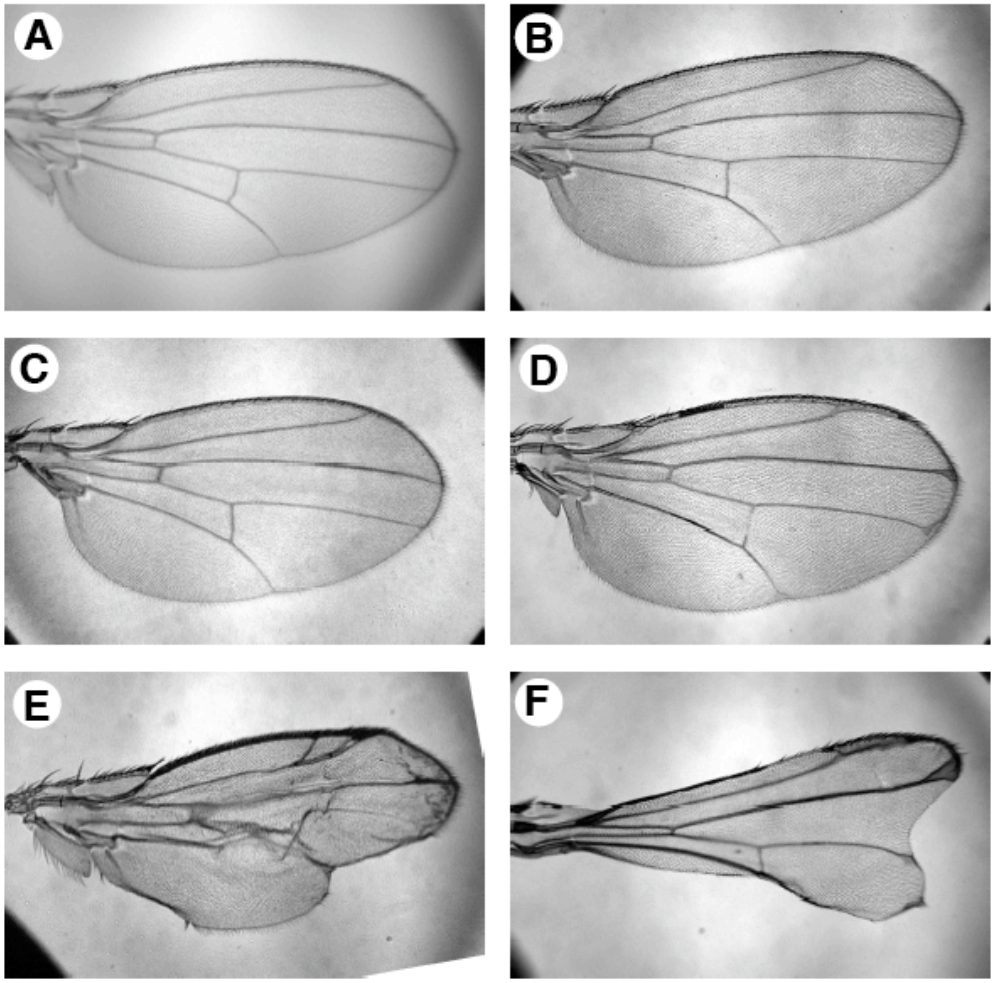

Figure 3.2. Expression of GFP-Clc enhances the *auxilin*$^{-}$ and *lqf* phenotypes. The wings of *auxilin*$^{-}$ and *lqf* are shown. The genotypes are wild-type (A), *Actin5C-gal4*/*UAS-gfp-clc* (B), aux^{K47}/aux^{D136} (C), lqf^{FDD9}/lqf^{FDD9} (D), *Actin5C-gal4*/*UAS-gfp*-clc; aux^{K47}/aux^{D136} (E), *Actin5C-gal4*/*UAS-gfp-clc*; lqf^{FDD9}/lqf^{FDD9} (F). There are abnormal phenotypes when GFP-Clc is expressed in wild-type background. However, in *auxilin*$^{-}$ and *lqf* hypomorphic background, it enhanced the wing phenotypes.

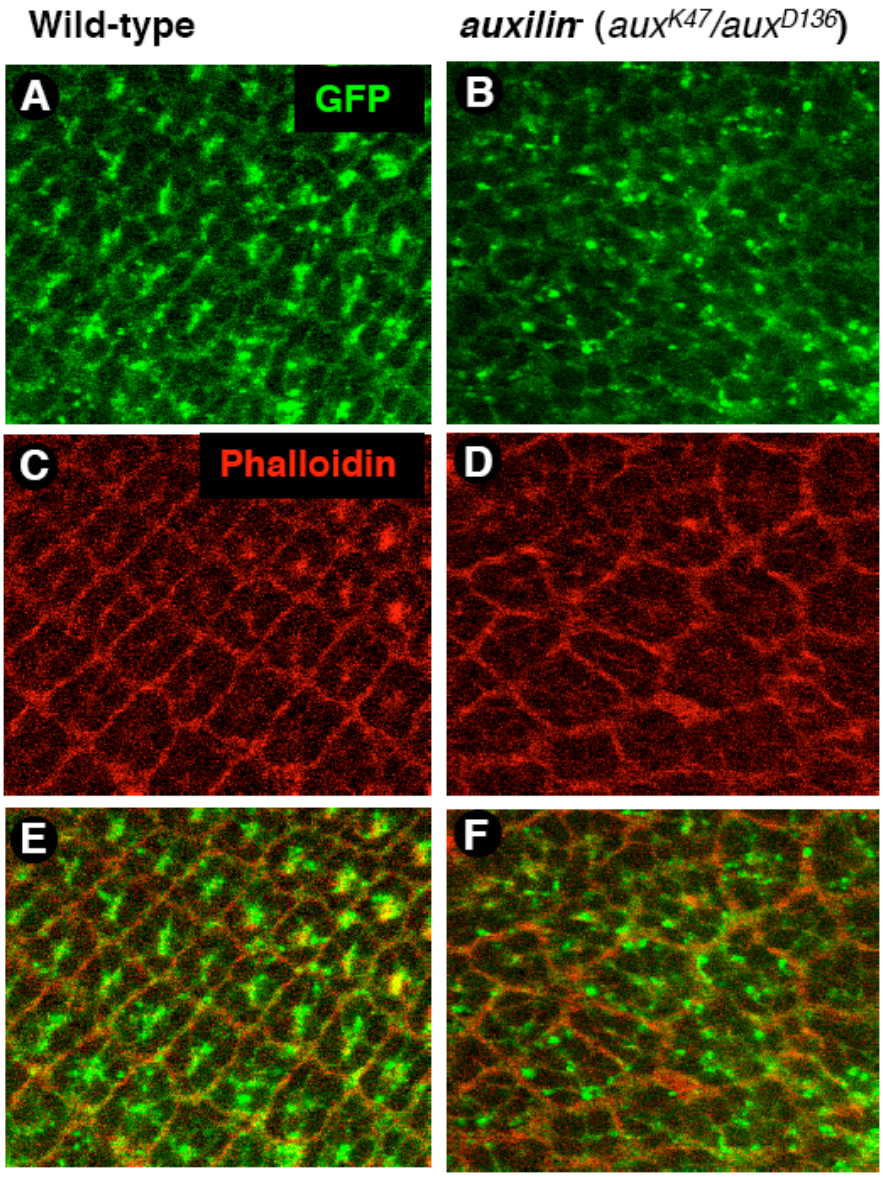

Figure 3.3. GFP-Clc staining pattern in auxilin hypomorphs. Confocal microscope images of third instar larval eye discs in wild-type (A,C,E) and auxilin hypomorph (aux^{K47}/aux^{D128}) (B,D,F) are shown. GFP-clc (Green) is localized near the plasma membrane stained by phalloidin (red). In *auxilin*$^{-}$, the number of GFP-clc puncta is reduced and the size is increased. E and F are merged image

I want to determine the function of *auxilin* in the eye disc. The strong alleles are homozygous lethal. To see the strong *auxilin* mutant phenotypes, I need to generate clones of homozygous mutant cells in otherwise heterozygous animals. I planned originally to perform three different kinds of mosaic clonal analysis: (1) FRT-induced mitotic recombination, (2) FLP-ing out of an *auxilin*$^{+}$ transgene, and (3) turning off *auxilin*$^{+}$ expression in specific cells using GAL80.

FRT-induced mitotic recombination is the more standard method for generating mutant clones in *Drosophila*. The second and the third methods were not performed previously in precisely the way I had planned and they presented potential difficulties. I tried these methods because I expected them to allow me to ask questions about auxilin function in more specific cells and developmental stages. However, they did not work (see Appendices).

The FRT-induced mitotic recombination technique allowed me to generate large *auxilin*$^{-}$ clones. To generate clones in the eye, I used *eyeless-FLP* (*eyFLP*) which is transcribed from an early developmental stage in the eye. Because the *auxilin* gene is located very close to the centromere, all available FRT sites are distal to it. To perform FRT-induced mitotic recombination, I needed to use an *auxilin*$^{+}$ rescue transgene located distal to an FRT site on a chromosome other than 3. The idea is to generate flies where the endogenous *auxilin* genes are mutant, so the only source of *auxilin*$^{+}$ activity is from the transgene. Clones are induced that lack the transgene. I obtained several genomic and cDNA rescue transgenes. Among these, I used a genomic rescue transgene located on the right arm of the second chromosome or a cDNA rescue transgene located on the left arm of the second chromosome. I generated fly stocks which allowed me to perform mosaic

clonal analysis by FRT/FLP-induced mitotic recombination. I dissected eye discs from flies whose genotype is *w, eyFLP/Y or +; FRT42D, P{w$^+$, gaux$^+$}, P{ w$^+$, ubiquitin-GFP}/FRT42D; aux^{D136}/aux^{727}*. I could identify the homozygous *auxilin$^-$* clones by the absence of GFP.

3.2.3 Auxilin is required for Notch activation during eye development

Notch signaling is important in several steps during *Drosophila* eye development. Among those, I can detect the consequences of Notch signaling failure near the morphogenetic furrow. In order to detect if Notch activation is affected by the lack of auxilin, I generated *auxilin$^-$* clones in heterozygous animals using FRT-induced mitotic

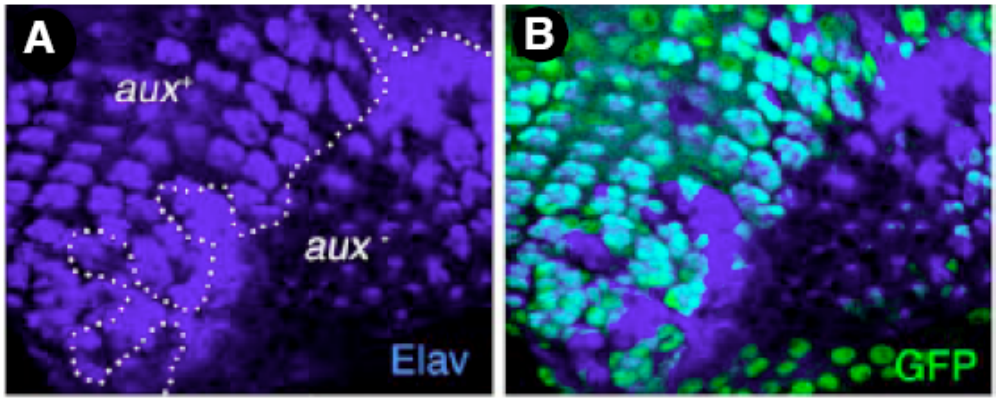

Figure 3.4. *auxilin$^+$* is required for Notch activation during proneural enhancement. Confocal microscope images of third instar larval eye discs are shown. A clone of *auxilin$^-$* (*aux^{727}/aux^{D136}*) cells outlined in A, marked by the absence of GFP, was generated in flies of the genotype *w, eyFLP; FRT42D gaux$^+$, Ubi-gfp / FRT42D; aux^{727}/aux^{D136}*. R-cell nuclei are blue. In the middle of *auxilin$^-$* clone, Elav$^+$ cells are absent.

recombination. Before the morphogenetic furrow, Notch activation is required for proneural enhancement in every cell to provide potency to become a neural cell. Expression of the proneural transcriptional factor, Atonal, is increased by Notch activation. The failure to enhance Atonal expression results in no photoreceptor cells. I stained *auxilin* mosaic eye discs with α-Elav antibody which labels the nuclei of neural cells (Fig. 3.4). In the middle of *auxilin*$^{-}$ mutant clones, there were no Elav^{+} cells. This is consistent with loss of proneural enhancement and failure to generate neural cells.

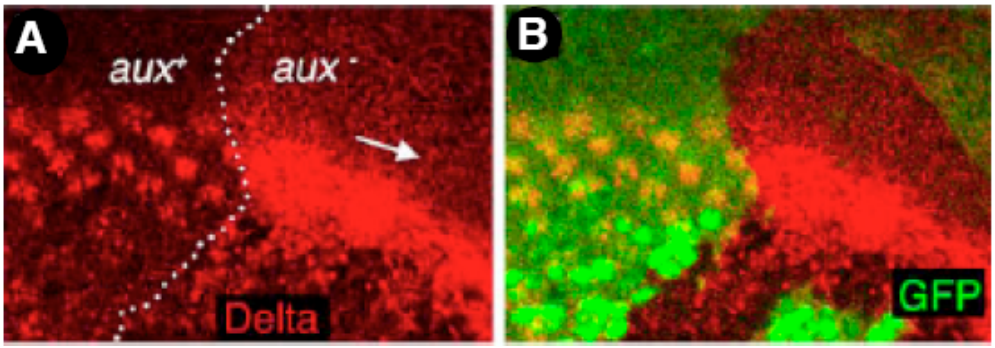

Figure 3.5. *auxilin*$^{+}$ is required for Notch activation during latral inhibition. Confocal microscope images of third instar larval eye discs are shown. A clone of *auxilin*$^{-}$ (*aux*^{727}/*aux*^{D136}) cells outlined in A, marked by the absence of GFP, was generated in flies of the genotype *w, eyFLP; FRT42D gaux*$^{+}$*, Ubi-gfp / FRT42D; aux*^{727}/*aux*^{D136}. Delta protein, which is punctate (in intracellular vesicles) in wild-type and both punctate and on the membrane in *auxilin*$^{-}$ cells, is red. In the *auxilin*$^{-}$ clone, Delta accumulates on the membrane at the morphogenetic furrow (arrow).

In the morphogenetic furrow, Notch activation is important for lateral inhibition to restrict neural potency into spatially organized neural clusters. *auxilin*$^{-}$ cells at clone borders are Elav^{+} because they are adjacent to Delta^{+} (wild-type) cells and therefore they upregulate Atonal. The failure of lateral inhibition among these *auxilin*$^{-}$ border cells results in disorganized clumps of neural clusters (Fig. 3.4.). Another indicator of lateral inhibition failure is elevated expression of Delta at the morphogenetic furrow. To detect the Delta expression level, I labeled eye discs with α-Delta antibody (Fig. 3.5). Similar to the hypomorphic phenotype, more Delta staining is detected in *auxilin*$^{-}$ clones. Also to observe the Delta transcription level, I used a *Dl-lacZ* enhancer trap. LacZ expression is

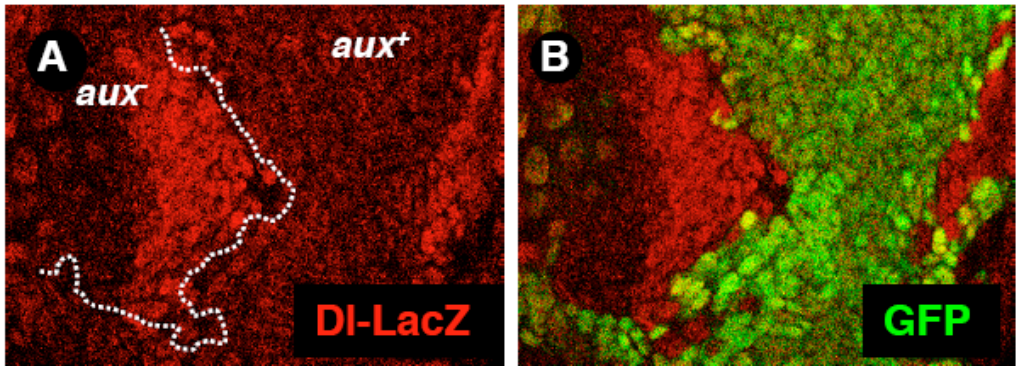

Figure 3.6. *auxilin*$^{+}$ is required for Notch activation during lateral inhibition. Confocal microscope images of third instar larval eye discs are shown. A clone of *auxilin*$^{-}$ (*aux*^{727}/*aux*^{D136}) cells in discs that express β-galactosidase from an enhancer trap in the *Delta* gene (*Dl-lacZ*) was generated in flies of the genotype *w, eyFLP; tubulin-aux*$^{+}$*, Ubi-gfp, FRT40A/ FRT40A; aux*^{D136}*, Dl-lacZ/aux*^{727}. Elevated cytoplasmic β-galactosidase (red) levels are observed in the clone near the furrow (arrow).

elevated within the *auxilin*$^{-}$ clone (Fig. 3.6). These results suggest that auxilin is required during lateral inhibition.

At row 2-3 posterior to the morphogenetic furrow, in order to limit the number of outer R-cells to six, Notch signaling must be activated in excess precluster cells by Delta presented in R2/5 and R3/4 cells. This phenomenon is called R-cell restriction. Lqf and Fat facets (Faf) are required in R2/5 and R3/4 cells for Delta endocytosis and signaling. Faf is a deubiquitinating enzyme that deubiquitinates Lqf and thus increases its level or activity. The eye phenotype in *lqf* hypomorphs and *faf* null mutants is rescued completely by a *RO-lqf* transgene, which express *lqf*$^{+}$ only in R2/5 and R3/4 cells (Cadavid et al., 2000). When a dominant negative form of Shibire or a dominant negative form of Delta that cannot be internalized is expressed by the RO vector, extra R-cells are generated. These results indicate that Delta endocytosis is important in R2/5 and R3/4 cells to prevent adjacent cells from becoming R-cells. To express *auxilin*$^{+}$ only in R2/5 and R3/4 cells, I generated *RO-auxilin* transgenic flies. In a hypomorphic *auxilin*$^{-}$ background, *RO-auxilin* rescues the *auxilin*$^{-}$ eye phenotype significantly but not completely (Fig. 3.7). The facets not rescued were disorganized. These facets might be due to the failure of lateral inhibition before transgene expression. The rescue by *RO-auxilin*$^{+}$ indicates that *auxilin* is required in R2/5 and R3/4 cells and might be required for the Delta endocytosis in these cells.

3.2.4. *auxilin*$^{+}$ is required only in the signal sending cells not in the receiving cells like *lqf*.

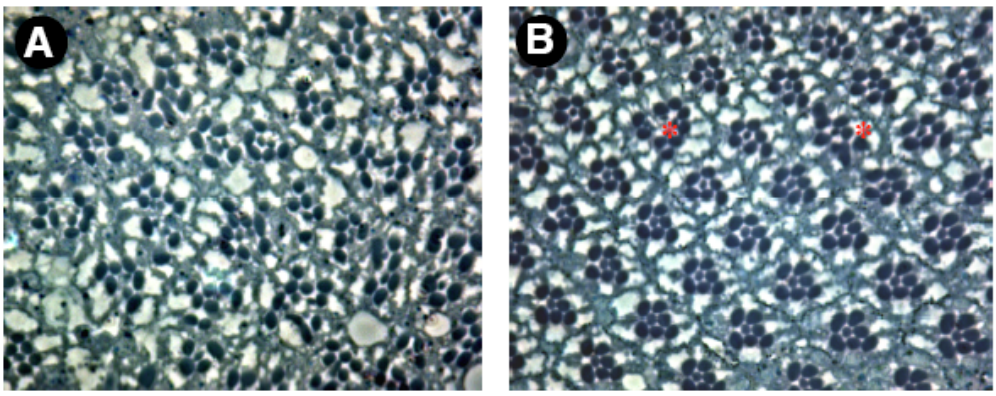

Figure 3.7. *auxilin*$^{+}$ is required in R2/5 and R3/4 cells. Tangential sections of adult eye are shown. Abnormal eye phenotype of *auxilin*$^{-}$ (*aux*^{K47}/*aux*^{D128}) (A) is suppressed by expression of *auxilin*$^{+}$ in R2/5 and R3/4 cells. The genotype of B is *w*; *RO-auxilin*$^{+}$/+; *aux*^{K47}/*aux*^{D128}. However, the complementation of *auxilin*$^{+}$ expression is not complete. Asterisks in B indicate mutant facets.

In order to activate Notch, endocytosis in the receiving cells as well as signaling cells are required. Interestingly, Lqf is required only in the signaling cells not in the receiving cells. The observation that Elav^{+} cells are present in *auxilin*$^{-}$ clones only at the clone borders where they are adjacent to *auxilin*$^{+}$ cells suggests that *auxilin*$^{+}$ is required in the signaling cells only. Also, suppression of the *auxilin*$^{-}$ eye phenotype by expression of auxilin in R2/5 and R3/4 cells suggests that *auxilin*$^{+}$ is required in the signaling cells.

I also asked whether Notch could be activated in *auxilin*$^{-}$ cells. I stained *auxilin*$^{-}$ mosaic clones with α-E(spl) antibody (Fig. 3.8.). The *E(spl)* gene is a direct target of Notch signaling. If I generate mosaic clones with genes required in the receiving cells such as *Notch*, I cannot detect the expression of the *E(spl)* gene in the mutant side, because *Notch* is required in the same cell where *E(spl)* is expressed. However, if I

generate mosaic clones with genes required only in the signaling cells such as *Delta* and *lqf*, I can detect the expression of the *E(spl)* gene in the mutant side at the border of the clone, because these cells can get signal from the adjacent wild-type cells. In the middle of large *auxilin*$^{-}$ clones, I could not detect the expression of *E(spl)*. Thus, *auxilin* is required for Notch activation during proneural enhancement. More importantly at the clone border, I could detect E(spl) in *auxilin*$^{-}$ cells. This result indicates that Notch can be activated in *auxilin*$^{-}$ cells as long as they are adjacent to *auxilin*$^{+}$ cells that can signal. Therefore, *auxilin* is required in the signaling cells not in the receiving cells.

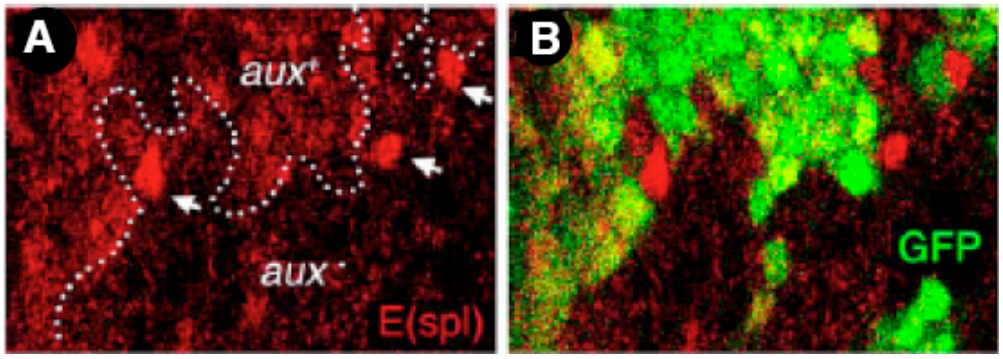

Figure 3.8. *auxilin*$^{+}$ is required in the signaling cells but not in the receiving cells. Confocal microscope images of third instar larval eye discs are shown. A clone of *auxilin*$^{-}$ (*aux*^{727}/*aux*^{D136}) cells outlined in A, marked by the absence of GFP, was generated in flies of the genotype *w, eyFLP; FRT42D gaux*$^{+}$*, Ubi-gfp / FRT42D; aux*^{727}/*aux*^{D136}. Red nuclei express E(spl), and the arrows indicate three red *auxilin*$^{-}$ nuclei. Near the border of the clone, *auxilin*$^{-}$ cells express E(spl).

3.2.5. Auxilin is required for Delta endocytosis.

auxilin mutants have shown endocytosis failure (Pishvaee et al., 2000; Umeda et al., 2000). Failure of the auxilin function during fission can result in an endocytosis defect. Also, clathrin depletion caused by failure of uncoating CCVs can result in an endocytosis defect. If Delta endocytosis for signaling requires clathrin, Delta internalization for signaling should be blocked in *auxilin* mutants. In *auxilin* hypomorphic eye discs, excessive Delta accumulates on *auxilin*$^{-}$ cell membranes beginning at the furrow like in *lqf* mutants (Fig. 3.9.A) (Overstreet et al., 2003; Overstreet et al., 2004). As described above, Delta transcription is increased by the

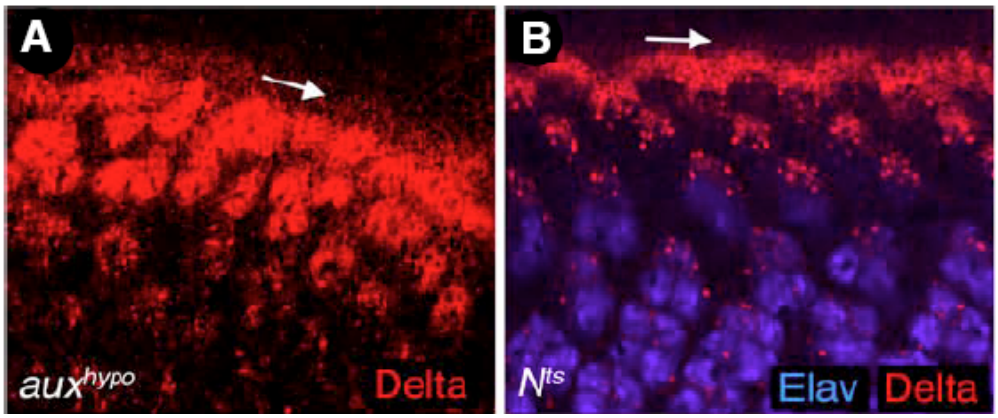

Figure 3.9. Auxilin is required for Delta endocytosis. (A) A disc hypomorphic for *auxilin* activity (aux^{K47}/aux^{D136}) has excessive Delta on plasma membranes near the furrow (arrow). (B)This picture was generated bt Erin Overstreet. A $Notch^{ts}$ (N^{ts}) disc from a larva incubated at the restrictive temperature (29 °C) for 6 hours prior to dissection. There is excessive Delta on the plasma membrane at the furrow (arrow). In *auxilin* hypomorphs, Delta on the membrane perdured further to the posterior than in $Notch^{ts}$.

failure of lateral inhibitory Notch signaling at the furrow (Baker and Yu, 1998; Wang and Struhl, 2004). When the *Notch*^{ts} is raised to the restrictive temperature for 6 hours, the similar phenomenon is detected in the eye discs (Fig. 3.9.B) (Baker and Yu, 1998). However, in *auxilin*$^{-}$ clones (Fig. 3.5.) and hypomorphs, Delta remained on the plasma membrane longer (further to the posterior) than in *Notch*^{ts}. One interpretation is that in *auxilin*$^{-}$ (and *lqf*) cells, Delta remains on the plasma membrane due to failure of endocytosis.

3.3. Discussion

3.3.1. Auxilin is required during Notch activation.

During *Drosophila* eye development, Notch activation functions in the several steps with different consequences. Complete failure of Notch signaling has a catastrophic effect on patterning in a clone of mutant cells. Therefore, only Notch signaling events that occur near the morphogenetic furrow are detectable. Together, the absence of Elav and E(spl) expression in the middle of *auxilin*$^{-}$ clones suggests that auxilin is required for proneural enhancement. Also, the failure of lateral inhibition is evident from clumped neural clusters as well as Delta and Dl-lacZ enhancer trap expression patterns.

Disorganized and clumped neural clusters result in the determination of more photoreceptor cells. Is more Delta expression caused by an increased number of Delta-expressing cells or by increased expression of Delta in each cell? Delta is expressed in

neural clusters and later in the photoreceptor cells. More Delta staining and more Dl-lacZ expression results from larger proneural clusters. However, there is prolonged Dl-lacZ expression in the *auxilin*$^{-}$ side of the clone meaning that stable LacZ protein is present in the cells for a longer time. If there were simply more neural clusters, I would expect to see more intensive staining at the morphogenetic furrow only.

Extra R-cells in *auxilin* hypomorphs and suppression of this phenotype by expressing auxilin in R2/5 and R3/4 cells indicates that auxilin is required during R-cell restriction. Thus, auxilin is required in all three Notch signaling events near the morphogenetic furrow. Hagedorn et al (2006) showed that the absence of auxilin results in overneuralized embryos. Probably, auxilin is essential for all Notch signaling events.

On *auxilin*$^{-}$ sides of clones, there are cells expressing Elav even though they are several cells away from the clone border and *auxilin*$^{+}$ cells. This phenotype is also observed in the *lqf* and *Delta*$^{-}$ mosaic clones. They must be have received Delta signal to get neural potency from *auxilin*$^{+}$ cells. One possible idea is that Delta is secreted to the extracellular matrix and in cultured mammalian cells and *C. elegans*, secreted forms of ligands can activate Notch. However, in most developmental contexts, Notch is activated by cell-cell interaction and in flies, a secreted form of ligand acts as a dominant negative (Hukriede and Fleming, 1997; Hukriede et al., 1997; Sun and Artavanis-Tsakonas, 1997). I don't think there is a simple explanation for this phenomenon.

3.3.2. Auxilin is required in the signaling cells not in the receiving cells.

Lqf is required only in the signaling cells to control Delta endocytosis. To ask whether auxilin is also required only in the signaling cells, I wanted to look at adult eyes

with mosaic ommatidia. The idea is to ask if in phenotypically mutant mosaic ommatidia with extra R-cells, the extra R-cells can be *auxilin*$^{+}$. If so, this would mean that cells failing to receive the Notch signal can be *auxilin*$^{+}$, and implies that other adjacent cells need to be *auxilin*$^{+}$ to send the signal. First, I embedded and sectioned eyes of flies whose genotype was *w*, *eyFLP*/*Y* or +; *FRT42D*, *P{w*$^{+}$, *gaux}*, *P{w*$^{+}$, *ubiquitin-GFP}*/*FRT42D*; *aux*^{D128}/*aux*^{K47}. The mutant phenotype in the mutant clones was too weak to generate many ommatidia containing extra R-cells and the *w*$^{+}$ transgenes were too weak to mark the *auxilin*$^{+}$ cells efficiently. In order to be able to use a good *Pw*$^{+}$, I used radiation (a cesium source) to induce mitotic recombination in the flies whose genotype is *w*; *auxilin*$^{-}$ /*Pw*$^{+}$. Radiation usually induces mitotic recombination close to the centromere. Even though the *auxilin* gene is close to the centromere, I expected to get some *auxilin*$^{-}$ mosaic clones. To mark wild-type cells, I used a *Pw*$^{+}$ which is located on 3R and which, we already know, is strong enough to produce pigment granules reliably in each *w*$^{+}$ R-cells. Auxilin is required from a very early stage of eye development, so I expected to see no R-cell differentiation in clones homozygous for strong alleles. To induce extra R-cells in the homozygous mutant, I used weaker mutant alleles such as *aux*^{N7}, *aux*^{D136}, and *aux*^{K48}. I embedded and sectioned several *w*$^{+}$ mosaic eyes from each allele. Many of them had no abnormal eye phenotype. It indicates that mitotic recombination happened between the *auxilin* mutant and the *Pw*$^{+}$. I could obtain only one mutant eye from *aux*^{K48} and it had ommatidia containing an extra R-cell (Fig. 3.10.). All rhabdomeres of R-cells had pigment granules which represented *auxilin*$^{+}$. This result suggests that a cell that fails to receive a Delta signal can be *auxilin*$^{+}$.

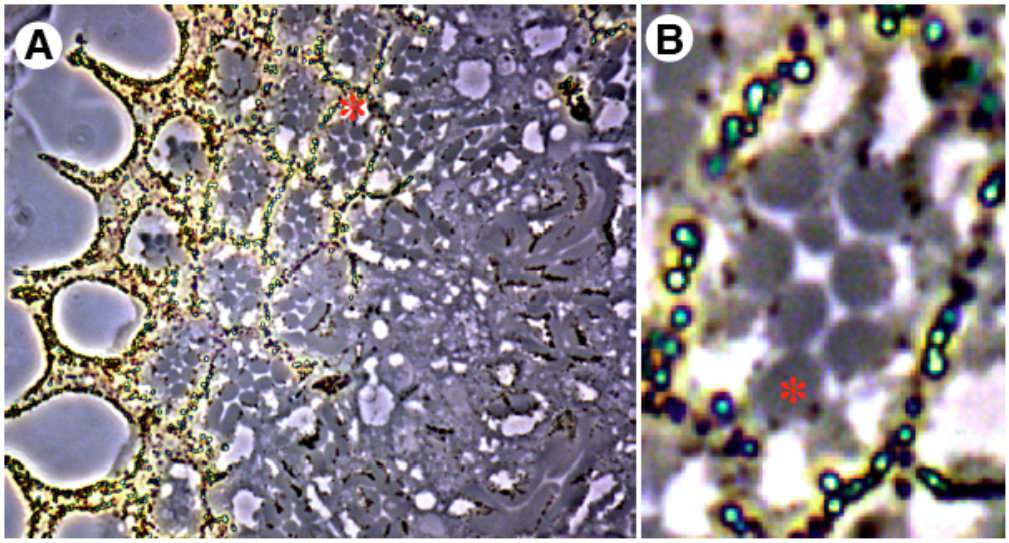

Figure 3.10 Auxilin is not required in the receiving cells. (A) A clone of *aux*^{K48} cells in the adult eye, indicated by the absence of pigment granules in pigment cells, is shown. The red asterisk indicates the ommatidium enlarged in B.(B) A phenotypically mutant facet at the clone border, in which all of the R-cells, including the ectopic R-cell (red asterisk), are w^{+} *aux*$^{+}$.

During R-cell restriction R2/5 and R3/4 cells send Delta signal to activate Notch in the neighbor cells to prevent these cells from becoming R-cells. One interesting observation of the mutant facets containing an extra R-cell in the *aux*^{K48} mosaic eye is that no R-cells are *auxilin*$^{-}$. The extra R-cell phenotype has been known to be caused by failure of Delta signaling from R2/5 and R3/4 cells. The extra R-cells in the *aux*^{K48} mosaic eye must fail to get Delta signal from the *auxilin*$^{-}$ cell which is not any of R2/5 and R3/4 because all of R2/5 and R3/4 are wild-type. I cannot explain the mechanism for

how the extra R-cell is generated and which cell fails to send a Delta signal. One possible interpretation is that lateral inhibition fails in those specific facets. It seems impossible to separate lateral inhibition and R-cell restriction sharply. Another interesting feature is that all R-cells in the mutant eye of aux^{K48} homozygous were $auxilin^{+}$ and I could not find any rhabdomere which did not contain pigment granules. Probably, *auxilin* is so important to generate R-cells that $auxilin^{-}$ cells died during early eye development.

To determine how the extra R-cells in aux^{K48} mutants appear and to generate more quantification of data of $auxilin^{+}$ extra R-cells, further experiments are required. To generate adult eye clones, I used X-rays. An efficient way to generate adult eye clones is to use FRT-induced mitotic recombination. To use this method, I would need to generate flies whose genotype is *w*, *eyFLP*/*Y* or +; *FRT42D*, $P\{w^{+}, gaux\}$, Pw^{+}/*FRT42D*; aux^{-}/aux^{-} or *w*, *eyFLP*/*Y* or +; $P\{w^{+}, caux\}$, Pw^{+}, *FRT40A*/*FRT40A*; aux^{-}/aux^{-}. The Pw^{+} which is used for the marker must be strong enough to produce pigment granules in each R-cell. There are two known Pw^{+} transgenes which are used for this purpose on each 2nd chromosome arm. Pw^{+} transgenes need to be recombined with a genomic or cDNA $auxilin^{+}$ rescue transgene first. If I generate adult eye clones using FRT-induced mitotic recombination, I would obtain more mosaic eyes and observe the extra R-cells caused by failure of R-cell restriction.

Chapter 4. Auxilin structure and functional analysis

4.1. Introduction

Drosophila has only one *auxilin* that is similar to GAK also known as mammalian auxilin2. Both *Drosophila* auxilin and GAK contain a kinase domain, a PTEN domain, a clathrin-binding domain and a J domain. *C. elegans* and yeast auxilin homologs do not contain the kinase and the PTEN domains. Thus, *Drosophila* auxilin might have more regulatory roles than *C. elegans* and yeast auxilin homologs. The presence of the kinase and PTEN domains, whose functions are controversial leave open the possibility that function of auxilin in Notch signaling might be complicated. In vitro, the kinase domain can phosphorylate the μ1 subunit of AP1 and the μ2 subunit of AP2 (Umeda et al., 2000; Korolchuk and Banting, 2002). AP1 and AP2 are clathrin adaptor proteins required at Golgi and plasma membrane respectively. Therefore, auxilin may control clathrin-dependent endocytosis via phosphorylation of an AP2 subunit. The PTEN protein functions as phosphoinositide phosphatase to regulate signal transduction pathway (Maehama and Dixon, 1999). However, The *Drosophila* PTEN domain does not contain essential amino acid for the catalytic activity. The PTEN domain is required for transient recruitment of auxilin to CCPs before fission (Lee et al., 2006). Also, right after CCV formation, auxilin is recruited to CCVs for uncoating using the PTEN domain (Massol et al., 2006). However, the PTEN domain is not required for uncoating CCVs in vitro (Holstein et al., 1996; Greener et al, 2000) and *C. elegans* and yeast auxilin homologs do

not contain the PTEN domain. The requirement of the PTEN domain is controversial. In *Drosophila*, two DPF motifs, which have been known to bind AP2, are located within the clathrin-binding domain. It has been shown that a DPF motif in mammalian auxilin binds directly to clathrin as well as AP2 (Scheele et al., 2003). The J domain is the most conserved domain. Using the J domain, auxilin recruits Hsc70 for removal of clathrin (Ungewickell et al., 1995; Holstein et al., 1996).

I wanted to determine which domains are required for auxilin function in Notch signaling. If the kinase domain and the PTEN domains are necessary and/or sufficient, this would suggest that auxilin function may be more complex than internalization and uncoating. If the clathrin-binding domain and the J domain are necessary and/or sufficient, this would suggest that the internalization and uncoating functions are important in the signaling cells.

4.2 Results

4.2.1. The functions of truncated auxilin proteins

To study which domains of *Drosophila* auxilin are important for the auxilin function in Notch signaling, I generated several auxilin cDNA constructs that encode partial proteins (Fig. 4.1.); Δkinase, ΔPTEN, CBD+J, kinase+PTEN, and ΔJ. I used the GAL4/UAS system to express them.

A.

B.

	complete rescue of *aux-*	rescue of *aux^{hypo}* eye + wing	causes lethality
Full Length	+ (1/1	+ (1/1	− (1/1
ΔKinase	•	•	+ (1)
ΔPTEN	− (1) •	+ (1) •	− (2) + (1)
CBD+J	+ (1/2	+ (1/2	− (1/4
K+PTEN	− (2)	− (2)	− (4)
ΔJ	− (1)	− (1)	− (3)

Figure 4.1. Auxilin domains required for Delta signaling. A diagram of the auxilin protein (1165 amino acids) is shown at top, and beneath are six transgene constructs (A). The arrows above indicate the positions of the nonsense (D128, 727, K48, D136) and missense (K47)mutations in *aux* alleles used in this work. B is a summary of the results. A "+" sign indicates that the construct rescued or caused lethality, a "–" sign indicates that the construct did not, and a "•" indicates that the experiment was not performed. The ΔPTEN construct showed different results for three transformant lines, most likely due to differences in expression levels. Two FL lines, one ΔKinase line, three Δ PTEN lines, one CBD+J line, and three K+PTEN lines were tested. The *auxilin*$^{-}$ genotype tested for rescue was aux^{727}/aux^{D128} and the *auxilin* hypomorph genotype was aux^{K47}/aux^{D128}. The numbers in parenthesis indicate the number of UAS constructs that I tested. If there are two numbers, the second number corresponds to genomic constructs.

First, I tested each line for dominant effects when expressed with *Act5c-gal4* in a wild-type background. I have only one line of the UAS-kinaseless transgenic line. Expression of the kinaseless protein with *Act5C-gal4* kills the flies. I have three lines of UAS-PTENless transgenic flies. Expression of one line of UAS-PTENless kills the flies and the others do not. I have only one line of the kinaseless+PTENless (CBD+J). The expression of CBD+J protein is not lethal without any noticeable phenotype. Among five lines of the CBDless+Jless (kinase+PTEN) protein, I tested two lines and neither showed any abnormality. In summary, expressions of the kinaseless protein and one PTENless line have dominant effects whereas the others do not show dominant effects.

Next, I tested rescue of *auxilin* hypomorphs (aux^{D128}/aux^{K47}) and strong mutants (aux^{D128}/aux^{727}) (Fig. 4.2.). Because expression of the kinaseless protein induces lethality, I was not able to test its rescuing activity. The expression of one PTENless line, which

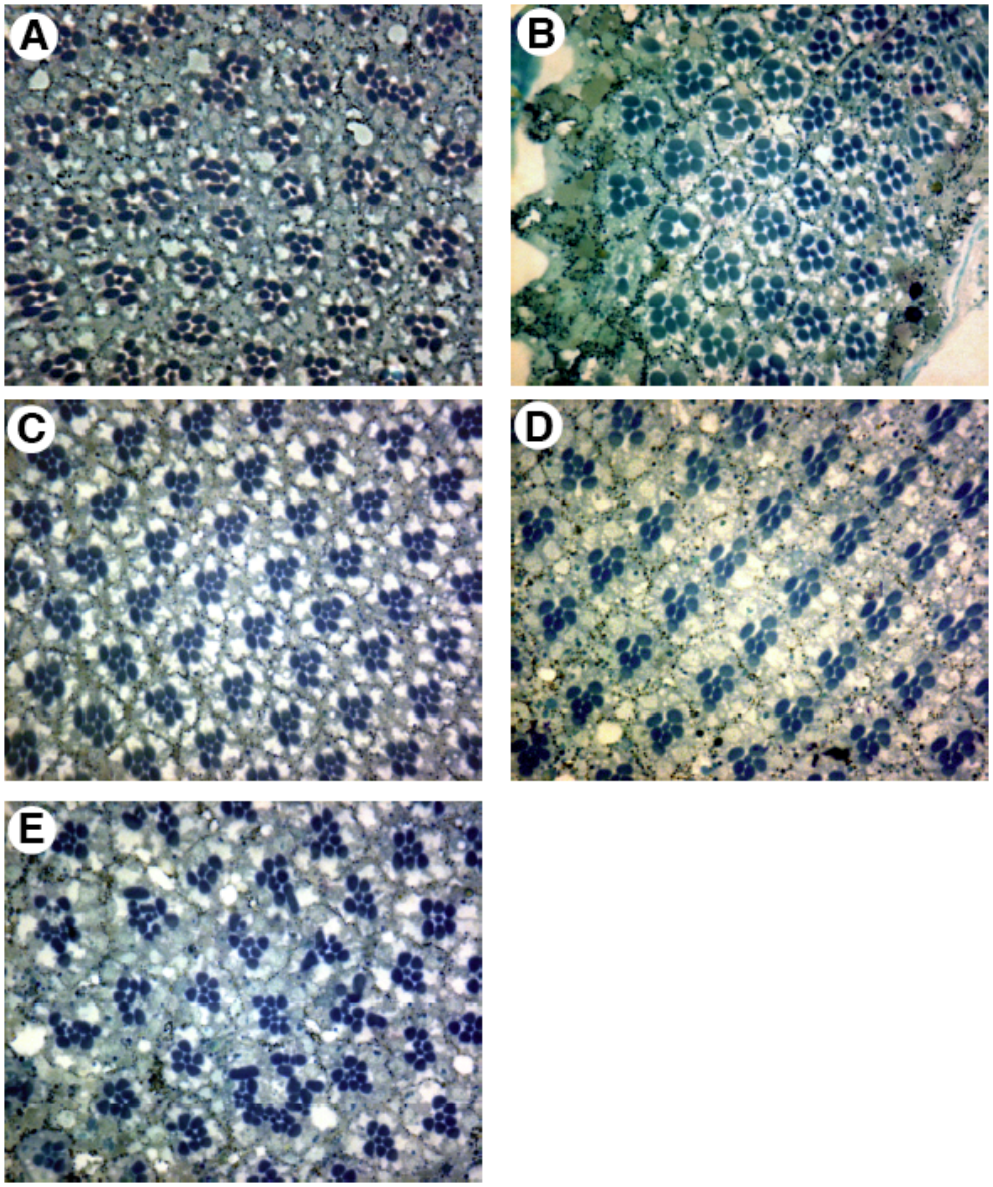

Figure 4.2. The eye phenotype of truncated auxilin proteins in *auxilin* mutants. The tangential sections of adult eyes are shown. The genotypes are: (A) aux^{K47}/aux^{D128}, (B) *Actin5C-gal4/UAS-ΔPTEN*; aux^{K47}/aux^{D128}, (C) *Actin5C-gal4/UAS-CBD+J*; aux^{K47}/aux^{D128}, (D) *Actin5C-gal4/UAS-CBD+J*; aux^{727}/aux^{D128}, (E) *Actin5C-gal4/UAS-Kinase+PTEN*; aux^{K47}/aux^{D128}.

does not induce lethality and is located on the 2nd chromosome, could not rescue the lethality of strong *auxilin* mutants but it rescues the eye phenotypes of weak mutants

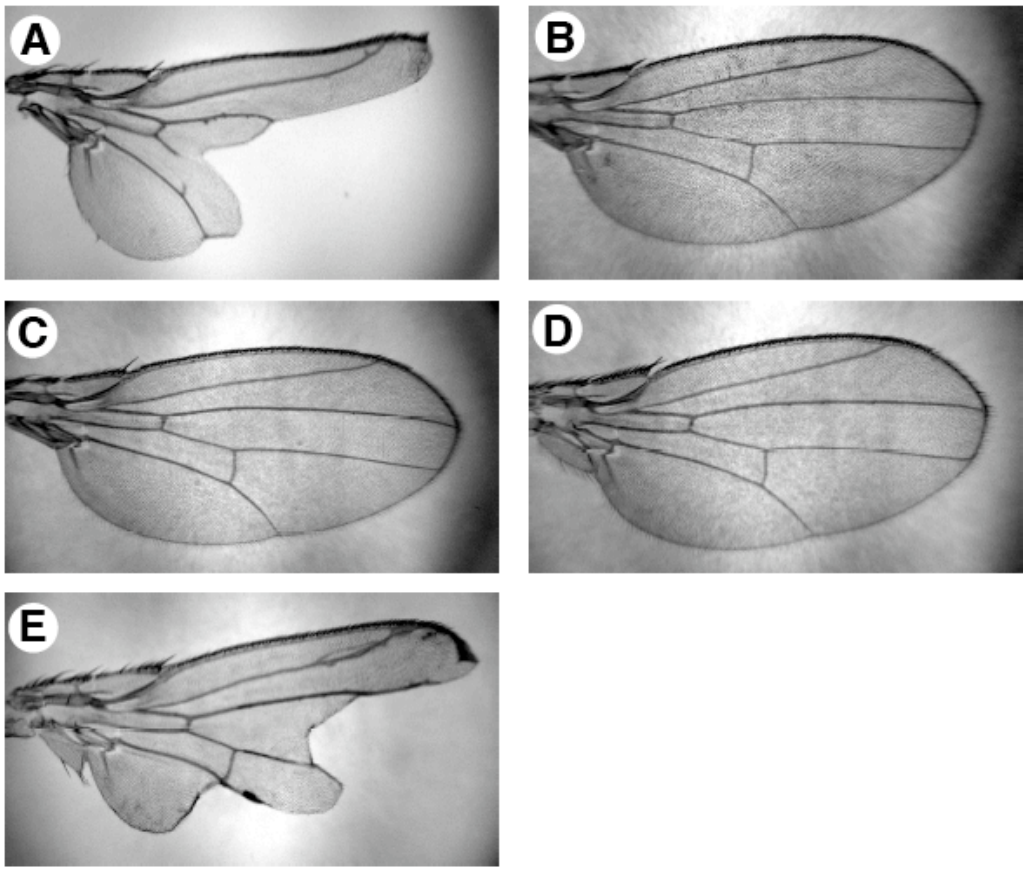

Figure 4.3. The wing phenotype of truncated auxilin proteins in *auxilin* mutants. The wings of truncated auxilin expression flies are shown. The genotypes are: (A) aux^{K47}/aux^{D128}, (B) *Actin5C-gal4/UAS-ΔPTEN*; aux^{K47}/aux^{D128}, (C) *Actin5C-gal4/UAS-CBD+J*; aux^{K47}/aux^{D128}, (D) *Actin5C-gal4/UAS-CBD+J*; aux^{727}/aux^{D128}, (E) *Actin5C-gal4/UAS-Kinase+PTEN*; aux^{K47}/aux^{D128}. The auxilin phenotypes are completely complemented by expression of CBD+J. Expression of ΔPTEN has partial rescue activity and Expression of Kinase+PTEN has no effect.

(Fig. 4.2.B, Fig. 4.3.B). The CBD+J protein rescues the lethality of strong *auxilin* mutants as well as the eye phenotype of weak *auxilin* mutants (Fig. 4.2.C,D, Fig 4.3. C,D). The clathrin-binding domain and the J domain are necessary and sufficient to

uncoat clathrin from CCVs in vitro (Holstein et al., 1996; Greener et al, 2000). The rescue activity indicates that overexpression of CBD+J protein is sufficient for the function of auxilin in Delta signaling. I also overexpressed the complement of CBD+J protein, kinase+PTEN protein, and it has no effect; the *auxilin*$^{-}$ phenotype was not rescued (Fig. 4.2.E, Fig. 4.3.E).

The relative expression levels of truncated proteins were compared in Western using α-auxilin Antibody (Fig. 4.4.). Anti-auxilin recognizes the CBD+J domain, which the first four constructs share. The expression level of the CBD+J protein was the lowest in Western data. This result reinforces that the rescue result of CBD+J protein is not due to simple overexpression of parts of auxilin. The expression level of kinaseless proteins was the highest so that one possible explanation is that high overexpression of parts of auxilin might cause lethality. However, the expression level of one PTENless, which causes lethality was lower than that of another PTENless, which has rescue activity. Thus, the expression level is not directly related with lethality. I cannot explain why less expression of PTENless protein causes lethality and more expression of PTENless protein rescues the *auxilin* phenotype.

To test the CBD+J domain in more physiological conditions, I generated transgenic flies containing a genomic *auxilin*$^{+}$ fragment with deletion of the kinase and the PTEN domains. I assumed that a genomic *CBD+J* fragment expresses the gene product more similar to the endogenous *auxilin* than the *UAS* constructs because it is expressed by the *auxilin* promoter and enhancers. None of the transgenic lines has dominant phenotypes. I tested two 2nd chromosome genomic CBD+J lines for rescue of *auxilin*$^{-}$. Both lines rescue the *auxilin*$^{-}$ phenotype completely including lethality.

Therefore, even under physiological conditions, CBD+J is sufficient to function for auxilin. Because α-auxilin antibody usually does not work on Westerns, I did not check the expression level of a genomic *auxilin*$^{+}$ transgene.

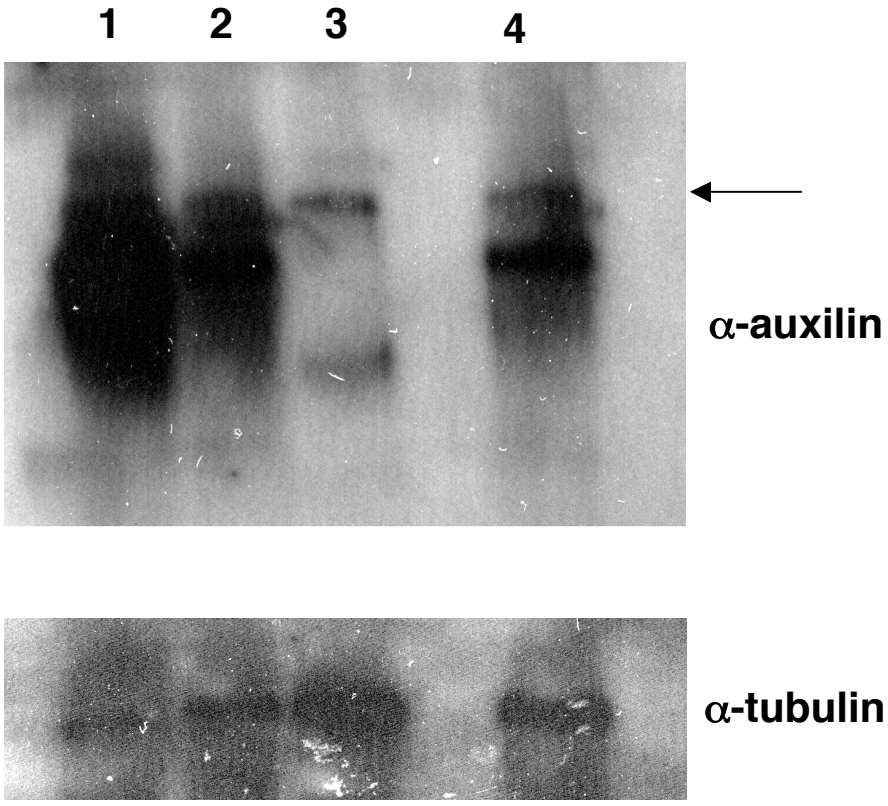

Figure 4.4. The expression level of truncated auxilin proteins. A Western blot of eye disc protein extracts from *ey-gal4*, *GMR-gal4>UAS-truncated auxilin* flies is shown. Lanes are ΔKinase (lane 1), ΔPTEN which does not cause lethality (lane 2), CBD+J (lane3), and ΔPTEN which cause lethality (lane 4). ΔKinase expressed the most. ΔPTEN which does not cause lethality when it is overexpressed has less expression level than ΔPTEN which causes lethality. CBD+J is expressed the least. The arrow indicates the endogenous auxilin protein. The total protein level was determined by α-tubulin antibody.

To address the importance of the J domain, I generated flies containing a *UAS-J-less* transgene. Because auxilin binds to CCVs using the clathrin-binding domain and recruits Hsc70 using the J domain, it is possible to see a dominant negative effect in J-less protein overexpression. However, there are *auxilin* alleles whose nonsense mutations are located right before the J domain. These alleles do not show a dominant effect so it is also possible that the J-less protein does not cause any mutant phenotypes. When I crossed three lines of the J-less protein with various GAL4 lines, I could not detect any dominant phenotypes. Then, I expressed the J-less protein in *auxilin* hypomorphs, to determine if this truncated protein possesses rescue activity. Interestingly, I could not obtain any adult flies whose genotype is *Actin5c-gal4/UAS-J-less*; aux^{K47}/aux^{D128}. This suggests that J-less expression might have a dominant negative effect in an *auxilin* hypomorphic background. I checked the phenotype of the expression of the J-less protein with one copy of $auxilin^{727}$. These flies showed eye and wing morphological phenotypes similar to *auxilin* hypomorphs (Fig. 4.5.). This indicates that expression of the J-less protein has dominant negative characteristics.

4.2.2. Suppression of *auxilin* phenotype by overexpression of Chc

When auxilin uncoats a vesicle, there are two products, free clathrin and uncoated vesicles. If the recycling model, in which Delta is endocytosed and recycled back to the plasma membrane in activated form, is correct, uncoated vesicles will be required. To test if one or both of these products are required for the function of auxilin in Notch signaling, we asked if overexpression of Chc could rescue $auxilin^{-}$ mutant phenotypes. The idea is that if free clathrin is generated in another way, the role for auxilin in Notch

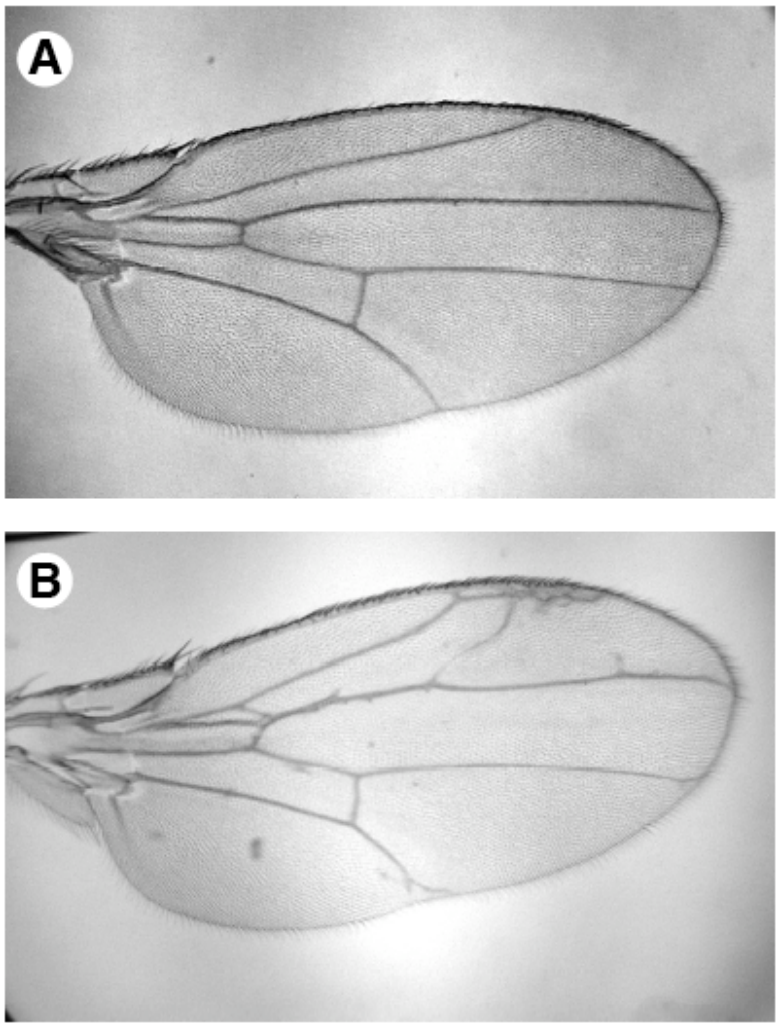

Figure 4.5. ΔJ auxilin has dominant negative charateristic. The genetypes are *Actin5C-gal4*/*UAS-ΔJ* (A) and *Actin5C-gal4*/*UAS-ΔJ*; *aux*^{727}/+ (B). Expression of ΔJ in wild-type background does not affect the wing phenotypes but it causes abnormal wing phenotype with one copy of *auxilin* mutant.

signaling could be bypassed if uncoated Delta-containing vesicles are not important but free clathrin is. To observe the effect on *auxilin* mutants of one additional copy of *chc*$^{+}$, I used a genomic *chc*$^{+}$ transgene that is on chromosome 2. I find that the *chc*$^{+}$ suppresses

the wing phenotype completely and eye phenotype significantly of viable hypomorphic *auxilin* mutants (Fig. 4.6.). By contrast, *Pchc*$^{+}$ fails to suppress the wing phenotypes of *lqf* mutants, which is weaker than that of *auxilin* mutants, and suppresses eye phenotype of *lqf* only a little (Fig. 4.6.). Clathrin is limiting when auxilin activity is low but not when Lqf activity is compromised. This result suggests that addition of *chc*$^{+}$ does not suppress Lqf-dependent endocytosis in general. Therefore, rescue by *chc*$^{+}$ is possible because *auxilin*$^{-}$ is depleting clathrin pool.

To strengthen this result, I tried to add more copies of *chc*$^{+}$ transgenes. When I tried to add 2 copies of the same transgene, it was homozygous lethal. One explanation is that the insertion locus of the transgene may cause the mutation of a gene which is homozygous lethal. Thus, I used two different transgenes to add two copies of *chc*$^{+}$ gene. However, I could not obtain any flies which contain two copies of *chc*$^{+}$ gene. These results suggest that two extra copies of *chc*$^{+}$ kill flies. I have one more *chc*$^{+}$ transgenic line which has insertion on the X chromosome and there are male flies. Due to dosage compensation, male X chromosome genes are transcribed twice as much as female X chromosome genes. Therefore, one copy of *chc*$^{+}$ on the male X chromosome is the same as two copies of *chc*$^{+}$ inserted on autosome. The viable male flies indicate that two copies of *chc*$^{+}$ on the X chromosome do not cause lethality. Using this X chromosome transgene, I tried to see the effect of more copies of the *chc*$^{+}$ transgene. With the combination of the 2nd chromosome transgene, I was able to obtain male flies containing 3 copies of *chc*$^{+}$ (1 on the X chromosome and 1 on the chromosome 2), female flies containing 2 copies of *chc*$^{+}$ (1 on the X chromosome and 1 on the chromosome 2), male flies containing 2 copies of *chc*$^{+}$ (1 on the X chromosome), and female flies containing 1

copies of chc^{+} (1 on the chromosome 2). There is not much difference of the eye phenotype among those flies. I cannot detect complete rescue of the eye phenotype even with 3 copies of chc^{+}.

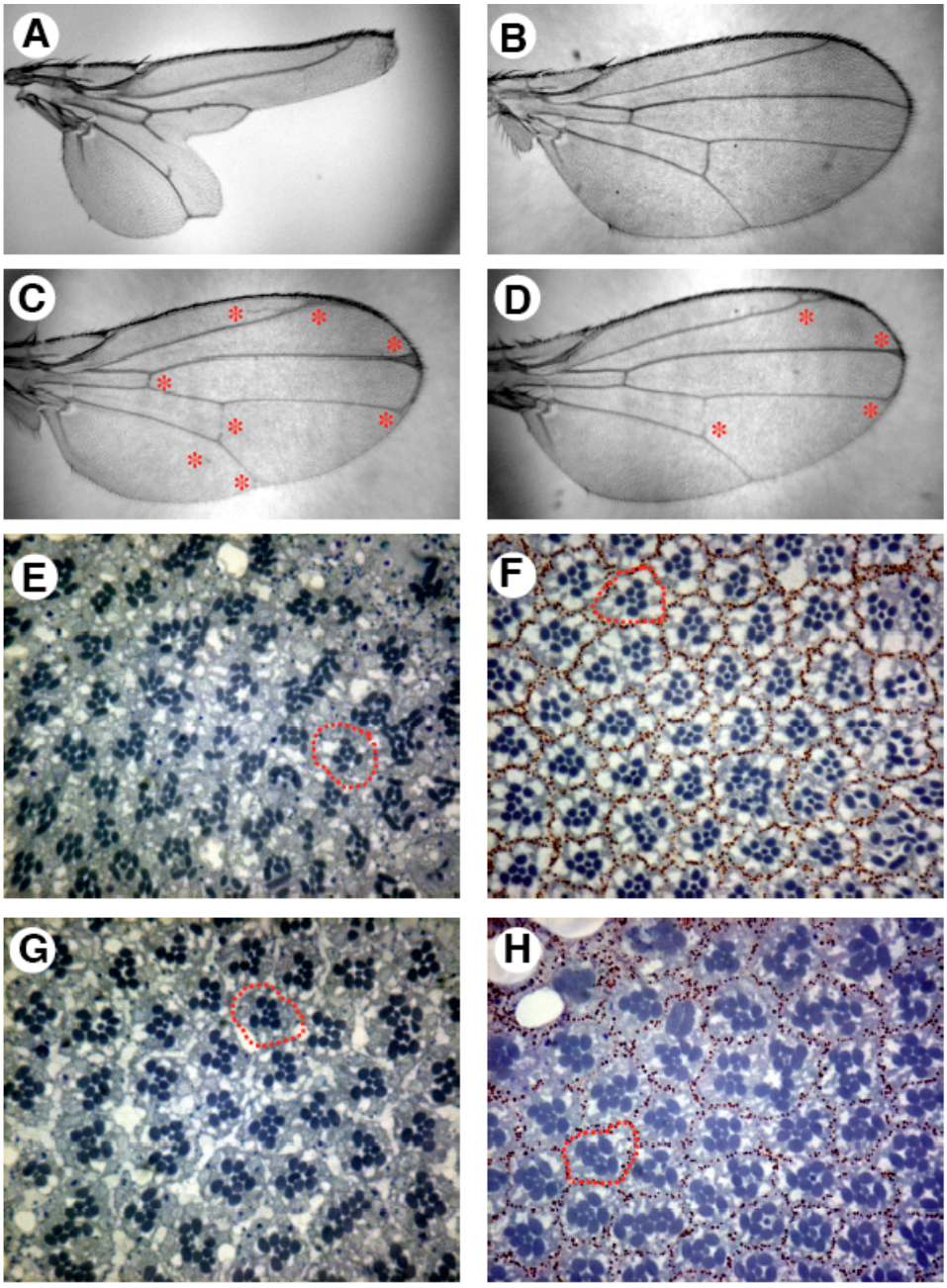

I

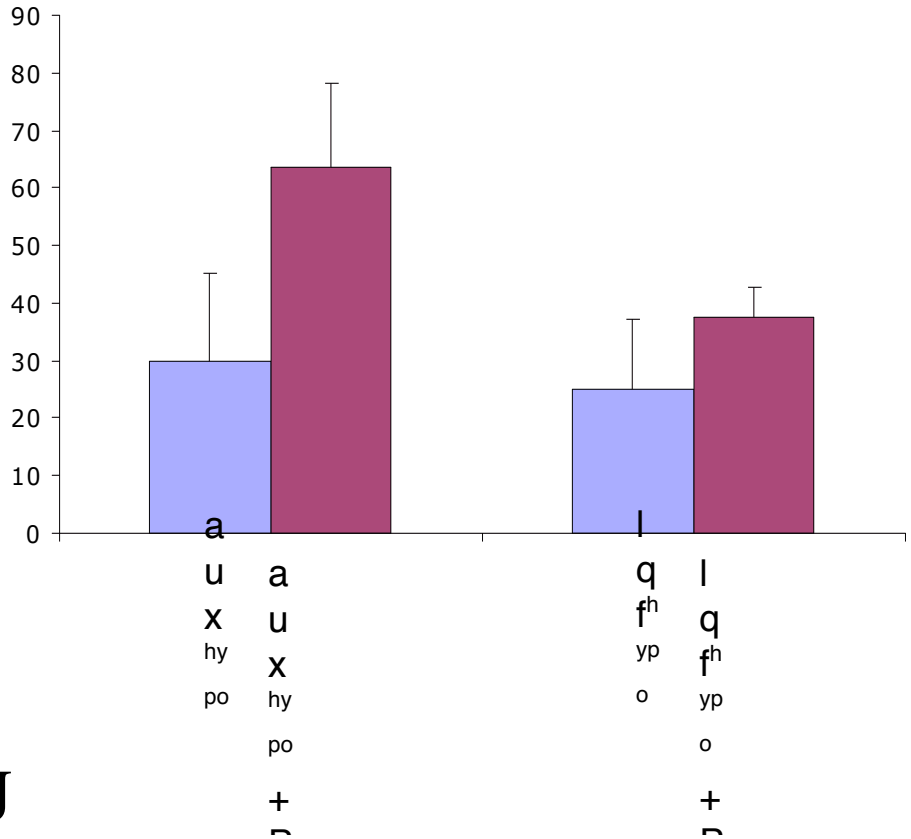

J

Genotypes	% of WT facets (mean ± s.d.)	no. of eyes	Total no. of facets
aux^{hypo}	30 ± 15	10	784
aux^{hypo} + $Pchc^{+}$	64 ± 15	10	871
lqf^{hypo}	25 ± 12	10	644
lqf^{hypo} + $Pchc^{+}$	37 ± 5	10	864

Figure 4.6. chc^+ overexpression suppresses *auxilin*$^-$ morphological phenotypes. (A-D) Wings of viable flies hypomorphic for *auxilin* or *lqf* are shown. The wing in B appears wild-type. The arrows in C and D indicate wing vein defects. (E-H) Tangential sections of adult eyes are shown as examples of the data tabulated in E. An example of a wild-type ommatidium is circled in each panel. $Pchc^+$ complements completely chc^1. (I) A bar graph showing the degree of suppression of *aux* and *lqf* hypomorphic eyes is shown. Y axis represents the ratio of wild-type facets. $aux^{hypo}= aux^{K47}/aux^{D128}$ and $lqf^{hypo}=lqf^{FDD9}/lqf^{FDD9}$. For each genotype, 51-124 facets in each of 10 eyes were examined. The error bars represent the standard deviation from the mean calculated for each eye. The effect of $Pchc^+$ is significant for both *auxilin* and *lqf* (Student's t-test; $P< 0.001$ and $P<0.01$, respectively). (J) A table for the numeric data of suppression of *aux* and *lqf* hypomorphic is are shown.

4.2.3. Subcellular location of auxilin

If I can determine the cellular localization of auxilin, it will be helpful to elucidate auxilin function in the cell. Two auxilin functions have been studied. First Auxilin is required at the fission step on the plasma membrane. Second, auxilin uncoats clathrin from CCVs in the cytosol. Thus, I expect to see auxilin on the membrane and in the cytosol.

I raised antibodies in rats using a protein made in bacteria containing the clathrin-binding domain and the J domain. To test antibody specifically for immunofluorescence, I stained eye discs containing *auxilin*$^-$ clones (aux^{D136}/aux^{727}) and saw no difference inside or outside the clone. Probably, aux^{D136} expresses some antigen because the nonsense mutation is located after the clathrin-binding domain. Then, I generated clones using an aux^{D128}/aux^{727} background. Nonsense mutations of both alleles are located earlier than the clathrin-binding domain. The α-auxilin antibody stained only *auxilin*$^+$ cells (Fig. 4.7.). Therefore, the α-auxilin antibody is specific enough to use for

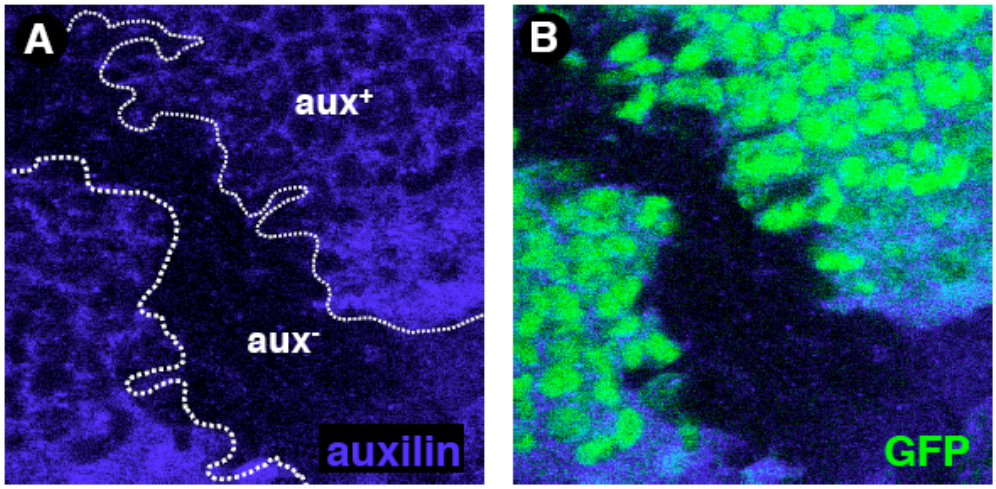

Figure 4.7. Specificity of α-auxilin antibody for immunostaining. Confocal microscope images of third instar larval eye discs are shown. A clone of *auxilin*$^{-}$ (*aux*^{727}/*aux*^{D128}) cells outlined in A, marked by the absence of GFP, was generated in flies of the genotype *w, eyFLP; FRT42D gaux*$^{+}$*, Ubi-gfp / FRT42D; aux*^{727}/*aux*^{D128}. α-auxilin antibody specifically stains only *auxilin*$^{+}$ cells.

immunostaining. To determine whether auxilin is localized on the membrane and/or cytosol, I costained with phalloidin which represents the plasma membrane. I observed many auxilin puncta in the cytosol near plasma membrane (Fig 4.8.). Delta endocytosis required for Notch signaling is only a small portion and most endocytosed Delta is not related with Notch activation. If auxilin were only required specifically for Delta endocytosis for Notch activation, I would see only a small number of *Delta*$^{+}$ puncta colocalized with auxilin. I costained wild-type eye discs with α-auxilin and α-Delta antibodies. All *Delta*$^{+}$ puncta were colocalized with auxilin (Fig. 4.8.D). One possible interpretation of this observation is that bulk endocytosis of Delta requires auxilin.

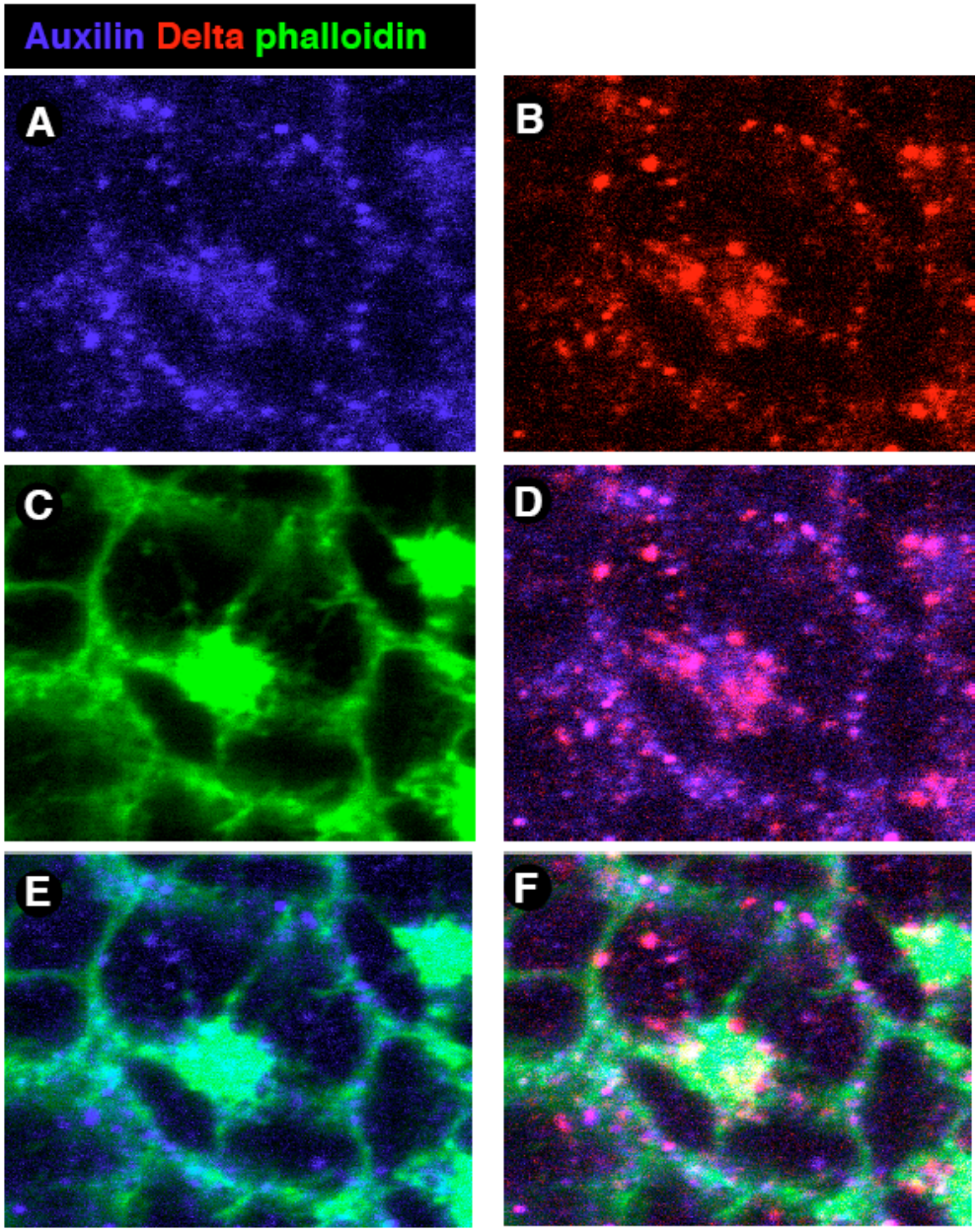

Figure 4.8. auxilin subcellular localization. Confocal images of third instar larval eye discs of wild-type flies are shown. (A) auxilin is punctate. (B) Delta is punctate. (C) Phalliodin stains plasma membrane. (D) Most Delta puncta colocalize (yellow) with auxilin. (E) The auxilin puncta concentrate near the plasma membrane. (E) All merged image.

Expression of *UAS-CBD+J* using *Actin5c-gal4* rescues completely the *auxilin*$^{-}$ phenotype including lethality. I stained eye discs of the flies whose genotype are *w; Actin5c-gal4/UAS-CBD+J;* aux^{727}/aux^{D128} (Fig. 4.9.G-E). In these flies, I can detect CBD+J truncated protein without any endogenous auxilin because both endogenous *auxilin* genes have nonsense mutations earlier than the antigen region of the antibody. I expected to observe CBD+J puncta only in the cytosol, maybe further from the plasma membrane, because this truncated protein does not contain the PTEN domain which has been shown to be required during the fission step of clathrin coated pits on the plasma membrane. As a control, I also stained eye discs which express full length auxilin without endogenous auxilin expression (Fig. 4.9.A-F). I detected identical staining patterns in both genotypes. The truncated and full length proteins are localized indistinguishly from endogenous auxilin.

As an alternative method to determine the subcellular localization of auxilin, I generated *UAS-gfp-auxilin* transgenic flies. Expression of full-length *auxilin* cDNA with the *Act5C-gal4* driver complements completely *auxilin*$^{-}$ phenotypes including lethality. When GFP-auxilin is expressed with the *Act5C-gal4* driver, it caused lethality. I also expressed this protein with several eye specific GAL4 lines. When I used *GMR-gal4*, I could not detect any phenotype. However, when I used *ey-gal4*, I could detect a very weak rough eye phenotype with less than 100% penetrance. I used *ey-gal4* and *GMR-gal4* at the same time and it caused a small and rough eye phenotype with variable expressivity (Fig. 4.10.). These results suggest that *UAS-gfp-auxilin* is not functional and also may have dominant negative characteristics. Thus, the subcellular localization of this chimeric protein is not informative so I did not observe the localization of the protein.

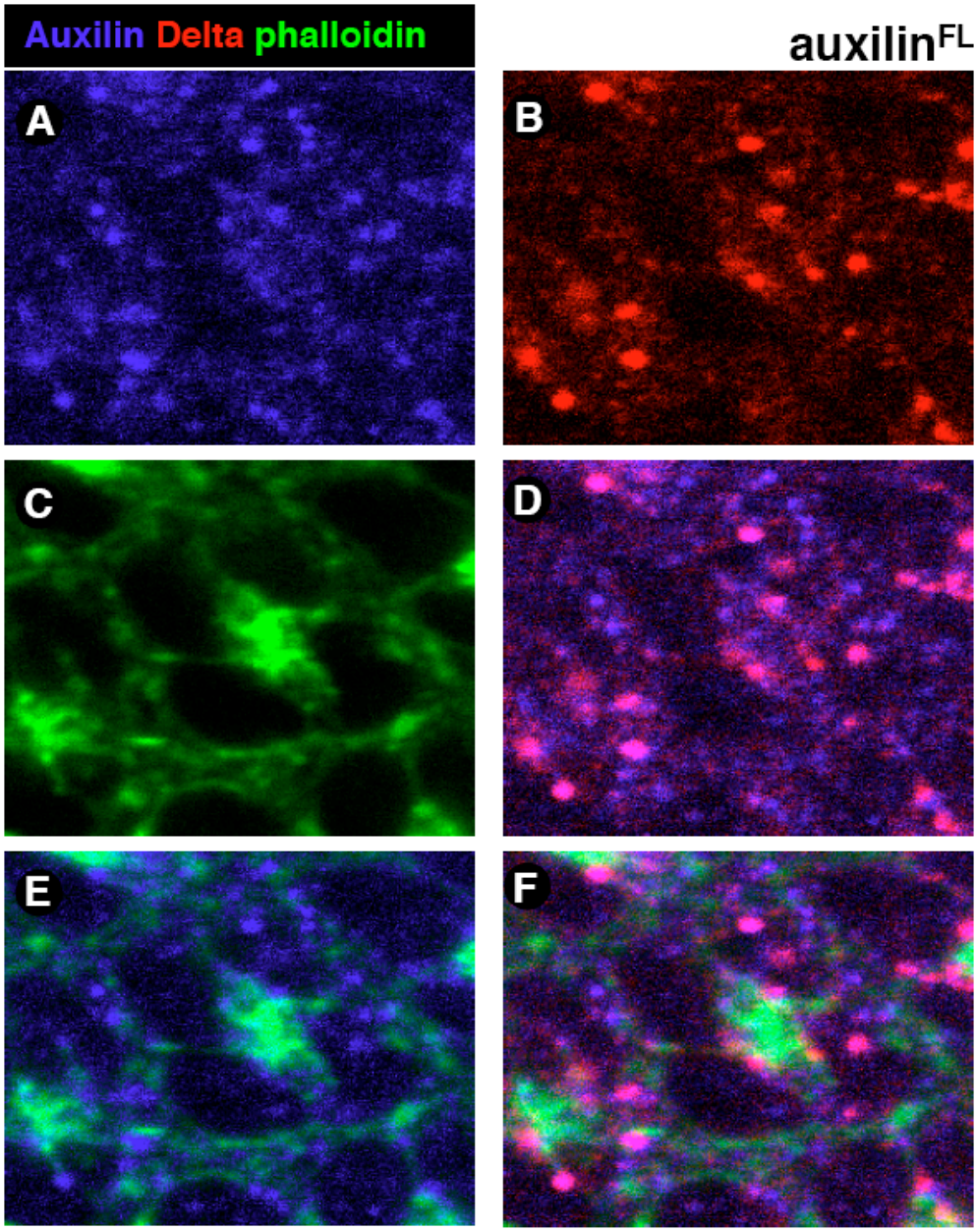

Figure 4.9. CDB+J subcellular localization. Confocal images of third instar larval eye discs are shown. (A-F) A developing ommatidium from an eye disc of the genotype *Act5C-gal4/UAS-aux*^{FL}; *aux*^{727}*/aux*^{D128}, where all of the auxilin protein is full-length expressed from the transgene. The aux^{FL} protein is localized similarly to wild-type and it colocalizes (yellow) with Delta.

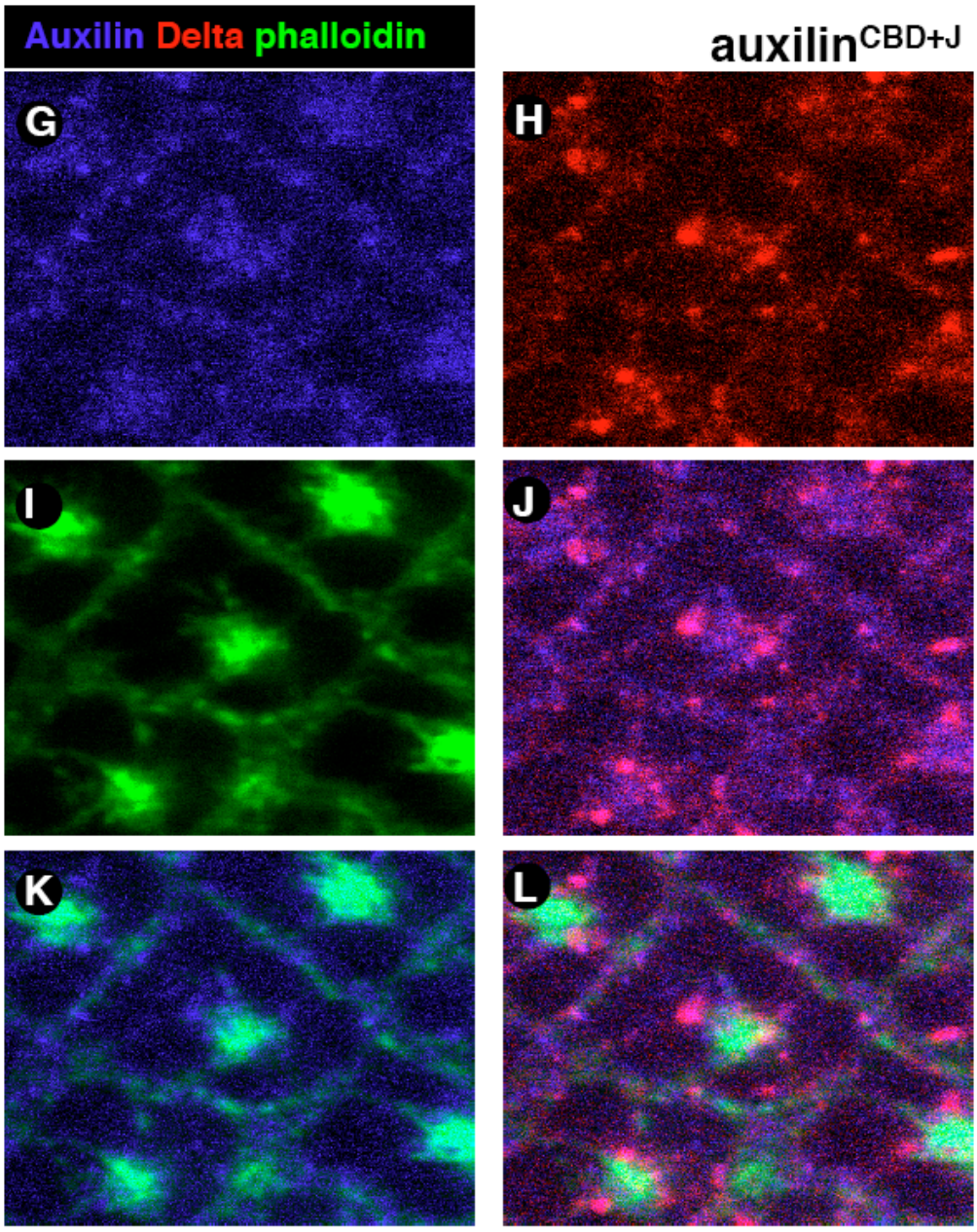

Figure 4.9. Continued. (G -L) A developing ommatidium from an eye disc of the genotype *Act5Cgal4/UAS-aux*$^{CBD+J}$; *aux*^{727}/*aux*^{D128}, where all of the auxilin protein is aux^{CBD+J} expressed from the transgene. aux^{CBD+J} localization is similar to that of aux^{FL} and endogenous auxilin and colocalizes (yellow) with Delta.

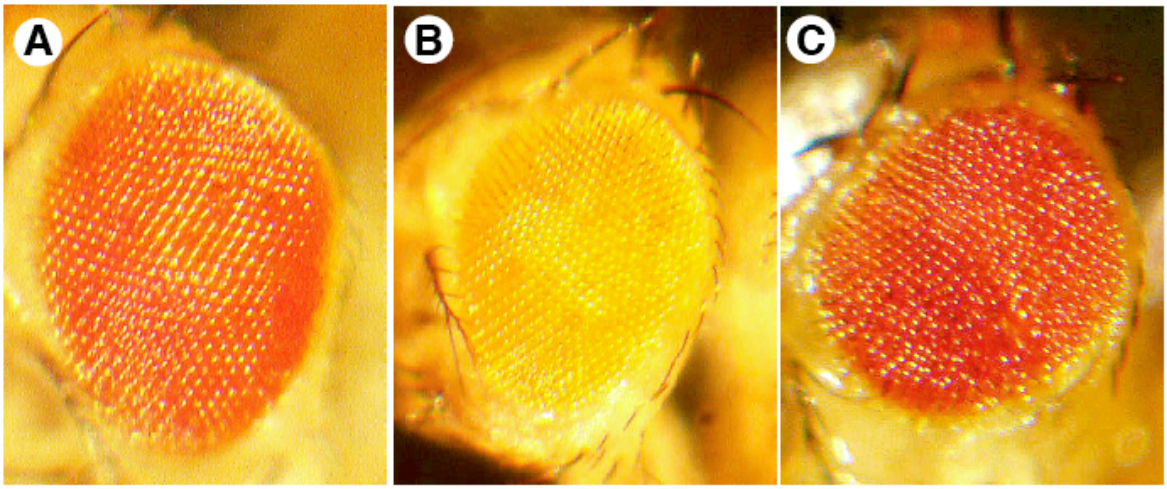

Figure 4.10. Expression of GFP-auxilin causes a mutant eye phenotype. Eyes of flies that express GFP-auxilin in the eyes with varous eye specific GAL4 lines: (A) *GMR-gal4*, (B) *ey-gal4*, and (C) *GMR-gal4* and *ey-gal4*. The eyes of *GMR-gal4*, *ey-gal4>UAS-GFP-auxilin* flies are small and rough.

4.3. Discussion

4.3.1. Addition of a genomic *chc*$^{+}$ transgene suppresses the *auxilin* phenotype.

In yeast and *C. elegans*, *auxilin*$^{-}$ causes depletion of free clathrin and failure of clathrin-dependent endocytosis and cargo transport (Gall et al., 2000; Pishvaee et al., 2000; Greener et al., 2001). In *C. elegans*, expression of *chc*$^{+}$ suppresses the *auxilin*$^{-}$ phenotype (Greener et al., 2001). Because uncoating fails in *auxilin*$^{-}$, most clathrin is stuck in the clathrin-coated vesicles and then clathrin-dependent endocytosis is

ineffective because of clathrin depletion. If *Drosophila auxilin*$^{-}$ causes free clathrin depletion, it may result in failure of Delta internalization. When I add one copy of genomic *chc*$^{+}$ transgene, it suppresses *auxilin*$^{-}$ phenotype. The result indicates that at least a part of the *Notch*-like phenotype of *auxilin* mutants is caused by clathrin depletion. Auxilin is thought to remodel clathrin on the plasma membrane for fission by exchanging free clathrin in the cytosol with membrane-bound clathrin. If *Drosophila* auxilin is required at the fission of CCVs directly, it may also lead to failure of Delta internalization. From two known auxilin functions (during fission and uncoating), I can think of three possible models for how *auxilin*$^{-}$ causes failure of Delta signaling (Fig.

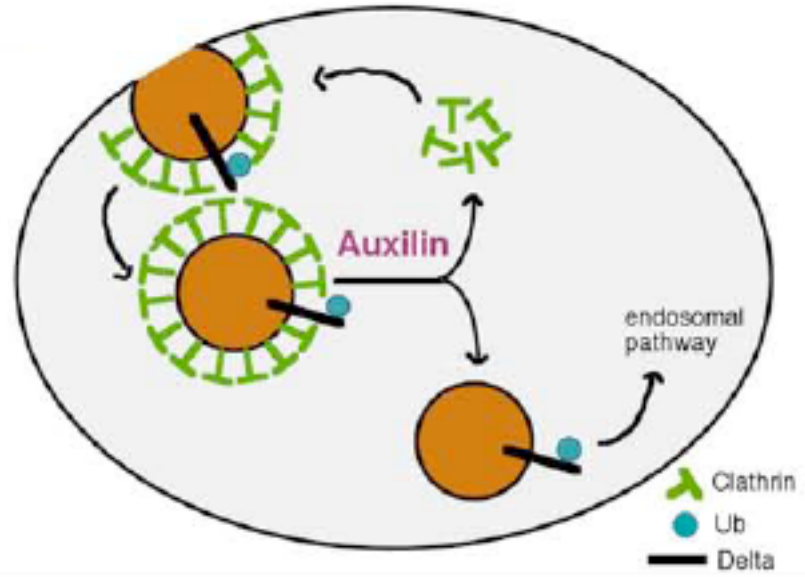

Figure 4.11. The possible roles of auxilin during Delta endocytosis. A diagram of the two products of auxilin activity downstream of vesicle scission are shown: clathrin and uncoated vesicles.

4.11.). ① If auxilin function at the fission step is important for Delta signaling, failure of fission may cause a *shibire*$^{-}$-like effect in the signaling cells. However, this effect will not be recovered by more clathrin. The *chc*$^{+}$ suppression data do not fit in this model. ② If the Delta recycling model is correct, endocytosed Delta should be transferred to the proper endosomes to be processed and recycled. Transfer of Delta must require the uncoating activity of auxilin. This uncoating activity also cannot be provided by the addition of clathrin. ③ The last model is failure of Delta internalization caused by clathrin depletion and thus indirectly, failure of Delta endocytosis for signaling. This model best fits into the *chc*$^{+}$ suppression result. However, I cannot completely rule out the first two models because the background I tested was hypomorphic. There should be some activity of *auxilin*$^{+}$. Also, I could not detect complete rescue. If the major role of auxilin uncoating function is to maintain free clathrin pool, and the other functions are also required but not as much, the partial rescue of the hypomorph also makes sense. If clathrin overexpression completely rescues the *auxilin* null mutant phenotype, this would be a strong argument against models where Delta^{+} endosomes must be recycled to the membrane for signaling. This result would indicate that uncoated vesicles *per se* are not needed for Delta signaling. There are two possible reasons why I could not detect complete rescue by addition of one copy of *chc*$^{+}$, even if it is feasible. First, the expression of Chc was not enough. Second, Clc is also required although it is not a target of uncoating. To achieve complete rescue, high-level expression of Chc (and Clc) using cDNA might be essential. Now I am trying to obtain transgeneic flies containing *ey-chc*, *ey-clc*, *UAS-chc*, and *UAS-clc* in order to express Chc and Clc simultaneously. Even partial suppression by *chc*$^{+}$ shows that clathrin is required for Delta signaling. This result

suggests that Delta is endocytosed in a clathrin-dependent way. Further, Delta endocytosis is Lqf-dependent so that Lqf-dependent Delta endocytosis requires clathrin. However, it does not necessarily mean that Delta is internalized though CCPs and CCVs. Clathrin could regulate Lqf recycling. Xuanhua Xie in our lab suggested a new model in which clathrin produced by auxilin is a positive regulator of Lqf function. The idea is that free clathrin binds Lqf in newly internalized vesicles, freeing Lqf from binding monoubiquitinated Delta, and recycling Lqf back to the plasma membrane. If clathrin is depleted in the cells, Lqf cannot be recruited to the plasma membrane because Lqf is quenched in internalized vesicles. This idea fits well with the observations that epsin induces cargo internalization clathrin-independently (Sigismund et al., 2005) and that epsin cannot bind to ubiquitin and clathrin simultaneously (Chen and De Camilli, 2005).

4.3.2. The clathrin-binding domain and the J domain are sufficient to function as auxilin

Surprisingly, not only expression of cDNA of CBD+J but also genomic CBD+J completely rescues *auxilin*$^{-}$ phenotypes including lethality. An in vitro study shows that the clathrin-binding domain and the J domain are essential and sufficient for uncoating function of auxilin (Holstein et al., 1996; Greener et al., 2000). Thus, it is possible that auxilin is required for uncoating. However, auxilin also functions for fission of CCVs which involves clathrin release. Maybe CBD+J is also sufficient to function for fission without the other domains. The kinase domain might regulate clathrin-dependent internalization via phosphorylation of the AP2 subunit (Umeda et al., 2000; Korolchuk and Banting, 2002). The observation that the kinase domain is not necessary for auxilin

function in Notch signaling suggests that the kinase activity of auxilin is not essential probably because of other proteins functioning abundantly and/or that AP2 is not required for Delta internalization (see below). It has been suggested that the *Drosophila* PTEN domain recruits auxilin to the plasma membrane. In mammalian cultured cells, the auxilin PTEN domain is essential to recruit auxilin to the plasma membrane for fission (Lee et al., 2006) and to the CCVs for uncoating (Massol et al., 2006). The localization of CBD+J is identical to the full-length auxilin. This result suggests that *Drosophila* auxilin can move to the plasma membrane and to the CCVs without the PTEN domain.

If CBD+J is sufficient for function, why are there other domains in *Drosophila* auxilin? When I expressed the kinaseless protein using the *Act5C-gal4* driver, it causes lethality. Also, expression of GFP-auxilin using the *Act5C-gal4* driver kills flies. GFP-auxilin expression with ey-Gal4 and GMR-Gal4 causes small and rough eye phenotype. Because GFP is directly connected to the kinase domain, GFP may block the kinase activity. These results suggest that blocking of the kinase domain causes a dominant effect. Expression of PTENless transgene sometimes casues lethality as well. The dominant effect of PTENless is not related with the expression level. One simple explanation is that kinase+PTEN has separate functions from CBD+J and that the function of kinase+PTEN is redundant with other protein(s). An in vitro study showed that GAK can phosphorylate AP1 and AP2. There is another kinase, AAK1, which phosphorylates AP1 and AP2 (Conner and Schmid, 2002). AAK1 is the major protein to control AP2 activity via phosphorylation. Kinase+PTEN may phosphorylate AP1 and AP2 and/or other proteins. PTEN may recruit auxilin to the substrates. In the absence of the kinase domain, PTEN binds to the substrates and blocks other kinases from

interacting with the substrates. Obviously, kinase+PTEN is not required for Delta signaling. Further experiments to identify the role of kinase+PTEN could be pursued. If Xuanhua Xie's model is correct, auxilin is required only to regenerate free clathrin and auxilin function at the fission step and/or activation of AP2 which may require the kinase and the PTEN domains is not necessary. His model fits well with the truncated auxilin data.

4.3.3. Previously suggested auxilin function in Notch signaling

Hagedorn et al (2006) suggested that 'auxilin regulates internalization of Delta.' However, they did not show any data to support their assertion. They insist that auxilin is required in the signaling cells from hypomorphic mosaic clonal analysis. In the adult eye section, they showed that near the clonal border there are more wild-type facets than in the center of the *auxilin*$^{-}$ clone. Delta is a transmembrane protein. To activate Notch, cell-to-cell interaction is required. A single facet contains about 20 cells. Looking at facets several rows away from the mutant clone cannot be informative to determine call autonomy. In addition, they said that *auxilin* mutant results support the recycling model and argue against the pulling model because uncoating must occur after internalization. Even though this paper came out earlier, it does not detract from the importance of my work. Here, I argue the opposite mechanism. Because uncoating failure in *auxilin* mutants causes free clathrin depletion required during internalization, *auxilin* data do not argue against the pulling model. Also, I showed that uncoated vesicles *per se* may not be necessary, which argues against the recycling model.

4.3.4. Why are general endocytic proteins required in the signaling cells?

Both epsin and auxilin are general endocytic proteins. How are these general endocytic factors required only in the signaling cells to regulate Delta endocytosis? It has been suggested that epsin performs 'specific functions' for Delta endocytosis to facilitate signaling. However, the requirement for auxilin in the signaling cells suggests that general endocytic factors are required for efficient Delta signaling and that epsin may not perform anything special necessarily. Rather, the requirement of both epsin and auxilin in the signaling cells suggests that Delta depends on general mechanisms of endocytosis. Perhaps, epsin and auxilin are usually redundant with other functions, at least enough to avoid cell lethality. Notch signaling calls may require highly efficient endocytosis, and thus epsin and auxilin become non-redundant specifically for this pathway.

Chapter 5. Examination of the possible role of Rab11 in the signaling cells during Notch activation.

5.1. Introduction

Rab proteins are Ras-like small GTPases which control membrane trafficking. Some Rabs have essential roles in endosomal pathways. Biological functions of Rab proteins have been studied mostly in the cultured cell system. Rab5 regulates membrane fusion between endocytosed vesicles and early endosomes and *rab5* mutants have endocytosis defects (Horiuchi et al., 1997; Christoforidis et al., 1999). Rab7 is localized on late endosomes and regulates late endosomal trafficking to the lysosomes through MVBs (Feng et al., 1995; Bucci et al., 2000). Rab11 is used as a marker for recycling endosomes. Rab11 functions in recycling through perinuclear recycling endosomes (Ullrich ey al., 1996) and during Golgi to plasma membrane trafficking (Chen et al., 1998). If Delta signaling requires recycling of Delta after endocytosis, *rab11* mutants should show defects in Delta signaling.

Drosophila Rab11 has been shown to function in recycling. In the embryo, transferrin receptor recycling fails in *rab11* mutants. Rab11 also has a role during Golgi to plasma membrane trafficking. In *rab11* mutants, rhodopsin trafficking from Golgi to rhabdomeres fails. Rhabdomeres are apically located membrane structures and is essentially plasma membrane. In *Drosophila*, viable *rab11* hypomorphs have fewer and shorter bristles. *Drosophila rab11* mutants have other phenotypes. Strong mutant alleles

of *rab11* are homozygous cell lethal. Therefore, it is almost impossible to generate *rab11* null clones. Also, *rab11* mutants have defects in generating rhabdomeres in the eye. These features make it hard to study *rab11* function in the eyes.

There are two papers that use studies of Rabs to support the recycling model. Both papers mention Rab11 as a marker of recycling endosomes. Jafar-Nejad et al. (2005) showed that Sec15 colocalizes with Rab11 and is required for Notch activation. Mutation of *sec15* causes a neurogenic phenotype and aberrant distribution of Rab11. Emery et al. (2005) showed that Rab11 positive vesicles appear only in the signaling cells during sensory organ precursor cell division. Nuclear fallout, a binding partner of Rab11, is essential for Rab11 positive vesicles. The receiving cells fail to recruit this protein to the centrosome to form Rab11 positive vesicles. Although these papers show that a Rab11 binding protein is required for Delta signaling, nobody has studied Delta signaling in *rab11* mutants directly. As suggested if the recycling model is correct, *rab11* mutant will cause similar phenotype with *Delta* and *lqf* mutants. Because *rab5* mutants result in internalization defects, they could serve as a positive control. As a negative control, *rab7* mutants could be used. Delta signaling is unaffected in *hrs* mutants which block cargo trafficking from late endosomes to lysosomes. Therefore, interruption of late endosomes using *rab7* mutants would not cause failure of Delta signaling.

Here I show that *rab11* mutants have the opposite phenotype of the Notch signaling component genes, for example fewer R-cells. I cannot explain how these phenotypes are generated. However, *rab11* mutant phenotypes argue against the Delta recycling model.

5.2. Results

5.2.1. Genetic interactions between *rab11* and *auxilin*, and *lqf*

If Rab11 is functioning in the signaling cells like Lqf and auxilin, I might detect genetic interaction between *rab11* and *auxilin* and between *rab11* and *lqf*. To determine whether *rab11* mutants dominantly enhance *auxilin* and/or *lqf* phenotypes, I used the $rab11^{EP3017}$ allele. Even though $rab11^{EP3017}$ is not a null allele, it is the strongest allele among those which are viable over $rab11^{93Bi}$, the weakest allele. Because all three genes are located on the 3rd chromosome, I needed to recombine chromosomes. The cytogenic locations of these genes are far enough to recombine mutant genes easily: *lqf* (66A), *auxilin*(82B), and *rab11*(93B). One copy of $rab11^{EP3017}$ does not enhance the phenotype of the *auxilin* hypomorph, $auxilin^{D128}/auxilin^{K47}$. Also, one copy of $rab11^{EP3017}$ does not enhance the phenotype of *lqf* hypomorph, lqf^{FDD9}/lqf^{FDD9}. However, one copy of a weak *auxilin* allele, $auxilin^{K47}$, and a strong *auxilin* allele, $auxilin^{D128}$, dominantly enhance a *rab11* hypomorph, $rab11^{EP3017}/rab11^{93Bi}$, to lethality. Also, one copy of a weak *lqf* allele, lqf^{FDD9} as well as a strong *lqf* allele, lqf^{ARI}, dominantly enhances *rab11* hypomorphs, $rab11^{EP3017}/rab11^{93Bi}$, to lethality. These genetic interactions between *lqf* and *rab11* as well as between *auxilin* and *rab11* suggest that *rab11* might function with *lqf* and *auxilin* in the same direction.

I expected that mutations in *auxilin* and/or *lqf* may affect the $Rab11^{+}$ vesicle structure or numbers if *rab11* functions downstream of *auxilin* and/or *lqf*. I detected α-Rab11 antibody staining pattern inside and outside of *auxilin* and *lqf* mosaic clones (Fig.

5.1.). There was no difference in Rab11 staining pattern and this result leads me to think that my expectation was naïve. Only a small amount of all the Delta in the cell is

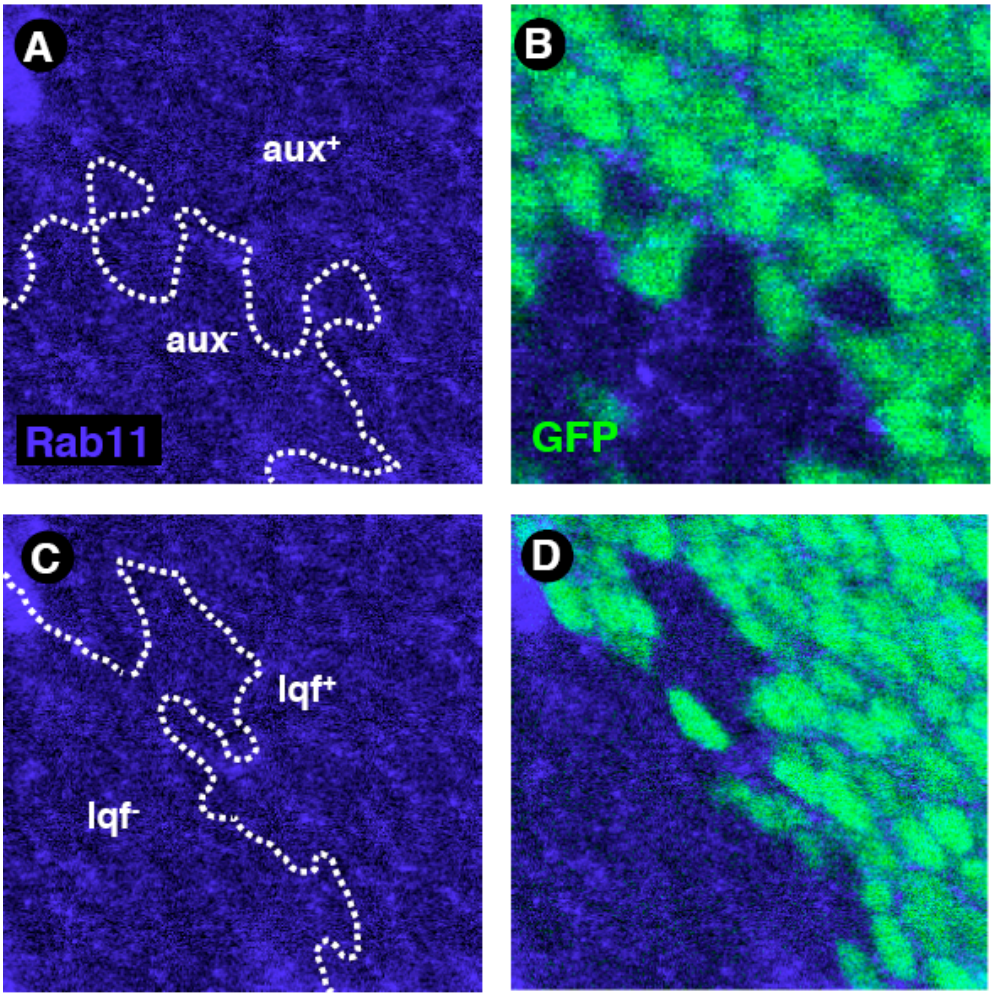

Figure 5.1. Rab11 staining is not altered in *auxilin*$^{-}$ cells. Confocal microscope images of third instar larval eye discs are shown. A clone of *auxilin*$^{-}$ (*aux*^{727}/*aux*^{D128}) cells outlined in A, marked by the absence of GFP, was generated in flies of the genotype *w, eyFLP; FRT42D gaux*$^{+}$*, Ubi-gfp / FRT42D; aux*^{727}/*aux*^{D128}. A clone of *lqf*^{L7} cells outlined in C, marked by the absence of GFP, was generated in flies of the genotype *w, eyFLP;; lqf*^{L7}*, FRT80B / Ubi-gfp, FRT80B*. α-Rab11 antibody staining pattern is the same in *auxilin*$^{-}$ and *auxilin*$^{+}$ cells as well as in *lqf*$^{-}$ and *lqf*$^{+}$ cells .

regulated by *auxilin* and *lqf* for Notch activation so the amount of Delta affected by *auxilin* and *lqf* mutants may be too little to be detected. In wild-type eye discs, Delta is not colocalized with Rab11 (Hagedorn et al., 2006). Also, there will be many other proteins excluding Delta to be recycled. Thus, less Delta for the recycling endosomes would not be expected to change the morphology of $Rab11^{+}$ puncta.

5.2.2. Eye phenotypes of *rab11* hypomorphic combinations

One described phenotype of *rab11* mutants is fewer and shorter bristles (Jankovics et al., 2001). This phenotype could be caused by failure of Notch activation. To determine whether *rab11* mutants cause Notch signaling defects in the eye, I generated mutant eyes with variable viable *rab11* mutant allele combination and I used the GMR-hid technique to generate whole eye clones of homozygous lethal alleles (Fig. 5.2.). The eyes of flies, whose genotype are *eyFLP/Y* or *+ ;; FRT82B, rab11*/*FRT82B, GMR-hid*, *cl* produce the whole eyes homozygous for *rab11*. The known hierarchy of the strength of the *rab11* mutants according to their bristle phenotype is $rab11^{93Bi}$, $rab11^{j2D1}$, $rab11^{EP3017}$, and $rab11^{ex}$ from the weakest and the strongest. Homozygous $rab11^{93Bi}$ flies are viable. The eyes of these flies show slight roughness. $rab11^{j2D1}$ is homozygous lethal. The exterior eyes of homozygous $rab11^{j2D1}$ generated by GMR-hid technique show no abnormality. Homozygous $rab11^{EP3017}$ or $rab11^{ex}$ generated by GMR-hid have no eyes. Previous studies suggest that strong *rab11* mutants cause cell lethality. The no eye phenotype confirms cell lethality of *rab11* mutants. The allelic combinations of both $rab11^{93Bi}$/$rab11^{j2D1}$ and $rab11^{93Bi}$/$rab11^{EP3017}$ are viable and the exterior eyes do not show detectable abnormality. Among *rab11* mutants, $rab11^{93Bi}$ is determined as the weakest

allele. It is surprising that among viable *rab11* hypomorphs, only *rab11*^{93Bi} homozygous flies show abnormality.

To determine more details of the *rab11* mutants eye phenotype, I sectioned the adult eyes of viable *rab11* hypomorphs. The eye sections of homozygous *rab11*^{93Bi} show a typical phenotype of the failure of Notch activation such as extra R-cells and disorganized facets (Fig. 5.3.A). The eye sections of *rab11*^{93Bi}/*rab11*^{j2D1} are completely normal (Fig. 5.3.B). The exterior eye of *rab11*^{93Bi}/*rab11*^{EP3017} is normal but I could not detect any rhabdomeres (Fig. 5.3.C). A previous study showed that the size of rhabdomeres is reduced when a dominant negative form of Rab11 is expressed (Satoh et al., 2005). Rhabdomeres are formed during pupal stages after cell fate is determined. Failure of rhabdomere formation does not affect the morphology of the exterior eye. Homozygous *rab11*^{j2D1} eyes have many facets with fewer R-cells (Fig. 5.3.D). I could not detect any facets containing extra R-cells. It is the opposite phenotype of what I detected in *rab11*^{93Bi} flies. To determine if the phenotypes are caused by *rab11* mutation only, a genomic *rab11*$^{+}$ rescue transgene was added in the *rab11*^{93Bi} homozygous and *rab11*^{j2D1} whole eye clone background (Fig. 5.4). The addition of the transgene could not rescue the *rab11*^{93Bi} homozygous phenotype. However, the *rab11*^{j2D1} homozygous phenotype is rescued by the addition of the *rab11*$^{+}$ rescue transgene. One copy of the transgene suppresses the phenotype and two copies of the transgene suppress more but not completely. Also, the addition of the transgene rescues the lethality of homozygous *rab11*^{j2D1}. Maybe the transgene does not include eye specific enhancers so that it cannot rescue the eye phenotype completely. In summary, I can say that the phenotype of R-cell loss is truly caused by *rab11* mutant.

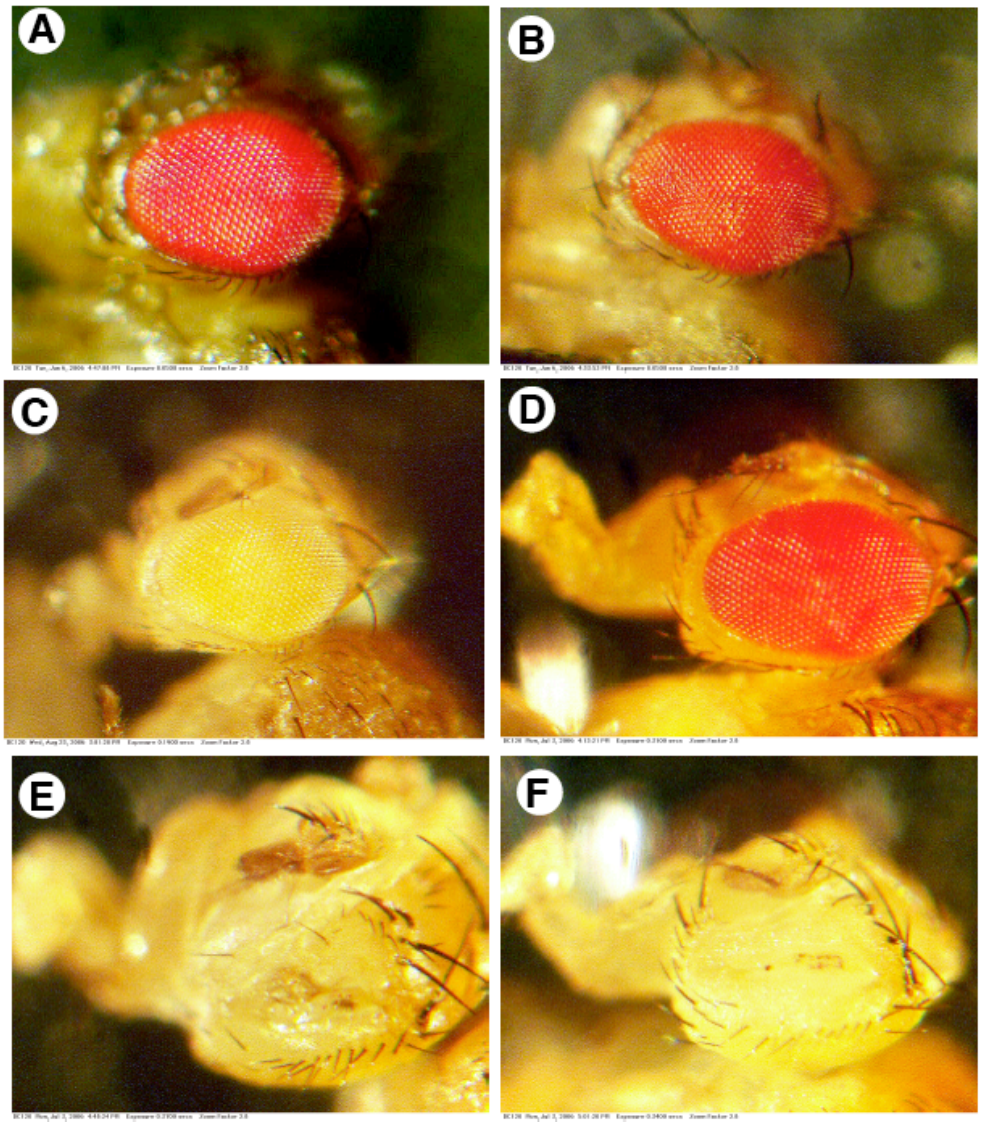

Figure 5.2. Eye phenotypes of *rab11* mutants. Adult eyes of various rab11 viable hypomophic combinations are shown. The genotypes are (A) *rab11*^{93Bi}/*rab11*^{93Bi}, (B) *rab11*^{93Bi}/*rab11*^{j2D1}, (C) *rab11*^{93Bi}/*rab11*^{EP3017}, (D) *ey-gal4*, *UAS-flp* / +; *FRT82B, GMR-hid, cl* / *FRT82B, rab11*^{j2D1}, (E) *ey-gal4*, *UAS-flp* / +; *FRT82B*, *GMR-hid, cl* / *FRT82B, rab11*^{EP3017}, and (F) *ey-gal4, UAS-flp* / +; *FRT82B, GMR-hid, cl* / *FRT82B, rab11*^{ex}. Homozygous *rab11*^{93Bi} flies have slightly rough eyes. Whole eye clones of *rab11*^{EP3017} and *rab11*^{ex} result in no eyes.

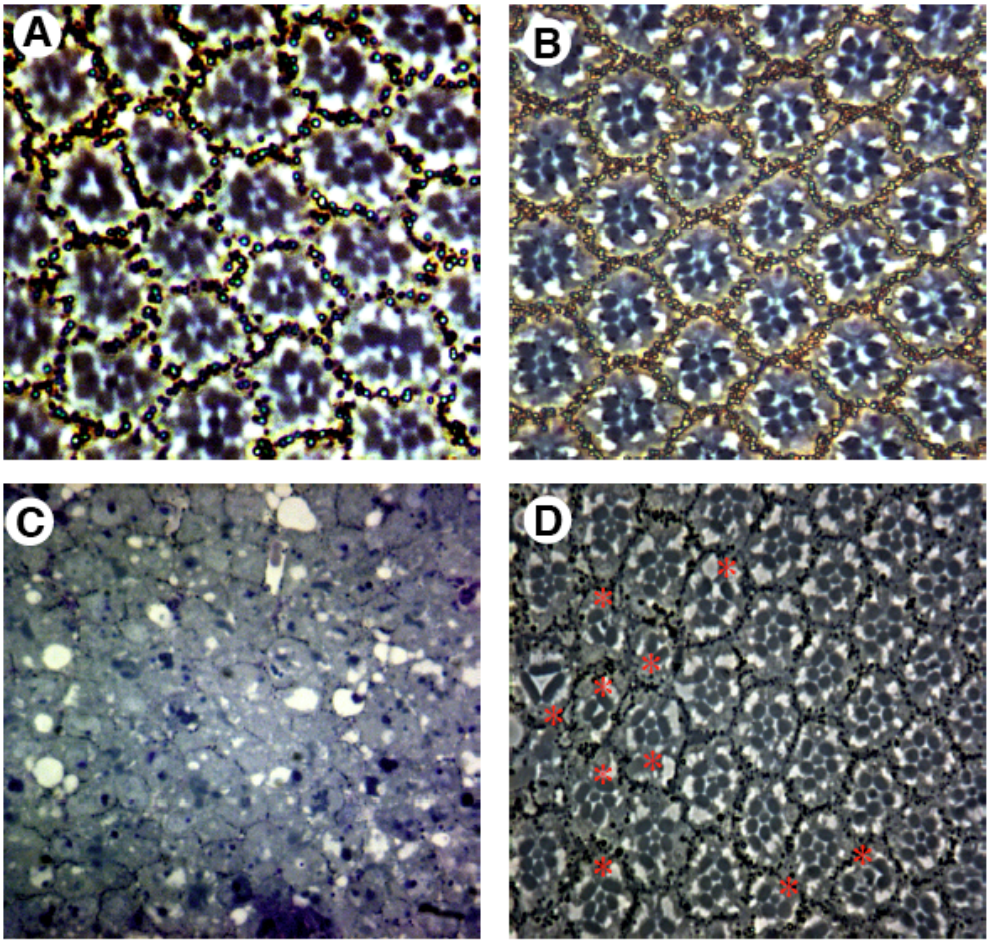

Figure 5.3. Eye phenotypes of *rab11* mutants. The tangential sections of adult eyes of various rab11 viable hypomophic combinations are shown. (A) Homozygous $rab11^{93Bi}$ flies have extra R-cells and disorganized facets. (B) There are no abnormal phenotypes in $rab11^{93Bi}/rab11^{j2D1}$ flies. (C) No rhabdomeres are detected in $rab11^{93Bi}/rab11^{EP3017}$ flies. (D) Some facets contains fewer facets in *ey-gal4*, *UAS-flp* / +; *FRT82B, GMR-hid, cl* / *FRT82B,* $rab11^{j2D1}$ flies. The asterisks in D indicate mutant facets containing fewer R-cells.

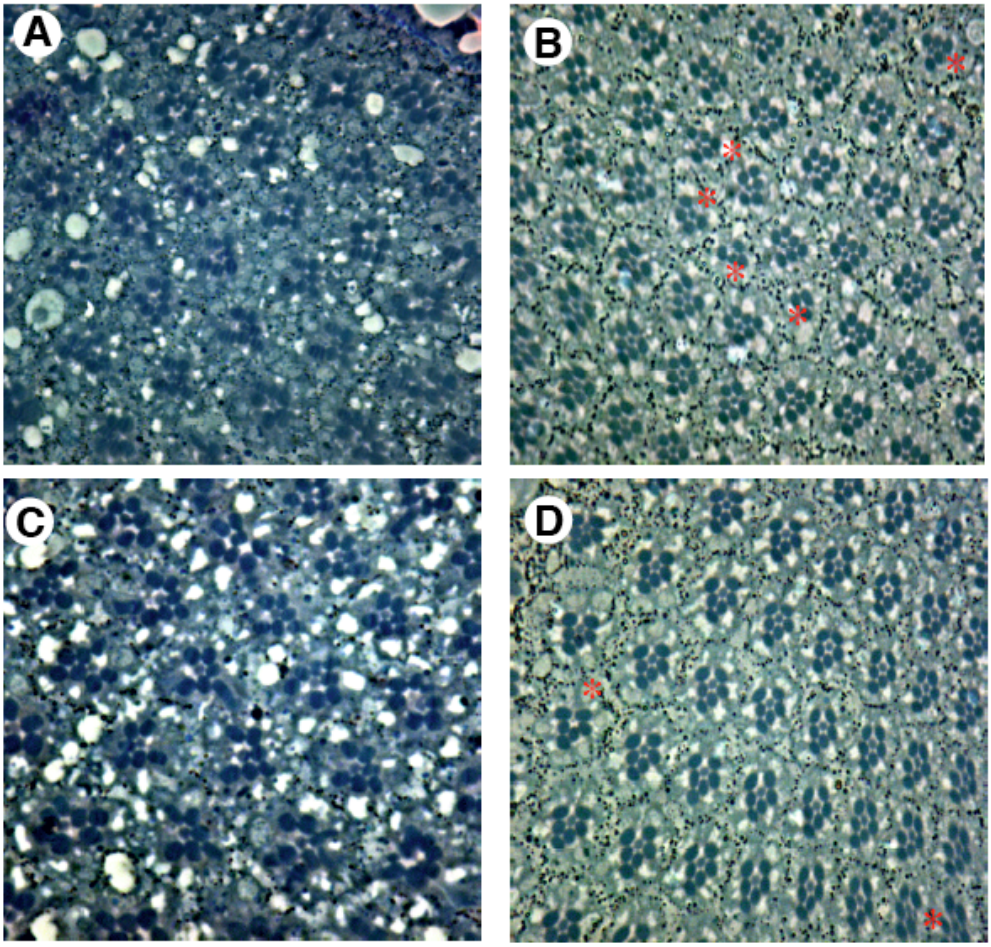

Figure 5.4. Suppression of *rab11* mutant eye phenotypes with *Prab11*$^{+}$. The tangential sections of adult eyes are shown. The eye phenotypes of homozygous *rab11*^{93Bi} flies are not suppressed with one copy of the *Prab11*$^{+}$ transgene (A) and with two copies of the *Prab11*$^{+}$ transgene (C). However, the eye phenotypes of homozygous *rab11*^{j2D1} flies are suppressed with one copy of the *Prab11*$^{+}$ transgene (B) and more with two copies of the *Prab11*$^{+}$ transgene (D) but not completely. The asterisks indicate mutant facets.

One of the indicators of failure of Notch activation during lateral inhibition is accumulation of Delta at the morphogenetic furrow. In *lqf* and *auxilin* mosaic clones, Delta accumulates at the furrow inside of the mutant clones. To detect the level of Delta presemt, I stained eye discs of $rab11^{93Bi}/rab11^{EP3017}$ flies with α-Delta antibody (Fig. 5.5. B). The staining pattern of these flies is not different from wild-type flies. The eye disc of $rab11^{j2D1}$ clone is also stained with α-Delta antibody (Fig. 5.5.C,D). I could not detect any aberrant Delta staining pattern in $rab11^{j2D1}$ homozygous cells. Maybe the allelic combinations of these *rab11* hypomorphs are too weak to produce mutant phenotypes. The other interpretation is that *rab11* is not needed for lateral inhibition. However, the staining results of $rab11^{j2D1}$ clone were not very clear. To determine Delta staining pattern in *rab11* mutants, staining of eye discs of $rab11^{j2D1}$ mosaic clone, $rab11^{EP3017}$ mosaic clone, and $rab11^{93Bi}/rab11^{ex}$ flies needs to be done. Big enough sized $rab11^{EP3017}$ clones in the eye discs can be obtained though whole eye clone of $rab11^{EP3017}$ results in no eyes.

5.2.3. *RO-gal4>UAS-rab11*^{DN} eye disc phenotype

Previously, it has been shown that Delta signaling and endocytosis are important in R2/5 and R3/4 cells. Expression of a dominant negative form of dynamin or Delta in these cells results in extra R-cells (Overstreet et al., 2004). If Delta recycling through recycling endosomes is required to send a signal, *rab11* mutants in the signaling cells will cause a similar phenotype to *Delta* mutants. To test this idea, I expressed dominant negative Rab11 in R2/5 and R3/4 cells using the UAS/Gal4 system. For $Rab11^{DN}$, I obtained a *rab11* cDNA in which amino acid 142 Asn is changed to Ile ($Rab11^{N142I}$) from

the Ready lab. This amino acid is important for GTP binding. This form of Rab11 dominant negative was used previously and its expression causes failure of protein

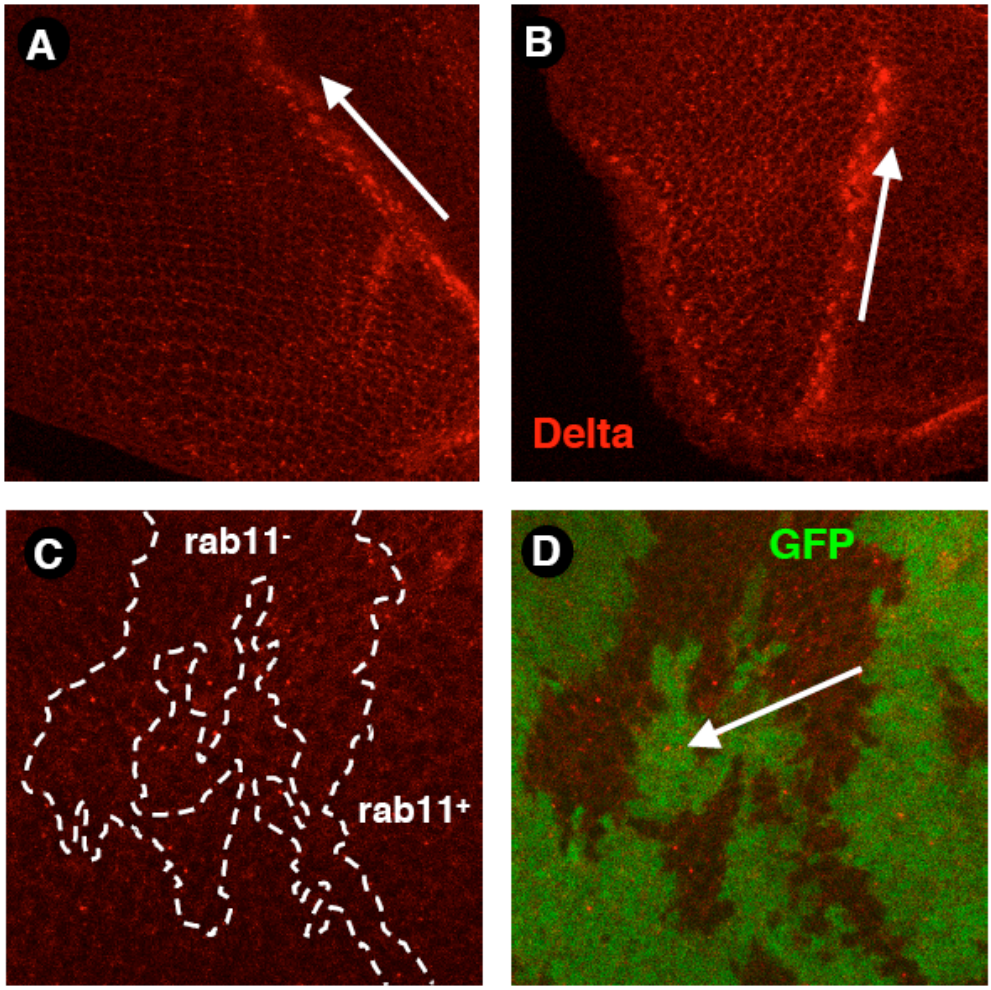

Figure 5.5. Delta staining pattern in *rab11* hypomorphs. Delta staining pattern is not altered in $rab11^{93Bi}/rab11^{EP3017}$ (B) compared to wild-type (A). A clone of $rab11^{j2D1}$ cells outlined in C, marked by the absence of GFP, was generated in flies of the genotype *w, eyFLP;; FRT82B, ubi-gfp / FRT82B,* $rab11^{j2D1}$. Delta staining pattern is not altered in $rab11^{j2D1}$ homozygous cells compared to wild-type (A). Arrows indicate the morphogenetic furrow.

transport to rhabdomeres. There is another form of Rab11^{DN} which is Rab11^{S25N}. Because I also obtained Rab5^{DN} (Rab5^{N142I}) from the Ready lab, I used Rab11^{N142I} for Rab11^{DN}. For Rab7^{DN}, I changed amino acid 125 Asn to Iso. The amino acid sequences including

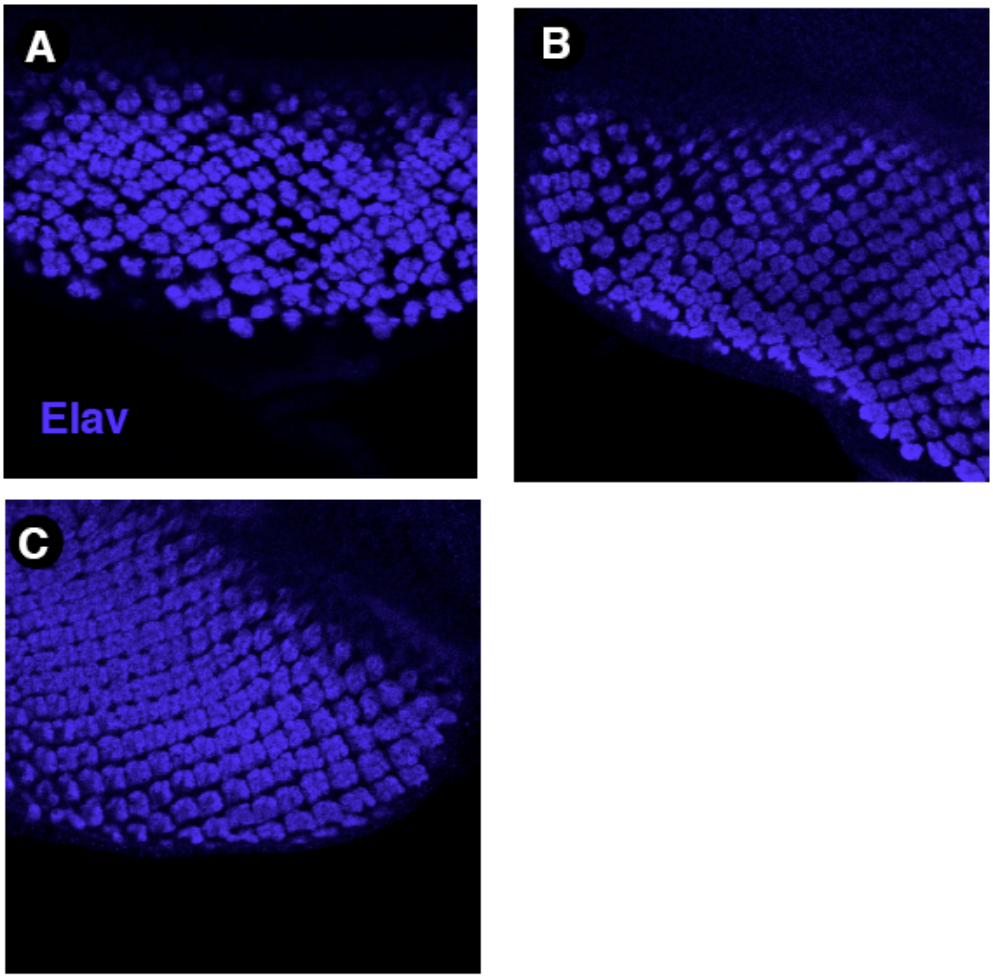

Figure 5.6. The number of R-cells are reduced when *rab11^{DN}* is expressed. Confocal microscope images of third instar larval eye discs are shown. When Delta *rab11^{DN}* is expressed in R2/5 and R3/4 cells, the number of Elav^{+} cells are reduced (A) compared with wild-type (C). However, expression of *rab5^{DN}* in R2/5 and R3/4 cells does not alter the number of Elav^{+} cells (B).

Rab7 amino acid 125 Asn is highly conserved with the Rab5 amino acid sequences including 142 Asn and the Rab11 amino acid sequences including 142 Asn. Bomsoo Cho helped me to generate DNA constructs of *UAS-rab7*^{DN}, *RO-rab5*^{DN}, *RO-rab7*^{DN} and *RO-rab11*^{DN}. I used Rab5^{DN} as a positive control and Rab7^{DN} as a negative control.

Interestingly, I could not acquire any adult flies expressing dominant negative forms of any three Rab proteins using UAS/GAL4 system with *RO-gal4*. When I detected a GFP expression pattern of *RO-gal4>UAS-gfp* in the eye disc, GFP is expressed only in R2/5 and R3/4 cells. Expression of *RO-Delta*^{DN} and *RO-shibire*^{DN} flies are not lethal and show an eye specific phenotype (Overstreet et al., 2004). It suggests that the *RO-vector* itself is very eye specific, but *RO-Gal4* express GAL4 in the some other places that are essential for the viability. Even though I could not collect adult flies, I was able to obtain larvae, which express dominant negative forms of Rab proteins when I used *RO-gal4*. I stained eye discs using α-Elav antibody. I could not detect any abnormality from *RO-gal4>UAS-rab5*^{DN} (Fig. 5.6.B) though I expected to detect extra R-cells because Rab5^{DN} causes defects in internalization (Satoh et al., 2005). However, flies of *RO-Gal4>UAS-rab11*^{DN} contain fewer R-cells (Fig. 5.6.A). This phenotype is consistent with the phenotype of *rab11*^{j2D1}. To test whether a fewer R-cell phenotype is related with Delta expression, I examined the level of Delta present when dominant negative forms of Rab5 and Rab11 are expressed in R2/5 and R3/4 cells (Fig. 5.7.). A previous study showed that expression of *Delta*^{DN} and *shibire*^{DN} using a *RO*-vector results in extra R-cells. It is thought that the extra R-cell phenotype is caused by the failure of R-cell restriction, which takes place later than lateral inhibition. Therefore, I did not expect to detect failure of lateral inhibition when dominant negative forms of Rabs were expressed in R2/5 and

R3/4 cells. I could not detect any aberrant Delta staining pattern in *RO-gal4>UAS-rab5*^{DN}

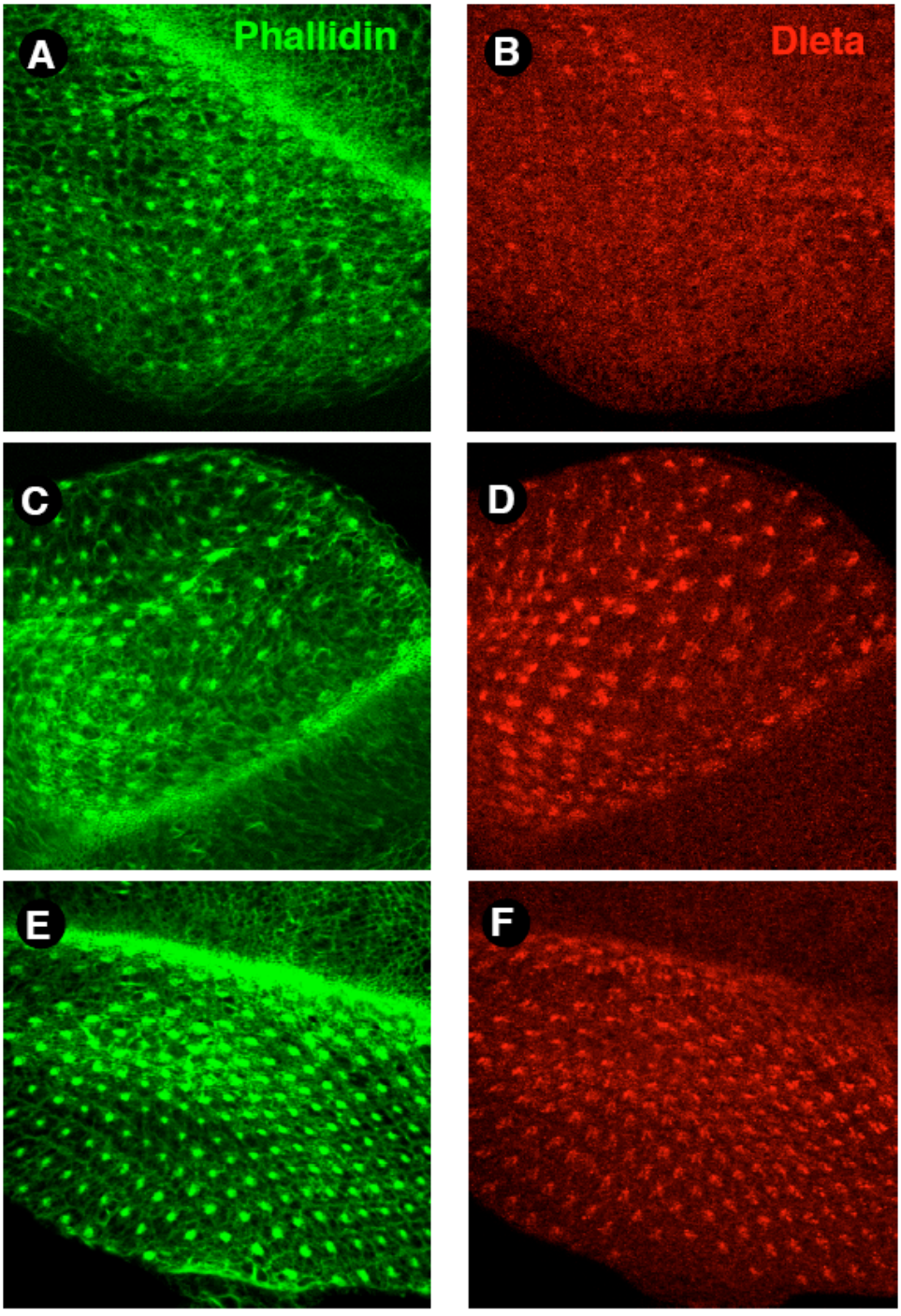

Figure 5.7. Delta staining is reduced when *rab11^{DN}* is expressed. Confocal microscope images of third instar larval eye discs are shown. When *rab11^{DN}* is expressed in R2/5 and R3/4 cells, Delta staining is reduced (A) compared with wild-type (E). However, expression of *rab5^{DN}* in R2/5 and R3/4 cells does not alter the Delta staining pattern (C).

flies. Because I could not a detect mutant phenotype from α-Elav staining, expression of Rab5^{DN} may not cause a defect of Notch signaling. Even if expression of Rab5^{DN} causes failure of R-cell restriction, it may not cause the failure of lateral inhibition. Interestingly, I detected less Delta in the eye disc of *RO-gal4>UAS-rab11^{DN}* flies. One possible explanation of this observation it that in *rab11* mutants, internalized Delta is transferred to the lysosomes for the degradation instead of being recycled on the plasma membrane. However, we do not know if internalized Delta is really recycled to the plasma membrane or not. Anyway, less Delta staining is also the opposite phenotype of Notch signaling defects which usually cause more Delta staining.

5.2.4. *RO-rab11^{DN}* adult eye phenotype

To detect the dominant negative phenotype of three Rabs in the adult eyes, I constructed *RO-rab5^{DN}*, *RO-rab7^{DN}*, and *RO-rab11^{DN}* and I obtained about 20 lines of each DNA construct. I could not detect any rough eye phenotype from *RO-rab5^{DN}* and *RO-rab7^{DN}* transgenic lines. Because I expected extra outer R-cells from *RO-rab5^{DN}*, I sectioned adult eyes from homozygous flies of several lines. I detected only one facet containing two inner R-cells (R7 or R8) (Fig. 5.8.). This phenotype is not what I expected and I found only one mutant facet. Thus, I cannot assert that this phenotype is really caused by blocking of Rab5 function in R2/5 and R3/4 cells. Some homozygous flies of

RO-rab11^{DN} show a slightly rough eye phenotype (Fig. 5.9.B). The facets of homozygous *RO-rab11*^{DN} lines contain fewer R-cells though the severity is different from each transgenic line (Fig. 5.9.C-F). This phenotype is consistent with the *rab11* hypomorph (*rab11*^{j2D1}) and eye discs of *RO-gal4>UAS-rab11*^{DN}. *Drosophila rab11* mutants show cell lethality and failure of rhabdomere formation. It is possible that the fewer R-cell phenotype is caused by cell lethality and failure of rhabdomere formation. From the arrangement of the R-cells, the identity of R-cells can be determined easily. In many cases, the missing cells (or rhabdomere) are R1 and/or R6 cells where Rab11^{DN} is not

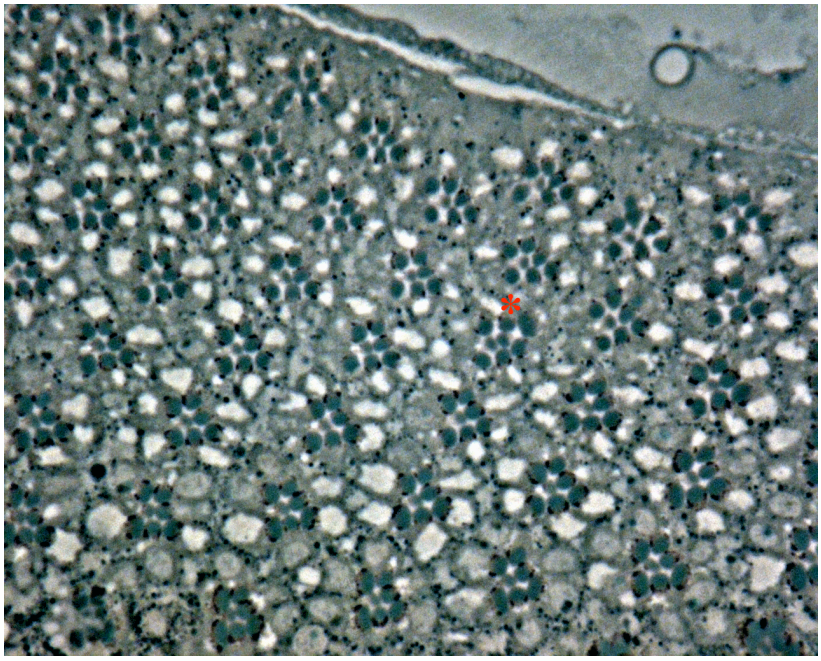

Figure 5.8. Eye phenotype of expression in R2/5 and R3/4 cells. The tangential sections of adult eyes of *RO-gal4>UAS-rab5*^{DN} are shown. All facets are normal except one, which contains an extra inner R-cell (asterisk).

expressed. It suggests that the fewer R-cell phenotype is not caused by cell lethality or failure of rhabdomere formation. Interestingly, some facets contain extra inner R-cells (R7 or R8).

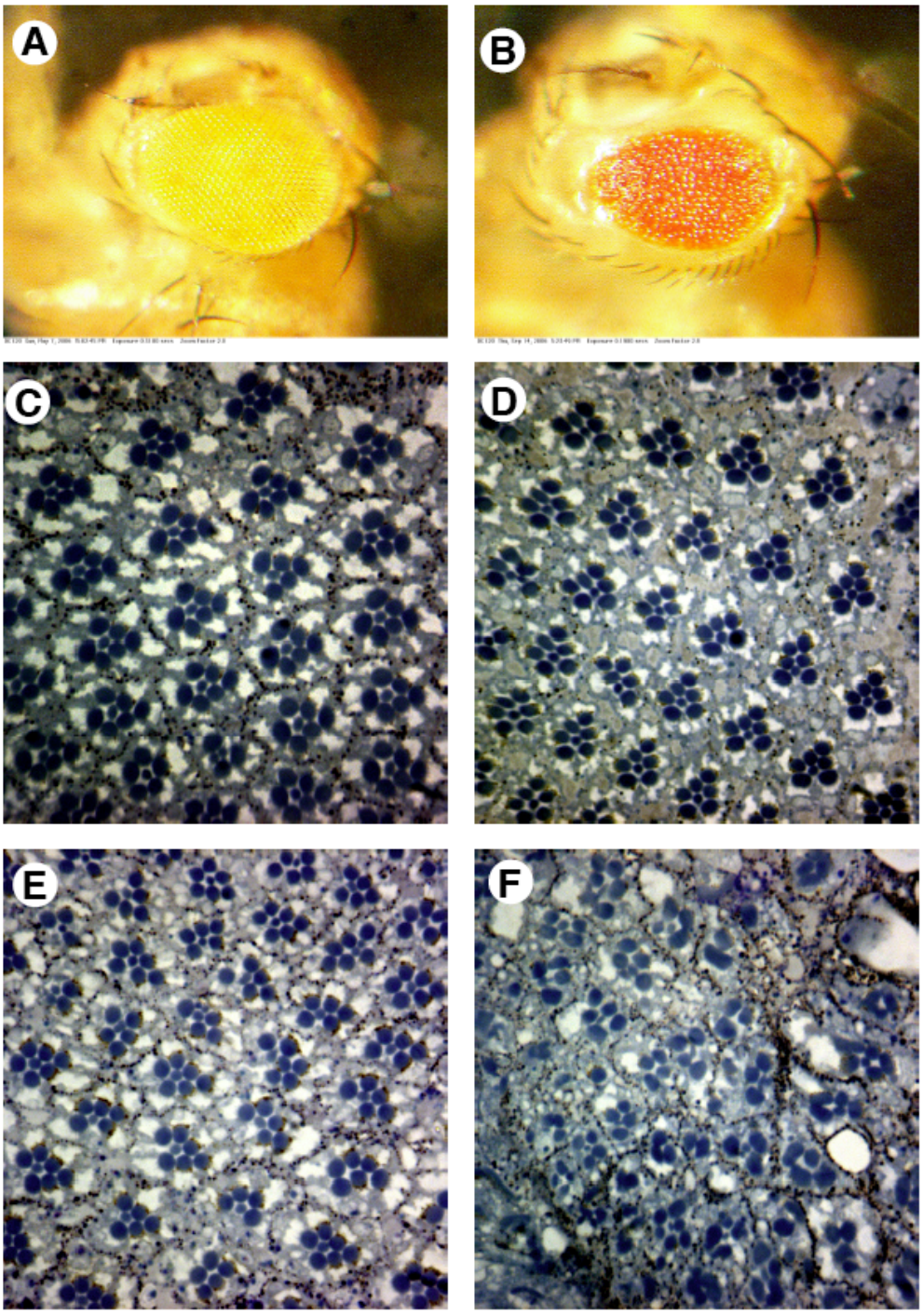

Figure 5.9. Expression of *rab11*^{DN} results in fewer R-cells. When *rab11*^{DN} is expressed in R2/5 and R3/4 cells, a rough eye phenotype is generated (B). (A) a wild-type eye is shown. The tangential sections of adult eyes of four *RO-rab11*^{DN} lies are shown (C-F). All sections have facets with fewer R-cells with various expressivity.

5.3. Discussion

5.3.1. *Rab11* mutant phenotype is the opposite of the phenotype of Notch signaling component mutants

5.3.1.1. *Rab11* mutants show the fewer R-cell phenotype.

Rab11 functions in the recycling endosomes. If the recycling model is correct, I would expecte to see a *rab11* phenotype similar to *Delta*, *lqf*, and *auxilin* mutants. Previous studies showed that *rab11* mutants have fewer and shorter bristles. For bristle formation, Notch signaling is required at two different stages during the sensory organ precursor (SOP) cell division. SOP cells are asymmetrically divided twice. At the first division, pIIb sends signal to pIIa to activate Notch in pIIa to prevent from becoming pIIb. The failure of Notch activation in this step causes a fewer-bristle phenotype. In the 2nd asymmetric division, pIIa is divided into the bristle cell and the socket cell. The bristle cell sends a signal to the socket cell to activate Notch to prevent it from becoming the bristle cells. The failure of Notch activation in this step causes the more-bristle phenotype. Notch signaling defects can cause either more- or fewer-bristle phenotype. However, the weak alleles of Notch signaling component genes usually cause a more-

bristle phenotype, for example *faf* and *lqf*. Probably, the second asymmetric division of SOP is more sensitive than the first one. The fewer-bristle phenotype in *rab11* hypomorphs are the opposite of the usual Notch signaling components mutants. Homozygous eye of a specific *rab11* allele, $rab11^{j2D1}$ shows a fewer R-cell phenotype. This is also the opposite phenotype of other Notch signaling components such as *faf*, *lqf*, *auxilin* and *Delta*. Theoretically, the fewer R-cell phenotype can be caused by failure of Notch activation. The proneural enhancement depends on Notch activation. Without proneural enhancement, R-cells cannot be generated. However, probably because of partial sensitivity of lateral inhibition and R-cell restriction, hypomorphs of the Notch signaling components show extra R-cells. The fewer-R-cell phenotype is consistently detected when $rab11^{DN}$ is expressed in R2/5 and R3/4 cells. Is the homozygous $rab11^{j2D1}$ phenotype also caused by a defect of Rab11 function in R2/5 and R3/4 cells? To answer this question, I need to add a $RO\text{-}rab11^{+}$ transgene in the $rab11^{j2D1}$ background. If the answer is yes, it means that R2/5 and R3/4 cells are very sensitive about the level and/or activity of Rab11. If Rab11 is required in the signaling cell for Delta signaling as suggested in the recycling model, expression of $Rab11^{DN}$ in R2/5 and R3/4 cells must show the extra R-cells as shown in $RO\text{-}Delta^{DN}$ and $RO\text{-}shibire^{DN}$ (Overstreet et al., 2004). However, I detected fewer R-cells. This phenotype is the opposite of blocking of Delta signaling in R2/5 and R3/4 cells. The *rab11* mutant phenotype argues against the recycling model.

5.3.1.2. Less Delta staining in *Rab11* mutant eye discs.

In *auxilin* and *lqf* mutant clones, Delta expression is increased due to lateral inhibition failure. However, there is no aberrant Delta staining pattern in the positive control, *RO-gal4>UAS-rab5*^{DN} flies. Elav staining, which represents R-cells, was not affected in the eye disc of *RO-gal4>UAS-rab5*^{DN} flies. The result indicates that expression of Rab5^{DN} in R2/5 and R3/4 cells does not cause any mutant phenotypes at least related with Delta signaling. Maybe the UAS-rab5^{DN} transgene is not functional or Delta internalization is not dependent on Rab5 function or expression level is not enough to antagonize endogenous Rab5. Interestingly, Delta staining was reduced in *RO-gal4>UAS-rab11*^{DN} flies. I cannot explain how there is less Delta staining when Rab11^{DN} is expressed in R2/5 and R3/4 cells. However, less Delta staining is also the opposite phenotype with mutation of the Notch signaling component genes. To reinforce the dominant negative characteristic, I tried to detect less Delta staining under more physiological conditions using loss-of-function alleles. However, I could not find any hypomorphs that showed aberrant Delta staining.

Do *rab11* mutant phenotypes completely rule out the recycling model? With *auxilin* results that suggest uncoated vesicles per se are not important for Delta signaling, I think that *rab11* mutant phenotypes argue against the recycling model. However, I cannot completely rule out the recycling model. Delta can be recycled in a Rab11-independent way. If so, the papers (Emery et al., 2005 and Jafer-Nejad et al., 2005) which used Rab11 binding partners to support the recycling model will be weakened. There is another explanation. Rab11 is pleiotropic. Some other functions are required earlier and at higher levels than those required for recycling of Delta, so it is impossible to detect Delta recycling failure in *rab11* mutants.

5.3.2. *Rab11* interacts genetically with *lqf* and *auxilin*.

Rab11 mutants did not enhance *lqf* and *auxilin* hypomorphs. However, not only strong alleles but also weak alleles of *lqf* and *auxilin* dominantly induce lethality of *rab11* hypomorphs. The genetic interaction among these three genes suggests that *rab11* may function in the same pathway in the same direction with *auxilin* and *lqf*. Why is this genetic interaction one direction? One possible explanation is that the *rab11* hypomorph is not sensitive to the change of the protein levels of *lqf* and *auxilin*, but *auxilin* and *lqf* hypomorphs are sensitive to the change of protein level of *rab11*. Another explanation is that the *rab11* hypomorph is very sick and the addition of one copy of either a *lqf* or *auxilin* mutation make it worse non-specifically. I could detect only lethality but not any enhancement of morphological phenotype so the second explanation is also possible. However, I think the first explanation is more likely for two reasons. First, because *rab11* hypomorphs have not many progenies, the flies would not be very sick. Second, the fact that weak alleles of two different genes enhance very strongly is not likely. To distinguish these two possibilities, it will be helpful to check whether or not *auxilin* and *lqf* mutants enhance the morphological phenotype of weaker rab11 hypomorphs such as $rab11^{93Bi}/rab11^{j2D1}$ and $rab11^{93Bi}/rab1^{jEP3017}$.

If *rab11* does not function during Delta signaling, how can *rab11* genetically interact with *auxilin* and *lqf*? One possibility is that Rab11 functions in the other pathway which is closely related with Notch signaling. Another possibility is that Rab11 functions only in a Notch signaling event in which failure of Notch activation generates the opposite phenotype of weak *auxilin* or *lqf*.

5.3.3. Is the *rab11^{DN}* phenotype related with *rough* gene?

The eye section pattern of expressing Rab11^{DN} in R2/5 and R3/4 cells is very similar to the null phenotype of the *rough* gene, such as fewer R-cells and extra inner R-cells. Rough is expressed at the morphogenetic furrow and then restrained into R2/5 and R3/4 cells. Atonal is a proneural transcriptional factor which is responsible for R8 cell specification (Baker et al., 1996; Baker, 2002). Atonal expression is negatively regulated by *rough*. (Dokucu et al., 1996). It is proposed that multiple R8 cells in *rough* mutant are caused by the failure of restriction of Atonal into a single cell. Rough is a transcriptional factor containing homeobox. Even Rough is expressed in R2/5 and R3/4 cells behind the morphogenetic furrow, it functions only in R2 and R5 cells (Tomlinson et al., 1988). The exact function and the direct target gene of Rough are not known yet. In *rough* mutants, R2 and R5 cells loose their identity and cannot recruit R1 and R6, resulting in fewer R-cells (Tomlinson et al., 1988). However, which signal to recruit R1 and R6 is defected in *rough* mutants is not known. Is Rab11 required in downsteam signaling of *rough*? I do not think that the similar phenotype of *RO-rab11^{DN}* and *rough* mutants necessarily supports the relationship between them. *RO*-vector does not express genes at the morphogenetic furrow. GFP is only expressed in R2/5 and R3/4 cells after 2-3 rows behind the morphogenetic furrow in *RO-gfp* and *RO-gal4>UAS*-gfp flies. If there is a small amount of expression at the morphogenetic furrow, which cannot be detected by GFP expression, *RO-Delta^{DN}* and *RO-shibire^{DN}* would have shown the defect of proneural enhancement. Therefore, multiple R8 cells caused by expression of Rab11^{DN} by *RO*-vector are not related with Rab11 function at the morphogenetic furrow. Just by looking at the eye section, it is hard to identify inner R-cell as R7 or R8. Maybe the

multiple inner R-cells are R7s rather than R8s. It is possible that *rough* mutants and *RO-rab11^{DN}* induce the same signaling defects in R2 and R5 to recruit R1 and R6.

5.3.4. Is the *rab11^{DN}* phenotype related with EGFR?

Many of the missing R-cells in *RO-rab11^{DN}* flies are the cells where *rab11^{DN}* is not expressed. This result indicates that the missing R-cells in *RO-rab11^{DN}* fail to get the signal to obtain R-cell identity. What are the possible signaling pathways? One is the EGFR signaling pathway. For R-cell specification, EGFR signaling as well as Notch signaling is important (Baker and Rubin, 1989; Cagan and Ready, 1989; Kumar and Moses, 2001) During lateral inhibition, EGFR is activated in the signaling cells and increases expression of Delta and decreases expression of Notch. However, in the receiving cells, EGFR is not activated and Delta expression decreases. When Rab11^{DN} was expressed in R2/5 AND R3/4 cells, I detected less Delta staining in the eye disc. Some exocyst components such as Sec15 have been known to function with Rab11. If Rab11 is required for secretion of Spitz, a ligand of EGFR, *rab11* mutant can cause failure of EGFR activation in neighboring cells. I think it is possible that failure of EGFR signaling in some cells may prevent them from becoming signaling cells expressing Delta. This hypothesis also fits well with the idea that R1 and R6 cells fail to activate EGFR and loose neural cell fate. However, there is a drawback in this hypothesis. The *RO*-vector expresses genes at 2 or 3 rows posterior to the morphogenetic furrow, which is later than lateral inhibition. When Delta^{DN} is expressed by the *RO*-vector, any phenotype related with a lateral inhibition defect was not detected. Another possible explanation for the less Delta staining pattern when Rab11^{DN} is expressed in R2/5 AND R3/4 cells is that

Delta was not transferred to the plasma membrane. Because Rab11 is required in Golgi to plasma membrane trafficking, Delta may not be able to be transferred to the plasma membrane in the *rab11* mutants. However, Delta staining decreases at the morphogenetic furrow where Rab^{DN} is not expressed in *RO-gal4>UAS- rab11*^{DN} eye discs. To verify whether Delta is less expressed or not, I will examine *Dl-lacZ* transgene expression in *RO-rab11*^{DN} flies. If LacZ staining is reduced, it would suggest that Delta transcription decreases in *rab11* mutants. If LacZ staining is not reduced, it would suggest that Delta transfer is defected in *rab11* mutants. It would be better if I can detect a *Dl-lacZ* expression pattern in *rab11* loss-of-function mutants. However, I could not find any viable *rab11* hypomorphs which show less Delta expression. Both the *Dl-lacZ* enhancer trap and *rab11* gene are located on the right arm of chromosome 3. If I generate mosaic clones of *rab11* using FRT-induced mitotic recombination, it will affect the number of copies of the *Dl-lacZ* enhancer trap. If *Dl-lacZ* is on the same chromosome with *rab11* mutant, the mutant clone will contain two copies of the enhancer trap and the twin spot will not contain any. If *Dl-lacZ* is on the opposite chromosome from the *rab11* mutant, the mutant clone will not contain the enhancer trap. Thus, I can use only the *Dl-lacZ* enhancer trap in *rab11*^{DN} flies.

In summary, *rab11* mutants have the opposite phenotypes from the Notch signaling defect. The phenotype of *rab11* mutants argues against the recycling model. However, I cannot completely rule out the recycling model. Delta might be recycled in a rab11-independent pathway. Why do *rab11* mutants show the opposite phenotype from Notch signaling components? To address this question, first I need to determine why

Delta is less expressed in *rab11* mutants. If Delta expression is reduced, then whether or not this phenotype is related with EGFR signaling defect needs to be tested using genes functioning in EFGR-dependent Delta transcription such as *sno* and *ebi*.

Appendices

Appendix 1. Miscellaneous experiments

A.1.1. FLP-out (Generation of *auxilin* mosaic clones)

Notch signaling is required in a variety of contexts at many different stages during eye development. FRT/FLP-induced mitotic recombination requires mitosis and most mitosis in the eye occurs before cell differentiation. Notch signaling has several different functions during this time and thus the phenotype of strong *auxilin*$^{-}$ mutants generated by mitotic recombination might be very complicated. If I can eliminate the *auxilin*$^{+}$ gene during a specific Notch signaling event, it will help to elucidate the *auxilin*$^{+}$ function in Notch signaling. This would be accomplished by the FLP-out technique. One advantage of this technique is that it does not require mitosis. I can turn off *auxilin*$^{+}$ even after the morphogenetic furrow, where only one more round of mitosis occurs. When two FRT sites are close to each other and in the same direction, the DNA fragment between two FRT sites is looped out when FLP is present (Fig. A.1). To perform FLP-out, I generated a construct where a genomic DNA fragment containing the *auxilin*$^{+}$ gene and a marker (*white*$^{+}$ for adult eyes and *tubulin-gfp* for larval eye discs) are flanked by two FRT sites and I obtained several transgenic flies. The transgene complements all *auxilin*$^{-}$ mutant phenotypes.

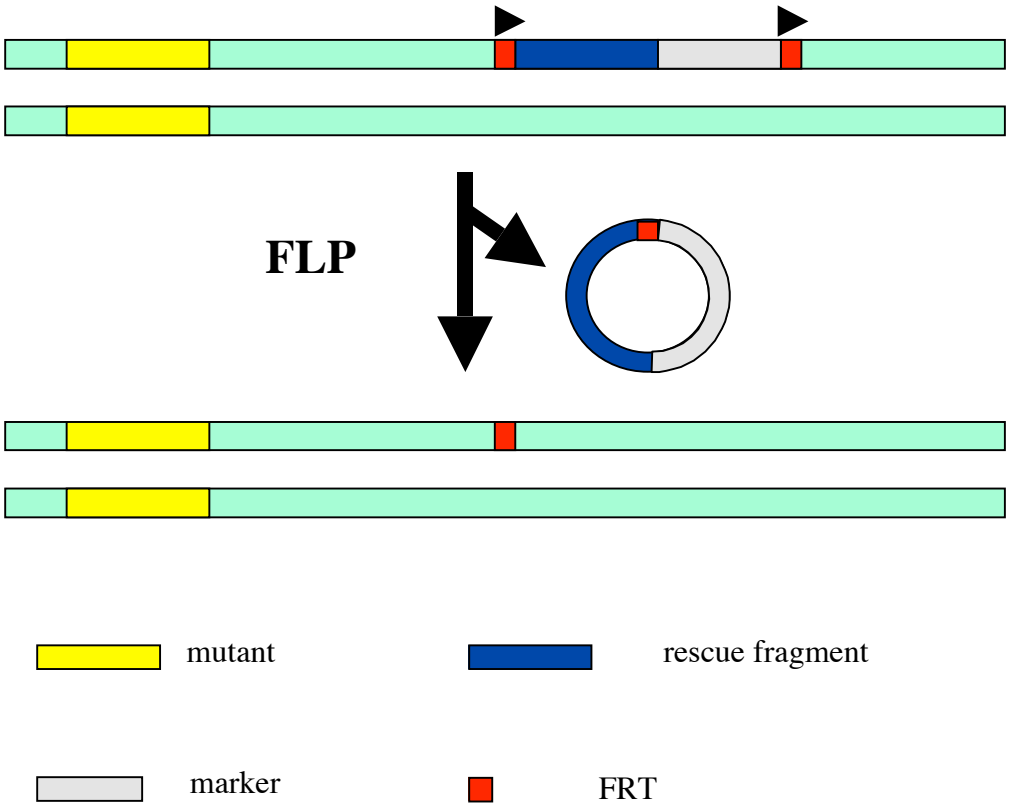

Figure A.1. FLP-out. A diagram of the FLP-out method is shown. The only functional gene in the homozygous mutant animals is looped out from the chromosome with a maker gene when two FRT-sites are flanked by these genes by activity of FLP recombinase. Color codes are indicated in the diagram.

To FLP-out, I used FLP lines driven by different kinds of eye specific promoters. First, I used ey-FLP. *Eyeless* expresses genes from a very early stage of eye development. When I FLPed-out the *auxilin*$^{+}$ rescue fragment with a marker using *ey-FLP*, I could not find any adult flies. It suggests that the *ey-FLP* line I have is not eye-specific. I tried

another *ey-FLP* line which is known to be more eye-specific. Again, when I FLPed-out the *auxilin*$^{+}$ rescue fragment, I could not find any adult flies. This suggests again the new *ey-FLP* line is not eye-specific, either. However, I was able to detect pupae after FLP-out. In the larvae, eye discs and antenna discs were not formed. I concluded that the FLP-out technique is working with *ey-FLP* and that *auxilin*$^{+}$ is required from an early stage of eye development for eye disc formation.

To FLP-out in more specific cells, I used *GMR-gal4>UAS-flp* and *RO-gal4>UAS-flp*. The *GMR* vector is active in all cells starting 3-4 rows posterior to the morphogenetic furrow and *RO* vector activity starts anterior to *GMR* in R2/5 and R3/4 precursor cells. In both cases, I could not detect any eye abnormalities. There are several possible explanations. First, as the GAL4/UAS system requires intermediates, the rescue fragment may be FLPed-out later than when the *auxilin*$^{+}$ gene is required. Second, the FLPed-out fragment may be stable as a circular form of DNA and mitosis might be required to eliminate it. I think the second model is more likely. If a unique DNA restriction site such as I-SceI, which is commonly used to introduce a cut during homologous recombination is added, it might be helpful to degrade this circular DNA. To add a restriction site in the circular DNA, I need to generate DNA constructs and then transgenic flies. This process will take a very long time and FRT-induced mitotic recombination is working well. Therefore, I did not pursue this experiment anymore.

A.1.2. GAL80 (Generation of *auxilin* mosaic clones)

GAL80 is a repressor of GAL4. GAL80 binds GAL4 and prevents GAL4 from activating transcription. If a gene is expressed using the GAL4/UAS system, the

expression can be blocked by temporal- and spatial-specific expression of GAL80. Using GAL80 expression, I wanted to turn off the *auxilin*$^{+}$ gene in specific cells during eye development. When *UAS-auxilin* is expressed by ubiquitously expressing GAL4 promoters such as *Act5C-gal4* and *Tubulin-gal4*, it completely rescues the *auxilin*$^{-}$ phenotype. I generated transgenic flies containing a *GMR-gal80* or a *RO-gal80* transgene. Using these transgenic flies, I generated flies whose genotype was *w*; *Act5C-gal4*/*GMR-gal80 (*or *RO-gal80)*; *aux*^{727}, *UAS-auxilin*/*aux*^{D136}. These flies appeared wild-type, indicating that GAL80 was not shutting down GAL4 function. The most likely reason for that is the amount of GAL80 expressed is too low. One thing I can try is to introduce more copies of RO-GAL80. As FRT/FLP induced mitotic recombination is working, I decided not to work on this technique any more.

A.1.3. Delta endocytosis is failed in *faf* mutant

In *auxilin* and *lqf* mutant eye discs, more Delta staining is easily detected. There are two possibilities for how there is more Delta staining. One is that Delta transcription is increased by the failure of Notch activation during lateral inhibition. The other is that Delta is failed to be endocytosed, so that Delta accumulates on the plasma membrane. Faf functions only during R-cell restriction (Overstreet et al., 2004). In *faf* mutant eye discs, Delta accumulates on the membrane. Therefore, I assumed that Delta accumulation on the membrane in *faf* mutants is caused by failure of Delta endocytosis. If Delta accumulation is solely caused by failure of Delta endocytosis in *faf* mutants, Delta transcription will not be increased.

I tried to check the transcription level of Delta using the *Dl-lacZ* enhancer trap. Because the *Dl-lacZ* enhancer trap is located in the same chromosome arm with *faf* gene, if I generate mutant clones of *faf* using FRT82B, it will also affect the *Dl-lacZ* enhancer trap. Therefore, to generate *faf* mutant clones, I used a faf^{+} transgene located on the X chromosome. I generated female flies whose genotype are w^{-}, $P\{w^{+}, faf^{+}\}$, $P\{w^{+}$, *ubi-gfp}, FRT19A/*w^{-}, *FRT19A;; Dl-lacZ,* faf^{BX4}*/ey-gal4, UAS-flp,* faf^{FO8}. Because one X chromosome needs to have 3 different transgenes, genomic faf^{+} transgene, cell maker *ubi-gfp* and *FRT19A*, it took very long time to generate this chromosome. Some of these genotype flies have completely normal eyes. GAL4 proteins sometimes rescue the *faf* mutant phenotype. Thus, this genotype is not good to detect the Delta transcription level in a *faf* mosaic. I dissected and stained *faf* mosaic eye discs with α-LacZ antibody. In some facets, I was able to detect more β-galactosidase protein in the *faf* side (Fig A.2.). Probably, the GAL4 protein did not rescue *faf* mutants in these specific flies. It suggests that Delta transcription is increased in *faf* cells. One interpretation is that Delta is more transcribed when R-cell restriction fails. Another interpretation is that R-cell restriction is not really separated from lateral inhibition. Maybe that is the reason why I detected extra R-cells, even though all R-cells were wild-type in aux^{K48} mutant clones and why I detect less Delta staining when I express $Rab11^{DN}$ in R2/5 and R3/4 cells.

To generate more convincing and consistent data, I need to use *ey-flp* instead of *ey-gal4, UAS-flp*. I am crossing flies to generate w^{-}, $P\{w^{+}, faf^{+}\}$, $P\{w^{+}$, *ubi-gfp}, FRT19A/*w^{-}, *FRT19A;; Dl-lacZ,* faf^{BX4}*/ey-flp,* faf^{FO8}. I expect to consistently detect more LacZ expression in *faf* clone sides.

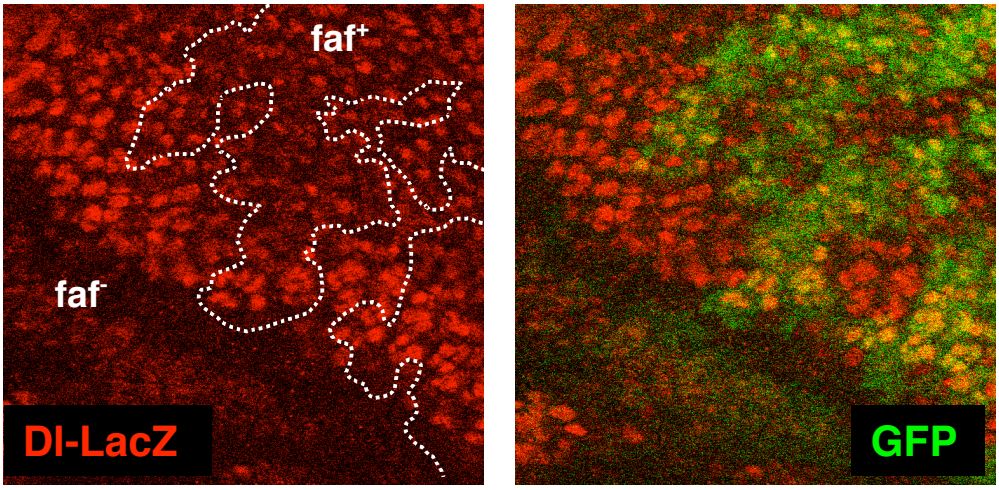

Figure A.2. Dl-lacZ staining pattern in *faf* hypomorphs. Confocal microscope images of third instar larval eye discs are shown. A clone of *faf- (faf^{BX4}/faf^{FO8})* cells outlined in A, marked by the absence of GFP, was generated in flies of the genotype *w^-, P{w^+, faf^+}, P{w^+, ubi-gfp}, FRT19A/w^-, FRT19A;; Dl-lacZ, faf^{BX4}/ey-gal4, UAS-flp, faf^{FO8}*. In faf- cells, Dl-lacZ staining is elevated.

A.1.4. Generation of *chc* mosaic clone

From *auxilin* mutant results, I showed that Delta is endocytosed in a clathrin-dependent way for Notch activation. A strong mutant allele of *chc* genetically interacts with *lqf* and *auxilin*. The addition of a chc^+ transgene suppresses the *auxilin* mutant phenotype. In *auxilin* mosaic eye discs, Delta is endocytosed in $auxilin^-$ cells. This result suggests that bulk endocytosis of Delta is not endocytosed in a clathrin-dependent way. However, in the wild-type eye discs, $Delta^+$ puncta are always colocalized with auxilin. This result conflicts with the idea that bulk endocytosis is independent from clathrin.

Because auxilin function involves clathrin, colocalization between auxilin and Delta suggests Delta bulk endocytosis is somehow related with clathrin. If I generate *chc* mosaic clones, I can answer whether Delta bulk endocytosis is clathrin-dependent or not. Also, I can test whether Delta endocytosis for Notch signaling is clathrin-dependent and I can determine whether clathrin is also required in the receiving cells.

In *Drosophila*, the *chc* gene is located on the X chromosome and there are several mutant alleles. Among those, chc^{1} is a null allele and chc^{4} is a hypomorph allele. Sometimes, chc^{4} male flies are viable without any morphological mutant phenotype. I decided to use the chc^{1} allele to generate mosaic clones. To use FRT-induced mitotic recombination, I tried to recombine chc^{1} and FRT19A. I balanced 20 recombined chromosomes with FM7. I collected chromosomes possibly containing chc^{1} using homozygous lethality. The chromosome containing chc^{1} is homozygous lethal and the lethality is rescued by addition of a chc^{+} transgene. Thus, chc^{1} is the only lethal mutation in this chromosome. I determined existence of FRT19A by crossing these chromosomes with *P{w^{+}, ubi-GFP}, FRT19A; eyFLP* flies. If the recombined chromosome contained FRT19A, I would see female progeny whose eyes were a mosaic of w^{+}. I could not find any flies containing FRT19A among homozygous lethal flies. I repeated the same experiment to eliminate possible errors and contamination. I failed to obtain any flies containing both chc^{1} and FRT19A. Because the cytological location of *chc* is 13F5, recombination of chc^{1} and FRT19A should not be very difficult. I then collected 40 recombined chromosomes, and I crossed all 40 chromosomes with *P{w^{+}, ubi-GFP}, FRT19A; eyFLP* flies. Among the 40 recombined lines, 18 lines have chc^{1} only (homozygous lethal), 19 lines have FRT19A only (w^{+} mosaic eyes), 3 lines have neither

of one and no lines have both *chc*^{1} and FRT19A. Three lines without *chc*^{1} and FRT19A indicate that there was recombination. Clathrin should be very important for the cell survival. If the null allele of *chc* is cell lethal, I would not obtain any mosaics of *chc* as in the case with *GMR-Hid*. A few of homozygous lethal 18 lines probably contain FRT19A but I cannot detect a mosaic eye because of *chc*^{1} cell lethality. In summary, I failed to generate *chc* clones using a *chc* null allele.

Expression of the dominant negative form of Chc in various locations and times will be helpful to determine clathrin function during Notch signaling. In the mammalian cells, expression of the hub fragment, C-terminal third of Chc, functions as a dominant negative. The hub fragment competes with endogenous Chc to bind to Clc (Liu et al., 1998). To express the hub fragment of *Drosophila* Chc, I generated *UAS-chc*^{hub} and *RO-chc*^{hub} transgeneic flies using cDNA encoding clathrin heavy chain residues 1074-1678, which correspond to bovine Chc^{hub}, with Bomsoo Cho's help. Expression of Chc^{hub} using various GAL4 lines does not induce any mutant phenotype and I could not find any mutant phenotype from the sections of *RO-chc*^{hub}flies. These results indicate the hub fragment does not work as dominant negative in *Drosophila*.

I tried to analyze clathrin function during Notch signaling using a *chc* null allele and a dominant negative. However, both methods do not allow me to generate mosaic clones. Other approaches need to be developed to generate *chc* clone.

Appendix 2. Materials and Methods

A.2.1. Materials and method (Chapter 2)

A.2.1.1. *Drosophila* genetics

All flies were grown on standard food at 25 °C or room temperature. In some cases, flies were grown at 18 °C or 29 °C for various experimental purposes. Fly crosses were performed in a typical manner.

A.2.1.1.1. *Drosophila* strains

Male recombination mapping of *auxilin*;

CyO, Δ2-3/Sco; th st aux^{727} sr e/TM6B (this study)

yw; P{w^{+} lacW}l(3)L5541 (78A5/6; FBst0010199)

yw; P{w^{+} lacW}l(3)L2100 (84B2/3; FBst0010219)

yw; P{w^{+} lacW}l(3)L1233 (82B1/2; FBst0012213)

yw; P{y^{+}w^{+}SUP}KG03264 (80A1; FBst0012935)

y; P{y^{+}w^{+}SUP }KG03229 (80A1; FBst0012934)

y; P{y^{+}w^{+}SUP}KG00844 (80A2; FBst0012963)

y; P{y^{+}w^{+}SUP}KG06133a (80B3; FBst0014143)

y; P{y^{+}w^{+}SUP}KG08740 (82A1; FBst0014969)

yw; P{y^{+}w^{+}EP}CG14641 (82A1; FBst0015525)

y; P{y^{+}w^{+}SUP}KG03023 (82A4; FBst0014427)

yw; P{y^{+}w^{+}EP}CG1103 (82A5; FBst0015295)

yw; P{w^{+} *lacW}j1E6* (82A3/5; FBst0010206)

yw; P{y^{+}*w*$^{+}$*EP}EY01545* (82B1; FBst0015360)

From this work;

w; aux^{727}*/TM6B*

w; aux^{727}*/TM6B gfp*

w; aux^{D136}*/TM6B*

w; aux^{D136}*/TM6B gfp*

w; aux^{D128}*/TM6B*

w; aux^{D128}*/TM6B gfp*

w; aux^{C2}*/TM6B*

w; aux^{C2}*/TM6B gfp*

w; aux^{N7}*/TM6B*

w; aux^{N7}*/TM6B gfp*

w; aux^{J26}*/TM6B*

w; aux^{J26}*/TM6B gfp*

w; aux^{K5}*/TM6B*

w; aux^{K5}*/TM6B gfp*

w; aux^{K47}*/TM6B*

w; aux^{K47}*/TM6B gfp*

w; aux^{K48}*/TM6B*

w; aux^{K48}*/TM6B, gfp*

w; aux^{L24}*/TM6B*

w; aux^{L24}/TM6B, gfp

w; aux^{F37}/TM6B

w; aux^{F37}/ TM6B, gfp

w; aux^{L7}/TM6B

w; aux^{727}, lqf^{FDD9}/TM6B

w; aux^{D136}, lqf^{FDD9}/TM6B

w; aux^{C2}, lqf^{FDD9}/TM6B

w; aux^{N7}, lqf^{FDD9}/TM6B

w; aux^{D128}, lqf^{FDD9}/TM6B

w; aux^{F37}, lqf^{FDD9}/TM6B

w; aux^{L7}, lqf^{FDD9}/TM6B

w; aux^{F37}, lqf^{ARI}/TM6B

w; aux^{L7}, lqf^{ARI}/TM6B

Rala^{EE1}

w; pgaux^{+}

w; pgchc^{+}

Other strains;

w; P{w^{1}, glrs-lqf} (our laboratoty stock)

lqf^{FDD9}/ TM6B (FBal0104483)

lqf^{ARI}/TM6B (FBal0104485)

Act5C-Gal4/ CyO (FBti0012293)

UAS-aux+ (FBal0190739; from I. Mellman)

w; Sb/TM6B (our laboratory stock)

w; Sco/CyO (our laboratory stock)

TM6B, GFP (FBst0004887)

w^{1118} (our laboratory stock)

A.2.1.1.2. Male recombination mapping of *auxilin* alleles

Enhancer *727* (aux^{727}) was mapped with respect to 12 different P elements located between polytene position 78A and 84B based on the methods described in Chen et al (1998). First, a *th st 727 sr ca* chromosome was generated. Males of the genotype *w; CyO, Δ2-3/Sco; th st 727 sr ca/TM6B* were crossed with virgins containing the P element to generate *CyO, Δ2-3/+; th st 727 sr ca P* males. These were crossed with *ru h th st cu sr e ca* virgins and the progeny were examined for male recombination events. The progeny with chromosomes that had recombined between *st* and *sr* could be distinguished easily by their eye colors. The vast majority of the progeny had wild-type (*P/ru h th st cu sr e ca*) or orange (*th st 727 sr ca/ru h th st cu sr e ca*) eyes, the latter because they are homozygous for *st ca*. Progeny with rare recombinant chromosomes (*th st* sr^+ ca^+*/ru h th st cu sr e ca* or th^+ st^+ *sr ca/ru h th st cu sr e ca*) had bright red (*st/st*) eyes or brown (*ca/ca*) eyes, respectively. Recombination between the markers *th* and *sr* served as a second check on the origins of the recombinant chromosomes. Recombinant chromosomes were scored for the presence or absence of *727* by crossing with *glrs-lqf*; if *727* is present, half of the progeny should have the enhanced rough eye phenotype and if *727* is absent, none of them should. Two P elements were found to flank *727* and these were used to map two other *auxilin* alleles (*L7* and *F37*) that were isolated as enhancers.

For this analysis, *st F37 sr e ca* and *st L7 sr e ca* chromosomes were used in identical experiments. Rare recombinant chromosomes were assayed for both the enhancer functions of *F37* and *L7* and also for their lethality in trans to *727*. Both the enhancer and lethality functions mapped between the two P elements that flanked *727*. Males of the genotype *w; CyO, Δ2-3/+; st F37 sr e ca/P* were crossed with *ru h th st cu sr e Pr ca/TM6B, Bri* virgins and rare recombinant chromosomes were identified in flies with bright red (*st/st*) or brown (*ca/ca*) eyes (*st* sr^+ e^+ ca^+*/ru h th st cu sr e Pr ca* or st^+*sr e ca/ru h th st cu sr e Pr ca*, respectively). The *sr* and *e* markers served as second checks on the origins of the chromosomes. The recombinant chromosomes were scored for the presence or absence of the lethal function of *F37* by crossing with *727/TM6B* and determining if any non-*Pr* and non-*TM6B* progeny were viable. Male progeny of this cross containing the recombinant chromosomes (*st* sr^+ e^+ ca^+*/TM6B* or st^+ *sr e ca/TM6B*) were crossed with *glrs-lqf* virgin females in order to assess if they carried the enhancer function of *F37*. If so, all of the non-*TM6B* progeny should have enhanced rough eyes and if not, none of them should. Both the enhancer and lethality in trans to aux^{727} functions of *L7* and *F37* mapped between the two P elements that flank the enhancer function of aux^{727}.

A.2.1.2. DNA constructs and transformants

pFOW: *pCMC105* (C.-m. Chen and G. Struhl, personal communication) was restricted with *Avr II*. The resulting plasmid was ligated with a 4.5 kb *Nhe I–Xba I* fragment of *pAT806* (K. Basler and G. Struhl, personal communication) containing a w^+ marker gene.

pgaux$^+$: A 21,081-bp DNA fragment containing the *auxilin*$^+$ gene was obtained by restricting BACR15O02 (Grumbling et al., 2006) with *NheI* and *SacII*. The *auxilin*$^+$ DNA fragment was ligated into the vector *pFOW* restricted with *NheI* and *SacII*. The *SacII* site in the resulting plasmid was changed to *NheI* by ligating annealed oligonucleotides of the sequence 59-TGCTAGCAGC-39 into the *SacII* site. A 21-kb *NheI* fragment containing the *auxilin*$^+$ gene was obtained from the resulting plasmid and ligated into the *XbaI* site of *pCasper4* (Thummeland Pirrotta 1992). Transformation of *paux*$^+$ was performed by Genetic Services, Inc (Sudbury, MA).

pgchc$^+$: A 14.3 kb *Avr II–Sac II* fragment of BAC22H11 (BACPAC Resources) containing *chc*$^+$ genomic DNA was ligated into a site restricted with *Avr II* and *Sac II*. The resulting plasmid was restricted with *Avr II*, and a 4.5 kb *Nhe I–Xba I* fragment of *pAT806* containing a *w*$^+$ marker gene was ligated in. Transformation of *pgchc*$^+$ was performed by Genetic Services, Inc (Sudbury, MA).

A.2.1.3. Molecular Biology and Histology

Molecular biology manipulations were performed using standard techniques or instructions from the manufacturers of enzymes and kits. Enzymes used for cloning were obtained from New England BioLabs, Roche, or Invitrogen. Oligonucleotides were synthesized by Integrated DNA Technologies.

DNA analysis of *auxilin*: Templates for DNA sequence determination of *auxilin* alleles were prepared by polymerase chain reaction (PCR) of genomic DNA from homozygous

larvae or from a single adult fly (*L7*). As most *auxilin* homozygotes die before the *Tb* marker on *TM6B* is evident in the larvae, stocks were balanced using *TM6B GFP* and 5–10 small nonfluorescing larvae were collected and homogenized in SB (10 mm Tris–HCl, pH 8.2, 1 mm EDTA, 25 mm NaCl). Template in SB (2–4 μl) was mixed with 2 μl primer (200 ng) and 45 μl of Platinum PCR SuperMix (Invitrogen). PCR conditions were 1 cycle of 1 min at 95 °C; 30 cycles of 1 min at 95 °C /1 min at 50 °C /1 min 40 sec at 72 °C; 1 cycle of 10 min at 72 °C. PCR products were purified by agarose gel electrophoresis and the QIAquick Gel extraction kit (QIAGEN, Chatsworth, CA). Four PCR primer pairs were used to amplify the aux gene in four overlapping parts: 5'-AGCAAACTGATTCCGCTC CAC-3' and 5'-GCATTGTTTGTTCTGAAGCAGTCC-3'; 59-TTGTCGCCTTTGTGG GTTCCAG-39 and 5'-TAAACTCGCAGGACCCAAGC ACTG-3'; 5'-AAGTGGATGTCTCTTGCCGACG-3' and 5'-TGTGCCCGAACTTTTG GTG-3'; 5'-AGCACGCTAAGTGGAAAGTCTCCC-3' and 5'-ACAGGGATACCAAT GAGTCACAGAG-3'. The same primers were used for automated fluorimetric DNA sequencing, and also an additional primer was used for the longest template: 5'-TTTCAC GCCCGCAAAGGAATGG-3'. Mutations found in *auxilin* alleles were confirmed by repeating the PCR and sequencing reactions.

DNA analysis of $Rala^{EE1}$: The *Rala* allele in *EE1* mutants was amplified by PCR from one adult male fly. The template was prepared as described above. PCR conditions were 1 cycle 1 min at 90 °C; 30 cycles of 1 min at 95 °C /1 min at 55 °C /1min at 72 °C; 1 cycle 10 min at 72 °C. Four primer pairs were used for both PCR and DNA sequencing:

5’-CTGTGAGCCGACTCCATAAGTTG-3’ and 5’-CCTGAGAGGAAAGCAAAACG C-3’; 5’-GCTACTTCGTTGCCATAACTCCC-3’ and 5’-TCCAGTGATGTTCTCGTTC GTAAG-3’; 5’-ATGTTGGTTCGGTCCTTG-3’ and 5’-CTGAAATGCTGCTGTGAAA-3’; 5’-TGACGGTTCTCTGGTGAATAAAGG-3’ and 5’-CGTCTGTGTGCTTTCGCTT G-3’. A Mutation found in a *Rala* allele were confirmed by repeating the PCR and sequencing reactions.

Analysis of eye and wing morphology: Scanning electron micrography and plastic sectioning of adult eyes were as described in Huang et al. (1995). Wings were mounted as described in Cadavid et al. (2000). Light photomicrographs of eyes was with an Olympus SZX12 microscope and a Kodak DC120 digital camera. Wings and eye sections were photographed with a Zeiss Axioplan and Axiocam. Immunostained eye discs were photographed with a Leica TCSSP2 confocal microscope. Adobe Photoshop 7.0 was used for processing images.

A.2.2. Materials and method (Chapter 3)

A.2.2.1. *Drosophila* strains

From Bloomington Stock Center:

FRT42D (FBti0002072)

Ubi-nGFP FRT40A/CyO (FBti0015576, FBti0002071)

CyO, YFP (FBti0058605)

w, eyFLP (FBti0015982)

Dl-lacZ (FBti0012268)

chc^{1} (FBal0033511)

UAS-gfp-clc (FBal0148099)

yw; UAS-FLP (FBst0004539)

UAS-FLP y w (FBst0008208)

From our laboratory:

w^{1118}

w; gaux+ (Chapter 2)

aux^{727} (Chapter 2)

aux^{D136} (Chapter 2)

aux^{K47}(Chapter 2)

aux^{D128} (Chapter 2)

aux^{K48} (Chapter 2)

lqf^{FDD9}/ TM6B (FBal0104483)

UAS-aux^{+} (FBal0190739; from I. Mellman)

Act5C-Gal4/ CyO

GMR-gal4

RO-gal4

Ey-gal4

Ey-gal4 GMR-gal4 (from H. Kramer)

w; FRT82B Pw+90E (FBti0002074, FBti0001288)

Generated in this work:

w; Ro-aux+

w; FRT42D, gaux^{+}, Ubi-gfp / CyO, yfp; aux^{727}/ TM6B

w; tub-aux^{+}, Ubi-gfp, FRT40A / CyO, yfp; aux^{727}/ TM6B

w, eyFLP; FRT40A/ CyO, yfp; aux^{D128}/ TM6B

w, eyFLP; FRT42D/ CyO, yfp; aux^{D136}/ TM6B

w, eyFLP; FRT42D/ CyO, yfp; aux^{D136} Dl-lacZ/ TM6B

w; Ro-aux^{+}/ CyO; aux^{K47}/ TM6B

A.2.2.2. P element constructs and transformation

Molecular biology was performed using standard procedures. Cloning enzymes and standard oligonucleotides were from New England Biolabs and Roche, custom oligonucleotides were from IDT, and DNA purification kits were from Qiagen.

Ro-aux+: An *aux+* cDNA in *pOT2* (*GH26574* from the DGRC) was purified as an *Xho I–Eco RI* fragment and ligated into those sites of *pBSKSII+* (Stratagene) to generate *pBS-aux+*. The *Eco RI* site in *pBS-aux+* was changed to *Asc I* by ligating annealed oligonucleotides of the sequence 5'-AATTGGCGCGCC-3' into the *Eco RI* site. Subsequently, the *Xho I* site in the resulting plasmid was changed to *Asc I* by ligating annealed oligonucleotides of the sequence 5'- TCGAGGCGCGCC-3' into the *Xho I* site. The 4.4 kb *Asc I* fragment containing the *aux+* cDNA was ligated into the *pRo* vector (Huang and Fischer-Vize, 1996) and the correct orientation determined by *Sal I* digestion. The *aux+* cDNA coding region is 3498 nt long, including start and stop codons, and it encodes a protein containing 1165 amino acids (AAs), including the Met initiator codon.

tub-aux+: A *tubulin* promoter fragment was excised from *pKB700* (Basler and Struhl, personal communication) as 2.6 kb *Not I–Kpn I* fragment and ligated into *pBSKSII* restricted with the same enzymes. The *Not I* site in the resulting plasmid was changed to *Avr II* by inserting the linker 5'-GGCCCCTAGG-3'. The *tubulin* promoter was excised as an *AvrII–Kpn I* (3' overhang removed) fragment. A 4.4 kb *Eco RI – Xho I* fragment containing the *aux*+ cDNA was excised from clone *GH26574* (Children's Hospital Oakland Research Institute) and ligated into *pBSKSII* restricted with the same enzymes. The *Xho I* site of the resulting plasmid was changed to *Nhe I* using the linker 5'-TCGAG CTAGC-3', the *Eco RI* site was changed to *Eco RV* using the linker 5'-AATTCGATATC G-3', and the *Not I* site was changed to *Avr II* using the linker 5'-GGCCCCTAGG-3'. The *tubulin* promoter fragment was ligated into the resulting plasmid restricted with *Eco RV* and *Avr II*, and an *Avr II-Nhe I* fragment containing *tubaux*+ was excised. A 1.2 kb *Spe I–Xba I* fragment containing transcription termination signals was excised from *pAT806* and ligated into *pCasper4* (Thummel and Pirotta, 1992) restricted with *Spe I*. A plasmid with the termination signal in the appropriate orientation was isolated, restricted with *Spe I*, and the *tub-aux*+ was ligated in.

Transformation: P element transformation of w^{1118} flies was performed according to standard methods in our laboratory.

A.2.2.3. Eye disc *auxilin*- clones and immunostaining

Third instar larval eye discs were fixed in PEMS and antibody incubations and

washes were in PBST (see Fischer-Vize et al., 1992). Primary antibodies used were mAb323 (1:2) obtained from Sarah Bray, mAB202 (1:10) from DSHB, rat anti-Elav (9:1) from DSHB, and anti-40-1a (1:50) from DSHB. Secondary antibodies (Molecular Probes) were Alexa^{568}-anti-mouse and Alexa^{633}-anti-rat (1:300). Alexa^{568}-phalloidin (Molecular Probes) was dried and resuspended in PBST at 0.1 unit/liter. Eye discs were mounted in Vectashield (Vector) and viewed with a Leica TCS SP2 confocal microsocpe. Images were processed with Adobe Photoshop. The number and the size of GFP-clc punta in the eye discs were analyzed with Image-Pro® Plus 6.1 software.

A.2.2.4. Adult eye analysis

Marked *w- aux-* homozygous clones were generated by radiation-induced mitotic recombination (1000 rads) in larvae of the genotype *w; aux^{K48}/ Pw+90E.* Of 8 *w-* clones observed, 7 were phenotypically wild-type and assumed to be genotypically wild-type due to mitotic recombination between *aux-* (at polytene position 82B) and *Pw+90E*. One clone had a mutant phenotype typical of *Dl* null or *lqf* null alleles and was assumed to be homozygous for *aux^{K48}*. Eyes were dissected, fixed and sectioned as described (Fischer-Vize et al., 1992). Light microscope images were acquired with a Zeiss Axioplan microscope and AxioCam, and processed using Adobe Photoshop.

A.2.2.5. Analysis of eye and wing morphology

Plastic sectioning of adult eyes were as described in Huang et al. (1995). Wings were mounted as described in Cadavid et al. (2000). Light photomicrographs of eyes was with an Olympus SZX12 microscope and a Kodak DC120 digital camera. Wings and eye

sections were photographed with a Zeiss Axioplan and Axiocam. Immunostained eye discs were photographed with a Leica TCSSP2 confocal microscope. Adobe Photoshop 7.0 was used for processing images.

A.2.3. Materials and method (Chapter 4)

A.2.3.1. *Drosophila* strains

From our laboratory:

w^{1118}

aux^{727} (Chapter 2)

aux^{K47}(Chapter 2)

aux^{D128} (Chapter 2)

lqf^{FDD9}/ TM6B (FBal0104483)

UAS-aux^{+} (Chapter 3)

Act5C-Gal4/ CyO

GMR-gal4

Ey-gal4

Ey-gal4 GMR-gal4

w; FRT42D, gaux^{+}*, Ubi-gfp / CyO, yfp;* aux^{727}*/ TM6B* (Chapter 3)

w, eyFLP; FRT40A/ CyO, yfp; aux^{D128}*/ TM6B* (Chapter 3)

Generated in this work:

w; Act5C-Gal4 / CyO; aux^{727}*/ TM6B*

w; Act5C-Gal4 / CyO; aux^{K47}*/ TM6B*

w; UAS-auxΔPTEN / CyO; aux^{D128}/ TM6B

w; UAS-auxCBD+J / CyO; aux^{D128}/ TM6B

w; UAS-auxK+PTEN/ CyO; aux^{D128}/ TM6B

w; UAS-auxΔJ/ CyO; aux^{D128}/ TM6B

w; gCBD+J/ CyO; aux^{D128}/ TM6B

w; UAS-auxΔKinase/ CyO

w; UAS-gfp-aux/ CyO

w; gchc^{+}/ CyO ; aux^{K47}/ TM6B

w; gchc^{+}/ CyO ; aux^{D128}/ TM6B

w; gchc^{+}/ CyO ; lqf^{FDD9}/ TM6B

A.2.3.2. P element constructs and transformation

UASt-auxΔKinase: This construct contains nts 997-3498 of the *aux*+ coding region corresponding to AAs P^{333}-A^{1165}. An *Eco RI* site followed by an ATG was introduced upstream of codon 333 by restricting *pBS-aux*+ with *Xba I*, and ligating in annealed oligonucleotides of the sequence 5'-CTAGAATTCATGCCT-3' and 5'-CTAGAGGCAT GAATT-3'. From the resulting plasmid, a 3.2 kb *Eco RI – Xho I* fragment containing *auxΔKinase* was isolated and ligated into *pUASt* restricted with *Eco RI* and *Xho I*.

UASt-auxΔPTEN: This construct contains nts 1-1197 + 2092-3498 of the *aux*+ cDNA coding region, corresponding to AAs M^{1} - V^{399} + P^{698}- A^{1165}. In addition, an *Avr II* linker sequence (5'-CCTAGG) between nts 1197 and 2092 resulted in the insertion of two

additional amino acids (PR) between V^{399} and P^{698}. The strategy was to use PCR to generate a 1.5 kb 5' *Eco RI – Avr II* fragment and a 2.1 kb 3' *Avr II – Xho I* fragment, which are then ligated together into *pUASt* restricted with *Eco RI* and *Xho I.* To generate the 5' fragment, the template was *pBS-aux*+, the primers were 5'-TGGGAATTCGGCAC GAGG-3' and 5'-ACCTAGGCACTTTGGTGGACGTATCTTTAATG-3', and Pfu Turbo DNA polymerase (Stratagene) was used. The amplification product was purified, A-tailed (Taq polymerase, Invitrogen), subcloned into pGEM-T Easy (Promega) and its DNA sequence confirmed. The 3' fragment was generated the same way, except that the primers were 5'-ACCTAGGCCAGACCCTGAGCAGGTGAC-3' and 5'-ACTCGAGTT CTACCTTTAACAGTGGCATTTCAC-3'.

UASt-CBD+J: This construct contains nts 2071-3498 of the *aux*+ cDNA coding region, corresponding to AAs N^{691}-A^{1165}. A 1.4 kb region of the *aux*+ coding region was amplified by PCR (Platinum PCR Supermix, Invitrogen) using *pBS-aux*+ as the template and the primer pair 5'-GGAATTCATGAACCAGGACTTGGATGATCTG-3'/5'-GTCTAGATT ACGCATTAAACATATTTTGCTG-3'. The PCR product was subcloned into pGEM-T Easy (Promega), and its DNA sequence was verified. A 1.4 kb *Eco RI–Xho I* fragment containing *auxCBD+J* was purified and ligated into *pUASt* restricted with *Eco RI* and *Xho I*.

UASt-auxK+PTEN: This construct contains nts 1-2103 of the *aux*+ cDNA coding region, corresponding to AAs M^{1} – E^{701}. A 2.1 kb *Asc I* fragment containing *auxK+PTEN* was generated by PCR using *pBS-aux*+ as a template, the primers 5'-AAAGGCGCGCCATG

GGCGAGTTCTTTAAGTCGCTC-3' and 5'-AAAGGCGCGCCTCACTCAGGGTCTG GCAGATCATCCA-3', and Pfu Turbo polymerase (Stratagene). The amplified product was gel-purified, restricted with *Asc I*, and ligated into *Asc I*-restricted *pUASt*. The DNA sequence of the insert was verified.

UASt-ΔJ: This construct contains nts 1-3291 of the *aux*+ cDNA coding region, corresponding to AAs M^{1} – D^{1097}. A 3.3 kb *Asc I-Nhe I* fragment containing *auxΔJ* was generated by PCR using *pBS-aux*+ as a template, the primers 5'-AAGGCGCGCCATGG GCGAGTTCTTTAAGTCGCTC-3' and 5'- GGCTAGCTTAATGTCCCACAACACTG TGTGCATAG -3', and Herculase DNA polymerase (Stratagene). The PCR product was subcloned into pGEM-T Easy (Promega), and its DNA sequence was verified. A 3.3 kb *Asc I-Nhe I* fragment containing *auxΔJ* was purified and ligated into *pUASt* restricted with *Asc I* and *Xba I*.

UASt-gfp-aux: A 3.2 kb *Asc I-Nhe I* fragment containing N-termini of *aux*+ cDNA from *pBS-aux*+ was isolated and ligated into the *UASt-gfp* vector (from our laboratory) restriced with *Asc I* and *Xba I*. An 1.0 kb *Xba I-Asc I* fragment was generated by PCR using *pBS-aux*+ as a template and the primers 5'-CTCGATGGGCATTATATGAAGG-3' and 5'-GGCGCGCCATGGGCGACTTCTTTAAGTCG-3'. The PCR product was subcloned into pGEM-T Easy, and its DNA sequence was verified. A 1.0 kb *Xba I-Asc I* fragment containing C-termini of *aux*+ cDNA was purified and ligated into *pUASt* containing *gfp* and N-termini of *aux*+ *cDNA* restricted with *Asc I* and *Xba I*.

pCasper3-gCBD+J: To remove the CBD+J domain, the 10 kb *Kpn I-Kpn I* fragment in *pgaux+* was exchanged with the 6.6 Kb *Kpn I-Kpn I* fragment with deletion of the CBD+J domain generated with threePCR products. A 21.0 kb *Nhe I-Nhe I* fragment from *pCasper4-aux+* was purified and ligated into *pCasper3* restriced with *Xba I.* A 1.0 kb *Xho I- Kpn I* fragment, in which the CBD+J is deleted, generated by PCR using *pgaux+* as a template and primers 5'-ACTCGAGAACCAGGACTTGGATGATCTGCCAG-3' and 5'-GGTACCGCCTGTGGCTGCG-3' using Herculase polymerase. The PCR product was subcloned into pGEM-T Easy, and its DNA sequence was verified. An A 1.0 kb *Xho I- Kpn I* fragment was isolated and subcloned into *pBSKSII+* restricted with *Xho I* and *Kpn I.* The 2.9 kb *Eco RV-Xho* I fragment was generated with the same way, except that the primers were 5'-AGATATCTCCGGATGGGCAGACACGAA-3' containing endogenous BspE I and 5'-ACTCGAGCATTTTGGTGGTGGCCAATGCTA-3' containing the start codon. The 2.9 kb *EcoR V-Xho I* fragment was ligated into the *pBSKSII+* already containing the 1.0 kb fragment restricted with *EcoR V* and *Xho I.* The 2.8 kb *Not I-BspE I* fragment was generated with the same way except that the primers were 5'-AGCGGCCGCGGTACCGCCCGAGCCCG-3' containing the endogenous KpnI site) and 5'-TCCGGATGTTGCAAACTTTCCAA-3' The 2.8 kb *Not I-BspE I* fragment was ligated into the *pBSKSII+* already containing the 1.0 kb and the 2.9 kb fragments restricted with *Not I* and *BspE I.* The 6.6 kb *Kpn I-Kpn I* fragment in *pBSKSII+* is ligated into *pCasper3-gaux+* restricted with *Kpn I.*

P element transformation of w^{1118} flies was performed according to standard methods in our laboratory. Transformation of *pCasper3-gCBD+J* was performed by

Genetic Services, Inc (Sudbury, MA).

A.2.3.3. Auxilin antibodies

Antibodies were generated to auxilin amino acids Q^{702}-A^{1165}. The corresponding DNA sequence was amplified by PCR using primers 5'-GGATCCCAGG TGACACCTC GGTTCTGCG-3' and 5'-GAATTCCGCATTAAACATATTTTGCTGCGTG-3', plasmid *GH26574* as a template, and subcloned into pGEMT. The sequence was verified, and a *Bam HI–Eco RI* fragment containing the *auxilin* coding sequences was ligated into pRSET (Invitrogen) restricted with the same enzymes, which added six His codons at the beginning of the open reading frame. Protein expression from pRSET-aux was in BL21-CodonPlus-RIL cells (Invtirogen) induced with 0.1 mM IPTG. The 6xHis-Aux protein was purified from sonicated cells using HisBind (Novagen), and used to raise antibodies in rats (Pocono Rabbit Farm and Laboratory). Prior to use for immunostaining and Western blots, the antisera were preadsorbed with fixed w^{1118} *Drosophila* embryos.

A.2.3.4. Western Blots

Eye disc protein extracts were generated and analyzed on protein blots, as described in Chen et al. (2002). Blots of extracts of eye discs were probed with rat α-aux at 1:1000 and mouse α-TubE7 at1:100 (DSHB). These were probed with secondaries HRP-conjugated α-rat (Santa Cruz Biochemicals) at 1:1,000 and HRP-conjugated anti-mouse (Santa Cruz Biochemicals) at 1:1,000.

A.2.3.5. Analysis of eye and wing morphology

Scanning electron micrography and plastic sectioning of adult eyes were as described in Huang et al. (1995). Wings were mounted as described in Cadavid et al. (2000). Light photomicrographs of eyes was with an Olympus SZX12 microscope and a Kodak DC120 digital camera. Wings and eye sections were photographed with a Zeiss Axioplan and Axiocam. Immunostained eye discs were photographed with a Leica TCSSP2 confocal microscope. Adobe Photoshop 7.0 was used for processing images.

A.2.4. Materials and method (Chapter 5)

A.2.4.1. *Drosophila* strains

From Bloomington Stock Center and other labs

rab11^{93Bi} (FBal0031959)

FTR82B, rab11^{j2D1} (FBal0010922, from R. Cohen)

FTR82B, rab11^{ep3017} (FBal0119426, from D. Ready)

FTR82B, rab11^{ex} (FBal0135841, from R. Cohen)

prab11+ (FBal0135843, from R. Cohen)

UAS-rab11^{N125I} (FBal0190955, from D. Ready)

UAS-rab5^{N145I} (FBal0182044, from D. Ready)

From our laboratory:

w^{1118}

aux^{727} (Chapter 2)

aux^{K47}(Chapter 3)

aux^{D128} (Chapter 3)

lqf^{FDD9} (FBal0104483)

lqf^{ARI} (FBal0104485)

lqf^{L7} *FRT80B*

RO-gal4

w; FRT42D, gaux^{+}*, Ubi-gfp / CyO, yfp; aux*^{727}*/ TM6B* (Chapter3)

w, eyFLP; FRT40A/ CyO, yfp; aux^{D128}*/ TM6B* (Chapter3)

w, eyFLP;; GMR-hid cl FRT80B

Generated in this work:

RO-rab11^{N124I}

RO-rab5^{N142I}

RO-rab7^{N124I}

UAS-rab7^{N142I}

A.2.4.2. P element constructs and transformation

Molecular biology was performed using standard procedures. Cloning enzymes and standard oligonucleotides were from New England Biolabs and Roche, custom oligonucleotides were from IDT, and DNA purification kits were from Qiagen.

RO-rab11^{N124I}: An *Asc I-Asc I* 0.6 kb fragment containing *UAS-rab11*^{N124I} was amplified by PCR using a single fly as a template and the primer pair 5'-AAAGGCGCGCCATGG GTGCAAGAGAAGACGA-3' and 5'- AAAGGCGCGCCTCACTGACAGCACTGTTT GC-3'. The PCR product was digested with *Asc I* and cloned into *pRo* vector restricted

with *Asc I*. The sequence and the orientation were confirmed by sequencing.

RO-rab5^{N145I}: An *Asc I-Asc I* 0.7 kb fragment containing *UAS-rab11*^{N145I} was amplified by PCR using a single fly as a template and the primer pair 5'-AAAGGCGCGCCATGG CAACCACTCCACGC-3' and 5'-AAAGGCGCGCCTCACTTGCAGCAGTTGTTCG-3'. The PCR product was digested with *Asc I* and cloned into *pRo* vector restricted with *Asc I*. The sequence and the orientation were confirmed by sequencing.

RO-rab7^{N142I}: An *Asc I-Asc I* 0.8 kb fragment containing *rab7*+ was amplified by RT-PCR with the primer pair 5'-AAAGGCGCGCCATGTCCGGACGTAAGAAATC-3' and 5'- AAAGGCGCGCCTTAGCACTGACAGTTGTCAG-3'. Total RNA was isolated from 10 *w*- flies using TRI reagent (molecular Research Center. OH) following the manufacturer's instruction. The reverse transcriptase reaction was performed using SuperScript® First Strand Synthesis System for RT-PCR (Invotrogen) following the manufacturer's instruction with 2 μg of total RNA and oligo-dT primer. By comparison with *rab5*^{N145I}, *rab11*^{N124I} and *rab7*+, N^{142} of Rab11 was determined to generate dominant negative Rab7. To change N to I, two separate PCR reactions were performed with a set of primers, 5'-AAAGGCGCGCCATGTCCGGACGTAAGAAATC-3' and 5'-TCCACC TTAATGCCCAACAC-3', and the other set of primers, 5'-GTGTTGGGCATTAAGGT GGA-3' and 5'-AAAGGCGCGCCTTAGCACTGACAGTTGTCAG -3'. Finally, an *Asc I-Asc I* 0.8 kb fragment containing *rab7*^{N142I} was amplified by RT-PCR with both PCR products as a template and the primer pair 5'-AAAGGCGCGCCATGTCCGGACGTAA GAAATC-3' and 5'-AAAGGCGCGCCTTAGCACTGACAGTTGTCAG-3' The PCR

product was digested with *Asc I* and cloned into *pRo* vector restricted with *Asc I*. The sequence and the orientation were confirmed by sequencing.

UAS-rab7^{N142I}: An *Asc I-Asc I* 0.8 kb fragment containing *rab7*^{N142I} was purified from *RO-rab7*^{N142I} and ligated into *pUASt* vector restricted with *Asc I*. The orientation and sequence was confirmed by sequencing.

Transformation: P element transformation of w^{1118} flies was performed according to standard methods in our laboratory. Transformation of *RO-rab11*^{N124I}, *RO-rab5*^{N145I} and *RO-rab7*^{N142I} was performed by Genetic Services, Inc (Sudbury, MA).

A.2.4.3. Eye disc immunostaining

Third instar larval eye discs were fixed in PEMS and antibody incubations and washes were in PBST (see Fischer-Vize et al., 1992). Primary antibodies used were rabbit anti-Rab11 (1:50) obtained from J. Knoblich, mAB202 (1:10) from DSHB, and rat anti-Elav (9:1) from DSHB. Secondary antibodies (Molecular Probes) were Alexa^{568}-anti-mouse, Alexa^{633}-anti-rabbit (1:500) and Alexa^{633}-anti-rat (1:300). Alexa^{488}-phalloidin (Molecular Probes) was dried and resuspended in PBST at 0.1 unit/liter. Eye discs were mounted in Vectashield (Vector) and viewed with a Leica TCS SP2 confocal microsocpe. Images were processed with Adobe Photoshop. Prior to use for immunostaining, the rabbit anti-Rab11 antiserum was preadsorbed with fixed w^{1118} *Drosophila* embryos.

A.2.4.4. Analysis of eye and wing morphology

Scanning electron micrography and plastic sectioning of adult eyes were as described in Huang et al. (1995). Wings were mounted as described in Cadavid et al. (2000). Light photomicrographs of eyes was with an Olympus SZX12 microscope and a Kodak DC120 digital camera. Wings and eye sections were photographed with a Zeiss Axioplan and Axiocam. Immunostained eye discs were photographed with a Leica TCSSP2 confocal microscope. Adobe Photoshop 7.0 was used for processing images.

A.2.5. Materials and method (Appendix 1)

A.2.5.1. *Drosophila* strains

Dl-lacZ (FBti0012268)

faf^{BX4} (FBal0028189)

faf^{FO8} (FBal0031258)

gfaf+ (from our laboratory)

FRT19A (FBst0001709)

ubi-GFP FRT18A (FBst0005623)

ey-gal4, UAS-flp (from our laboratory)

chc^{1} (FBal0033511)

aux^{727}

aux^{D136}

pFOW-gaux+ (Chapter 2)

Generated in this work:

pFOG-gaux+

Ey-gal80

Ro-gal80

w; pFOW-gaux+/ CyO ; aux^{727}/ TM6B

w, ey-FLP ; aux^{D136}/ TM6B

w; GMR-Gal4, UAS-FLP ; aux^{D136}/ TM6B

w, Ro-gal4, UAS-FLP ; aux^{D136}/ TM6B

w; Ro-gal80/ CyO yfp; aux^{D136}, UAS-gfp/ TM6B

w; GMR-gal80/ CyO yfp; aux^{D136}, UAS- gfp/ TM6B

w; Act5c- gal4/ CyO yfp; aux^{727}, UAS-aux/ TM6B

w^{-} gfaf^{+} ubi-gfp FRT19;; Dl-lacZ faf^{BX4}/TM6B

w^{-} FRT19A;; ey-gal4 UAS-flp faf^{FO8}/TM6B

A.2.5.2. P element constructs and transformation

Molecular biology was performed using standard procedures. Cloning enzymes and standard oligonucleotides were from New England Biolabs and Roche, custom oligonucleotides were from IDT, and DNA purification kits were from Qiagen.

pFOG-gaux+: A 2.6 kb *Not I-Kpn I* fragment containing the *tubulin* promoter was purified from *pKB700* and subcloned into *pUASt* vector containing the *gfp* transgene (from our laboratory) restricted with *Not I* and *Kpn I*. A 3.4 kb *Not I-Avr II* fragment containing the *tubulin* promoter and the *gfp* transgene was isolated from the resulting plasmid and subcloned into *pCMC105* restricted with *Not I* and *Avr II*. A 1.2 kb *Spe I – Xba I* fragment containing transcription termination signals was excised from *pAT806*

and ligated into the resulting plasmid restricted with *Avr II* site. The orientation was checked with *Not I* and *BamH I* digestion. The final plasmid was named *pFOG*. A 21.0 kb *Nhe I-Nhe I* fragment from *pCasper4-aux+* was purified and ligated into *pFOG* restriced with *Xba I*.

Ey-gal80: The plasmid containing *gal80* was obtained from L. Luo. A 1.3 kb *Not I-Xba I gal80* fragment was ligated with *pEy* vector restricted with *Not I* and *Xab I*.

RO-gal80: A 1.3 kb *Not I-Xba I gal80* fragment was subcloned into *pBSKSII+,* in which *Sma I* site was converted with *Asc I* site, (from our laboratory) restricted with *Not I* and *Xab I*. The *Sac II* site of the resulting plasmid was changed to *Asc I* site by inserting the linker, 5'-GGCGCGCCGC-3'. A 1.3 kb *Asc I-Asc I* fragment was ligated into *pRO* vector restricted with *Asc I*.

RO-chc^{hub}: The *Drosophila chc^{hub}* region was determined by comparison of bovine *chc^{hub}*. This construct contains nts 3220-5037 of the *chc+* cDNA coding region, corresponding to AAs K^{1074} – L^{1678}. A 1.8 kb *Asc I-Asc I* fragment was amplified by RT-PCR using primers 5'-AAAGGCGCGCCATGAAGAAGTTCGATGTGAACACATC-3' and 5'-AAAGGCGCGCCCTACAAGTAGGGATAGCCCATG-3'. The PCR product was digested by *Asc I* and cloned into *pRO* vector restricted with *Asc I*. The orientation and sequence was confirmed by sequencing.

UAS-chc^{hub}: A 1.8 kb *Asc I-Asc I* fragment containing was *chc^{hub}* purified from *RO-chc^{hub}*

and ligated into *pUASt* vector restricted with *Asc I*. The orientation and sequence was confirmed by sequencing.

A.2.5.3. Eye disc immunostaining

Third instar larval eye discs were fixed in PEMS and antibody incubations and washes were in PBST (see Fischer-Vize et al., 1992). Primary antibodies used was m40-1 (1:50) from DSHB. Secondary antibodies (Molecular Probes) was Alexa^{568}-anti-mouse (1:300). Alexa^{488}-phalloidin (Molecular Probes) was dried and resuspended in PBST at 0.1 unit/liter. Eye discs were mounted in Vectashield (Vector) and viewed with a Leica TCS SP2 confocal microsocpe. Images were processed with Adobe Photoshop. Prior to use for immunostaining rabbit anti-Rab11 antisera were preadsorbed with fixed w^{1118} *Drosophila* embryos.

References

Andres, DA, Seabra, MC, Brown, MS, Armstrong, SA, Smeland, TE, Cremers, FP, Goldstein, JL. 1993. cDNA cloning of component A of Rab geranylgeranyl transferase and demonstration of its role as a Rab escort protein. *Cell*. 73:1091-9

Baker, NE, Rubin, GM. 1989. Effect on eye development of dominant mutations in *Drosophila* homologue of the EGF receptor. *Nature*. 340:150-3

Baker, NE, Yu, S, Han, D. 1996. Evolution of proneural atonal expression during distinct regulatory phases in the developing *Drosophila* eye. *Curr Biol*. 6:1290-301

Baker, NE, Yu, SY. 1997. Proneural function of neurogenic genes in the developing *Drosophila* eye. *Curr Biol*. 7:122-32

Baker, NE, Zitron, AE. 1995. *Drosophila* eye development: *Notch* and *Delta* amplify a neurogenic pattern conferred on the morphogenetic furrow by scabrous. *Mech Dev*. 49:173-89

Baker, N. E. 2002. Notch and the patterning of ommatidial founder cells in the developing *Drosophila* eye. In *Drosophila Eye Development* (ed. K. Moses), pp.35-58. Berlin: Springer-Verlag.

Barriere, H, Nemes, C, Lechardeur, D, Khan-Mohammad, M, Fruh, K, Lukacs, GL. 2006. Molecular basis of oligoubiquitin-dependent internalization of membrane proteins in Mammalian cells. *Traffic*. 7:282-97

Berdnik, D, Torok, T, Gonzalez-Gaitan, M, Knoblich, JA. 2002. The endocytic protein alpha-Adaptin is required for numb-mediated asymmetric cell division in *Drosophila*. *Dev Cell*. 3:221-31

Bilodeau, PS, Urbanowski, JL, Winistorfer, SC, Piper, RC. 2002. The Vps27p Hse1p complex binds ubiquitin and mediates endosomal protein sorting. *Nat Cell Biol*. 4:534-9

Blatch, GL, Lassle, M. 1999. The tetratricopeptide repeat: a structural motif mediating protein-protein interactions. *Bioessays*. 21:932-9

Bray, S, Furriols, M. 2001. Notch pathway: making sense of suppressor of hairless. Curr Biol. 11:R217-21

Brodsky, FM, Chen, CY, Knuehl, C, Towler, MC, Wakeham, DE. 2001. Biological basket weaving: formation and function of clathrin-coated vesicles. *Annu Rev Cell Dev Biol*. 17:517-68

Bruckner, K, Perez, L, Clausen, H, Cohen, S. 2000. Glycosyltransferase activity of Fringe modulates Notch-Delta interactions. *Nature*. 406:411-5

Bucci, C, Thomsen, P, Nicoziani, P, McCarthy, J, van Deurs, B. 2000. Rab7: a key to lysosome biogenesis. Mol Biol *Cell*. 11:467-80

Bukau, B, Horwich, AL. 1998. The Hsp70 and Hsp60 chaperone machines. *Cell*. 92:351-66

Cagan, RL, Ready, DF. 1989. *Notch* is required for successive cell decisions in the developing *Drosophila* retina. *Genes Dev*. 3:1099-112

Chang, HC, Newmyer, SL, Hull, MJ, Ebersold, M, Schmid, SL, Mellman, I. 2002. Hsc70 is required for endocytosis and clathrin function in Drosophila. *J Cell Biol*. 159:477-87

Chappell, TG, Welch, WJ, Schlossman, DM, Palter, KB, Schlesinger, MJ, Rothman, JE. 1986. Uncoating ATPase is a member of the 70 kilodalton family of stress proteins. *Cell*. 45:3-13

Chastagner, P, Israel, A, Brou, C. 2006. Itch/AIP4 mediates Deltex degradation through the formation of K29-linked polyubiquitin chains. *EMBO Rep*. 7:1147-53

Chavrier, P, Gorvel, JP, Stelzer, E, Simons, K, Gruenberg, J, Zerial, M. 1991. Hypervariable C-terminal domain of rab proteins acts as a targeting signal. *Nature*. 353:769-72

Chen, B, Chu, T, Harms, E, Gergen, JP, Strickland, S. 1998. Mapping of *Drosophila* mutations using site-specific male recombination. *Genetics*. 149:157-63

Chen, H, De Camilli, P. 2005. The association of epsin with ubiquitinated cargo along the endocytic pathway is negatively regulated by its interaction with clathrin. *Proc Natl Acad Sci U S A*. 102:2766-71

Chen, H, Fre, S, Slepnev, VI, Capua, MR, Takei, K, Butler, MH, Di Fiore, PP, De Camilli, P. 1998. Epsin is an EH-domain-binding protein implicated in clathrin-mediated endocytosis. *Nature*. 394:793-7

Chen, W, Feng, Y, Chen, D, Wandinger-Ness, A. 1998. Rab11 is required for trans-golgi network-to-plasma membrane transport and a preferential target for GDP dissociation inhibitor. *Mol Biol Cell*. 9:3241-57

Chen, X, Zhang, B, Fischer, JA. 2002. A specific protein substrate for a deubiquitinating enzyme: Liquid facets is the substrate of Fat facets. Genes Dev. 16:289-94

Cho, KO, Choi, KW. 1998. Fringe is essential for mirror symmetry and morphogenesis in the *Drosophila* eye. *Nature*. 396:272-6

Christoforidis, S, McBride, HM, Burgoyne, RD, Zerial, M. 1999. The Rab5 effector EEA1 is a core component of endosome docking. *Nature*. 397:621-5

Conner, SD, Schmid, SL. 2002. Identification of an adaptor-associated kinase, AAK1, as a regulator of clathrin-mediated endocytosis. *J Cell Biol*. 156:921-9

Conner, SD, Schmid, SL. 2003. Regulated portals of entry into the cell. *Nature*. 422:37-44

Cooper, MT, Bray, SJ. 1999. Frizzled regulation of Notch signalling polarizes cell fate in the *Drosophila* eye. *Nature*. 397:526-30

Cooper, MT, Bray, SJ. 2000. R7 photoreceptor specification requires Notch activity. *Curr Biol*. 10:1507-10

Cremona, O, Di Paolo, G, Wenk, MR, Luthi, A, Kim, WT, Takei, K, Daniell, L, Nemoto, Y, Shears, SB, Flavell, RA, McCormick, DA, De Camilli, P. 1999. Essential role of phosphoinositide metabolism in synaptic vesicle recycling. *Cell*. 99:179-88

Cullis, DN, Philip, B, Baleja, JD, Feig, LA. 2002. Rab11-FIP2, an adaptor protein connecting cellular components involved in internalization and recycling of epidermal growth factor receptors. *J Biol Chem*. 277:49158-66

de Celis, JF, Bray, S. 1997. Feed-back mechanisms affecting Notch activation at the dorsoventral boundary in the *Drosophila* wing. *Development*. 124:3241-51

DerMardirossian, C, Bokoch, GM. 2005. GDIs: central regulatory molecules in Rho GTPase activation. *Trends Cell Biol*. 15:356-63

Diederich, RJ, Matsuno, K, Hing, H, Artavanis-Tsakonas, S. 1994. Cytosolic interaction between deltex and Notch ankyrin repeats implicates deltex in the Notch signaling pathway. *Development*. 120:473-81

Dokucu, ME, Zipursky, SL, Cagan, RL. 1996. Atonal, rough and the resolution of proneural clusters in the developing *Drosophila* retina. *Development*. 122:4139-47

Dollar, G, Struckhoff, E, Michaud, J, Cohen, RS. 2002. Rab11 polarization of the *Drosophila* oocyte: a novel link between membrane trafficking, microtubule organization, and *oskar* mRNA localization and translation. *Development*. 129:517-26

Dominguez, M, de Celis, JF. 1998. A dorsal/ventral boundary established by Notch controls growth and polarity in the *Drosophila* eye. *Nature*. 396:276-8

Drab, M, Verkade, P, Elger, M, Kasper, M, Lohn, M, Lauterbach, B, Menne, J, Lindschau, C, Mende, F, Luft, FC, Schedl, A, Haller, H, Kurzchalia, TV. 2001. Loss of caveolae, vascular dysfunction, and pulmonary defects in caveolin-1 gene-disrupted mice. *Science*. 293:2449-52

Dupre, S, Urban-Grimal, D, Haguenauer-Tsapis, R. 2004. Ubiquitin and endocytic internalization in yeast and animal cells. *Biochim Biophys Acta*. 1695:89-111

Edidin, M. 2003. The state of lipid rafts: from model membranes to cells. *Annu Rev Biophys Biomol Struct*. 32:257-83

Emery, G, Hutterer, A, Berdnik, D, Mayer, B, Wirtz-Peitz, F, Gaitan, MG, Knoblich, JA. 2005. Asymmetric Rab 11 endosomes regulate delta recycling and specify cell fate in the *Drosophila* nervous system. *Cell*. 122:763-73

Eun, SH, Lea, K, Overstreet, E, Stevens, S, Lee, JH, Fischer, JA. 2007. Identification of genes that interact with Drosophila *liquid facets*. *Genetics*. 175:1163-74

Fanto, M, Mlodzik, M. 1999. Asymmetric Notch activation specifies photoreceptors R3 and R4 and planar polarity in the *Drosophila* eye. *Nature*. 397:523-6

Feig, LA. 2003. Ral-GTPases: approaching their 15 minutes of fame. *Trends Cell Biol*. 13:419-25

Feng, Y, Press, B, Wandinger-Ness, A. 1995. Rab 7: an important regulator of late endocytic membrane traffic. *J Cell Biol*. 131:1435-52

Fielding, AB, Schonteich, E, Matheson, J, Wilson, G, Yu, X, Hickson, GR, Srivastava, S, Baldwin, SA, Prekeris, R, Gould, GW. 2005. Rab11-FIP3 and FIP4 interact with Arf6 and the exocyst to control membrane traffic in cytokinesis. *Embo J*. 24:3389-99

Fischer, JA, Eun, SH, Doolan, BT. 2006. Endocytosis, endosome trafficking, and the regulation of *Drosophila* development. *Annu Rev Cell Dev Biol*. 22:181-206

Fischer, JA, Leavell, SK, Li, Q. 1997. Mutagenesis screens for interacting genes reveal three roles for *fat facets* during *Drosophila* eye development. *Dev Genet*. 21:167-74

Fischer-Vize, JA, Rubin, GM, Lehmann, R. 1992. The *fat facets* gene is required for *Drosophila* eye and embryo development. *Development*. 116:985-1000

Fitzgerald, K, Greenwald, I. 1995. Interchangeability of *Caenorhabditis elegans* DSL proteins and intrinsic signalling activity of their extracellular domains in vivo. *Development*. 121:4275-82

Fleming, RJ. 1998. Structural conservation of Notch receptors and ligands. *Semin Cell Dev Biol*. 9:599-607

Fleming, RJ, Gu, Y, Hukriede, NA. 1997. *Serrate*-mediated activation of *Notch* is specifically blocked by the product of the gene *fringe* in the dorsal compartment of the *Drosophila* wing imaginal disc. *Development*. 124:2973-81

Flores, GV, Duan, H, Yan, H, Nagaraj, R, Fu, W, Zou, Y, Noll, M, Banerjee, U. 2000. Combinatorial signaling in the specification of unique cell fates. *Cell*. 103:75-85

Ford, MG, Mills, IG, Peter, BJ, Vallis, Y, Praefcke, GJ, Evans, PR, McMahon, HT. 2002. Curvature of clathrin-coated pits driven by epsin. *Nature*. 419:361-6

Fortini, ME, Rebay, I, Caron, LA, Artavanis-Tsakonas, S. 1993. An activated Notch receptor blocks cell-fate commitment in the developing *Drosophila* eye. Nature. 365:555-7

Fotin, A, Cheng, Y, Grigorieff, N, Walz, T, Harrison, SC, Kirchhausen, T. 2004. Structure of an auxilin-bound clathrin coat and its implications for the mechanism of uncoating. *Nature*. 432:649-53

Fra, AM, Williamson, E, Simons, K, Parton, RG. 1995. De novo formation of caveolae in lymphocytes by expression of VIP21-caveolin. *Proc Natl Acad Sci U S A*. 92:8655-9

Frise, E, Knoblich, JA, Younger-Shepherd, S, Jan, LY, Jan, YN. 1996. The *Drosophila* Numb protein inhibits signaling of the Notch receptor during cell-cell interaction in sensory organ lineage. Proc Natl Acad Sci U S A. 93:11925-32

Fryer, CJ, White, JB, Jones, KA. 2004. Mastermind recruits CycC:CDK8 to phosphorylate the Notch ICD and coordinate activation with turnover. *Mol Cell*. 16:509-20

Gad, H, Ringstad, N, Low, P, Kjaerulff, O, Gustafsson, J, Wenk, M, Di Paolo, G, Nemoto, Y, Crun, J, Ellisman, MH, De Camilli, P, Shupliakov, O, Brodin, L. 2000. Fission and uncoating of synaptic clathrin-coated vesicles are perturbed by disruption of interactions with the SH3 domain of endophilin. *Neuron*. 27:301-12

Gaidarov, I, Santini, F, Warren, RA, Keen, JH. 1999. Spatial control of coated-pit dynamics in living cells. *Nat Cell Biol*. 1:1-7

Gall, WE, Higginbotham, MA, Chen, C, Ingram, MF, Cyr, DM, Graham, TR. 2000. The auxilin-like phosphoprotein Swa2p is required for clathrin function in yeast. *Curr Biol*. 10:1349-58

Grabher, C, von Boehmer, H, Look, AT. 2006. Notch 1 activation in the molecular pathogenesis of T-cell acute lymphoblastic leukaemia. *Nat Rev Cancer*. 6:347-59

Greener, T, Grant, B, Zhang, Y, Wu, X, Greene, LE, Hirsh, D, Eisenberg, E. 2001. *Caenorhabditis elegans* auxilin: a J-domain protein essential for clathrin-mediated endocytosis *in vivo*. *Nat Cell Biol*. 3:215-9

Greener, T, Zhao, X, Nojima, H, Eisenberg, E, Greene, LE. 2000. Role of cyclin G-associated kinase in uncoating clathrin-coated vesicles from non-neuronal cells. *J Biol Chem*. 275:1365-70

Gridley, T. 2003. Notch signaling and inherited disease syndromes. *Hum Mol Genet*. 12 Spec No 1:R9-13

Grumbling, G, Strelets, V. 2006. FlyBase: anatomical data, images and queries. *Nucleic Acids Res*. 34:D484-8

Guo, M, Jan, LY, Jan, YN. 1996. Control of daughter cell fates during asymmetric division: interaction of Numb and Notch. *Neuron*. 17:27-41

Hagedorn, EJ, Bayraktar, JL, Kandachar, VR, Bai, T, Englert, DM, Chang, HC. 2006. *Drosophila melanogaster auxilin* regulates the internalization of Delta to control activity of the Notch signaling pathway. *J Cell Biol*. 173:443-52

Haglund, K, Sigismund, S, Polo, S, Szymkiewicz, I, Di Fiore, PP, Dikic, I. 2003. Multiple monoubiquitination of RTKs is sufficient for their endocytosis and degradation. *Nat Cell Biol*. 5:461-6

Hales, CM, Griner, R, Hobdy-Henderson, KC, Dorn, MC, Hardy, D, Kumar, R, Navarre, J, Chan, EK, Lapierre, LA, Goldenring, JR. 2001. Identification and characterization of a family of Rab11-interacting proteins. *J Biol Chem*. 276:39067-75

Hao, W, Luo, Z, Zheng, L, Prasad, K, Lafer, EM. 1999. AP180 and AP-2 interact directly in a complex that cooperatively assembles clathrin. *J Biol Chem*. 274:22785-94

Harper, JA, Yuan, JS, Tan, JB, Visan, I, Guidos, CJ. 2003. Notch signaling in development and disease. *Clin Genet*. 64:461-72

Hawryluk, MJ, Keyel, PA, Mishra, SK, Watkins, SC, Heuser, JE, Traub, LM. 2006. Epsin 1 is a polyubiquitin-selective clathrin-associated sorting protein. *Traffic*. 7:262-81

Hayashi, I, Urano, Y, Fukuda, R, Isoo, N, Kodama, T, Hamakubo, T, Tomita, T, Iwatsubo, T. 2004. Selective reconstitution and recovery of functional gamma-secretase complex on budded baculovirus particles. *J Biol Chem*. 279:38040-6

Heerklotz, H. 2002. Triton promotes domain formation in lipid raft mixtures. *Biophys J*. 83:2693-701

Heitzler, P, Bourouis, M, Ruel, L, Carteret, C, Simpson, P. 1996. Genes of the *Enhancer of split* and *achaete-scute* complexes are required for a regulatory loop between *Notch* and *Delta* during lateral signalling in *Drosophila*. *Development*. 122:161-71

Heitzler, P, Simpson, P. 1991. The choice of cell fate in the epidermis of Drosophila. *Cell*. 64:1083-92

Heymann, JB, Iwasaki, K, Yim, YI, Cheng, N, Belnap, DM, Greene, LE, Eisenberg, E, Steven, AC. 2005. Visualization of the binding of Hsc70 ATPase to clathrin baskets: implications for an uncoating mechanism. *J Biol Chem*. 280:7156-61

Hicke, L. 2001. A new ticket for entry into budding vesicles-ubiquitin. *Cell*. 106:527-30

Hicke, L, Dunn, R. 2003. Regulation of membrane protein transport by ubiquitin and ubiquitin-binding proteins. *Annu Rev Cell Dev Biol*. 19:141-72

Hicke, L, Riezman, H. 1996. Ubiquitination of a yeast plasma membrane receptor signals its ligand-stimulated endocytosis. *Cell*. 84:277-87

Hicks, C, Ladi, E, Lindsell, C, Hsieh, JJ, Hayward, SD, Collazo, A, Weinmaster, G. 2002. A secreted Delta1-Fc fusion protein functions both as an activator and inhibitor of Notch1 signaling. *J Neurosci Res*. 68:655-67

Hinshaw, JE. 2000. Dynamin and its role in membrane fission. *Annu Rev Cell Dev Biol*. 16:483-519

Holstein, SE, Ungewickell, H, Ungewickell, E. 1996. Mechanism of clathrin basket dissociation: separate functions of protein domains of the DnaJ homologue auxilin. *J Cell Biol*. 135:925-37

Hori, K, Fostier, M, Ito, M, Fuwa, TJ, Go, MJ, Okano, H, Baron, M, Matsuno, K. 2004. *Drosophila* deltex mediates suppressor of Hairless-independent and late-endosomal activation of Notch signaling. *Development*. 131:5527-37

Horiuchi, H, Lippe, R, McBride, HM, Rubino, M, Woodman, P, Stenmark, H, Rybin, V, Wilm, M, Ashman, K, Mann, M, Zerial, M. 1997. A novel Rab5 GDP/GTP exchange factor complexed to Rabaptin-5 links nucleotide exchange to effector recruitment and function. *Cell*. 90:1149-59

Huang, Y, Baker, RT, Fischer-Vize, JA. 1995. Control of cell fate by a deubiquitinating enzyme encoded by the *fat facets* gene. *Science*. 270:1828-31

Huang, Y, Fischer-Vize, JA. 1996. Undifferentiated cells in the developing *Drosophila* eye influence facet assembly and require the Fat facets ubiquitin-specific protease. *Development*. 122:3207-16

Huber, LA, Ullrich, O, Takai, Y, Lutcke, A, Dupree, P, Olkkonen, V, Virta, H, de Hoop, MJ, Alexandrov, K, Peter, M, et al. 1994. Mapping of Ras-related GTP-binding proteins

by GTP overlay following two-dimensional gel electrophoresis. *Proc Natl Acad Sci U S A*. 91:7874-8

Hukriede, NA, Fleming, RJ. 1997. *Beaded of Goldschmidt*, an antimorphic allele of *Serrate*, encodes a protein lacking transmembrane and intracellular domains. *Genetics*. 145:359-74

Hukriede, NA, Gu, Y, Fleming, RJ. 1997. A dominant-negative form of *Serrate* acts as a general antagonist of *Notch* activation. *Development*. 124:3427-37

Hutterer, A, Knoblich, JA. 2005. Numb and alpha-Adaptin regulate Sanpodo endocytosis to specify cell fate in *Drosophila* external sensory organs. *EMBO Rep*. 6:836-42

Hyman, J, Chen, H, Di Fiore, PP, De Camilli, P, Brunger, AT. 2000. Epsin 1 undergoes nucleocytosolic shuttling and its eps15 interactor NH(2)-terminal homology (ENTH) domain, structurally similar to *Armadillo* and HEAT repeats, interacts with the transcription factor promyelocytic leukemia Zn(2)+ finger protein (PLZF). *J Cell Biol*. 149:537-46

Itoh, M, Kim, CH, Palardy, G, Oda, T, Jiang, YJ, Maust, D, Yeo, SY, Lorick, K, Wright, GJ, Ariza-McNaughton, L, Weissman, AM, Lewis, J, Chandrasekharappa, SC, Chitnis, AB. 2003. Mind bomb is a ubiquitin ligase that is essential for efficient activation of Notch signaling by Delta. *Dev Cell*. 4:67-82

Itoh, T, Koshiba, S, Kigawa, T, Kikuchi, A, Yokoyama, S, Takenawa, T. 2001. Role of the ENTH domain in phosphatidylinositol-4,5-bisphosphate binding and endocytosis. *Science*. 291:1047-51

Jafar-Nejad, H, Andrews, HK, Acar, M, Bayat, V, Wirtz-Peitz, F, Mehta, SQ, Knoblich, JA, Bellen, HJ. 2005. Sec15, a component of the exocyst, promotes notch signaling during the asymmetric division of *Drosophila* sensory organ precursors. *Dev Cell*. 9:351-63

Jankovics, F, Sinka, R, Erdelyi, M. 2001. An interaction type of genetic screen reveals a role of the *Rab11* gene in *oskar* mRNA localization in the developing *Drosophila* melanogaster oocyte. *Genetics*. 158:1177-88

Jiang, R, Gao, B, Prasad, K, Greene, LE, Eisenberg, E. 2000. Hsc70 chaperones clathrin and primes it to interact with vesicle membranes. *J Biol Chem*. 275:8439-47

Ju, BG, Jeong, S, Bae, E, Hyun, S, Carroll, SB, Yim, J, Kim, J. 2000. Fringe forms a complex with Notch. *Nature*. 405:191-5

Kanaoka, Y, Kimura, SH, Okazaki, I, Ikeda, M, Nojima, H. 1997. GAK: a cyclin G associated kinase contains a tensin/auxilin-like domain. *FEBS Lett*. 402:73-80

Katic, I, Vallier, LG, Greenwald, I. 2005. New positive regulators of *lin-12* activity in *Caenorhabditis elegans* include the BRE-5/Brainiac glycosphingolipid biosynthesis enzyme. *Genetics*. 171:1605-15

Katz, M, Shtiegman, K, Tal-Or, P, Yakir, L, Mosesson, Y, Harari, D, Machluf, Y, Asao, H, Jovin, T, Sugamura, K, Yarden, Y. 2002. Ligand-independent degradation of epidermal growth factor receptor involves receptor ubiquitylation and Hgs, an adaptor whose ubiquitin-interacting motif targets ubiquitylation by Nedd4. *Traffic*. 3:740-51

Kidd, S, Lieber, T. 2002. Furin cleavage is not a requirement for *Drosophila* Notch function. *Mech Dev*. 115:41-51

Klapisz, E, Sorokina, I, Lemeer, S, Pijnenburg, M, Verkleij, AJ, van Bergen en Henegouwen, PM. 2002. A ubiquitin-interacting motif (UIM) is essential for Eps15 and Eps15R ubiquitination. *J Biol Chem*. 277:30746-53

Korolchuk, VI, Banting, G. 2002. CK2 and GAK/auxilin2 are major protein kinases in clathrin-coated vesicles. *Traffic*. 3:428-39

Kuang, B, Wu, SC, Shin, Y, Luo, L, Kolodziej, P. 2000. *split ends* encodes large nuclear proteins that regulate neuronal cell fate and axon extension in the *Drosophila* embryo. *Development*. 127:1517-29

Kumar, JP, Moses, K. 2001. EGF receptor and Notch signaling act upstream of Eyeless/Pax6 to control eye specification. *Cell*. 104:687-97

Kumar, JP, Moses, K. 2001. The EGF receptor and Notch signaling pathways control the initiation of the morphogenetic furrow during *Drosophila* eye development. *Development*. 128:2689-97

Lai, EC. 2004. Notch signaling: control of cell communication and cell fate. Development. 131:965-73

Lai, EC, Roegiers, F, Qin, X, Jan, YN, Rubin, GM. 2005. The ubiquitin ligase *Drosophila* Mind bomb promotes Notch signaling by regulating the localization and activity of Serrate and Delta. *Development*. 132:2319-32

Lamaze, C, Dujeancourt, A, Baba, T, Lo, CG, Benmerah, A, Dautry-Varsat, A. 2001. Interleukin 2 receptors and detergent-resistant membrane domains define a clathrin-independent endocytic pathway. *Mol Cell*. 7:661-71

Lasky, JL, Wu, H. 2005. Notch signaling, brain development, and human disease. *Pediatr Res*. 57:104R-9R

Le Borgne, R, Remaud, S, Hamel, S, Schweisguth, F. 2005. Two distinct E3 ubiquitin ligases have complementary functions in the regulation of delta and serrate signaling in *Drosophila*. *PLoS Biol*. 3:e96

Le Borgne, R, Schweisguth, F. 2003. Notch signaling: endocytosis makes delta signal better. *Curr Biol*. 13:R273-5

Le, PU, Guay, G, Altschuler, Y, Nabi, IR. 2002. Caveolin-1 is a negative regulator of caveolae-mediated endocytosis to the endoplasmic reticulum. *J Biol Chem*. 277:3371-9

Le, PU, Nabi, IR. 2003. Distinct caveolae-mediated endocytic pathways target the Golgi apparatus and the endoplasmic reticulum. *J Cell Sci*. 116:1059-71

Lee, DW, Zhao, X, Zhang, F, Eisenberg, E, Greene, LE. 2005. Depletion of GAK/auxilin 2 inhibits receptor-mediated endocytosis and recruitment of both clathrin and clathrin adaptors. *J Cell Sci*. 118:4311-21

Lee, DW, Wu, X, Eisenberg, E, Greene, LE. 2006. Recruitment dynamics of GAK and auxilin to clathrin-coated pits during endocytosis. *J Cell Sci*. 119:3502-12

Li, L, Milner, LA, Deng, Y, Iwata, M, Banta, A, Graf, L, Marcovina, S, Friedman, C, Trask, BJ, Hood, L, Torok-Storb, B. 1998. The human homolog of rat *Jagged1* expressed by marrow stroma inhibits differentiation of 32D cells through interaction with Notch1. *Immunity*. 8:43-55

Lieber, T, Kidd, S, Alcamo, E, Corbin, V, Young, MW. 1993. Antineurogenic phenotypes induced by truncated Notch proteins indicate a role in signal transduction and may point to a novel function for Notch in nuclei. *Genes Dev*. 7:1949-65

Lieber, T, Kidd, S, Young, MW. 2002. *kuzbanian*-mediated cleavage of *Drosophila* Notch. *Genes Dev*. 16:209-21

Lindsay, AJ, McCaffrey, MW. 2002. Rab11-FIP2 functions in transferrin recycling and associates with endosomal membranes via its COOH-terminal domain. *J Biol Chem*. 277:27193-9

Liu, SH, Marks, MS, Brodsky, FM. 1998. A dominant-negative clathrin mutant differentially affects trafficking of molecules with distinct sorting motifs in the class II major histocompatibility complex (MHC) pathway. *J Cell Biol*. 140:1023-37

Logeat, F, Bessia, C, Brou, C, LeBail, O, Jarriault, S, Seidah, NG, Israel, A. 1998. The Notch1 receptor is cleaved constitutively by a furin-like convertase. *Proc Natl Acad Sci U S A*. 95:8108-12

Maehama, T, Dixon, JE. 1999. PTEN: a tumour suppressor that functions as a phospholipid phosphatase. *Trends Cell Biol*. 9:125-8

Mammoto, A, Ohtsuka, T, Hotta, I, Sasaki, T, Takai, Y. 1999. Rab11BP/Rabphilin-11, a downstream target of rab11 small G protein implicated in vesicle recycling. *J Biol Chem*. 274:25517-24

Massol, RH, Boll, W, Griffin, AM, Kirchhausen, T. 2006. A burst of auxilin recruitment determines the onset of clathrin-coated vesicle uncoating. *Proc Natl Acad Sci U S A*. 103:10265-70

Matsuno, K, Diederich, RJ, Go, MJ, Blaumueller, CM, Artavanis-Tsakonas, S. 1995. Deltex acts as a positive regulator of Notch signaling through interactions with the Notch ankyrin repeats. *Development*. 121:2633-44

Matsuno, K, Ito, M, Hori, K, Miyashita, F, Suzuki, S, Kishi, N, Artavanis-Tsakonas, S, Okano, H. 2002. Involvement of a proline-rich motif and RING-H2 finger of Deltex in the regulation of Notch signaling. *Development*. 129:1049-59

Mayer, MP, Bukau, B. 1998. Hsp70 chaperone systems: diversity of cellular functions and mechanism of action. *Biol Chem*. 379:261-8

McGill, MA, McGlade, CJ. 2003. Mammalian numb proteins promote Notch1 receptor ubiquitination and degradation of the Notch1 intracellular domain. *J Biol Chem*. 278:23196-203

McMahon, HT. 1999. Endocytosis: an assembly protein for clathrin cages. *Curr Biol*. 9:R332-5

Minshall, RD, Tiruppathi, C, Vogel, SM, Niles, WD, Gilchrist, A, Hamm, HE, Malik, AB. 2000. Endothelial cell-surface gp60 activates vesicle formation and trafficking via G(i)-coupled *Src* kinase signaling pathway. *J Cell Biol*. 150:1057-70

Moloney, DJ, Shair, LH, Lu, FM, Xia, J, Locke, R, Matta, KL, Haltiwanger, RS. 2000. Mammalian Notch1 is modified with two unusual forms of *O*-linked glycosylation found on epidermal growth factor-like modules. *J Biol Chem*. 275:9604-11

Mousavi, SA, Malerod, L, Berg, T, Kjeken, R. 2004. Clathrin-dependent endocytosis. *Biochem J*. 377:1-16

Mumm, JS, Schroeter, EH, Saxena, MT, Griesemer, A, Tian, X, Pan, DJ, Ray, WJ, Kopan, R. 2000. A ligand-induced extracellular cleavage regulates gamma-secretase-like proteolytic activation of Notch1. *Mol Cell*. 5:197-206

Nabi, IR, Le, PU. 2003. Caveolae/raft-dependent endocytosis. *J Cell Biol*. 161:673-7

Newmyer, SL, Christensen, A, Sever, S. 2003. Auxilin-dynamin interactions link the uncoating ATPase chaperone machinery with vesicle formation. *Dev Cell*. 4:929-40

Nichols, B. 2003. Caveosomes and endocytosis of lipid rafts. *J Cell Sci*. 116:4707-14

Nichols, BJ. 2002. A distinct class of endosome mediates clathrin-independent endocytosis to the Golgi complex. *Nat Cell Biol*. 4:374-8

Nichols, BJ, Lippincott-Schwartz, J. 2001. Endocytosis without clathrin coats. *Trends Cell Biol*. 11:406-12

Nichols, JT, Miyamoto, A, Olsen, SL, D'Souza, B, Yao, C, Weinmaster, G. 2007. DSL ligand endocytosis physically dissociates Notch1 heterodimers before activating proteolysis can occur. *J Cell Biol*. 176:445-58

O'Connor-Giles, KM, Skeath, JB. 2003. Numb inhibits membrane localization of Sanpodo, a four-pass transmembrane protein, to promote asymmetric divisions in *Drosophila*. *Dev Cell*. 5:231-43

Okajima, T, Xu, A, Irvine, KD. 2003. Modulation of notch-ligand binding by protein *O*-fucosyltransferase 1 and fringe. *J Biol Chem*. 278:42340-5

Oldham, CE, Mohney, RP, Miller, SL, Hanes, RN, O'Bryan, JP. 2002. The ubiquitin-interacting motifs target the endocytic adaptor protein epsin for ubiquitination. *Curr Biol*. 12:1112-6

Olusanya, O, Andrews, PD, Swedlow, JR, Smythe, E. 2001. Phosphorylation of threonine 156 of the μ2 subunit of the AP2 complex is essential for endocytosis in vitro and in vivo. *Curr Biol*. 11:896-900

Orlandi, PA, Fishman, PH. 1998. Filipin-dependent inhibition of cholera toxin: evidence for toxin internalization and activation through caveolae-like domains. *J Cell Biol*. 141:905-15

Ostermeier, C, Brunger, AT. 1999. Structural basis of Rab effector specificity: crystal structure of the small G protein Rab3A complexed with the effector domain of rabphilin-3A. *Cell*. 96:363-74

Overstreet, E, Chen, X, Wendland, B, Fischer, JA. 2003. Either part of a *Drosophila* epsin protein, divided after the ENTH domain, functions in endocytosis of Delta in the developing eye. *Curr Biol*. 13:854-60

Overstreet, E, Fitch, E, Fischer, JA. 2004. Fat facets and Liquid facets promote Delta endocytosis and Delta signaling in the signaling cells. *Development*. 131:5355-66

Panin, VM, Papayannopoulos, V, Wilson, R, Irvine, KD. 1997. Fringe modulates Notch-ligand interactions. *Nature*. 387:908-12

Parks, AL, Huppert, SS, Muskavitch, MA. 1997. The dynamics of neurogenic signalling underlying bristle development in *Drosophila melanogaster*. Mech Dev. 63:61-74

Parks, AL, Klueg, KM, Stout, JR, Muskavitch, MA. 2000. Ligand endocytosis drives receptor dissociation and activation in the Notch pathway. *Development*. 127:1373-85

Parton, RG. 1996. Caveolae and caveolins. *Curr Opin Cell Biol*. 8:542-8

Pavlopoulos, E, Pitsouli, C, Klueg, KM, Muskavitch, MA, Moschonas, NK, Delidakis, C. 2001. *neuralized* Encodes a peripheral membrane protein involved in delta signaling and endocytosis. *Dev Cell*. 1:807-16

Pelissier, A, Chauvin, JP, Lecuit, T. 2003. Trafficking through Rab11 endosomes is required for cellularization during *Drosophila* embryogenesis. *Curr Biol*. 13:1848-57

Pelkmans, L, Kartenbeck, J, Helenius, A. 2001. Caveolar endocytosis of simian virus 40 reveals a new two-step vesicular-transport pathway to the ER. *Nat Cell Biol*. 3:473-83

Pereira-Leal, JB, Seabra, MC. 2000. The mammalian Rab family of small GTPases: definition of family and subfamily sequence motifs suggests a mechanism for functional specificity in the Ras superfamily. *J Mol Biol*. 301:1077-87

Pfeffer, SR. 2005. Structural clues to Rab GTPase functional diversity. *J Biol Chem*. 280:15485-8

Pickart, CM, Fushman, D. 2004. Polyubiquitin chains: polymeric protein signals. *Curr Opin Chem Biol*. 8:610-6

Pishvaee, B, Costaguta, G, Yeung, BG, Ryazantsev, S, Greener, T, Greene, LE, Eisenberg, E, McCaffery, JM, Payne, GS. 2000. A yeast DNA J protein required for uncoating of clathrin-coated vesicles *in vivo*. *Nat Cell Biol*. 2:958-63

Pitsouli, C, Delidakis, C. 2005. The interplay between DSL proteins and ubiquitin ligases in Notch signaling. *Development*. 132:4041-50

Polo, S, Sigismund, S, Faretta, M, Guidi, M, Capua, MR, Bossi, G, Chen, H, De Camilli, P, Di Fiore, PP. 2002. A single motif responsible for ubiquitin recognition and monoubiquitination in endocytic proteins. *Nature*. 416:451-5

Poodry, CA. 1990. *shibire*, a neurogenic mutant of *Drosophila*. *Dev Biol*. 138:464-72

Prekeris, R, Klumperman, J, Scheller, RH. 2000. A Rab11/Rip11 protein complex regulates apical membrane trafficking via recycling endosomes. *Mol Cell*. 6:1437-48

Raiborg, C, Bache, KG, Gillooly, DJ, Madshus, IH, Stang, E, Stenmark, H. 2002. Hrs sorts ubiquitinated proteins into clathrin-coated microdomains of early endosomes. *Nat Cell Biol*. 4:394-8

Rand, MD, Grimm, LM, Artavanis-Tsakonas, S, Patriub, V, Blacklow, SC, Sklar, J, Aster, JC. 2000. Calcium depletion dissociates and activates heterodimeric notch receptors. *Mol Cell Biol*. 20:1825-35

Razani, B, Engelman, JA, Wang, XB, Schubert, W, Zhang, XL, Marks, CB, Macaluso, F, Russell, RG, Li, M, Pestell, RG, Di Vizio, D, Hou, H, Jr., Kneitz, B, Lagaud, G, Christ, GJ, Edelmann, W, Lisanti, MP. 2001. Caveolin-1 null mice are viable but show evidence of hyperproliferative and vascular abnormalities. *J Biol Chem*. 276:38121-38

Razzaq, A, Robinson, IM, McMahon, HT, Skepper, JN, Su, Y, Zelhof, AC, Jackson, AP, Gay, NJ, O'Kane, CJ. 2001. Amphiphysin is necessary for organization of the excitation-contraction coupling machinery of muscles, but not for synaptic vesicle endocytosis in *Drosophila*. *Genes Dev*. 15:2967-79

Riggs, B, Rothwell, W, Mische, S, Hickson, GR, Matheson, J, Hays, TS, Gould, GW, Sullivan, W. 2003. Actin cytoskeleton remodeling during early *Drosophila* furrow formation requires recycling endosomal components Nuclear-fallout and Rab11. *J Cell Biol*. 163:143-54

Roehl, H, Kimble, J. 1993. Control of cell fate in *C. elegans* by a GLP-1 peptide consisting primarily of ankyrin repeats. *Nature*. 364:632-5

Roy, M, Pear, WS, Aster, JC. 2007. The multifaceted role of Notch in cancer. *Curr Opin Genet Dev*. 17:52-9

Sakata, T, Sakaguchi, H, Tsuda, L, Higashitani, A, Aigaki, T, Matsuno, K, Hayashi, S. 2004. *Drosophila* Nedd4 regulates endocytosis of notch and suppresses its ligand-independent activation. *Curr Biol*. 14:2228-36

Santolini, E, Puri, C, Salcini, AE, Gagliani, MC, Pelicci, PG, Tacchetti, C, Di Fiore, PP. 2000. Numb is an endocytic protein. *J Cell Biol*. 151:1345-52

Satoh, AK, O'Tousa, JE, Ozaki, K, Ready, DF. 2005. Rab11 mediates post-Golgi trafficking of rhodopsin to the photosensitive apical membrane of *Drosophila* photoreceptors. *Development*. 132:1487-97

Scheele, U, Alves, J, Frank, R, Duwel, M, Kalthoff, C, Ungewickell, E. 2003. Molecular and functional characterization of clathrin- and AP-2-binding determinants within a disordered domain of auxilin. *J Biol Chem*. 278:25357-68

Schmid, SL. 1997. Clathrin-coated vesicle formation and protein sorting: an integrated process. *Annu Rev Biochem*. 66:511-48

Schroeter, EH, Kisslinger, JA, Kopan, R. 1998. Notch-1 signalling requires ligand-induced proteolytic release of intracellular domain. *Nature*. 393:382-6

Schuck, S, Honsho, M, Ekroos, K, Shevchenko, A, Simons, K. 2003. Resistance of cell membranes to different detergents. *Proc Natl Acad Sci U S A*. 100:5795-800

Schweisguth, F. 2004. Regulation of notch signaling activity. *Curr Biol*. 14:R129-38

Seabra, MC. 1998. Membrane association and targeting of prenylated Ras-like GTPases. *Cell Signal*. 10:167-72

Seabra, MC, Wasmeier, C. 2004. Controlling the location and activation of Rab GTPases. *Curr Opin Cell Biol*. 16:451-7

Selkoe, DJ. 2004. Cell biology of protein misfolding: the examples of Alzheimer's and Parkinson's diseases. *Nat Cell Biol*. 6:1054-61

Seugnet, L, Simpson, P, Haenlin, M. 1997. Requirement for dynamin during Notch signaling in *Drosophila* neurogenesis. *Dev Biol*. 192:585-98

Sever, S, Skoch, J, Bacskai, BJ, Newmyer, SL. 2005. Assays and functional properties of auxilin-dynamin interactions. *Methods Enzymol*. 404:570-85

Shiba, T, Koga, H, Shin, HW, Kawasaki, M, Kato, R, Nakayama, K, Wakatsuki, S. 2006. Structural basis for Rab11-dependent membrane recruitment of a family of Rab11-interacting protein 3 (FIP3)/Arfophilin-1. *Proc Natl Acad Sci U S A*. 103:15416-21

Sigismund, S, Woelk, T, Puri, C, Maspero, E, Tacchetti, C, Transidico, P, Di Fiore, PP, Polo, S. 2005. Clathrin-independent endocytosis of ubiquitinated cargos. *Proc Natl Acad Sci U S A*. 102:2760-5

Simons, K, Ikonen, E. 1997. Functional rafts in cell membranes. *Nature*. 387:569-72

Simons, K, Toomre, D. 2000. Lipid rafts and signal transduction. *Nat Rev Mol Cell Biol*. 1:31-9

Skeath, JB, Doe, CQ. 1998. Sanpodo and Notch act in opposition to Numb to distinguish sibling neuron fates in the *Drosophila* CNS. Development. 125:1857-65

Sonnichsen, B, De Renzis, S, Nielsen, E, Rietdorf, J, Zerial, M. 2000. Distinct membrane domains on endosomes in the recycling pathway visualized by multicolor imaging of Rab4, Rab5, and Rab11. *J Cell Biol*. 149:901-14

Sorsa, V. 1988. Electron microscopic mapping of polytene chromosomes, pp. 29-107 in *Chromosome maps of Drosophila, Vol. II*, *CRC Press*, Boca Raton.

Spradling, KD, McDaniel, AE, Lohi, J, Pilcher, BK. 2001. Epsin 3 is a novel extracellular matrix-induced transcript specific to wounded epithelia. *J Biol Chem*. 276:29257-67

Stan, RV. 2002. Structure and function of endothelial caveolae. *Microsc Res Tech*. 57:350-64

Stifani, S, Blaumueller, CM, Redhead, NJ, Hill, RE, Artavanis-Tsakonas, S. 1992. Human homologs of a *Drosophila Enhancer of split* gene product define a novel family of nuclear proteins. *Nat Genet*. 2:119-27

Struhl, G, Fitzgerald, K, Greenwald, I. 1993. Intrinsic activity of the Lin-12 and Notch intracellular domains in vivo. *Cell*. 74:331-45

Sun, X, Artavanis-Tsakonas, S. 1997. Secreted forms of DELTA and SERRATE define antagonists of Notch signaling in *Drosophila*. *Development*. 124:3439-48

Takai, Y, Sasaki, T, Matozaki, T. 2001. Small GTP-binding proteins. *Physiol Rev*. 81:153-208

Takei, K, Haucke, V. 2001. Clathrin-mediated endocytosis: membrane factors pull the trigger. *Trends Cell Biol*. 11:385-91

Tanzi, RE, Bertram, L. 2001. New frontiers in Alzheimer's disease genetics. *Neuron*. 32:181-4

Terrell, J, Shih, S, Dunn, R, Hicke, L. 1998. A function for monoubiquitination in the internalization of a G protein-coupled receptor. *Mol Cell*. 1:193-202

Thummel, C. S. and Pirrotta, V. (1992). Technical notes: new pCaSpeR P element vectors. *Dros. Inf. Serv.* **71**, 150.

Tomlinson, A, Kimmel, BE, Rubin, GM. 1988. *rough*, a Drosophila homeobox gene required in photoreceptors R2 and R5 for inductive interactions in the developing eye. Cell. 55:771-84

Tsuda, L, Nagaraj, R, Zipursky, SL, Banerjee, U. 2002. An EGFR/Ebi/Sno pathway promotes delta expression by inactivating Su(H)/SMRTER repression during inductive notch signaling. *Cell*. 110:625-37

Ullrich, O, Reinsch, S, Urbe, S, Zerial, M, Parton, RG. 1996. Rab11 regulates recycling through the pericentriolar recycling endosome. *J Cell Biol*. 135:913-24

Umeda, A, Meyerholz, A, Ungewickell, E. 2000. Identification of the universal cofactor (auxilin 2) in clathrin coat dissociation. *Eur J Cell Biol*. 79:336-42

Ungewickell, E, Ungewickell, H, Holstein, SE, Lindner, R, Prasad, K, Barouch, W, Martin, B, Greene, LE, Eisenberg, E. 1995. Role of auxilin in uncoating clathrin-coated vesicles. *Nature*. 378:632-5

Urbe, S, Sachse, M, Row, PE, Preisinger, C, Barr, FA, Strous, G, Klumperman, J, Clague, MJ. 2003. The UIM domain of Hrs couples receptor sorting to vesicle formation. *J Cell Sci*. 116:4169-79

Verstreken, P, Koh, TW, Schulze, KL, Zhai, RG, Hiesinger, PR, Zhou, Y, Mehta, SQ, Cao, Y, Roos, J, Bellen, HJ. 2003. Synaptojanin is recruited by endophilin to promote synaptic vesicle uncoating. *Neuron*. 40:733-48

Wang, S, Sdrulla, AD, diSibio, G, Bush, G, Nofziger, D, Hicks, C, Weinmaster, G, Barres, BA. 1998. Notch receptor activation inhibits oligodendrocyte differentiation. *Neuron*. 21:63-75

Wang, W, Struhl, G. 2004. *Drosophila* Epsin mediates a select endocytic pathway that DSL ligands must enter to activate Notch. *Development*. 131:5367-80

Wang, W, Struhl, G. 2005. Distinct roles for Mind bomb, Neuralized and Epsin in mediating DSL endocytosis and signaling in *Drosophila*. *Development*. 132:2883-94

Wang, Y, Shao, L, Shi, S, Harris, RJ, Spellman, MW, Stanley, P, Haltiwanger, RS. 2001. Modification of epidermal growth factor-like repeats with *O*-fucose. Molecular cloning

and expression of a novel GDP-fucose protein *O*-fucosyltransferase. *J Biol Chem*. 276:40338-45

Wei, J, Hemmings, GP. 2000. The *NOTCH4* locus is associated with susceptibility to schizophrenia. *Nat Genet*. 25:376-7

Wendland, B, Steece, KE, Emr, SD. 1999. Yeast epsins contain an essential N-terminal ENTH domain, bind clathrin and are required for endocytosis. *Embo J*. 18:4383-93

Weng, AP, Ferrando, AA, Lee, W, Morris, JPt, Silverman, LB, Sanchez-Irizarry, C, Blacklow, SC, Look, AT, Aster, JC. 2004. Activating mutations of *NOTCH1* in human T cell acute lymphoblastic leukemia. *Science*. 306:269-71

Wilkin, MB, Carbery, AM, Fostier, M, Aslam, H, Mazaleyrat, SL, Higgs, J, Myat, A, Evans, DA, Cornell, M, Baron, M. 2004. Regulation of notch endosomal sorting and signaling by *Drosophila* Nedd4 family proteins. *Curr Biol*. 14:2237-44

Wilson, AL, Erdman, RA, Maltese, WA. 1996. Association of Rab1B with GDP-dissociation inhibitor (GDI) is required for recycling but not initial membrane targeting of the Rab protein. *J Biol Chem*. 271:10932-40

Wolfe, MS, Haass, C. 2001. The Role of presenilins in gamma-secretase activity. *J Biol Chem*. 276:5413-6

Wolfe, MS, Kopan, R. 2004. Intramembrane proteolysis: theme and variations. *Science*. 305:1119-23

Wolff, T. and Ready, D. F. (1993). Pattern formation in the Drosophila retina. In *The Development of* Drosophila melanogaster, Vol. 2. M. (ed. M. Bate and A. Martinez rias), pp. 1277-1325. Cold Spring Harbor: Cold Spring Harbor Laboratory Press.

Wu, X, Zhao, X, Baylor, L, Kaushal, S, Eisenberg, E, Greene, LE. 2001. Clathrin exchange during clathrin-mediated endocytosis. *J Cell Biol*. 155:291-300

Zeng, J, Ren, M, Gravotta, D, De Lemos-Chiarandini, C, Lui, M, Erdjument-Bromage, H, Tempst, P, Xu, G, Shen, TH, Morimoto, T, Adesnik, M, Sabatini, DD. 1999. Identification of a putative effector protein for rab11 that participates in transferrin recycling. *Proc Natl Acad Sci U S A*. 96:2840-5

Zerial, M, McBride, H. 2001. Rab proteins as membrane organizers. *Nat Rev Mol Cell Biol*. 2:107-17

Zhang, CX, Engqvist-Goldstein, AE, Carreno, S, Owen, DJ, Smythe, E, Drubin, DG. 2005. Multiple roles for cyclin G-associated kinase in clathrin-mediated sorting events. *Traffic*. 6:1103-13

Zhang, J, Schulze, KL, Hiesinger, PR, Suyama, K, Wang, S, Fish, M, Acar, M, Hoskins, RA, Bellen, HJ, Scott, MP. 2007. Thirty-one flavors of Drosophila rab proteins. *Genetics*. 176:1307-22

Zhang, XM, Ellis, S, Sriratana, A, Mitchell, CA, Rowe, T. 2004. Sec15 is an effector for the Rab11 GTPase in mammalian cells. *J Biol Chem*. 279:43027-34

Vita

Suk Ho Eun is the son of Hee Chang Eun and Moon Ja Kim. He was born on February 11, 1973 in Seoul, Korea. He graduated from Kyung Hee University with a B.S. in Genetic engineering in February, 1998 and from Yonsei University with a M.S. in Biochemistry in February, 2000. He began his graduate education in Molecular Cell and Developmental Biology in July 2002 at the Institute of Cell and Molecular Biology at the University of Texas at Austin. He joined Dr. Fischer's laboratory in the Spring of 2003. In 2006, he was awarded a Graduate Student Summer Fellowship from The University of Texas at Austin. His graduate training has allowed him to make important scientific contributions to understanding the role of auxilin in important developmental processes. He was awarded the degree of Doctor of Philosophy in December, 2007.

Permanent address: Sangwolgok-dong 55-35. Sungbuk-gu, Seoul, Korea 136-120

This dissertation was typed by Suk Ho Eun.